ARO 26644.19-PH

AD-A257 001

(2)

Nonlinear Optical Studies of Resonant Systems

FINAL REPORT

Duncan G. Steel

August 1992

Submitted to the U.S. Army Research Office

ARO PROPOSAL NUMBER: 26644-PH
CONTRACT/GRANT NUMBER: DAAL03-89-K-0099
Research Period: 1 May 1989 through 30 April 1992

University of Michigan

DTIC
ELECTE
OCT 26 1992
S A D

APPROVED FOR PUBLIC RELEASE:

DISTRIBUTION UNLIMITED

The views, opinions, and/or findings contained in this report are those of the author and should not be construed as an official Department of the Army position, policy, or decision, unless so designated by other documentation.

228600

92-27526

MASTER COPY KEEP THIS COPY FOR REPRODUCTION PURPOSES

REPORT DOCUMENTATION PAGE

Form Approved
OMB No 0704-0188

Public reporting burden for this collection of information is estimated to average 1 hour per response, including the time for reviewing instructions, searching existing data sources, gathering and maintaining the data needed, and completing and reviewing the collection of information. Send comments regarding this burden estimate or any other aspect of this collection of information, including suggestions for reducing this burden, to Washington Headquarters Services, Directorate for information Operations and Reports, 1215 Jefferson Davis Highway, Suite 1204, Arlington, VA 22202-4302, and to the Office of Management and Budget, Paperwork Reduction Project (0704-0188), Washington, DC 20503.

1. AGENCY USE ONLY (Leave blank)	2. REPORT DATE	3. REPORT TYPE AND DATES COVERED
	Sept 1992	Final 1 May 89-1 Jun 92

4. TITLE AND SUBTITLE

Nonlinear Optical Studies of Resonant Systems

5. FUNDING NUMBERS

DAAL03-89-K-0099

6. AUTHOR(S)

Duncan G. Steel

7. PERFORMING ORGANIZATION NAME(S) AND ADDRESS(ES)

University of Michigan
Ann Arbor, MI 48104

8. PERFORMING ORGANIZATION REPORT NUMBER

9. SPONSORING / MONITORING AGENCY NAME(S) AND ADDRESS(ES)

U. S. Army Research Office
P. O. Box 12211
Research Triangle Park, NC 27709-2211

10. SPONSORING / MONITORING AGENCY REPORT NUMBER

ARO 26644.19-PH

11. SUPPLEMENTARY NOTES

The view, opinions and/or findings contained in this report are those of the author(s) and should not be construed as an official Department of the Army position, policy, or decision, unless so designated by other documentation.

12a. DISTRIBUTION / AVAILABILITY STATEMENT

Approved for public release; distribution unlimited.

12b. DISTRIBUTION CODE

13. ABSTRACT *(Maximum 200 words)*

Work has concentrated on the development of high resolution frequency domain nonlinear spectroscopy methods as well as the use of picosecond coherent techniques such as the stimulated photon echo and time resolved free polarization decay. Using these methods, new understanding has been obtained on the dynamics associated with excitons in GaAs/AlGaAs quantum well structures, particularly as these dynamics are affected by disorder.

14. SUBJECT TERMS

Resonant Systems, Excitons, Quantum WEll Structures, Semiconductor Heterostructures, Nonlinear Spectroscopy

15. NUMBER OF PAGES

16. PRICE CODE

17. SECURITY CLASSIFICATION OF REPORT	18. SECURITY CLASSIFICATION OF THIS PAGE	19. SECURITY CLASSIFICATION OF ABSTRACT	20. LIMITATION OF ABSTRACT
UNCLASSIFIED	UNCLASSIFIED	UNCLASSIFIED	UL

INTRODUCTION

The study of the nonlinear optical response of materials is important for potential applications of these materials for opto-electronic devices and as a very effective means for the study of basic physics in these systems. The nonlinear response is particularly useful for the measurement of the dynamical evolution of resonant systems due to the interactions with the surrounding environment (i.e., the reservoir). Such spectroscopic studies provide considerable information on the effects of the reservoir on the system as well as providing information on the reservoir. The understanding is of fundamental interest as well as practical interest since these interactions ultimately limit the speed of these materials for electronic and optical applications.

Nonlinear laser spectroscopy based on studies of the third order susceptibility represents an extremely powerful method for studying both energy level structure as well as relaxation in complex systems. In general, it has been established in our earlier work and the work of others that it is possible to study the relaxation of any optically excited state or arbitrary superposition state. In addition, it is possible to eliminate the effects of inhomogeneous broadening due to random crystal fields or other potential fluctuations which in a quantum well can be due for example to interface roughness caused by nonideal growth conditions. Spatial diffusion coefficients can be measured and the presence and degree of spectral diffusion due, for example, to the emission or absorption of acoustic phonons, can be determined. Finally, it should be noted that the study of optical materials by nonlinear laser spectroscopy provides the basic understanding which is important for the potential application of these materials to nonlinear optical devices.

In this final report, we summarize the results of experiments which we have been performing on excitons in semiconductor quantum wells. Our results have focussed on the use of frequency domain nonlinear spectroscopy methods which we have developed based on four-wave mixing as well as coherent transient techniques such as photon echoes.

Accesion For
NTIS CRA&I
DTIC TAB
Unannounced
Justification
By
Distribution /
Availability Codes
Dist
A-1

PROGRAM SUMMARY

Research Progress

An important objective of our research has been the development and application of nonlinear laser spectroscopy methods for the study of excitation dynamics near the band edge of semiconductor heterostructures. Current work has been in semiconductor quantum wells grown by MBE and is significant for several reasons: we have obtained new understanding of the basic physics of exciton dynamics and the nonlinear optical excitonic response; we have obtained new insight into the fundamental physics associated with disorder induced localization of excitons; we have determined in part the effects of disorder on the nonlinear response as well as used the nonlinear response to provide some further understanding of the disorder induced localization; and finally, we have observed new aspects of the nonlinear response important for potential applications.

Our work has concentrated on the development of high resolution frequency domain nonlinear spectroscopy methods as well as the use of picosecond coherent techniques such as the stimulated photon echo and time resolved free polarization decay. As stated above, using these methods, new understanding has been obtained on the dynamics associated with excitons in GaAs/AlGaAs quantum well structures, particularly as these dynamics are affected by disorder. A summary of some of the more important results shows:

We have made the first demonstration of stimulated photon echoes from excitons in GaAs quantum well structures. These measurements enabled the simultaneous determination of both the excitation (longitudinal) relaxation rates as well as the polarization decay (also called dephasing or transverse decay) rates. One result of these measurements is that they show the nonlinear response in these experiments is due to excitons localized by interface disorder and confirm the theoretical predictions of decay dominated by phonon assisted tunneling.

We have *time resolved the emission in the stimulated photon echo experiment* by cross correlation techniques and have shown that at moderate excitation densities, the time dependence of the emission is highly complex, consisting of a prompt component (i.e., zero delay with respect to the third pulse) due to a free polarization decay and a delayed component corresponding to the stimulated photon echo.

We have shown by studying the polarization properties of the stimulated photon echo and picosecond four-wave mixing that two classes of excitons are present in these disordered systems and contribute to the optical response. Interpretation of these results is being explored in light of recent studies suggesting a bimodal distribution of roughness scales at the GaAs/AlGaAs interface.

High resolution frequency domain nonlinear spectroscopy methods developed on this program have been used to obtain a direct measurement of the quasi-equilibrium

distribution of excitons that result from phonon assisted migration between localization sites due to spectral diffusion.

Using frequency domain four-wave mixing, we have shown that there exist multiple decay channels for excitation decay extending over several orders of magnitude in time.

We have analytically solved the modified optical Bloch equations to determine and provide physical insight into the effects of spectral diffusion on frequency domain four-wave mixing line shapes and the origin of interference effects.

Using the frequency domain four-wave mixing methods developed on this program, we have made the first direct measurement of the exciton Zeeman doublet in the presence of a magnetic field. The new developments in four-wave mixing were critical since they enabled us to eliminate not only the contributions from inhomogeneous broadening, but also spectral diffusion.

Below, we summarize the basis for frequency domain nonlinear laser spectroscopy which includes the development of new theoretical understanding based on simple resonant systems and describe experimental results of exciton relaxation obtained using both frequency domain as well as picosecond time domain coherent spectroscopy methods. The theoretical basis for coherent time domain methods has been described by several groups and is provided in the cited references. The review begins with a brief discussion of the general nature of exciton relaxation and the complexity that arises in experimental studies due to the presence of disorder.

The relaxation of an exciton resonantly excited by coherent radiation is described by two general types of decays, the excitation or longitudinal decay and the polarization or transverse decay. For a simple exciton in an ideal quantum well (at liquid helium temperatures) at $\mathbf{k}=0$, the first decay would be the simple recombination time (typically 0.5-1.0 ns [1] or faster [2]) In the presence of phonon scattering along the exciton dispersion curve, the measured decay would be much faster (~10 ps [3]). In the simple picture the optical dipole vanishes for excitons away from $\mathbf{k}=0$ and hence these excitons are not directly observable. However, the temporal dependence of an optical probe at $\mathbf{k}=0$ would be described by a bi-exponential: a fast component due to phonon scattering and a slower component due to the recombination decay of the quasi-equilibrium distribution of excitons *produced by the phonon scattering*. The polarization decay rate is proportional to the sum of the excitation decay rates plus an additional so-called pure dephasing rate due to elastic scattering which changes the phase of exciton coherence but leaves the state of the exciton unchanged. In such an ideal system, the linear absorption line width is determined only by these decay rates.

However, disorder due to the interface roughness resulting from nonideal growth conditions during molecular beam epitaxial growth [4-9] results in considerable complications of

the above simple picture. Figure 1 schematically compares an exciton in an ideal quantum well and a more realistic quantum well characterized by disorder (the possibility of a bimodal distribution for roughness scale suggested by [6] and [9] is not represented in the figure.) In the first case, the exciton is described by an extended state wave function whereas in the second case, the exciton is localized by defect scattering at sites of local energy minima. Localization of the exciton leads to considerable complexity of the problem. The distribution of localization sites leads to inhomogeneous broadening of the linear absorption spectrum, typically 1-3 meV or larger. (We are distinguishing here between excitons localized by disorder and excitons bound to impurities which occur at lower energy [3]). Localized excitons can migrate between different localization sites by emission and absorption of acoustic phonons. The time dependent change in exciton energy is called spectral diffusion and the rate of migration has been predicted to depend on the exciton energy [10, 11], as we confirm experimentally, below. The spectral diffusion of excitons leads to a quasi-equilibrium distribution of excitons at the different localization sites, and the magnitude of the different relaxation rates associated with the exciton depend on the energy of the exciton. However as we show below, it is possible to observe the exciton energy distribution using an optical probe. In addition, excitons excited above the elastic cutoff [12] would be delocalized, suggesting the possibility of the presence of an exciton mobility edge [13, 14]. Evidence for this in our work is presented below as well as suggestions for additional studies.

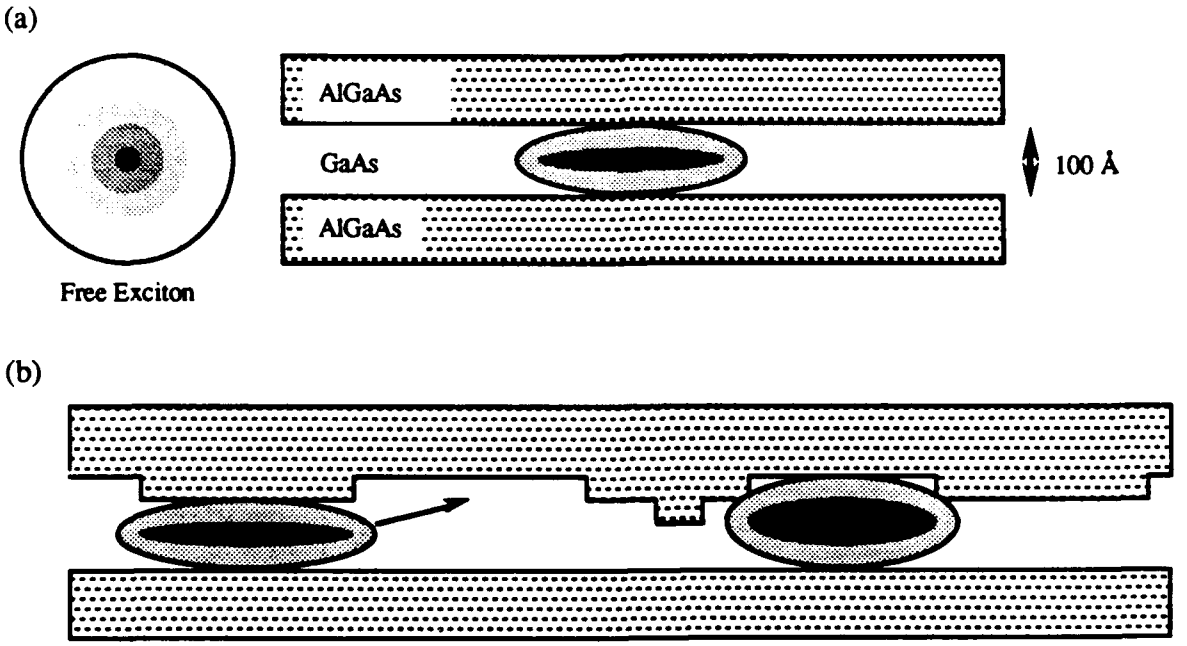

Figure 1. (a) In an ideal quantum well, an exciton is confined between the potential barriers, but is described as an extended Bloch state. (b) In the presence of disorder, scattering results in localization of the exciton, described by exponentially decaying wave functions.

The spectroscopy problem in the study of such a complex resonant structure is obvious. Measurement of the different excitation relaxation rates depends on the energy of the exciton involved and hence the wavelength of excitation. Furthermore, spectral diffusion results in a redistribution of excitons, thus complicating the interpretation of any so-called homogeneous line shape that could be measured, assuming the contributions by inhomogeneous broadening are eliminated. Nonlinear laser spectroscopy methods provide a powerful set of tools for studying these phenomena. The need to obtain wavelength resolved data such as the distribution of excitons suggests the use of nonlinear frequency domain nonlinear spectroscopy based on four-wave mixing. These methods have been developed by us in a series of earlier experimental and theoretical studies of simple resonant systems such as atoms. In this section we present new theoretical understanding we have developed as well as experimental results obtained in studies of excitons in GaAs/AlGaAs multiple quantum wells. While considerable new information has been obtained in these frequency domain measurements, complimentary time domain methods based on coherent techniques have been important to obtain a more nearly complete understanding of the dynamical nature of this complex problem. These measurements are described following the frequency domain studies. In addition to the new understanding we have regarding exciton relaxation, these studies show that in complex systems, it is useful to *combine both time and frequency domain measurements.*

Our frequency domain four-wave mixing spectroscopy measurements are based on the following experimental configuration:

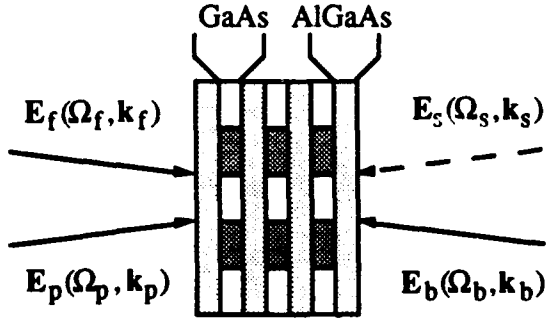

Figure 2. Schematic representation for spectroscopic measurements of relaxation. Measuring the signal amplitude as a function of detuning either Ω_p or Ω_f yields a line width determined by excitation relaxation. Tuning Ω_b provides a line shape free of inhomogeneous broadening and determined by homogeneous broadening and spectral diffusion. The open and shaded regions in the GaAs layer represent the spatial modulation of excitation due to the interaction of $E_f E_p^*$.

In these experiments, a cw forward pump and probe beam intersect in the material to create a spatial and temporal modulation of the absorption and dispersion. The cw backward pump beam

scatters from this grating giving rise to the signal. As we have shown in several theoretical papers [15, 16], measurement of the various signal line shapes as a function of tuning of the input frequencies enables characterization of many of the relaxation phenomena associated with the resonance. In addition, as we show below, determination of the signal properties as a function of the angle of the forward pump and probe as well as the relative electric field polarizations and amplitudes also provides important new information.

Analytical determination of the different line shapes in the presence of inhomogeneous broadening and spectral diffusion has been obtained by our group by analysis of the modified optical Bloch equations (MOBE) developed by Berman [17] for a two level system undergoing spectral diffusion. In this model, the excitation at an individual site can transfer to neighboring sites through an inter-site interaction (such as dipole-dipole interaction). The excitation transfer is assumed to be characterized by a redistribution kernel $W(\omega, \omega')$ representing the rate for populations in the excited state to be transferred from a site with resonant frequency ω to sites with resonant frequency ω'. The overall spectral diffusion rate is then $\Gamma(\omega) = \int W(\omega,\omega')d\omega'$. $W(\omega, \omega')$ is analogous to collision kernels that are used to describe velocity changing collisions in atomic vapor [18]. In addition, since the excitation transfer is likely to be associated with emission or absorption of thermal phonons, we assume that at the new site the excitation transfer does not induce a superposition state of the ground and excited state that is coherent with the input fields. Such a model has been discussed in detail elsewhere [17], and is closely related to the problem of excitation transfer between ions embedded in a crystal [19, 20].

The interaction of the system with optical fields can be described by the following modified optical Bloch equations assuming a classical representation for the optical fields:

$$i\hbar\frac{\partial}{\partial t}\rho_{22}(\omega) = -\{V\rho_{21}(\omega) - c.c.\} - i\hbar\{\gamma_{sp} + \Gamma(\omega)\}\rho_{22}(\omega) + i\hbar\int W(\omega',\omega)\rho_{22}(\omega')d\omega' \quad (1)$$

$$i\hbar\frac{\partial}{\partial t}\rho_{12}(\omega) = V\{\rho_{22}(\omega) - \rho_{11}(\omega)\} - \hbar\omega\rho_{12}(\omega) - i\hbar\{\gamma + \Gamma_{12}(\omega)\}\rho_{12}(\omega) \quad (2)$$

where level $|2\rangle$ is the excited state and level $|1\rangle$ is the ground state, $\rho_{ij}(\omega)$ is the usual *population* density matrix element for systems with a resonant frequency ω, $\Gamma_{12}(\omega)$ represents the dephasing rate of the system due to spectral diffusion, $V=-\mu\cdot\mathbf{E}$ is the interaction energy with μ the dipole moment (assumed to be real) and $\mathbf{E} = \frac{1}{2}\sum \mathbf{E}_j \exp(i\mathbf{k}_j\cdot\mathbf{x} - i\Omega_j t) + c.c.$ summed over all applied electric fields. Eq. (2) takes into consideration pure dephasing of the optically induced coherence by letting the dephasing rate $\gamma=\gamma_{sp}/2+\gamma_{ph}$, where γ_{sp} is the spontaneous emission rate, and γ_{ph} is the pure dephasing rate, due for example to elastic scattering. In addition, we have also assumed that the system is quantum mechanically closed, i.e., the probability that an atom is in the ground

or the excited state is unity. This leads to the condition $\rho_{11}(\omega)+\rho_{22}(\omega)=G(\omega)$ where $G(\omega)$ is the density of atoms at frequency ω. Note that spectral diffusion due to intersite energy transfer is also accompanied by a corresponding change in location of the excitation. However, if the effective mean free path for excitation transfer is small, then the effect would be described by a spatial diffusion process. This effect can be phenomenologically included as a spatial diffusion decay term in the equation for ρ_{22}, and the decay rate is given by $\Gamma_d= 4\pi^2 D/L^2$ where D is the diffusion coefficient and L is the spatial period of the modulation. (This aspect of the response has been used to measure exciton diffusion coefficients, [16] and Appendix.)

The model discussed above may not accurately represent the physical process of exciton migration during nonlinear optical interaction, since a simple two level model does not reflect the the many-body nature of the excitonic nonlinear optical response [21]. Moreover, description of the spectral diffusion process in general, and exciton migration in particular is much more complicated than a simple transfer of the excited state population [10]. Nevertheless, recent theoretical work has shown that in the limit that phase space filling dominates the exciton nonlinear optical response, the equation of motion governing the nonlinear optical process in semiconductors is nearly identical to the optical Bloch equation of an atomic system [22]. Hence, we expect predictions from the above simple two level model to reflect the qualitative features of four-wave mixing line shapes of more complicated systems, in particular excitons in QW structures, and provide guidance for more detailed studies.

Even with the above assumptions, it is rather difficult to obtain analytical solutions for frequency domain four-wave mixing line shapes for a general distribution kernel. However, using a strong redistribution model for the spectral diffusion process we may further simplify the above equations. In this model, the spectral diffusion process is independent of the resonant frequency of the initial site, and each transfer on average leads to a complete redistribution of the excited state population [23], i.e. $W(\omega',\omega)=\Gamma F(\omega)$ with $F(\omega)$ satisfying $\int d\omega F(\omega) = 1$ where Γ is the overall spectral diffusion rate for the excited state. For the qualitative discussions of this work, the dephasing rate due to spectral diffusion is taken to be $\Gamma_{12}(\omega)=\Gamma/2$ (the coupling giving rise to spectral diffusion may also lead to pure-dephasing effects which could be included in γ_{ph}).

With these simplifications, the off diagonal matrix element to the third order in applied fields for a signal nearly counter-propagating to the probe (proportional to $E_f E_p^* E_b$) can be obtained resulting in the corresponding third order polarization following integration over the inhomogeneous distribution:

$$P^{(3)}(\Omega_s) = -2\mu\left(\frac{\mu}{2\hbar}\right)^3 E_f E_p^* E_b \exp\{i(\mathbf{k}_f + \mathbf{k}_b - \mathbf{k}_p)\cdot\mathbf{x} - i\Omega_s t\}\frac{1}{\Delta_{fp} + i(\gamma_{sp} + \Gamma)}$$

$$\left\{\frac{1}{\Delta_{sp} + 2i\Gamma_h}[A(\Omega_s) - A^*(\Omega_p)] - \frac{1}{\Delta_{sf}}[A(\Omega_s) - A(\Omega_f)] + \right.$$

$$\left.\frac{i\Gamma}{\Delta_{fp} + i\gamma_{sp}}Q(\Omega_s)[A(\Omega_f) - A^*(\Omega_p)]\right\} + \text{c.c.}$$

where $\Gamma_h=\gamma_{sp}/2+\Gamma/2+\gamma_{ph}$ is the total dephasing rate, $\Omega_S=\Omega_f+\Omega_b-\Omega_p$ is the signal frequency, and $\Delta_{ij}=\Omega_i-\Omega_j$ with i,j=f,b,p. $A(\Omega)$ is given by

$$A(\Omega) = \int \frac{1}{\Omega - \omega + i\Gamma_h} G(\omega)d\omega$$

The imaginary part of the $A(\Omega)$ is related to the inhomogeneous linear absorption profile of the system and the real part corresponds to the dispersion. $Q(\Omega_S)$ is related to the redistribution kernel:

$$Q(\Omega_s) = \int \frac{1}{\Omega_s - \omega + i\Gamma_h} F(\omega)d\omega$$

The nonlinear optical signal is determined by a solution of the appropriate Maxwell wave equation where the nonlinear polarization is the source term. In the limit that all fields are weak and there is no depletion of any of the applied fields, the nonlinear signal is simply proportional to $\left|P^{(3)}(\Omega_s)\right|^2$.

Examination of the different FWM line shapes that can be obtained from this expression and their dependence on the different relaxation parameters provides considerable insight into the interpretation of the line shapes observed in the GaAs spectroscopy measurements discussed below. We consider a strongly inhomogeneously broadened system and a Gaussian kernel associated with spectral diffusion. With all laser frequencies tuned within the inhomogeneous width, and $\Omega_b=\Omega_p$, we see the FWM response obtained by tuning Ω_f in Fig. 3. This profile reflects, in the frequency domain, the dynamics associated with the excitation dynamics. Without the contribution of spectrally diffused excitation, a broad resonance (the dashed line) reflects the fast decay out of the energy state probed by the laser. However, in the presence of spectral diffusion, the excitation redistributes to different energy states and establishes a quasi-equilibrium distribution which decays at the slower recombination rate. The complete FWM response is shown as the solid line in Fig. 3. The width of the narrow feature is determined by the recombination time.

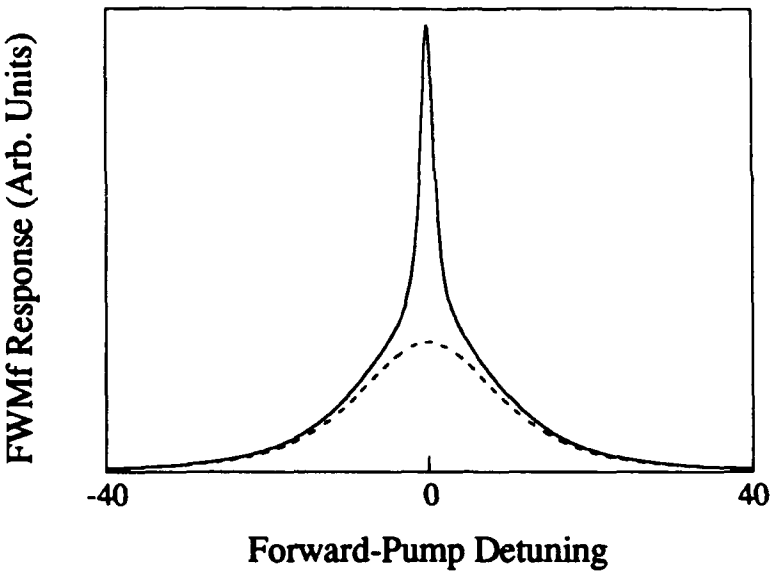

Figure 3. FWM response obtained by tuning the forward pump. The line shape is determined by the *excitation* relaxation rates. All the frequency and decay rates are normalized to the spontaneous emission rate. Γ=15, $\Delta\omega_{inh}$=1000, $\Delta\omega_o$=400, $\omega_o-\omega_{inh}$=-100, $\Omega_p=\omega_o$. The response shows a prominent narrow component due to the spectral diffusion process.The width of this component is determined by the spontaneous emission rate. The dashed line represents the nonlinear response without contribution from the spectrally diffused excitations. Compare with experimental results in Figure 5b.

The linear absorption profile in this system provides little information on the homogeneous line shape because of the large inhomogeneous broadening. However, the FWM response obtained by tuning Ω_b eliminates inhomogeneous broadening and provides a line shape determined by the homogeneous width of the spectral hole produced by the forward pump and probe excitation as well as a contribution from the quasi-equilibrium distribution of excitation due to spectral diffusion. A remarkable and powerful result of FWM is that it is possible to eliminate the contribution due to spectral diffusion in FWM by setting the forward pump probe detuning equal or larger than the recombination rate. In this way, it is possible to obtain just the homogeneous response of the system. Figure 4 shows two line shapes obtained by tuning Ω_b. The dotted line shape is the response with Ω_f-Ω_p=0 and shows a narrow resonance due to the homogeneous line width of the excitation and a broad feature resulting from spectrally diffused excitation. The solid line is just the homogeneous response which is measured by setting Ω_f-Ω_p=Γ. The contribution due to spectral diffusion is greatly reduced, providing information

on the pure homogeneous line width. The results are discussed in more detail in several reprints and preprints included in the Appendix.

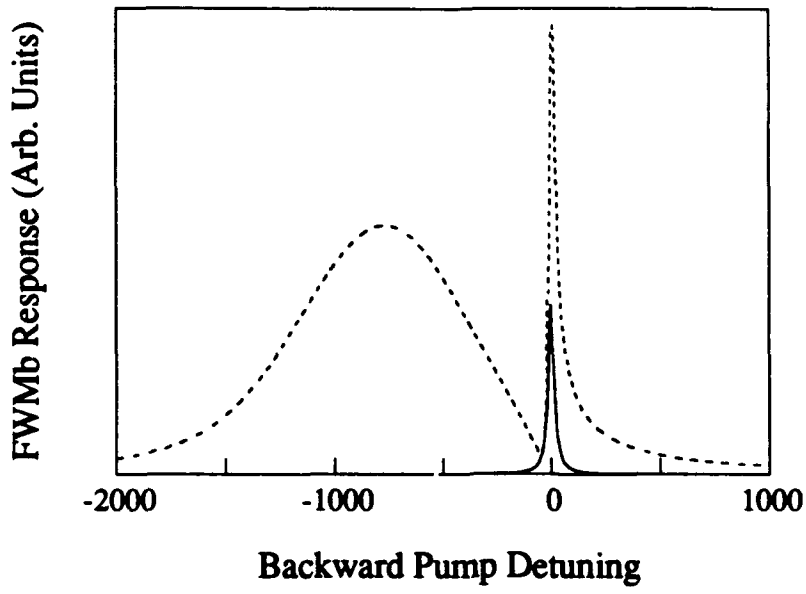

Figure 4. The FWM response obtained by tuning the backward pump. The line shape is determined by the *polarization* relaxation rates and spectral diffusion. All the frequency and decay rates are normalized to the spontaneous emission rate. Γ=15, $\Delta\omega_{inh}$=1000, $\Delta\omega_o$=400, Ω_p–ω_{inh}=–100, ω_o-ω_{inh}=–850, where ω_{inh} and $\Delta\omega_{inh}$ are the center and half-width of the inhomogeneous distribution respectively, and ω_o and $\Delta\omega_o$ are the center and half-width of the redistribution kernel respectively. The backward pump detuning is measured with regard to Ω_p-Δ_{fp}. The solid line is the line shape obtained with Δ_{fp}=Γ. The line width is the homogeneous linewidth with no inhomogeneous broadening. The dashed line is the line shape obtained with Δ_{fp}=0, where the effects of spectral diffusion are clearly observed. Compare with experimental results in Figure 6.

Experimental studies have been performed on both MBE grown single and multiple GaAs/$Al_{0.3}Ga_{0.7}As$ quantum wells as well as high purity bulk GaAs. Sample characterization including luminescence, absorption and photoluminescence excitation are performed in our own laboratory. The experimental studies are performed on samples as a function of temperature between 1.8 and 25 K and are based on frequency domain four-wave mixing using two or three frequency stabilized cw dye lasers, two variable pulsewidth picosecond/femtosecond dye laser systems, or a self mode locked Ti-sapphire laser. Highlights of the published experimental results are presented below. Detailed discussions can be found in the reprints in the Appendix.

As anticipated above, the presence of disorder in a quantum well is predicted to lead to exciton localization and phonon assisted tunneling between localization sites. Measurements of

the excitation relaxation time would be expected to be comprised of two components, a fast component due to spectral diffusion and a slow component due to recombination. Figure 5 shows two characteristic four-wave mixing line shapes (tuning the forward pump to get the *excitation relaxation rate*) obtained below line center. Below absorption line center, we observe a two component spectrum. The width of the wide feature is temperature dependent and is due to spectral diffusion of the excitons. Our studies of the temperature and wavelength dependence of this feature [16, 24, 25] indicates that at low temperatures the origin is due to acoustic phonon assisted tunneling between localization sites [10] The narrow feature shown at the tip of Fig. 5a corresponds to the slower exciton recombination time. This feature is enhanced at higher temperatures (Fig. 5b) since the spectral diffusion rate has increased considerably. Above the absorption line center, excitons are expected to be delocalized [26]. The response is dominated by a nearly temperature independent slow component due to recombination. The phonon scattering time for these states has been measured by other groups [3] along with our own work (below) and is much faster. The rapid time scale (<5 ps) for this scattering results in a small broad pedestal underneath a narrow feature (data not shown, see Appendix).

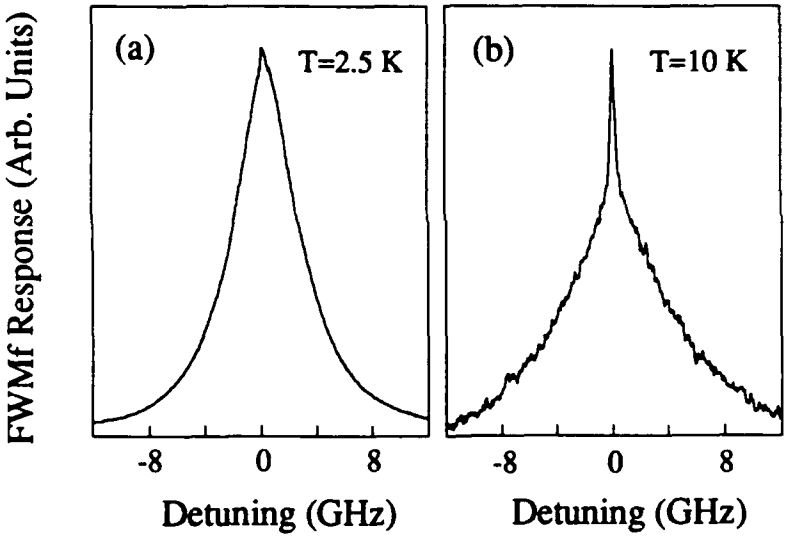

Figure 5. The FWM line shapes corresponding to excitation (longitudinal) decay processes obtained by tuning the forward pump (See Fig. 3). (a). Obtained below the absorption line center at 2K. The wide feature corresponds to a decay time of 60 ps and is the spectral diffusion time (see text for origin). The narrow feature at the top is enhanced in (b) when the temperature is increased to 10K. The wide feature has increased in width owing to the faster spectral diffusion rate, while the narrow feature is more prominent. The width is 1 ns and is due to slower exciton recombination processes.

Localized excitons are characterized by an optical dipole, and based on the above analytical discussion, it is clear that the excitons that have been excited at one energy and then emit acoustic phonons to migrate to other localization sites should be directly observable in

FWM by tuning the backward pump. Figure 6 shows the measurement providing the first direct observation of the quasi-equilibrium distribution of excitons. There are several features of this result which are quite important. First, we note that the inhomogeneous broadening is completely eliminated in the response. The narrow feature is the spectral hole produced by the forward pump and probe beam and corresponds to a line width of 40 meV. The broad feature measures the quasi-equilibrium distribution of spectrally diffused excitons and can be compared directly to calculations of the scattering kernel.

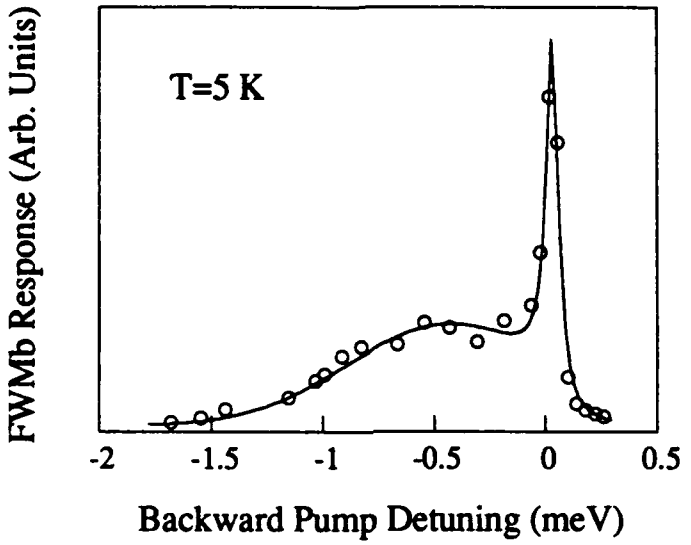

Figure 6. The FWM spectrum obtained by tuning the backward pump providing a measurement of the exciton homogeneous line width and the contribution due to spectral diffusion (See Fig. 4).

More detailed discussions are provided in the references where these techniques have been used to determine the temperature and energy dependence of the relaxation rates predicted by Takagahara as well as the spatial diffusion coefficient.

While the discussion up to this point has emphasized the use of cw FWM for measurements of relaxation, the great precision afforded in such measurements and the ability to eliminate inhomogeneous broadening can also be used to obtain new information on energy level structure. This is especially powerful in cases where linear spectroscopic methods fail due to the large inhomogeneous broadening compared to the relevant energy scale. The capability has been critical in our studies of spin flip induced hole burning and measurements of the exciton Zeeman splitting in modest magnetic fields.

To understand these experiments, we note that the electronic energy spectrum of quantum well structures is fully quantized under a magnetic field parallel to the growth axis. Optical absorption reveals a ladder of magnetoexcitons corresponding to transitions between electron and hole Landau levels [27]. The accompanying Zeeman splitting lifts the Kramers degeneracy and is characterized by an effective g-factor which depends sensitively on the details of the band structure. In addition, the energy separation between the different spin leads to an increase in the spin relaxation time since now spin relaxation can only take place via inelastic processes [28].

There have been numerous studies of the electron g-factor, however, determination of the Zeeman splitting has been more difficult because of the large inhomogeneous broadening due to disorder [29] and the fact that the exciton Zeeman splitting in a quantum well is much smaller than in the bulk for small magnetic fields. Earlier magneto-reflectance measurements were able to resolve Zeeman splittings for the light-hole but not the heavy-hole exciton [30]. More recent measurements have inferred the exciton g-factor from nonlinear quantum beat spectroscopy [31]. However, using the methods described above, we have been able to obtain the first direct measurements of the exciton Zeeman splitting in GaAs quantum wells [32]. The measurements reveal a heavy-hole splitting much smaller than that reported for bulk GaAs at low magnetic field, and show a nonlinear dependence of the splitting on magnetic field strength. The results reflect the effects of the complex band structure of a quantum well.

In these experiments, a nearly monochromatic optical beam with σ_- circular polarization is used to excite a narrow spectral-hole at the lowest heavy-hole (HH1) exciton associated with the 3/2 to 1/2 transition (see Fig. 7 for the 2-D exciton energy level diagram in a magnetic field). The width of the spectral-hole is determined by the homogeneous line width. Spin relaxation of these excitons generates a spectral-hole of excitons associated with the -3/2 to -1/2 transition. The induced spectral hole burning is probed using an optical beam with σ_+ circular polarization. Zeeman splitting can then be obtained by measuring the energy spacing between the spin-flip-induced spectral hole and the original spectral hole resonance.

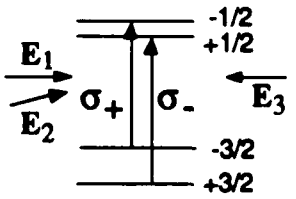

Figure 7 Energy level diagram and experimental configuration for FWM studies of magnetoexcitons in a quantum well.

In practice, the measurements proposed above are complicated by strong spectral diffusion of the localized excitons, as seen in Fig. 6. In the limit where the spin-flip time is long compared with the spectral diffusion time, nearly all spin-flipped excitons have diffused in energy. Hence, the spin-flip-induced spectral hole burning resonance will be completely smeared out by the spectral diffusion process. To avoid the above complications, we exploit the power of FWM spectroscopy which enables us to eliminate the spectral diffusion contribution to the response. As before, nearly degenerate beams $\mathbf{E}_1$ and $\mathbf{E}_2$ interfere in the sample to excite a traveling wave grating which oscillates at a frequency equal to the detuning between the two beams $\delta=|\omega_1-\omega_2|$. The amplitude of the grating is proportional to $(\delta+i\Gamma_{pop})^{-1}$. Measuring the FWM signal as a function of ω_3 probes the spectral profile of the grating. In the presence of spectral diffusion, the spectral-hole excited by $\mathbf{E}_1\cdot\mathbf{E}_2^*$ diffuses in energy and the FWM response arises from both the spectral-hole and the quasi-equilibrium distribution of the exciton population as discussed above. The decay of the spectral hole is determined by the sum of the exciton spectral diffusion and recombination rates. However, the life time of the quasi-equilibrium distribution is determined solely by the recombination time of the exciton as we discussed earlier . In the limit where the spectral diffusion rate is much larger than the exciton recombination rate, detuning $\mathbf{E}_1$ and $\mathbf{E}_2$ by an amount large compared with the recombination rate (but still smaller than or comparable with the spectral diffusion rate) significantly decreases the amplitude of the grating associated with the quasi-equilibrium distribution. As a result, the FWM nonlinear optical response will be dominated by the spectral hole burning resonance [16].

For these measurements, experiments were carried out at 2.5 K using a split-coil superconducting magnet. The effects of spectral diffusion were reduced on the spectral hole burning resonance by using two acousto-optic modulators to set the detuning between $\mathbf{E}_1$ and $\mathbf{E}_2$ to 140 MHz. In the first set of measurements, we used three circularly polarized optical beams rotating in the same direction in the lab frame. The nonlinear optical response, shown as squares in Fig. 8, involves only the σ_- excitons associated with the 3/2 to 1/2 transition. As expected, the contribution from spectral diffusion is nearly nonexistent.

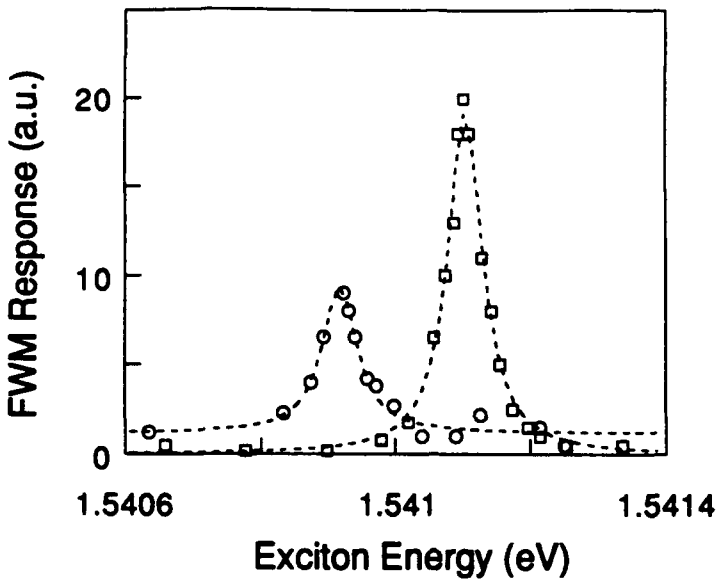

Figure 8. The FWM response of magnetoexcitons in a quantum well obtained by tuning ω_3. The grating is written using σ_- polarized $\mathbf{E}_1$ and $\mathbf{E}_2$ The high frequency resonance is the original spectral hole observed when $\mathbf{E}_3$ is σ_- polarized while the lower frequency resonance is the result of spin flip induced hole burning, observed when $\mathbf{E}_3$ is σ_+ polarized.

When the electron or hole associated with a σ_- exciton created with $\mathbf{E}_1 \cdot \mathbf{E}_2^*$ flip their spin, the nonlinear response probed by reversing the polarization direction of the third beam will exhibit a resonance associated with a spectral hole located at the energy of the σ_+ exciton. The nonlinear response at the σ_+ exciton arises due to phase space filling caused by the presence of electrons (holes) with -1/2 (+3/2) angular momentum. The resulting resonance, shown as circles in Fig. 8 clearly shows narrow spectral hole burning at a lower energy. The energy difference is the exciton Zeeman splitting, which is 0.19 meV at 4T. The nearly constant background signal in Fig. 8 is due to excitons that have spectrally diffused. Note that spin-flips of σ_+ excitons require absorption of acoustic phonons, and are slower compared with spin-flips of σ_- excitons. The observed spin-flip-induced spectral hole burning resonance is considerably weaker at 4T when $\mathbf{E}_1 \cdot \mathbf{E}_2^*$ excites σ_+ excitons.

Using linearly polarized light for the third beam, we can simultaneously probe the spectral hole burning and the spin-flip-induced resonance. With $\mathbf{E}_1 \cdot \mathbf{E}_2^*$ exciting only the σ_- excitons, the FWM response obtained (see attached reprint) shows the well resolved Zeeman doublet.

Recent measurements have shown that at low and intermediate magnetic field, the electron g-factor at the lowest Landau level in GaAs quantum wells is close to the value for bulk GaAs [33]. In contrast, the Zeeman splitting of the HH1 exciton obtained above is very small in comparison with that reported for bulk GaAs [34]. Our results seem to be in agreement with the earlier magneto-reflectance measurements where the heavy hole Zeeman doublet was not resolved. Small Zeeman splittings attributed to the strong valence band mixing in quantum well structures have been recently predicted by numerical calculations of magnetoexcitons using the Luttinger Hamiltonian [35, 36]. In particular, the mixing of σ_- excitons with excitons at higher energy pushes the σ_- exciton to lower energy. The theory also predicts an eventual sign change of the Zeeman splitting at higher magnetic fields where the band mixing effects overcome those of the Zeeman interaction. However, theoretical determination of the magnetic field at which the zero crossing occurs is difficult since the cancellation of the two competing contributions depends strongly on parameters of the model [36]. The sign change of the splitting has not been observed in our measurements up to 6 T.

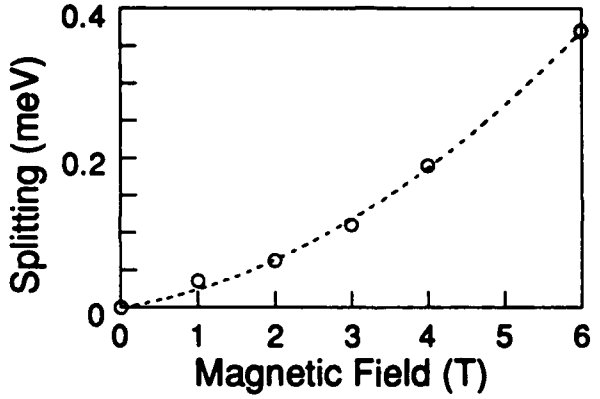

Figure 9. Magnetic field dependence of the magnetoexciton Zeeman splitting.

Figure 9 displays the magnetic field dependence of the Zeeman splitting for the HH1 exciton. The validity of the quadratic dependence indicated in the figure (dashed line) is clearly questionable since our data covers only a relatively small field range. Nevertheless, the observed field dependence is somewhat surprising since the calculations predict a field dependence slower than linear. The observed dependence may be due in part to the nonparabolicity of the conduction band [37], which was not included in the calculations. Note that our results differ considerably from those obtained from nonlinear quantum beats in a 30 Å stepped GaAs quantum well [31]. Zeeman splittings reported in the quantum beat measurements are proportional to magnetic fields with a field strength ranging from 1 to 5 T, and are very close to those measured for impurity bound excitons in bulk GaAs [38].

Time domain measurements are important in systems such as this since they can provide a measure of dynamics on a time scale short compared to spectral diffusion times. For this work, we have used the stimulated backward photon echo (or three pulse echo) first developed by Hartmann's group [39] and recently used in the study of mixed crystal semiconductors [40]. In these experiments, it is possible to simultaneously determine both the excitation relaxation time and the pure dephasing time. These experiments are based on the usual backward four-wave mixing geometry shown in Fig. 10.

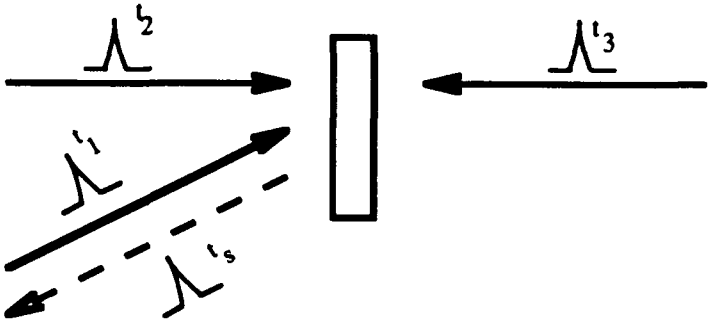

Figure 10. Experimental configuration for stimulated photon echo and transient four-wave mixing studies.

The pulse sequence for emission in the direction of the dotted line is given by t_1 followed by t_2 followed by t_3 (specific for inhomogeneous broadening due to random crystal fields, and different than the time sequence for inhomogeneous broadening due to velocity). If the medium is homogeneously broadened, the signal emission is prompt with respect to the third pulse as shown in Fig. 11a, and is called a free polarization decay signal. However, if the resonant

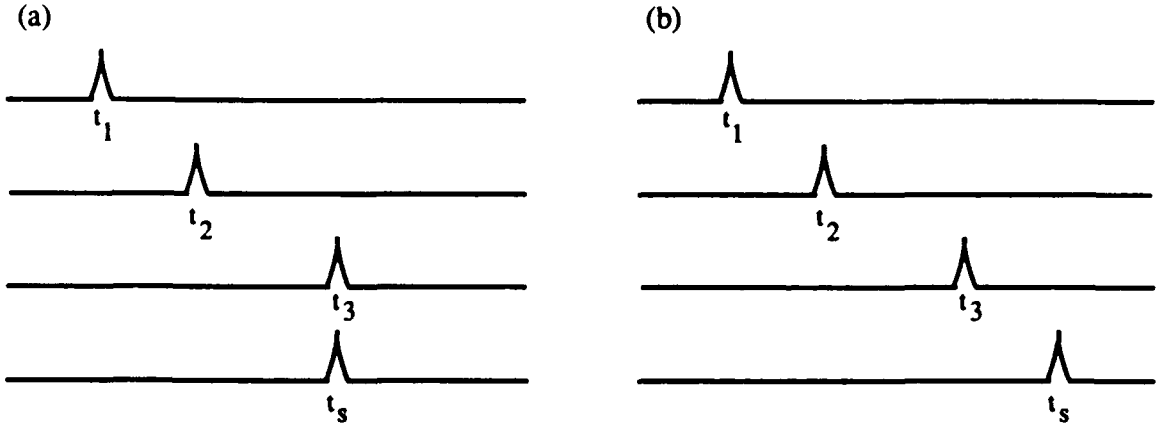

Figure 11. (a) The signal is coincident with t_3 for a homogeneously broadened system and is called a free polarization decay signal (b). If the resonant system is inhomogeneously broadened, the signal emission is delayed by an amount given by $t_2 - t_1$ and is called a stimulated photon echo.

system is inhomogeneously broadened, then the signal is delayed with respect to the third pulse by an amount given by $t_2 - t_1$, as shown in Fig. 11b, and is called a stimulated photon echo. The stimulated photon echo becomes nearly identical to an ordinary two pulse photon echo in the limit $t_3 - t_2 = 0$. In the usual way with picosecond laser systems, the signal is integrated in a detector. Determination of whether the signal is a photon echo or a free polarization signal is determined indirectly by looking at the symmetry of the scattered amplitude with respect to $t_2 - t_1 = 0$ [41]. In measurements presented below, however, we present the first time resolved measurements of the stimulated photon echo in GaAs quantum wells and show that in many cases of interest the temporal structure of the output is considerably more complicated for excitons. The results demonstrate the importance of time resolving the emission in these experiments.

Initial experiments in the time domain gave results at considerable variance with the cw measurements discussed above. Time scales for relaxation were considerably faster. However, we determined that all of the time scales were exciton density dependent, even at densities as low as 5×10^8 excitons/cm^2/layer, compared to densities in the cw experiments of order 10^7 excitons/cm^2/layer or less. Experiments with picosecond lasers at this low density required considerable improvements in noise reduction. After reducing scatter and improving signal processing techniques, we succeeded in operating at very low exciton densities and achieving the longer time scales observed in the cw measurements.

In the first measurements we compared the dephasing rate to the excitation decay rate as a function of both excitation wavelength and temperature. The results are shown in Fig. 12.

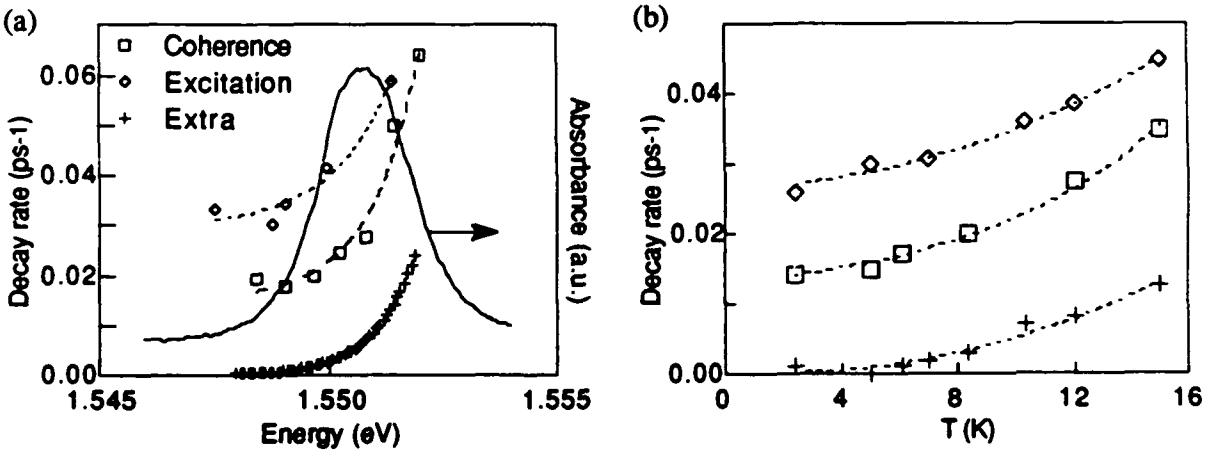

Figure 12. Measurement of the photon energy and temperature dependence of the dephasing rate (coherence, squares) and excitation decay rate (diamonds) measured by the stimulated photon echo at low excitation density. The crosses represent possible evidence of extra dephasing and come from difference between the measured dephasing rate and one half the excitation decay rate.

The measurements are very distinctive. First we note that at low energy and low temperature, the dephasing rate is half the excitation rate, exactly what is expected in the absence of pure dephasing by elastic scattering. At higher temperature and energy, we note both rates increase. As we show below, this is due to phonon assisted tunneling and thermal activation, as anticipated earlier. However, we also note that the difference between the dephasing rate and the excitation rate is not a constant, but increases as a function of both energy and temperature. One possible explanation of this is the presence of an elastic scattering component in the exciton dephasing. Since the scattering is elastic and temperature dependent, it is clearly a *higher order* phonon process. The scattering at low temperature is clearly due to phonon assisted tunneling by localized excitons. An Arrhenius plot of the excitation decay rate is shown in Figure 13 along

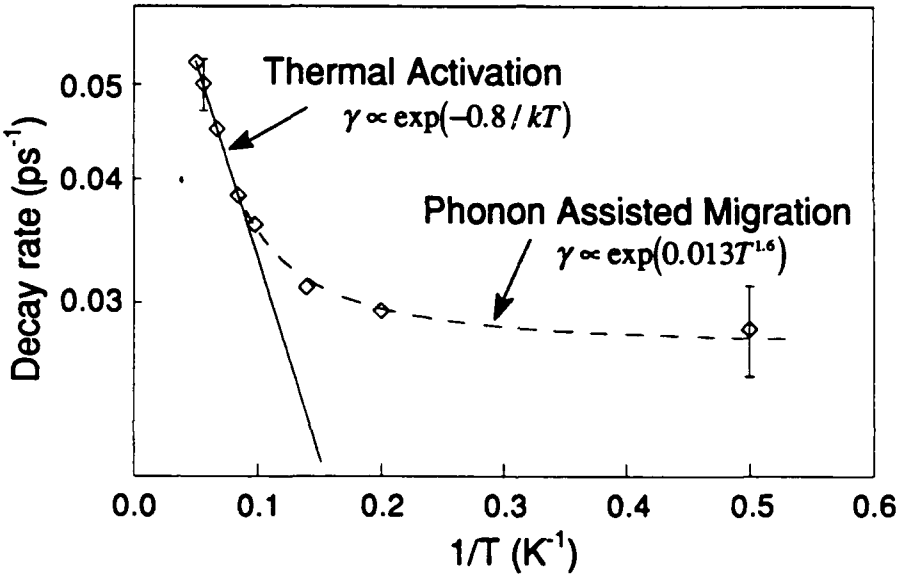

Figure. 13. Measurement of the excitation decay rate as a function of temperature. The low temperature region of the curve is fit by the phonon assisted tunneling model while the higher temperature region if fit by thermal activation

with a plot of the recent theoretical predictions for excitation decay by Takagahara [10]. At higher temperatures, the decay is dominated by thermal activation to quasi-delocalized states. At lower temperatures, phonon assisted tunneling between different localization sites dominates the decay rate. The data in Fig. 6 showed clear evidence for spectrally diffused excitons. The data in Fig. 13 confirms the mechanism of spectral diffusion. Particularly convincing for the phonon assisted migration model proposed by Takagahara is the unique temperature dependence for the spectral diffusion rate at the lowest temperatures given by $\beta\exp(\alpha T^{1.6})$ where α is a positive number. The dashed line in the Fig. 13 is a fit of this function. At higher temperatures the decay

rate is determined by thermal activation and shows an activation energy corresponding to the difference between absorption line center and the photon excitation energy.

In the above experiments, we directly confirmed that the signal was indeed an echo, as expected by comparison of the long dephasing time shown in Fig. 12 to the absorption line width. To confirm this and determine directly the magnitude of inhomogeneous broadening, we time resolved the echo by frequency up conversion with a reference beam from the laser. This is particularly challenging, given the low exciton densities we are using. The results are shown in Fig. 14. The data clearly shows the signal is a pure echo, where the delay is given by

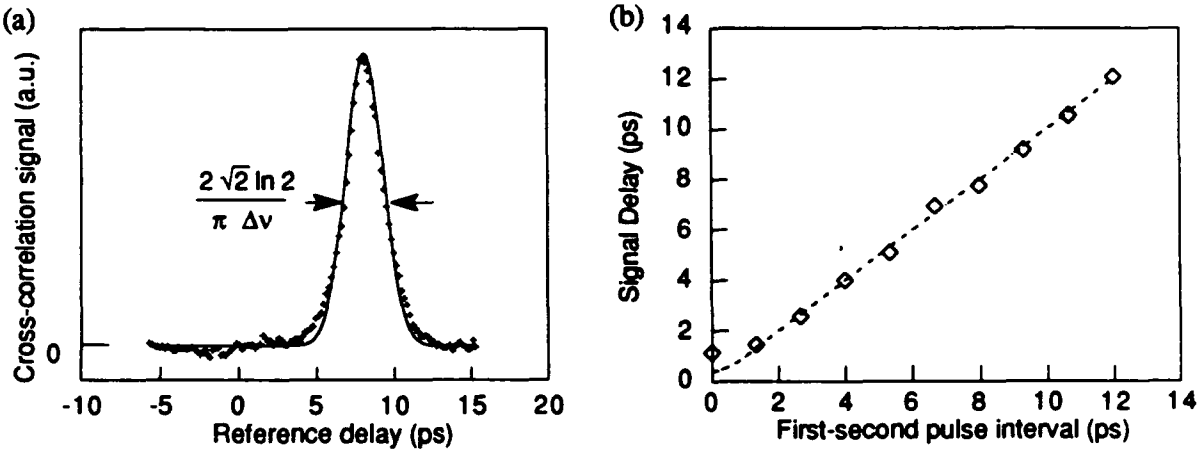

Figure 14. (a) Time resolved emission of the stimulated photon echo and (b) measurement of the echo delay as a function of the time difference between the first and second pulses. The solid line in (a) is a numerical fit of the calculated echo time dependence, including finite pulse width effects. The fit enables us to directly determine the inhomogeneous width.

the time between the first and second pulse except at short time due to finite pulse effects (the solid line is an exact numerical calculation). The width of the SPE emission is given by the inhomogeneous width. In this experiment, it is in good agreement with the absorption width.

At higher excitation densities (typically above 10^9 excitons/cm^2/layer), we find the overall dynamical behavior in the time integrated stimulated photon echo studies is considerably more complex, with both excitation and dephasing decay rates becoming multiexponential. The origin of this behavior is partially resolved by time resolving the emission. Figure 15 shows the complex emission associated with the three pulse experiment. Recalling the timing sequences of Fig. 11, we see that the emission is comprised of two pulses. The first pulse is not present in Fig. 11 and is *coincident with the third pulse* and is called a free polarization decay emission. The second pulse is delayed and corresponds to the stimulated photon echo. Measurements of the spectral dependence of the free polarization signal show that it is nearly identical to the measured

spectral dependence of the stimulated photon echo. The data shows that indeed, the optical response arises from two different kinds of resonances: the echo is from an inhomogeneously broadened resonance while the free polarization decay is from a homogeneously broadened resonance as seen by comparison with Fig. 11. Such a response is obtained in an analytical development if the distribution is the sum of an inhomogeneous function such as a Gaussian and

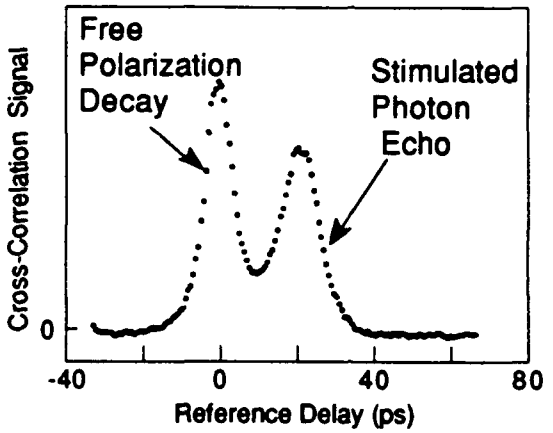

Figure 15. Measurement of the time resolved emission in the time separated transient four-wave mixing experiment at higher excitation density (>10^9 excitons/cm^2/layer). Temporal evolution was obtained by cross correlating the signal with a reference pulse. The emission shows the echo seen in Figure 14 but also shows the presence of a prompt free polarization decay signal.

a Dirac delta function located at some specific frequency:

$$P^{(3)} = \int d\omega_o P^{(3)}(\omega_o)\left[f(\omega_o) + \beta\delta(\omega_o - \Omega_o)\right]$$

This conclusion is further verified by the experimental determination that compared to the echo, the prompt signal is characterized by faster (intensity independent) excitation and dephasing decay rates as well as different excitation saturation parameters. One possible explanation for this behavior is that the density of localization sites is spatially inhomogeneous, resulting in regions of higher exciton density and possible strong exciton-exciton interactions that cause an increased dephasing rate. However, we have new results described in the attached preprint reporting studies of the polarization dependence that suggest that this behavior may be the result of a contribution to the signal from both localized and delocalized excitons.

In summary, our measurements show that not only is the nonlinear response highly complex, but that studies of the nonlinear response provide considerable new insight into fundamental physics associated with these systems. As we show in the reprints, these

experiments have led to the observation of the unexpected polarization properties of the time separated transient four-wave mixing measurements as well as enabled us to move into new areas including the first studies of high resolution nonlinear spectroscopy of magnetoexcitons and Landau resonances observed in a strong magnetic field.

IIB. Published Paper Summary and Educational Activity

Journal Papers

J.T. Remillard, H. Wang, D.G. Steel, J. Oh, J. Pamulapati, and P.K. Bhattacharya, "High Resolution Nonlinear Laser Spectroscopy of the Heavy Hole Exciton in a GaAs/AlGaAs Quantum Well Structure: A Direct Measure of the Exciton Line shape," Phys. Rev. Lett. **62**, pp. 2861-2864 (1989).

H. Wang, M. Jiang, D. G. Steel, "Measurement of phonon assisted migration of localized excitons in GaAs/AlGaAs multiple quantum well structures," Phys. Rev. Lett. **65**, pp1255-1258 (1990).

D.G. Steel, H. Wang, J.T. Remillard, M. Jiang, "High resolution nonlinear laser spectroscopy measurements of exciton dynamics in GaAs quantum well structures," invited paper, in *Laser Optics of Condensed Matter*, Vol. 2, E. Garmire, Alexei A. Maradudin, Karl K. Rebane, eds., Plenum Press (1991), pp265-271. Presented at the Fourth US-USSR Binational Symposium, Irvine, January, 1990

Hailin Wang, J.T. Remillard, M.D. Webb, and D.G. Steel, "High Resolution Laser Spectroscopy of Relaxation and the Excitation Line Shape of Excitons in GaAs Quantum Well Structures," Surf. Sci. 228 pp69-73 (1990).

M.D. Webb, S.T. Cundiff, D.G. Steel, "Stimulated Photon Echoes and Free Polarization Decay Signals in GaAs Quantum Wells: Evidence for Localized and Delocalized Excitons" Ultrafast Phenomena VII, pp. 233-235, C.B. Harris, E.P. Ippen, G.A. Mourou, and A.H. Zewail, eds. (Springer-Verlag, Berlin 1990).

M.D. Webb, S.T. Cundiff, D.G. Steel, "Observation of time-resolved stimulated photon echoes and free polarization decay in GaAs/AlGaAs multiple quantum wells," Phys. Rev. Let. **66**, 934 (1991).

Hailin Wang and Duncan G. Steel, "High resolution laser spectroscopy of exciton relaxation in GaAs quantum wells," invited paper, Applied Physics A, Solids and Surfaces **53**, pp 514-544 (1991).

D.G. Steel and J. Shah, "Coherent transient optical phenomena in semiconductors," Opt. Phot. **2**, pp 25-26 (1991).

M. D. Webb, S. T. Cundiff, D. G. Steel, "Stimulated Picosecond Photon Echo Studies of Localized Exciton Relaxation due to Phonon Assisted Migration and Thermal Activation in GaAs/AlGaAs Multiple Quantum Wells, " Phys. Rev. B **43**, 12658 (1991).

S.T. Cundiff, H. Wang, D.G. Steel, "Picosecond Excitonic Optical Nonlinearities: A Probe for the Complexities of Disorder", to be published, Phys. Rev. B. (1992).

S.T. Cundiff, H. Wang, D.G. Steel, "Coherent transient spectroscopy of excitons in GaAs/AlGaAs quantum wells," invited paper, to be published IEEE J. Quan. Elec. (1992).

H. Wang, M. Jiang, D.G. Steel, "Spin Flip Induced Hole Burning in Quantum Wells," Phys. Rev. Lett. **69**,, 804 (1992).

D.G. Steel, H. Wang, S.T. Cundiff "Four-wave mixing in quantum well systems," invited chapter in *Optics of Semiconductor Nanostructures*, Fritz Henneberger and Stefan Schmitt-Rink, eds (VCH-Germany, 1992).

S.T. Cundiff and D.G. Steel, "Excitonic picosecond coherence effects in the presence of disorder," Ultrafast Phenomena VIII, 1992.

D. G. Steel, S. T. Cundiff and H. Wang, "Coherent Nonlinear Laser Spectroscopy of Excitons in Quantum Wells," to be published in Proceedings of NATO ARW in Frontiers in Optical Phenomena in Semiconductors of Reduced Dimensions.

Invited papers

D.G. Steel, "High Resolution Spectroscopy and Photon Echoes in GaAs Quantum Wells," invited paper at the APS March Meeting, Bull. Am. Phys. Soc. **36**, p338 (1991).

D. G. Steel, J. T. Remillard, Hailin Wang, M. D. Webb, J. Oh, J. Pamulapati, and P. K. Bhattacharya, "High Resolution Nonlinear Laser Spectroscopy of GaAs/AlGaAs Multiple Quantum Wells," OSA Topical Meeting on Quantum Wells for Optics and Optoelectronics, OSA Tech. Dig. **10**, pp. 62-65 (1989).

D. G. Steel, P. K. Bhattacharya, J. T. Remillard Hailin Wang, M. D. Webb, J. Pamulapati, J. Oh, "High Resolution Nonlinear Laser Spectroscopy of Excitons in GaAs Quantum Well Structures," Quantum Electronics and Laser Science Conference (QELS/CLEO '89), OSA Tech. Dig. **12**, pp. 4-7 (1989).

D. G. Steel, J. T. Remillard, H. Wang, and M. D. Webb, "Application of Four-Wave Mixing Spectroscopy to Semiconductor Material Studies," Conference on Lasers and Electro-Optics, Technical Digest Series **7**, pp. 260-261 (1988).

D. G. Steel, Hailin Wang, J. T. Remillard, M. D. Webb, J. Pamulapati, J. Oh, P. K. Bhattacharya, "High Resolution Nonlinear Laser Spectroscopy of Excitons in GaAs/AlGaAs Mulitple Quantum Well Structures", in Laser Spectroscopy IX, (Academic Press 1989).

H. Wang, J. T. Remillard, M. Jiang, M. D. Webb, D. G. Steel, "Frequency Domain Nonlinear Optical Studies of Multiple Quantum Well Structures," Proceedings of SPIE Symposium on Opto Electronics, Conference 1216 (1990)).

D. G. Steel, H. Wang, J. T. Remillard, M. Jiang, "Application of Frequency Domain High Resolution Nonlinear Laser Spectroscopy to the Study of Excitons in GaAs/AlGaAs Quantum Well Structures," presented at the Fourth US-USSR Binational Symposium, Irvine, CA, 1990 (see above citation).

D.G. Steel, H. Wang, S.T. Cundiff, M. Jiang, "Coherent Nonlinear Spectroscopy of Excitons in GaAs/AlGaAs Mulitple Quantum Wells", Conference on Lasers and Electro-Optics, CLEO '91, Technical Digest Series **10**, pp308-309 (1991)

D.G. Steel, "High Resolution Spectroscopy and Photon Echoes in GaAs Quantum Wells," invited paper at the APS March Meeting, Bull. Am. Phys. Soc. **36**, p338 (1991).

D.G. Steel, H. Wang, S.T. Cundiff, M. Jiang, "Nonlinear Optics and Spectroscopy in Systems with Reduced Dimensionality," Nonlinear Optics Gordon Conference, (1991).

D. G. Steel, H. Wang, S. T. Cundiff, M. Jiang, "Nonlinear Spectroscopy of Excitons: A Probe of Disorder," ILS Symposium on "Frontiers in Laser-Condensed Matter Interaction," (1992).

Refereed Contributed Conference Presentations with Published Proceedings

H. Wang, J. T. Remillard, D. G. Steel, J. Oh, J. Pamulapati, and P. K. Bhattacharya, "High Resolution Laser Spectroscopy of Relaxation and the Excitation Line Shape of Excitons at Low Temperature in GaAs Quantum Well Structures," in the Proceedings of 4th International Conference on Modulated Semiconductor Structures, 1989 (see above citation to Surf. Sci.).

H. Wang, J. T. Remillard, M. D. Webb, and D. G. Steel, "High Resolution Nonlinear Laser Spectroscopy and Efficient Optical Phase Conjugation in Semiconductor Microcrystallite Doped Glasses," Conference on Lasers and Electrooptics (CLEO '89), OSA Tech. Dig. **11**, pp. 156-157 (1989).

H. Wang, J.T. Remillard, M Jiang, and D.G. Steel, "Precision Nonlinear Laser Spectroscopy of Exciton Dynamics in GaAs/AlGaAs Multiple Quantum Well Structures," Nonlinear Optics, NLO'90, IEEE, p121 (1990).

D.G. Steel, H. Wang, J.T. Remillard, M. Jiang, "Application of Frequency Domain High Resolution Nonlinear Laser Spectroscopy to the Study of Excitons in GaAs/AlGaAs Quantum Well Structures," invited paper to be published in the Fourth US-USSR Binational Symposium, Plenum Press (1990). Presented at Irvine, January, 1990 (see above citation).

H. Wang, J.T. Remillard, M. Jiang, M.D. Webb, D.G. Steel, "Frequency Domain Nonlinear Optical Studies of Multiple Quantum Well Structures," invited paper, Proceedings of SPIE Symposium on Nonlinear Optical Materials and Devices for Photonic Switching 1216, pp206-214 (1990).

M.D. Webb, S. Cundiff, D.G. Steel, "Stimulated Photon Echoes (SPE) and Free Polarization Decay (FPD) in Time Resolved Four-Wave Mixing Spectroscopy of HH1 Excitons in GaAs/AlGaAs Multiple Quantum Well (MQW) Structures at 5K," International Quantum Electronics Conference (IQEC '90) Technical Digest **8**, pp102-103 (1990).

H. Wang, M. Jiang, D.G. Steel, J.E. Cunningham, "Studies of Exciton Recombination and Transport in High Purity GaAs Using High Resolution Nonlinear Spectroscopy," International Quantum Electronics Conference (IQEC '90), Technical Digest **8**, pp310-311 (1990).

H. Wang, M. Jiang, and D.G. Steel, "High Resolution nonlinear spectroscopy studies of the dynamics of localized excitons in GaAs/AlGaAs quantum wells," International Quantum Electronics Conference (IQEC '90), Technical Digest **8**, pp60-61 (1990).

Ming Jiang, Hailin Wang, D.G. Steel, "Anomalous Nonlinear Optical Processes in GaAs/AlGaAs Quantum Wells," Quantum Electronics and Laser Science (QELS'91), Technical Digest Series **11**, pp252-253 (1991).

S.T. Cundiff, M.D. Webb, D.G. Steel, "Measurement of picosecond excitation relaxation and dephasing of localized excitons in GaAs/AlGaAs Mulitple Quantum Wells," Quantum Electronics and Laser Science (QELS'91), Technical Digest Series **11**, pp200-201 (1991).

D.G. Steel, S.T. Cundiff, M. Jiang, Hailin Wang, M.D. Webb, "Coherent Nonlinear Laser Spectroscopy Studies of Exciton Relaxation, Dephasing and Energy Transport in GaAs Quantum Wells", Quantum Optoelectronics, OSA Technical Digest, **7** (1991).

S.T. Cundiff, V. Subramaniam, H. Wang, D.G. Steel, "Coupling between excitonic magnetic substates in GaAs multiple quantum wells," QELS'92, OSA Technical Digest **13**, 218-219 (1992).

S.T. Cundiff, H. Wang, D.G. Steel, "Picosecond photon echoes and free polarization decay from localized and delocalized statein GaAs quantum wells," QELS'92, OSA Technical Digest **13**, 34-35 (1992).

H. Wang, M. Jiang, R. Merlin, D.G. Steel, "Spin-flip induced spectral hole burning of magnetoexcitons in GaAs/AlGaAs quantum wells", QELS'92, OSA Technical Digest **13**, 36-37 (1992)

M. Jiang, H. Wang, R. Merlin, D.G. Steel, "High resolution spectroscopic measurements of magneto-excitons in thin film GaAs," QELS'92, OSA Technical Digest **13**, 214-215 (1992).

S.T. Cundiff and D.G. Steel, "Excitonic picosecond coherence effects in the presence of disorder," Ultrafast Phenomena VIII, 1992.

S.T. Cundiff and D.G. Steel., "Polarization dependent coherent nonlinear spectroscopy: A probe of exciton localization in quantum wells," XVIII International Quantum Electronics Conference, Technical Digest **9**, p30-32 (1992).

Conference Papers

H. Wang, M. Jiang, R. Merlin, D.G. Steel, "Spin-flip induced spectral hole burning of magnetoexcitons in GaAs/AlGaAs quantum wells," APS March Meeting, APS Bull. **37**, p 708 (1992).

Educational Activity

Four students have received their Ph.D. through support of this program and a fifth student will receive the Ph. D. in Fall of 1992. Three other students are currently being supported by this program as well as the laboratory and instructional support for one NSF predoctoral fellow. In addition, this program has made possible the continuing involvement of undergraduates in this laboratory. We have had five undergraduates involved in this work at different times. We have weekly group meetings where all students make presentations of their progress followed by technical discussions of the research activity.

REFERENCES

[1] J. Feldmann, G. Peter, E.O. Göbel, P. Dawson, K. Moore, C. Foxon, and R.J. Elliott, Phys. Rev. Lett. **59**, 2337 (1987).

[2] B. Deveaud, F. Clerot, N. Roy, K. Satski, B. Sermage, and D.S. Katzer, Phys. Rev. Lett. **67**, 2355 (1991).

[3] L. Schultheis, A. Honold, J. Kuhl, K. Kohler, and C.W. Tu, Phys. Rev. B **34**, 9027 (1986).

[4] C. Weisbuch, R. Dingle, A.C. Gossard, and W. Wiegmann, Solid State Comm. **38**, 709 (1981).

[5] B. Deveaud, A. Regreny, J.-Y. Emery, and A. Chomette, J. Appl. Phys. **59**, 1633 (1986).

[6] A. Ourmazd, D.W. Taylor, J. Cunningham, and C.W. Tu, Phys. Rev. Lett. **62**, 933 (1989).

[7] B. Deveaud, B. Guenais, A. Poudoulec, and A. Regreny, Phys. Rev. Lett. **65**, 2317 (1990).

[8] A. Ourmazd and J. Cunningham, Phys. Rev. Lett **65**, 2318 (1990).

[9] D. Gammon, B.V. Shanabrook, and D.S. Katzer, Phys. Rev. Lett. **67**, 1547 (1991).

[10] T. Takagahara, Phys. Rev. B **31**, 6552 (1985).

[11] T. Takagahara, Jr. Lumin. **44**, 347 (1989).

[12] P.A. Lee and T.V. Ramakrishnan, Rev. Mod. Phys. **57**, 287 (1985).

[13] N.F. Mott, Adv. Phys. **16**, 49 (1967).

[14] N.F. Mott and E.A. Davis, *Electronic Processes in Non-Crystalline Materials*, 2nd ed. (Clarendon Press, Oxford, 1979).

[15] D.G. Steel and J.T. Remillard, Phys. Rev. A **36**, 4330 (1987).

[16] H. Wang and D.G. Steel, Phys. Rev. A **43**, 3823 (1991).

[17] P.R. Berman, J. Opt. Soc. Am. B. **3**, 564 (1986).

[18] P.R. Berman, Phys. Rep. **43**, 101 (1978).

[19] D.L. Dexter, J. Chem. Phys. **21**, 836 (1953).

[20] T.F. Soules and C.B. Duke, Phys. Rev. B **3**, 262 (1971).

[21] S. Schmitt-Rink, D.A.B. Miller, and D.S. Chemla, Phys. Rev. B **35**, 8113 (1987).

[22] M. Lindberg and S.W. Koch, Phys. Rev. B **38**, 3342 (1988).

[23] P.R. Berman and R.G. Brewer, Phys. Rev. A **32**, 2784 (1985).

[24] J.T. Remillard, H. Wang, M.D. Webb, D.G. Steel, J. Oh, J. Pamulapati, and P.K. Bhattacharya, Opt. Lett. **14**, 1131 (1989).

[25] H. Wang, M. Jiang, and D.G. Steel, Phys. Rev. Lett. **65**, 1255 (1990).

[26] J. Hegarty and M.D. Sturge, J. Opt. Soc. Am. B **2**, 1143 (1985).

[27] M. Shinada and K. Tanaka, J. Phys. Soc. Jpn **29**, 1258 (1970).

[28] M. Potemski, J.C. Maan, A. Fasolino, K. Ploog, and G. Weimann, Phys. Rev. Lett. **63**, 2409 (1989).

[29] M.J. Snelling, E. Blackwood, C.J. McDonagh, and R.T. Harley, Phys. Rev. B **45**, 3922 (1992).

[30] S.G. Elkomoss and G. Munschy, J. Phys. Chem. Solids **42**, 1 (1981).

[31] S. Bar-Ad and I. Bar-Joseph, Phys. Rev. Lett. **66**, 2491 (1991).

[32] H. Wang, M. Jiang, R. Merlin, and D.G. Steel, Phys. Rev. Lett. **69**, 804 (1992).

[33] M. Dobers, K. Klitzing, and G. Weimann, Phys. Rev. B **38**, 5453 (1988).

[34] B. Bimberg, Advan. in Solid State Phys. **XVIII**, 195 (1977).

[35] G.E.W. Bauer and T. Ando, Phys. Rev. B **37**, 3130 (1988).

[36] G.E.W. Bauer, High Magnetic Fields in Semiconductor Physics II, G. Landwehr, Ed. , Springer-Verlag (Berlin) 240 (1989).

[37] G. Lommer, F. Malcher, and U. Rossler, Phys. Rev. B **32**, 6965 (1985).

[38] A.M. White, I. Hinchliffe, and P.J. Dean, Solid State Commun. **10**, 497 (1972).

[39] T.W. Mossberg, R. Kachru, and S.R. Hartmann, Phys. Rev. A **20**, 1976 (1979).

[40] G. Noll, U. Siegner, S.G. Shevel, and E.O. Göbel, Phys. Rev. Lett. **64**, 792 (1990).

[41] A.M. Weiner, S. De Silvestri, and E.P. Ippen, J. Opt. Soc. Am. B. **2**, 654 (1985).

Spin-Flip-Induced Hole Burning in GaAs Quantum Wells: Determination of the Exciton Zeeman Splitting

H. Wang, M. Jiang, R. Merlin, and D. G. Steel

Harrison M. Randall Laboratory of Physics, The University of Michigan, Ann Arbor, Michigan 48109-1120

(Received 18 February 1992)

A new method of four-wave-mixing spectroscopy in GaAs quantum wells reveals spectral hole burning due to spin relaxation of magnetoexcitons. The measurements resolve the Zeeman doublet of the lowest-energy heavy-hole exciton where the doublet splitting is much less than the exciton inhomogeneous width. The Zeeman splitting depends nonlinearly on the magnetic field and is small compared with that of bulk GaAs. The results reflect effects of the complex band structure of quantum wells. Information on exciton spin relaxation is also provided by the hole-burning measurements.

PACS numbers: 71.35.+z, 71.70.Ej, 73.20.Dx, 78.65.Fa

The electronic energy spectrum of quantum well structures is fully quantized under a magnetic field parallel to the growth axis. Optical absorption reveals a ladder of magnetoexcitons corresponding to transitions between electron and hole Landau levels [1]. Magnetic fields also lift the Kramers degeneracy with the resultant Zeeman splitting depending on details of the band structure. The removal of this degeneracy is also expected to lead to a substantial increase of the spin relaxation time between Zeeman-split Landau levels since now spin relaxation can only take place via inelastic processes.

The electron g factor in GaAs heterostructures has been extensively studied. Earlier magnetotransport measurements have shown large exchange-induced enhancement of the electron g [2]. Recent electron-spin-resonance studies have revealed the magnetic field dependence of the electron g for different Landau levels [3]. These results were explained in terms of the nonparabolicity of the conduction band [4]. Determination of the exciton Zeeman splitting has proven to be more elusive [5–7]. Earlier magnetoreflectance measurements were able to resolve Zeeman splittings for the light-hole but not the heavy-hole exciton [5]. More recent measurements have inferred the exciton g from nonlinear quantum-beat spectroscopy [6]. A precise determination of the exciton Zeeman splitting in a quantum well using linear optical spectroscopy is difficult since interface disorder leads to exciton localization and subsequent inhomogeneous broadening of the absorption profile [8]; the resultant inhomogeneous broadening varies from 1 meV to several meV, much larger than the splitting in moderate fields.

A related area is relaxation of carrier and exciton spins in semiconductor heterostructures. Polarization-dependent measurements of interband optical transitions have shown an interesting dependence of spin relaxation on growth conditions, carrier confinement, and temperature [9]. Various physical mechanisms for spin relaxation have also been discussed [9,10]. In addition, luminescence measurements at high magnetic fields have revealed a much larger spin relaxation time due to the full quantization of the energy spectrum [11].

In this paper, we report frequency-domain nonlinear optical studies of exciton Zeeman splitting and spin relaxation in GaAs quantum wells. Using selective optical excitation and nonlinear optical methods similar to spectral hole burning (SHB, also referred to as saturation spectroscopy or differential transmission), we are able to probe spin relaxation of magnetoexcitons and measure directly their Zeeman splitting. The measurements reveal a heavy-hole splitting much smaller than that reported for bulk GaAs at low magnetic field and show a nonlinear dependence of the splitting on magnetic field strength. The results reflect effects of the complex band structure of a quantum well.

Nonlinear optical methods such as SHB have the advantage of being able to eliminate inhomogeneous broadening and accurately measure small energy separations as shown in precision measurements in atomic vapors [12]. For GaAs/AlGaAs quantum wells, a nearly monochromatic optical beam with σ_- circular polarization can be used to excite a narrow spectral hole (say at energy E_- within the inhomogeneous absorption profile) of the lowest heavy-hole (HH1) exciton associated with the $\frac{1}{2}$ to $\frac{1}{2}$ transition (see the inset in Fig. 1 for the energy-level diagram in a magnetic field). The width of the spectral hole is determined by the homogeneous linewidth. Spin flips of electrons and holes associated with these excitons generate a spectral hole at the energy of the $-\frac{1}{2}$ to $-\frac{1}{2}$ exciton transition, designated E_+. The *spin-flip-induced* SHB at E_+ results from the reduced absorption due to the presence of carriers that have flipped their spins from E_-. This SHB can be probed using an optical beam with σ_+ circular polarization. Zeeman splitting can then be obtained by measuring the energy spacing between the spin-flip-induced SHB and the original SHB resonance.

In practice the measurements proposed above are complicated by strong spectral diffusion of the localized excitons. Once created, localized excitons migrate rapidly among localization sites with different energies leading to *a broad quasiequilibrium distribution in energy* as we demonstrated earlier using four-wave mixing [13]. In the normal SHB measurement discussed above, the nonlinear

© 1992 The American Physical Society

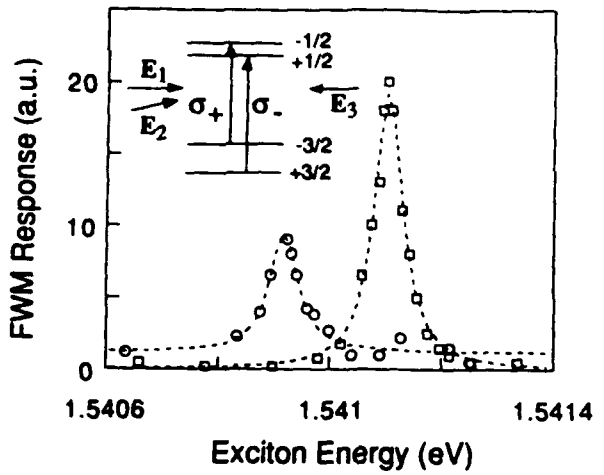

FIG. 1. Hole-burning FWM responses at 4 T. All three beams are circularly polarized with E_1 and E_2 exciting the $\sigma-$ exciton. Squares represent the response when the probe beam E_3 interacts with the $\sigma-$ exciton. Circles represent the response when E_3 interacts with the $\sigma+$ exciton. Dashed lines are Lorentzian fits to the response. Inset: Conduction-band and heavy-hole valence-band energy levels in a GaAs quantum well for a magnetic field parallel to the growth axis.

optical signal may be dominated by this distribution. In the limit that the spin relaxation time is long compared with the spectral diffusion time, nearly all spin-flipped excitons have diffused in energy. Hence, the spin-flip-induced SHB resonance will be overwhelmed by the spectral diffusion process.

To avoid the above complications, we have used a new method of SHB based on nearly degenerate four-wave mixing (FWM) [14,15]. This method can significantly reduce the contribution of the quasiequilibrium exciton distribution to the nonlinear optical response and, hence, allows us to recover the spin-flip-induced SHB resonance. The experimental configuration is based on backward FWM and uses three optical beams. Two nearly degenerate beams designated $E_1(\omega_1,\mathbf{k}_1)$ and $E_2(\omega_2,\mathbf{k}_2)$ interact in the sample with a third probing beam designated $E_3(\omega_3,\mathbf{k}_3)$. The SHB response is obtained by measuring the backward FWM signal (propagating in a direction determined by $\mathbf{k}_1-\mathbf{k}_2+\mathbf{k}_3$) as a function of ω_3. Detailed analytical discussions of frequency-domain FWM spectroscopy have been presented elsewhere [14,15]; however, the underlying physics can be understood as follows: Nearly degenerate beams E_1 and E_2 interfere in the sample to excite a traveling-wave grating which oscillates at a frequency equal to the detuning between the two beams $\delta=|\omega_1-\omega_2|$ ($\ll$homogeneous linewidth). The grating is a spatially modulated pattern of spectral hole burning at ω_1 ($\approx\omega_2$) with amplitude proportional to $(\delta+i\gamma)^{-1}$, where γ is the grating decay rate determined by relaxation and spatial transport of excitons. Measuring the FWM signal as a function of ω_3 probes the spectral profile of the grating within the inhomogeneous profile. In the absence of spectral diffusion, the *spectral* width of the grating is given by the exciton homogeneous linewidth as expected from SHB, and the width of the FWM response is twice the homogeneous linewidth [15]. Note that although both FWM and the traditional SHB (i.e., differential transmission) signals result from the induced nonlinear optical polarization, the FWM signal includes contributions from both the real and the imaginary part of the nonlinear susceptibility while the traditional SHB measures only the imaginary part [12].

In the presence of spectral diffusion, the spectral hole excited by $E_1\cdot E_2^*$ diffuses in energy resulting in a spectral redistribution of the excitation. In this case, the FWM response arises from both the spectral hole and the quasiequilibrium distribution of the exciton population as discussed above. The decay of the SHB population is determined by the sum of the exciton spectral diffusion, spin relaxation, and recombination rates. However, the lifetime of the quasiequilibrium distribution is determined by the *recombination time of the exciton* [13]. In the limit that the spectral diffusion rate is much larger than the rate for exciton recombination, setting δ large compared with the recombination rate (but still smaller than or comparable with the spectral diffusion rate) significantly decreases the relative amplitude of the grating associated with the quasiequilibrium distribution. Hence, the FWM response will be dominated by the SHB resonance [14].

The quantum well samples used in our measurements consist of ten periods of 100-Å GaAs wells and 100-Å $Al_{0.3}Ga_{0.7}As$ barriers, grown at 750 °C by molecular-beam epitaxy on semi-insulating (100) GaAs substrates using interrupted growth. The structures show a 1-meV absorption linewidth with a Stokes shift of the luminescence of order 0.3 meV for the HH1 exciton. The nonlinear measurements were carried out at 2.5 K using a split-coil superconducting magnet. δ was set at 140 MHz using two acousto-optic modulators. The exciton density was of order $10^7/cm^2$.

In the first set of measurements, we used three circularly polarized optical beams rotating in the same direction in the laboratory frame. The nonlinear optical response, shown as squares in Fig. 1, involves only the $\sigma-$ excitons associated with the $\frac{1}{2}$ to $\frac{1}{2}$ transition. The width of the response corresponds to a homogeneous linewidth of 0.03 meV. The small linewidth confirms the localized and inhomogeneous broadening nature of the magnetoexciton [8,13].

As discussed earlier, if electrons or holes associated with $\sigma-$ excitons created with $E_1\cdot E_2^*$ flip their spin at the same localization site, it will produce SHB at the energy of the $\sigma+$ exciton. Experimentally, spin-flip-induced SHB can be probed by reversing the polarization direction of E_3. The resulting resonance, shown as circles in Fig. 1, clearly shows narrow SHB at a lower energy with

the energy difference being the exciton Zeeman splitting: 0.19 meV at 4 T. The small signal at the original SHB position is most likely due to the residual ellipticity of the circularly polarized beams. The nearly constant background signal in the inset in Fig. 1 is due to excitons that have spectrally diffused. Nonlinear signals due to the spectrally diffused excitons overwhelm the spin-flip-induced SHB when $\delta = 0$. Note that spin relaxation of σ_+ excitons requires absorption of acoustic phonons and is slower than spin relaxation of σ_- excitons. The observed spin-flip-induced SHB is considerably weaker at 4 T when $\mathbf{E}_1 \cdot \mathbf{E}_2^*$ excites σ_+ excitons.

In further experiments, we used linearly polarized light for the third beam. With $\mathbf{E}_1 \cdot \mathbf{E}_2^*$ exciting only the σ_- excitons, we can simultaneously probe the SHB and the spin-flip-induced SHB resonance. The FWM response (Fig. 2) shows the well-resolved Zeeman doublet. Because of possible interference between the two resonances, the Zeeman splitting determined from Fig. 2 is less accurate than that from Fig. 1.

Recent measurements have shown that at low and intermediate magnetic field, the electron g factor at the lowest Landau level in GaAs quantum wells is close to the value for bulk GaAs [3,16]. In contrast, the Zeeman splitting of the HH1 exciton obtained above is very small in comparison with that reported for bulk GaAs [17]. Our results seem to be in agreement with the earlier magnetoreflectance measurements where the heavy-hole Zeeman doublet was not resolved. The small Zeeman splitting attributed to the strong valence-band mixing in quantum well structures has been recently predicted by numerical calculations of magnetoexcitons using the Luttinger Hamiltonian [18]. In particular, the mixing of σ_- excitons with excitons at higher energy pushes the σ_- exciton to lower energy. The above calculation also predicts an eventual sign change of the Zeeman splitting at higher magnetic fields where the band-mixing effects overcome those of the Zeeman interaction. However, theoretical determination of the magnetic field at which the zero crossing occurs is difficult since the cancellation of the two competing contributions depends strongly on parameters of the model [18]. The sign change of the splitting has not been observed in our measurements up to 6 T. It is interesting to note that disorder-induced localization is expected to enhance the band-mixing effects if the localization scale is smaller than the exciton Bohr radius. Using the recombination rate of the localized exciton, we have estimated the localization scale to be comparable to the exciton Bohr radius.

Figure 3 displays the magnetic field dependence of the Zeeman splitting for the HH1 exciton. The dashed line in the figure represents a quadratic dependence. Clearly the quadratic behavior may not extend into the high-field region. The observed field dependence is somewhat surprising since the calculations predict a field dependence slower than linear. The observed dependence may be due in part to the nonparabolicity of the conduction band [4], which was not included in the calculations. Note that our results differ considerably from those obtained from nonlinear quantum beats in a 30-Å stepwise GaAs quantum well [6]. Zeeman splittings reported in the quantum-beat measurement (0.5 meV at 4 T) are proportional to magnetic fields with a field strength ranging from 1 to 5 T, and are very close to those measured for impurity-bound excitons in bulk GaAs [19]. The sign of the Zeeman splitting cannot be determined in quantum-beat measurements.

The relative amplitude of the two SHB resonances shown in Fig. 2 is determined by the spin relaxation rates as well as the spectral diffusion rate of the exciton (assuming equal oscillator strengths). As expected, exciton spin relaxation rates decrease with increasing magnetic fields, resulting in a decrease in the relative peak height of the spin-flip-induced SHB. The ratio of σ_+ to σ_- exciton SHB amplitudes decreases approximately by a factor of 4 when the field increases from 2 to 6 T. Using a simple rate equation and a lifetime of 50 ps for the σ_+ exciton SHB (determined independently [20]), we are able to estimate an effective spin relaxation rate of 100 ps for the σ_- exciton at 4 T. The estimated spin relaxation

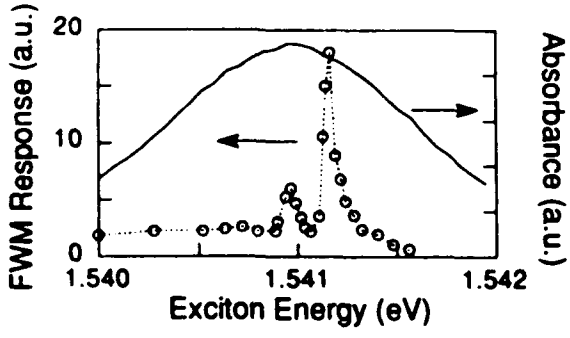

FIG. 2. FWM hole-burning response at 4 T with E_3 linearly polarized. E_1 and E_2 interact only with the σ_- exciton. The line shape shows the well-resolved Zeeman doublet. The solid line is the exciton absorption spectrum. The dotted line is a guide to the eye.

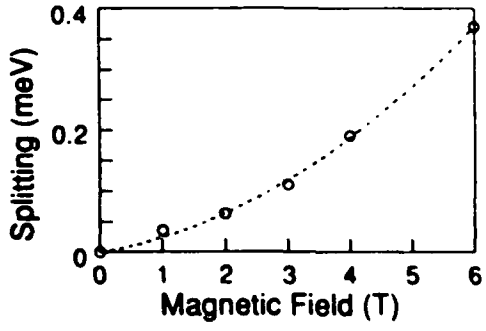

FIG. 3. Magnetic field dependence of the exciton Zeeman splitting. The dashed line is a least-squares fit with a quadratic dependence.

rate is smaller than the spectral diffusion rate, but is much larger than the rate for exciton recombination. Hence, most of the spectrally diffused $\sigma-$ excitons changed their spins before recombination, which explains the negligible nonlinear optical response from the spectrally diffused $\sigma-$ excitons in Fig. 1.

Finally, we note that although spin relaxation of magnetoexcitons in a quantum well is presumably an inelastic process, the relaxation may also proceed via an elastic process due to disorder-induced localization. A localized magnetoexciton with a specific spin orientation may have the same energy as magnetoexcitons at another localization site with different spin orientation. Strong resonant excitation transfer may occur between the two sites. The resonant transfer should depend strongly on the intersite distance as well as on the Zeeman splitting, providing a good probe for the interface disorder. In the SHB measurement, the resonant intersite transfer is characterized by a spin-flip-induced SHB resonance at the energy of the nearly degenerate E_1 and E_2 beams. However, conclusive evidence for the transfer has not been observed in samples used in our measurements.

This work was supported by the Army Research Office and the Air Force Office of Scientific Research.

[1] M. Shinada and K. Tanaka, J. Phys. Soc. Jpn. **29**, 1258 (1970).

[2] See, for example, Th. Englert and K. von Klitzing, Surf. Sci. **73**, 70 (1978); T. Ando and Y. Uemura, J. Phys. Soc. Jpn. **37**, 1044 (1974).

[3] D. Stein, K. von Klitzing, and G. Weimann, Phys. Rev. Lett. **51**, 130 (1983); M. Dobers, K. von Klitzing, and G. Weimann, Phys. Rev. B **38**, 5453 (1988).

[4] G. Lommer, F. Malcher, and U. Rossler, Phys. Rev. B **32**, 6965 (1985).

[5] P. Lefebvre, B. Gil, J. P. Lascaray, H. Mathieu, D. Bimberg, T. Fukunaga, and H. Nakashima, Phys. Rev. B **37**, 4171 (1988).

[6] S. Bar-Ad and I. Bar-Joseph, Phys. Rev. Lett. **66**, 2491 (1991).

[7] M. J. Snelling, E. Blackwood, C. J. McDonagh, R. T. Harley, and C. T. B. Foxon, Phys. Rev. B **45**, 3922 (1992).

[8] J. Hegarty and M. D. Sturge, J. Opt. Soc. Am. B **2**, 1143 (1985).

[9] M. Kohl, M. R. Freeman, D. D. Awschalom, and J. M. Hong, Phys. Rev. B **44**, 5923 (1991); T. C. Damen, Luis Vina, J. E. Cunningham, Jagdeep Shah, and L. J. Sham, Phys. Rev. Lett. **67**, 3432 (1991); T. C. Damen, Karl Leo, Jagdeep Shah, and J. E. Cunningham, Appl. Phys. Lett. **58**, 1902 (1991).

[10] T. Uenoyama and L. J. Sham, Phys. Rev. Lett. **64**, 3070 (1990); R. Ferreira and G. Bastard, Phys. Rev. B **43**, 9687 (1991).

[11] M. Potemski, J. C. Maan, A. Fasolino, K. Ploog, and G. Weimann, Phys. Rev. Lett. **63**, 2409 (1989).

[12] See, for example, Marc D. Levenson and Satoru S. Kano, *Introduction to Nonlinear Laser Spectroscopy* (Academic, Boston, 1988); S. Stenholm, *Foundations of Laser Spectroscopy* (Wiley, New York, 1984).

[13] H. Wang, M. Jiang, and D. G. Steel, Phys. Rev. Lett. **65**, 1255 (1990).

[14] Hailin Wang and Duncan G. Steel, Appl. Phys. A **53**, 514 (1991).

[15] D. G. Steel and J. T. Remillard, Phys. Rev. A **36**, 4330 (1987); Hailin Wang and Duncan G. Steel, Phys. Rev. A **43**, 3823 (1991).

[16] M. J. Snelling, G. P. Flinn, A. S. Plaut, R. T. Harley, A. C. Tropper, R. Eccleston, and C. C. Phillips, Phys. Rev. B **44**, 11345 (1991).

[17] See, for example, D. Bimberg, Adv. Solid State Phys. **18**, 195 (1977).

[18] G. E. W. Bauer, in *High Magnetic Fields in Semiconductor Physics II*, edited by G. Landwehr (Springer-Verlag, Berlin, 1989); G. E. W. Bauer and T. Ando, Phys. Rev. B **37**, 3130 (1988).

[19] A. M. White, I. Hinchliffe, and P. J. Dean, Solid State Commun. **10**, 497 (1972).

[20] Obtained by measuring the FWM signal as a function of the detuning between the two excitation beams. See also Ref. [13].

Observation of Time-Resolved Picosecond Stimulated Photon Echoes and Free Polarization Decay in GaAs/AlGaAs Multiple Quantum Wells

M. D. Webb, S. T. Cundiff, and D. G. Steel

Harrison M. Randall Laboratory of Physics, The University of Michigan, Ann Arbor, Michigan 48109

(Received 25 July 1990)

We report measurements of exciton dynamics in GaAs multiple-quantum-well structures at low temperature using three-pulse picosecond four-wave mixing. The *time-resolved measurements of the emission* show both a delayed signal (stimulated photon echo) and a prompt signal (free polarization decay) with different decay times. The results suggest that, in addition to the inhomogeneously broadened resonance, a homogeneously broadened resonance contributes to the optical response of the exciton.

PACS numbers: 78.47.+p, 42.50.Md, 42.65.Re, 71.35.+z

Transient nonlinear laser spectroscopy methods provide a powerful experimental tool for the study of electronic excitation in solids. In the simplest experiment, optical excitation by a short pump pulse, with wave vector $\mathbf{k}_1$, creates a nonequilibrium state of the system and modifies the absorption, which can be measured as a function of time and frequency with a second beam with wave vector $\mathbf{k}_2$. The decay rates reflect the return to equilibrium and arise from several mechanisms such as radiative decay and scattering due to interactions with other perturbers. The time evolution may be very complex. Using the language developed for simpler systems, this decay can be referred to as longitudinal relaxation. Electronic excitation by coherent optical radiation also creates a macroscopic polarization reflecting the fact that the system is in a superposition of states that give rise to the dipole. This polarization is characterized by a decay that is usually distinct from the longitudinal relaxation and can be designated transverse or dephasing relaxation, corresponding to the homogeneous linewidth in the frequency domain. In the time domain, the dephasing rate can be measured by transient four-wave mixing[1] (FWM) where two beams separated in time (with wave vectors $\mathbf{k}_1$ and $\mathbf{k}_2$) create a spatial modulation that results in scattering of the incident beams in direction $2\mathbf{k}_1-\mathbf{k}_2$ or $2\mathbf{k}_2-\mathbf{k}_1$. For a homogeneously broadened system, the signal is prompt [called a free polarization decay (FPD)] with respect to the second pulse, while for an inhomogeneously broadened system, the signal emission is delayed [called a two-pulse photon echo (PE)] and the delay time is the interval between the input pulses. In this paper we examine both the longitudinal and transverse relaxation of resonantly excited excitons in GaAs/AlGaAs multiple-quantum-well (MQW) structures using a powerful extension of the above techniques based on time-separated, three-pulse excitation[2] in a backward FWM geometry.

In an ideal quantum well at low temperature, the quasi-two-dimensional excitons are delocalized. For the HH1 exciton (HH denotes heavy hole), phonon and defect scattering result in rapid dephasing [measured using transient FWM in a single high-quality QW, width $=13.5$ nm, to be of order 2 ps corresponding to the homogeneous linewidth of order 0.6 meV (Ref. 3)]. This scattering also gives rise to an initial fast decay in the longitudinal relaxation rate measurement due to scattering to exciton k values away from the initial $k=0$ (i.e., spectral diffusion, defined as the scattering of excitation at energy E to E'); a longer decay component due to exciton recombination follows the rapid decay. However, nonideal growth conditions result in interface roughness leading to inhomogeneous broadening of the absorption spectrum[4] and to localization of low-energy excitons due to fluctuations in the potential. Recent measurements of relaxation and spatial diffusion of these localized excitons in GaAs MQWs show a slower relaxation rate than for the delocalized excitons.[5,6] The rates depend on the excitation energy, increasing near the line center, suggesting the presence of a mobility edge where higher-energy excitons are delocalized. The temperature dependence of the relaxation rates of the lower-energy excitons indicates the origin is due to thermal activation to extended states[5,7] and spectral diffusion of excitons between localization sites is due to phonon-assisted migration.[8-10]

The experimental measurements presented below show this discussion is incomplete. Using transient FWM and *time resolving the emission*, we find both a FPD and a PE signal with strong spectral overlap and different decay times. The results are consistent with the interpretation that both an inhomogeneously broadened resonance and a homogeneously broadened resonance comprise the linear response of the system.

The experimental geometry is illustrated in the upper left inset of Fig. 1(a). The laser produces nearly transformed-limited pulses (1 or 8 ps) at the exciton transition wavelength ($\lambda \approx 800$ nm). Three beams with wave vectors $\mathbf{k}_1$, $\mathbf{k}_2$, and $\mathbf{k}_3$ ($=-\mathbf{k}_2$) are incident on the sample at time t_1, t_2, and t_3, respectively, producing a coherent signal in the direction $-\mathbf{k}_1$. The dephasing (longitudinal) decay rate results in the decay of the signal as a function of t_2-t_1 (t_3-t_2).

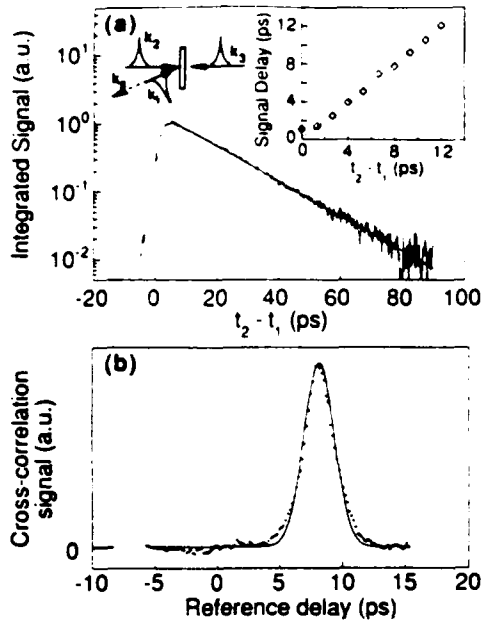

FIG. 1. (a) SPE signal as a function of delay. The solid line is a fit, corresponding to a dephasing time of 68 ps. Upper left inset: Experimental geometry. Upper right inset: Delay of the peak of the photon echo signal. The dashed line is the theoretically calculated delay, assuming a laser pulse width of 1 ps, and a phase coherence time of 68 ps. (b) The SPE signal as a function of time, measured with a 1.6-ps laser pulse width, and a corresponding theoretical fit showing that the inhomogeneous width of the resonance giving rise to the SPE is 2.5 ± 0.25 meV.

Three MBE-grown MQW samples were examined, with similar results. The data presented in this paper were obtained on a sample consisting of 65 periods of GaAs (96 Å) and $Al_{0.3}Ga_{0.7}As$ (98 Å) layers with the substrate removed. At 1.8 K, the HH1 exciton absorption linewidth is 2.35 meV, and the luminescence exhibits a small (~1 meV) Stoke's shift.

Figure 1(a) illustrates the decay of the integrated signal as a function of $t_2 - t_1$ due to dephasing at $T = 2.0$ K (for $t_3 - t_2 = 0$). The decay rate ($\gamma^{-1} = 68 \pm 2$ ps) (Ref. 11) corresponds to excitons excited 1 meV below the absorption line center, where excitons are expected to be localized, and is independent of excitation density for densities below 8×10^7 excitons/cm^{2}layer. The decay rate implies a homogeneous linewidth of 0.019 meV. This decay is slower than previously reported values,[12,13] most likely due to differences in the microscopic details of interface roughness that determines the phonon-assisted tunneling rate. The narrow homogeneous linewidth demonstrates that the linear absorption spectrum is strongly inhomogeneously broadened and that the signal is a simple PE.

The inhomogeneous broadening of the optical response is confirmed at low excitation densities by demonstrating the response is asymmetric as a function of $\tau = t_2 - t$ (i.e., 0 for $t_2 < t_1$) for $t_3 - t_2 > 0$ (Ref. 2) (see Ref. 14 for effects of local-field corrections in semiconductors). For $t_3 - t_2 > 0$, the coherent emission is a stimulated photon echo (SPE).[15] Time resolving the signal by cross correlating with a reference pulse directly verifies the echo. The upper right inset in Fig. 1(a) shows the linear dependence of the echo delay on τ. Numerical integration of the density matrix equations shows that the flattening of the curve near $\tau = 0$ is due to finite-pulse-width effects.

The amplitude of the SPE signal as a function of $t_2 - t_1$ provides a measure of the dephasing rate, but the *temporal evolution of the emission* [Fig. 1(b)] provides a direct measurement of the inhomogeneous broadening. In the simple case of δ-function excitation pulses and strong inhomogeneous broadening by a Gaussian distribution, the FWHM in time of the SPE signal is given by $\Delta t = 2\sqrt{2}\ln 2/\pi\Delta\nu$, where $\Delta\nu$ is the FWHM of the absorption profile. The solid curve in the figure shows the numerically determined SPE signal including finite-pulse-width effects. A best fit shows the linewidth is 2.5 ± 0.25 meV, in good agreement with the linear absorption measurement. The measurement supports the earlier claim that the absorption spectrum is completely inhomogeneously broadened. Small deviations between theory and experiment are most likely the result of a non-Gaussian absorption spectrum. It is important to note that including the wavelength dependence of the dephasing rate[12,16] in our calculations does not affect this conclusion.

The SPE technique enables measurement of lifetime dynamics of the exciton by measuring the signal amplitude as a function of $t_3 - t_2$, in contrast to the ordinary PE. The measured excitation lifetime is 34 ± 1 ps, suggesting that the dephasing time (measured as twice the excitation decay time) is due to decay of the excitation. This short lifetime is in qualitative agreement with earlier transient hole-burning measurements[17] and is clearly not due to recombination ($\tau_{rec} \approx 1$ ns), but rather to phonon-assisted migration (spectral diffusion) between localization sites of excitons localized by disorder.[9] Detailed studies of the time-integrated relaxation measurements of these excitons are presented elsewhere.[16] It is useful to note that with a large, fixed delay in the third pulse, the measurements show a sharp decrease in the phase coherence when the delay between the first and second pulses is greater than the pulse width. This is the standard signature of spectral diffusion.[2] In addition, measurement of the temperature dependence of the decay rate shows that phonon-assisted migration and thermal activation determine the relaxation.[10]

At the higher excitation densities ($> 10^9$ cm^{-2}layer, common in transient FWM), the nonlinear response shows contributions from higher-order terms (as determined by the dependence of the signal strength on exci-

tation beam intensities) and the decay of dynamics become complex. The time evolution of the signal becomes multiexponential and the exponential prefactors depend on intensity and temperature. However, the nonexponential decay of the signal as a function of the delay time t_2-t_1 is not simply the result of complex decay dynamics but rather the unexpected result that *two signals contribute to the time-integrated response.* Figure 2(a) shows the time-resolved emission at a density of 5×10^9 cm^{-2}layer. In addition to the delayed pulse corresponding to the SPE, we observe an additional prompt signal (the FPD signal) that is nearly coincident with the third incident pulse, independent of t_2-t_1. (The FPD signal is observable at this excitation density because the SPE has saturated while the FPD signal continues to increase as the cube of the input intensities. Saturation of the SPE signal is possibly the result of an increase in the dephasing rate due to exciton-exciton interactions[18] or the result that at high excitation, the number of localization sites is significantly depleted.) The physical interpretation of this result based on the usual picture of FWM is

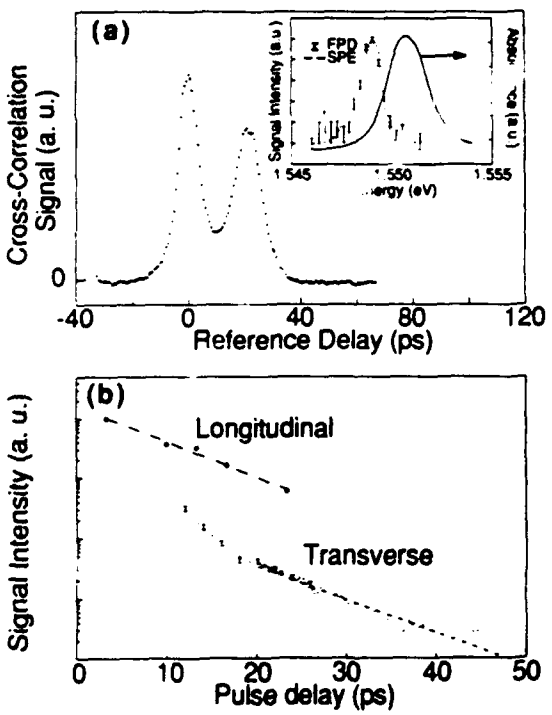

FIG. 2. (a) The cross-correlation signal showing both a SPE signal (at 20-ps delay) and FPD signal (at 0 delay), measured with an 8-ps laser pulse width. Inset: Spectral dependence of both signals. (b) The FPD signal as a function of pulse delay, measured with a 1-ps laser pulse width. The lower curve is a measurement of the dephasing decay as a function of t_2-t_1, corresponding to a two-component decay time of <5 and 16 ps. The upper curve is a measurement of the longitudinal relaxation decay as a function of t_3-t_2 corresponding to a single-component decay time of 14 ps.

that the electronic transition giving rise to the emission is comprised of an inhomogeneously broadened resonance (creating the SPE) and a homogeneously broadened resonance (creating the FPD). Such behavior has been reported in a simpler system.[19]

The spectral dependence of the two signals [Fig. 2(a), inset] was determined using the 8-ps pulse to provide adequate spectral resolution. To avoid saturation effects, the SPE spectral measurement was made at an excitation density near 5×10^7 cm^{-2}layer. t_2-t_1 was set at 20 ps to enable adequate temporal resolution between the FPD and PE signals. Such data by themselves are not complete since both the longitudinal and transverse decay rates depend on wavelength (as indicated earlier for the SPE signal[12]); nevertheless, the data clearly show two resonances with strong spectral overlap of both signals.

In addition to a different saturation intensity, the resonance giving rise to the FPD signal is also characterized by transverse and longitudinal relaxation times which differ considerably from the corresponding time associated with the SPE signal. Figure 2(b) shows the decay of the signal as a function of t_2-t_1 yielding a two-component decay corresponding to dephasing times of 6 and 16 ps.[20] Superimposed on these data is the signal as a function of t_3-t_2 yielding a longitudinal decay time of 14.5 ps (longer delay times are limited by the small signal-to-noise ratio due to the finite t_2-t_1 needed to provide separation between the prompt and delayed signal). Both measurements were shown to be independent of excitation density.

Hence, the data strongly support the presence of two separate resonances contributing to the signal. Numerical calculations of the SPE signals using finite-pulse-width excitation in the presence of different distributions, wavelength-dependent dephasing, and spectral diffusion do not predict the temporal structure seen in Fig. 2(a) unless two separate resonances are assumed where one resonance is inhomogeneously broadened. More formally, the linear absorption spectrum can be described as an inhomogeneously broadened resonance where the decay rates depend on excitation frequency and the distribution function is the sum of a continuous function such as a Gaussian and a weighted δ function.

Excitons localized by potential fluctuations, which also results in inhomogeneous broadening, provide a satisfactory explanation for the origin of the SPE signal and the corresponding relaxation. The short dephasing times of the FPD signal are comparable to those expected for delocalized excitons;[3] however, the FPD resonance would be blueshifted (above the exciton mobility edge) with respect to the SPE resonance, in contrast to the inset in Fig. 2(a). In addition, the measured longitudinal relaxation time is longer than expected for delocalized excitons. (Note that above the line center, our decay rate measurements confirm that both the longitudinal and trans-

verse relaxation times are of order 1 ps and arise from a FPD signal, as expected from earlier work.[3]) The long longitudinal relaxation rate also makes it unreasonable to suggest that the FPD signal arises from delocalized excitons produced in a few high-quality (no interface roughness) QWs within the MQW or from excitons above the mobility edge in QWs which are wider than those QWs giving rise to the SPE. These latter two possibilities are also unlikely since in the first case, we have observed the same spectral structure in different MQW structures; and in the second case, this explanation would produce a low-energy tail in the SPE spectrum not seen in the data. An alternate explanation is based on the fact that exciton-exciton interactions result in a strong exciton density-dependent dephasing. In this sample, the total dephasing rate is measured to be $\gamma_{ph}=\gamma_{ph}^{0}\times(1+n/n_0)$, where $n_0=5\times10^8$ excitons/cm^{2}layer (assuming a uniform distribution of excitons) and the dephasing rate varies linearly with density. This leads to the unlikely result that an average exciton separation much greater than the exciton Bohr radius results in a contribution to the dephasing time due to exciton-exciton interactions of order 70 ps. More likely is that due to variations in interface roughness, some regions are more densely populated with localized excitons, leading to strong dephasing, and regions which are homogeneously broadened giving rise to the FPD signal.

In summary, the time-resolved measurements show the presence of two resonant components in the exciton response. The origin of the SPE is explained by excitons localized by interface roughness. However, while the optical properties of the FPD have been determined, the origin of this signal remains unclear.

The authors would like to thank P. K. Battacharya for sample preparation, and S. R. Hartmann for helpful discussions. This work was supported by the U.S. Army Research Office.

[1]T. Yajima and Y. Taira, J. Phys. Soc. Jpn. 47, 1620 (1979).

[2]A. M. Weiner, S. De Silvestri, and E. P. Ippen, J. Opt Soc Am. B 2, 654 (1985).

[3]L. Schultheis, A. Honold, J. Kuhl, K. Kohler, and C W Tu, Phys. Rev. B 34, 9027 (1986).

[4]C. Weisbuch, R. Dingle, A. C. Gossard, and W. Wiegmann, Solid State Commun. 38, 709 (1981).

[5]J. Hegarty, L. Goldner, and M. D. Sturge, Phys. Rev. B 30, 7346 (1984).

[6]J. Hegarty and M. D. Sturge, J. Opt. Soc. Am. B 2, 1143 (1985).

[7]J. E. Zucker, A. Pinczuk, D. S. Chemla, and A. C. Gossard, Phys. Rev. B 35, 2892 (1987).

[8]J. Hegarty, K. Tai, and W. T. Tsang, Phys. Rev. B 38, 7843 (1988).

[9]T. Takagahara, J. Lumin. 44, 347 (1989), reviews recent theory and experiments.

[10]H. Wang, M. Jiang, and D. G. Steel, Phys. Rev. Lett. 65, 1255 (1990).

[11]The signal varies as $e^{-\tau/T}$, where τ is t_2-t_1 or t_3-t_2. For inhomogeneous broadening, the dephasing time is 4 T (2 T) in a time-integrated (time-resolved) measurement and 2 T for a homogeneous broadening. The longitudinal decay time is 2 T for either system (see Ref. 2).

[12]J. Hegarty *et al.*, Phys. Rev. Lett. 49, 930 (1982).

[13]L. Schultheis, M. D. Sturge, and J. Hegarty, Appl. Phys. Lett. 47, 995 (1985).

[14]K. Leo *et al.*, Phys. Rev. Lett. 65, 1340 (1990).

[15]T. Mossberg, A. Flusberg, R. Kachru, and S. R. Hartmann, Phys. Rev. Lett. 42, 1665 (1979); G. Noll, U. Siegner, S. G. Shevel, and E. O. Gobel, Phys. Rev. Lett. 64, 792 (1990).

[16]M. D. Webb, S. T. Cundiff, and D. G. Steel, Phys. Rev. B (to be published).

[17]J. Hegarty and M. D. Sturge, J. Lumin. 31&32, 494 (1984).

[18]A. Honold, L. Schultheis, J. Kuhl, and C. W. Tu, Phys. Rev. B 40, 6442 (1990).

[19]E. I. Shtyrkov, V. S. Lobkov, and N. G. Yarmukhametov, Pis'ma Zh. Eksp. Teor. Fiz. 27, 685 (1978) [JETP Lett. 27, 648 (1978)].

[20]In an infinitely fast medium using the decay time of the pulse determined by autocorrelation, the observed FWM decay rate of the signal would be 1.9 ps, compared to the 3 and 8 ps observed.

Measurement of Phonon-Assisted Migration of Localized Excitons in GaAs/AlGaAs Multiple-Quantum-Well Structures

H. Wang, M. Jiang, and D. G. Steel
Harrison M. Randall Laboratory of Physics, The University of Michigan, Ann Arbor, Michigan 48109
(Received 18 May 1990)

We report high-resolution nonlinear-laser-spectroscopy measurements of relaxation of lowest-energy heavy-hole excitons in GaAs multiple-quantum-well structures. We show that excitons below the absorption line center are spatially localized, and migrate among localization sites with a time scale of order 100 ps. The measurements give the resultant quasiequilibrium energy distribution of the scattered excitons and, based on the temperature dependence of the migration rate, confirm the theoretical model for phonon-assisted migration.

PACS numbers: 71.35.+z, 42.65.−k, 78.47.+p, 78.65.Fa

Optical resonant excitation of excitons with nearly monochromatic light of energy E leads to an optically induced polarization (coherence) and a population of excitons within ΔE of E where $\Delta E \sim \hbar\Gamma_h$ (Γ_h is the homogeneous linewidth of the exciton). The decay of this excitation must be characterized by decay of the polarization (often called dephasing) as well as decay of the population about energy E. In a simple ideal quantum well, quasi-two-dimensional excitons are described by a Bloch type of wave function and are free to move in the well plane. At low exciton density, decay of the excitation is then expected to be predominantly due to exciton-phonon scattering along with exciton recombination. In practice, however, the problem becomes more complicated due to nonideal growth processes. Recent transport and chemical lattice-imaging measurements[1,2] have shown the interface of GaAs/AlGaAs multiple-quantum-well (MQW) samples exhibits islandlike structures with a height of one monolayer and a lateral size of order 50 Å. For an exciton confined to a thin GaAs layer in a MQW, its energy depends strongly on the well thickness. For example, well width fluctuations of one monolayer in a 100-Å GaAs/$Al_{0.3}Ga_{0.7}As$ MQW can result in a change of exciton energy on the order of several meV. Therefore, at low temperature in the low-energy region of the heavy-hole exciton (HH1) absorption spectrum, excitons can be localized in the well with an energy determined by the local environment[3] leading to inhomogeneous broadening of the linear absorption spectrum. Excitons in the high-energy region may still be delocalized.[3] These excitons are expected to experience additional dephasing due to elastic scattering from potential fluctuations in addition to the decay due to exciton-phonon scattering and exciton recombination.

Localized excitons are in a local minimum in energy, and at very low temperature, decay of the localized exciton at energy E is expected to be dominated by migration between localization sites. The migration is accompanied by absorption or emission of acoustic phonons to compensate for the energy difference. Indeed, phonon-assisted migration was proposed to explain the slow and nonexponential energy relaxation observed in time-resolved luminescence measurements in a GaAs MQW.[4] While the migration is due to the overlap of the exciton wave functions between different sites for small intersite distances, the intersite dipole-dipole interaction mediates the migration process when the intersite distance is much greater than the localization length.[5] It is estimated that the typical magnitude of participating phonon wave vectors is within a few times of the inverse of the localization length, which indicates the energy of participating phonons is on the order of 0.01–0.1 meV. At higher temperatures (>10 K), thermal activation of localized excitons to delocalized states becomes important. This process is associated with phonon absorption, and has been observed in GaAs MQW structures using resonant Rayleigh scattering[3] and resonant Raman scattering.[6] The estimated activation energy indicates that the onset for the delocalized exciton is near the absorption line center.

A distinctive signature for phonon-assisted migration is the temperature dependence. Recent work by Takagahara[5] has shown the temperature dependence of the migration rate in MQW structures has a form given by $\exp(BT^{\alpha})$, and has been observed in transient hole-burning experiments in an InGaAs/InP MQW.[7] In this expression, B is positive and independent of temperature but is expected to increase with the exciton energy and depends on the details of interface roughness; α is estimated to be between 1.6 and 1.7. The predicted temperature dependence is quite different from that of variable-range hopping used by Mott to interpret electronic conduction in the localized regime,[8] and is attributed to the role of the long-range dipole-dipole interaction involved in the migration of the localized exciton.[5]

In this paper, we present results of high-resolution nonlinear laser spectroscopy of lowest-energy heavy-hole excitons in a GaAs/AlGaAs MQW at temperatures between 2.5 and 15 K. Using frequency-domain four-wave mixing (FWM), we are able to obtain relaxation rates

for the exciton population at a given energy E, and to directly measure the steady-state exciton redistribution under narrow-band cw excitation. The measurement shows that excitons below the absorption line center are localized and migrate among localization sites on a time scale of order 100 ps. The predicted temperature dependence of the migration rate is also confirmed.

The experimental configuration, discussed elsewhere,[9] is based on the use of two frequency stabilized tunable cw dye lasers. Three incident beams $\mathbf{E}_f(\omega_f,\mathbf{k}_f)$, $\mathbf{E}_b(\omega_b,\mathbf{k}_b)$, and $\mathbf{E}_p(\omega_p,\mathbf{k}_p)$ (f, b, and p represent forward, backward, and probe, respectively, and $\mathbf{E}_p \| \mathbf{E}_f \perp \mathbf{E}_b$) interact in the sample to generate a signal beam $\mathbf{E}_s(\omega_s,\mathbf{k}_s)$ which is proportional to $\chi^{(3)}\mathbf{E}_f\mathbf{E}_p^*\mathbf{E}_b$, where $\omega_s=\omega_f+\omega_b-\omega_p$. $\mathbf{E}_f\cdot\mathbf{E}_p^*$ results in a spatial and temporal modulation of the exciton population[10] which modifies the optical response of the sample through exciton phase-space filling and exchange effects.[11] The signal arises from coherent scattering of the backward beam from the modulation. Spectroscopic information related to the energy-level structure and relaxation of the system is obtained by measuring the nonlinear response as a function of the frequency of any of the three input beams. Depending on which frequency is tuned, the resultant line shape is designated the FWMi line shape ($i=f,b,p$). The physical meaning of the different line shapes can be understood based on the following simple picture (a more rigorous analysis based on effective optical Bloch equations is presented elsewhere[12]).

In the FWMb measurement, $\mathbf{E}_f\cdot\mathbf{E}_p^*$ ($|\omega_f-\omega_p|\ll\Gamma_h$) excites an exciton population in a spectral hole with a half-width $\Delta E=\hbar\Gamma_h$ within the inhomogeneous width. A resonance as a function of ω_b occurs when ω_s is resonant with the exciton dipoles induced by $\mathbf{E}_f\cdot\mathbf{E}_p^*$. This leads to a simple resonance represented by the hole-burning denominator $(\omega_s-\omega_p+2i\Gamma_h)^{-1}$ (note the extra factor of 2 over ordinary linear spectroscopy).[13,14] In addition, since $\mathbf{E}_b$ detects the exciton dipole, localized excitons that are scattered to other energy states will also contribute to the FWMb response, allowing for the direct measurement of the exciton spectral redistribution. While delocalized excitons can also be scattered to other energies by inelastic processes such as exciton-phonon interactions, these states have nonzero momentum, and, as a result, a zero dipole moment. In this case, the FWMb line shape simply provides a measure of the exciton homogeneous line shape.

In the FWMf measurement, we hold $\omega_p=\omega_b$ and tune ω_f by an amount $\delta=\omega_f-\omega_p$ producing a traveling-wave modulation of excitation. The nonlinear response as a function of δ then measures the decay rate Γ of the modulation formed by excitons that are resonant with ω_s; Γ includes contributions from exciton recombination as well as scattering of excitons from energy E to E' where $|E-E'|>\Gamma_h$. Spatial diffusion of the exciton also contributes to the decay and manifests itself as a dependence of the decay rate on the spatial period of the modulation.[15] In the limiting case where $\Gamma_h\sim\Gamma/2$, the FWMf line shape is complicated by the fact tuning ω_f tunes ω_s. The FWMf response then experiences an additional resonant effect from the hole-burning denominator appearing as $(\delta+2i\Gamma_h)^{-1}$, resulting in a deviation from a simple Lorentzian and requiring a small correction (of order 1) in relating Γ to the FWHM for *absolute* decay-rate measurements. The FWMp response provides a measurement similar to the FWMf response. However, since $\omega_f=\omega_b$, the hole-burning denominator appears as $(\delta+i\Gamma_h)^{-1}$ resulting in a slightly larger correction. In the case $\Gamma_h\gg\Gamma/2$, the FWMp and FWMf line shapes are the same and independent of Γ_h.

Samples consisted of 65 periods of 96-Å GaAs wells and 98-Å $Al_{0.3}Ga_{0.7}As$ barriers, grown at 630°C by molecular-beam epitaxy on semi-insulating (100) GaAs substrates with interrupted growth. They are mounted on a sapphire disk (c-axis normal) with the substrate removed. The data presented in this paper were obtained on a sample that is characterized by an absorption linewidth of 2.2 meV for the HH1 exciton, and a Stokes shift of 1 meV between the HH1 exciton absorption and emission. Similar results were also obtained on other samples. All the nonlinear measurements are carried out on the HH1 exciton with an exciton density on the order of $10^7/cm^2$.

The complex decay dynamics of the exciton population is seen in the FWMf response. A typical line shape below the absorption line center is shown in Fig. 1(a). The FWHM corresponds to a relaxation time of 60 ps, which is too slow to be due to phonon scattering of the delocalized exciton (typically[16] on a time scale of several ps), and is over an order of magnitude faster than the exciton recombination time. Furthermore, the FWHM is independent of the grating period, indicating the contribution from exciton diffusion is negligible and that excitons are localized in this spectral region. Hence, the data suggest that the decay is due to spectral diffusion as

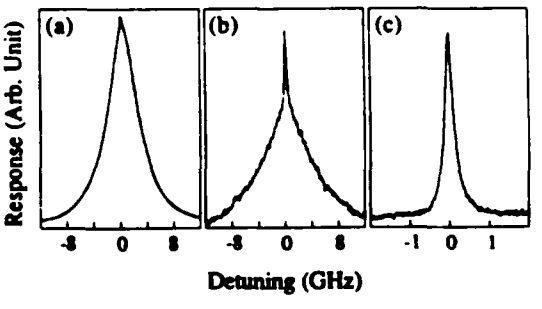

FIG. 1. The FWMf responses (where energy shifts are given, they refer to the absorption line center at 1.5508 eV): (a) at 1.5 meV below line center and at 2.5 K, (b) at 0.6 meV below line center and at 10 K, and (c) at 2 meV above line center and at 10 K.

a result of scattering of localized excitons from energy E to E' ($|E-E'|>\Gamma_h$). In fact, the decay rate is in agreement with a recent calculation based on phonon-assisted migration of the localized exciton.[5] In addition, excitons that are scattered from E to E' can later be scattered back to energy E establishing a quasiequilibrium exciton population about E before they eventually recombine. This quasiequilibrium population contributes to the FWMf response with a decay rate characterized by the exciton recombination rate.[12] The FWMf response shown in Fig. 1(a) indeed shows a small and narrow feature at the top of the line shape. The narrow feature becomes more pronounced at higher temperature due to faster exciton migration as shown in Fig. 1(b). The width associated with the feature corresponds to a decay time of 1.2 ns, consistent with the exciton recombination rate.[17]

We further examine the relaxation mechanism of the localized exciton by studying the temperature dependence of the exciton relaxation rate. Figure 2(a) shows the temperature dependence of the exciton relaxation rate obtained at 0.6 and 1.5 meV below the absorption line center using the FWMf response. The data are in good agreement with the theory of phonon-assisted migration discussed above with $\alpha=1.6$. The measurement indicates that the dominant contribution to relaxation of the localized exciton is phonon-assisted migration up to a temperature of 15 K. Note that earlier measurements[3,6] have reported observations of an activation type of temperature dependence for the localized exciton at temperatures between 7 and 20 K, indicating that in this temperature region, relaxation for the localized exciton is dominated by thermal activation to delocalized states. It has been suggested[18] that sample-dependent variations in the thermal activation energy are the result of differences in the nature of interface roughness. Hence, the effective activation energy can be much higher than simply the energy difference between the mobility edge and the localized exciton resulting, at low temperature (<15 K), in a thermal activation rate much smaller than the phonon-assisted migration rate.

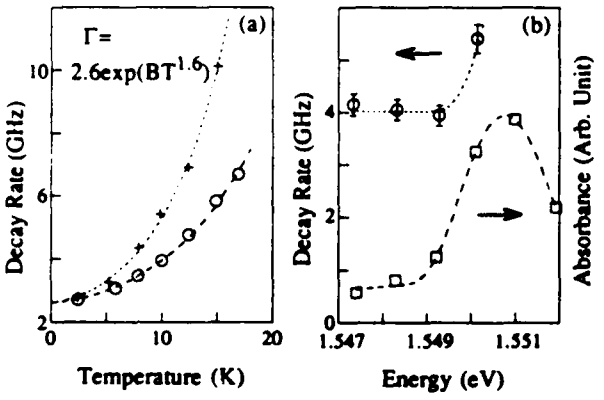

FIG. 2. (a) The temperature dependence of the exciton decay rate. Circles and crosses are data obtained at 1.5 and 0.6 meV below line center, respectively. Dashed lines are fits by the theory of phonon-assisted migration. (b) The energy dependence of the exciton decay rate at 10 K. The dashed line is only a guide to the eye.

The energy dependence of the decay of the exciton population below the absorption line center is shown in Fig. 2(b). For exciton energies less than 1.5 meV below the absorption line center, the decay rate depends very weakly on the energy. The rate increases rapidly when the exciton energy approaches the absorption line center, suggesting a transition from localized to delocalized excitons.[3]

If we imagine that localized excitons are optically excited at energy E and then migrate among localization sites to different energies, a quasiequilibrium exciton population over a broad spectral range can be established assuming the exciton migration rate is large compared with the recombination rate. As indicated earlier, it is the decay of this quasiequilibrium distribution that gives rise to the narrow features in Figs. 1(a) and 1(b). The spectral redistribution of the population can be directly measured in the FWMb response by scanning ω_b while keeping ω_f and ω_p fixed at E. Figure 3 shows a FWMb line shape where excitons are optically excited at 1.5 meV below the absorption line center. The nonlinear response is corrected for sample absorption, and is proportional to the quasiequilibrium exciton population assuming all excitons in the spectral region concerned give rise to the same cw nonlinear response.

To improve the qualitative understanding of the exciton migration process, we introduce a distribution kernel $f(E,E')$, the rate for an exciton to migrate from energy E to E'. $f(E,E')$ is analogous to collision kernels which are used to describe velocity-changing collisions in atomic vapor.[19] Decay of the exciton population can then be described by the following transport equation:

$$\dot{\rho}(E)=-(\gamma+\Gamma_E)\rho(E)+\int f(E',E)\rho(E')dE',$$

where $\rho(E)$ is the density of the excitons at E, γ is the

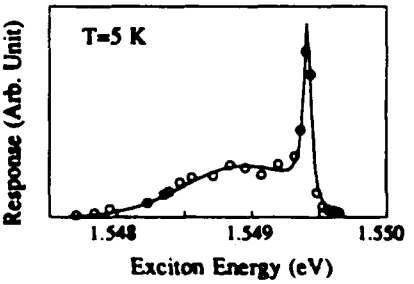

FIG. 3. The FWMb response with the frequencies of the forward and probe beams at 1.5 meV below line center.

recombination rate, $\Gamma_E = \int f(E,E')dE'$ is the overall rate at which excitons migrate out of states with energy E. In principle, the transport equation, together with the equation for the nonlinear polarization,[11,20] can provide a description for the FWMf and FWMb line shapes, though, in general, $f(E,E')$ is unknown and has to be determined by experiments. However, by assuming $f(E,E')$ to be independent of the initial-state energy, analytical solutions[12] can be obtained for standard distributions and can show that the FWMf response has an additional component with a width given by γ as anticipated based on physical arguments. The FWMb line shape in Fig. 3 can be described by a simple model which neglects migration to states above the excitation energy, and is based on the understanding of the solution to the above transport equation. The model assumes a Gaussian distribution for the quasiequilibrium population of excitons that have migrated to states below the excitation energy. The result is plotted as a solid line in Fig. 3.

Finally, we note that earlier measurements have suggested that excitons above the absorption line center are weakly delocalized.[3] Indeed, our measurements of the FWMf response show a quadratic dependence[15] of the modulation decay rate on the inverse of the spatial period of the modulation yielding a diffusion coefficient on the order of 4 cm^2/s. More strikingly, for large spatial modulation spacing where there is negligible contribution from exciton spatial diffusion, the FWMf line shape is completely dominated by the recombination component due to the rapid exciton-phonon scattering [on the order of several ps (Ref. 16)]. A typical FWMf line shape in this case is shown in Fig. 1(c). The FWHM of the line shape corresponds to an exciton recombination time of 1.2 ns. Using the FWMb response, we also determined the homogeneous width to be on the order 0.5 meV (corresponding to a dephasing time of 1.3 ps) at a temperature of 5 K, consistent with what is expected for the delocalized exciton.[16]

This work was supported by the Air Force Office of Scientific Research.

[1]R. Gottinger, A. Gold, G. Abstreiter, G. Weiman, and W. Schlapp, Europhys. Lett. **6**, 183 (1988).

[2]A. Ourmazd, D. W. Taylor, J. Cunningham, and C. W. Tu, Phys. Rev. Lett. **62**, 933 (1989).

[3]J. Hegarty, L. Goldner, and M. D. Sturge, Phys. Rev. B **30**, 7346 (1984).

[4]Yasuaki Masumoto, Shigeo Shionoya, and Hitoshi Kawaguchi, Phys. Rev. B **29**, 2324 (1984).

[5]T. Takagahara, J. Lumin. **44**, 347 (1989); Phys. Rev. B **32**, 7013 (1985).

[6]J. E. Zucker, A. Pinczuk, D. S. Chemla, and A. C. Gossard, Phys. Rev. B **35**, 2892 (1987).

[7]J. Hegarty, K. Tai, and W. T. Tsang, Phys. Rev. B **38**, 7843 (1988).

[8]N. F. Mott, and E. A. Davis, *Electronic Processes in Noncrystalline Materials* (Oxford Univ. Press, New York, 1979), 2nd ed.

[9]J. T. Remillard, H. Wang, D. G. Steel, J. Oh, J. Pamulapati, and P. K. Bhattacharya, Phys. Rev. Lett. **62**, 2861 (1989).

[10]For cw measurements, the orientational grating ($E_p \perp E_f \| E_s$) has not been observed.

[11]S. Schmitt-Rink, D. S. Chemla, and D. A. B. Miller, Adv. Phys. **38**, 89 (1989).

[12]H. Wang and D. G. Steel (to be published).

[13]J. L. Oudar and Y. R. Shen, Phys. Rev. A **22**, 1141 (1980).

[14]D. G. Steel and J. T. Remillard, Phys. Rev. A **36**, 4330 (1987).

[15]J. T. Remillard, H. Wang, D. G. Steel, J. Oh, J. Pamulapati, and P. K. Bhattacharya, Opt. Lett. **14**, 1131 (1989).

[16]L. Schultheis, A. Honold, J. Kuhl, K. Kohler, and C. W. Tu, Phys. Rev. B **34**, 9027 (1986).

[17]J. Feldman, G. Peter, E. O. Gobel, P. Dawson, K. Moore, C. Foxon, and R. J. Elliott, Phys. Rev. Lett. **55**, 2337 (1987).

[18]T. Takagahara (private communication).

[19]Paul R. Berman, Phys. Rep. **43**, 102 (1978).

[20]M. Lindberg and S. W. Koch, Phys. Rev. B **38**, 3342 (1988).

Accepted for Publication
Phys. Rev. B Rapid. Comm.

Polarization Dependent Picosecond Excitonic Nonlinearities and the Complexities of Disorder

S.T. Cundiff, H. Wang and D.G. Steel

Harrison M. Randall Laboratory of Physics, The University of Michigan, Ann Arbor, Mi. 48109

Time resolved emission of the hh1 exciton transient four-wave-mixing (TFWM) response in multiple quantum wells (MQW) shows the unexpected result that the signal emission is either a photon echo or a free polarization decay, depending on the relative polarization of the excitation beams. The energy and temperature dependences of the dephasing rates and the transport and saturation characteristics show that the two excitations are significantly different. Explanations for the disappearance of the echo, which arises due to the presence of disorder, and the origin of the prompt signal are considered.

Picosecond optical excitation of excitons in semiconductors leads to coherent nonlinear optical effects such as photon echoes, free polarization decay and quantum beat phenomena. The physics underlying these interactions was first described in simple systems based on the optical Bloch equations (OBE). In semiconductors the description is complicated by the Coulomb interaction and the fermionic nature of the carriers. However, progress in the development of a parallel treatment of optical interactions in semiconductors resulting in a set of semiconductor OBE [1] has greatly facilitated understanding. Work in this area is the subject of numerous recent studies, not only because this is a challenging manybody problem important for application to optoelectronic devices, but also because nonlinear spectroscopy is a powerful means of studying materials.

The nonlinear response and excitation dynamics in semiconductor heterostructures, however, is qualitatively changed due to the presence of disorder such as monolayer fluctuations at the GaAs/AlGaAs interface. Early measurements demonstrated that the low temperature exciton line width in GaAs MQW is inhomogeneously broadened by the corresponding confinement potential fluctuations [2]. It was initially believed that there were large regions at the interface that were atomically flat. More recent studies have shown that the disorder is due to the presence of monolayer flat islands with a spatial extent of 50-100 Å [3] suggesting the existence of at least two scale lengths for interface roughness [4, 5].

Nonlinear optical measurements of excitons in MQW at low temperature have improved the understanding. TFWM showed that in MQW the emission is a photon echo, confirming the resonance is inhomogeneously broadened [6]. Measurements on a single QW with a much narrower hh1 absorption line demonstrated that the resonance was homogeneously broadened [7]. In MQW TFWM measurements of the diffusion coefficient [8] showed a strong dependence on photon energy. The diffusion rate increased through the absorption line center which is evidence for the exciton mobility edge. Theoretical [9] and experimental [10, 11] work showed that exciton relaxation ($T<15K$) proceeds by phonon assisted migration between localization sites. In this paper, we report new unexpected features regarding the polarization dependence of the time resolved emission in TFWM. The results can not be explained based on existing theoretical

models and show the importance of including the effects of polarization dependent interactions as well as the effects of disorder.

Based on the solution of the ordinary OBE, it is well known that for a single resonance the emission in three pulse TFWM (Fig. 1a, left inset) is a free polarization decay (FPD) emitted coincident with the third pulse [12]. If the system is inhomogeneously broadened, the FPD from the different resonant groups destructively interfere and the prompt coherent emission vanishes. However, at a time following the third pulse given by the time difference between the first two pulses, the interference becomes constructive, leading to an emitted signal (a stimulated photon echo, SPE) for a duration determined by the inverse inhomogeneous width.

Recently however, it has been shown theoretically that this simple picture based on non-interacting two level systems is not adequate for describing the temporal structure of coherent radiation produced in TFWM resonant with excitons in an ideal semiconductor. Lindberg et al with similar results by Schäfer et al. [13] show that even for resonant excitation of a homogeneously broadened exciton, the time dependent emission in TFWM can be complex due to exciton-exciton interactions and contributions from the continuum states, leading to additional temporal structure and delay in the emission.

Measurements presented in this paper were obtained on two samples grown by molecular beam epitaxy and gave qualitatively similar results. The first sample consisted of 65 periods of 96 Å GaAs wells and 98 Å $Al_{0.3}Ga_{0.7}As$ barriers. The hh1 absorption width was 2.2 meV (1.2 meV luminescence Stokes shift.) The second sample, with only 10 periods, had an absorption line width less than 1.0 meV (luminescence Stokes shift < 0.2 meV.) Energy resolved measurements were obtained using the first sample since the narrow absorption resonance of the higher quality sample was on the order of the inverse pulse width necessary to complete the measurements. The TFWM signal was time resolved by the usual cross-correlation technique. Unless otherwise stated, all measurements were performed at 5.5K and the autocorrelation width was 3 ps.

As we discuss in more detail below, it is expected that other than rotating the polarization of the signal, no difference in the FWM response is expected for either all excitation beams linearly co-

polarized or for $E_1 \perp E_2 \| E_3$, $E_s \| E_1$. Figure 1 shows the surprising result that in the first case the emission is delayed with respect to the third field given by the time between E_1 and E_2 (as shown earlier [11]) while in the second case ($E_1 \perp E_2$ excitation) the signal is prompt (i.e., independent of time delay) with respect to the third pulse. (An additional delayed signal is also evident in Fig. 1b arising from a strong resonance with a long dephasing time and Stokes shifted by 2.5 meV, most likely due to an impurity bound exciton). Both signals are *strongly resonant* with the hh1 exciton, approximately centered at the hh1 absorption line center (after corrections for absorption and wavelength dependent coherence decay rates). Furthermore, we note that at low excitation density, there is no combination of circularly polarized input beams (the natural polarization for this discussion) which gives rise to the rapid dephasing associated with the prompt signal (see below). In the following, we present data which further distinguishes these two signals as well as providing insight into possible explanations.

The exponential decrease in the peak signal strength as a function delay, τ, between E_1 and E_2 is determined by dephasing [12]. Experiments show both signals in Fig. 1 decay monoexponentially, though the dephasing rate in the delayed signal is much slower than for the prompt signal. (The increase in dephasing rate for orthogonal excitation has been reported earlier [14].) In addition, the dephasing rates differ considerably in energy and temperature dependence. Since delay in emission in Fig 1a varies linearly with the delay τ, we assume the dependence on dephasing is given by $\exp(-4\Gamma_{ph}\tau)$ whereas for the signal in Fig 1b, the dependence is given by $\exp(-2\Gamma_{ph}\tau)$ [12] Figure 2a and 2b show the corresponding energy [15] and temperature dependence (1 meV below line center).

The linear dependence of signal emission on τ coupled with the long dephasing time (in agreement with earlier spectral hole burning measurements [10]) shows that the signal is Fig. 1a is a classical stimulated photon echo arising from localized excitons. This is further supported by Fig 2a showing the increase in dephasing rate through line center as demonstrated earlier for localized excitons[8] as well as the fact that the temperature dependence follows that due to phonon assisted migration and thermal activation (dashed line) for localized states [10, 16]. As seen in the upper

inset of Fig. 1b, this signal also saturates at low intensity (~5×10^8 excitons/cm^{-2} assuming the absorption is due to the resonance associated with the SPE) due to the finite number of localization sites. In addition the observed exact correspondence between the time delay in the signal and the time τ is not expected at low excitation for homogeneously broadened excitons [13].

In comparison with the delayed signal, we see that the dephasing rate for the prompt signal is larger and nearly energy independent (Fig. 2a). In addition, the temperature dependence of the dephasing rate for the prompt signal (Fig. 2b) is linear and the magnitude and temperature dependence is in agreement with the earlier work discussed above in a homogeneously broadened single QW [7] (where the hh1 absorption line width was 0.4 meV, in agreement with the reported dephasing rate.) In those experiments, it was believed that the exciton was described by an extended state and dephasing was due to single photon scattering. We also note that while the amplitude of the delayed signal saturates at low intensity, the onset of saturation for the prompt signal occurs at a much higher intensity. At high intensities (10^{11}photons/cm^2/sec), the delayed signal saturates, and the prompt signal becomes observable under co-polarized excitation. In constrast in the absence of disorder, Lindberg [13] shows the presence of the (second) delayed contribution to the response increases with respect to the first peak with increasing excitation density rather than decreasing.

It is important to note that that after accounting for the finite pulse width in the current experiments, the spectral width of the nonlinear response from the prompt signal is considerably narrower than that associated with the echo [17]. The temporal width of the echo is also in agreement with that expected from the linear absorption line width [11].

Finally we determined the mobility associated with the echo and prompt signal by transient grating experiments [8]. As expected the diffusion coefficient, D, varied between samples. We found that D increases though line center for the echo signal, in agreement with earlier work on localized excitons [8]. However, we found that the D (10.1 and 14 cm^2/sec for the two samples examined) associated with the prompt signal was independent of the excitation wavelength over the

resonance and was considerably larger than the *D* for localized excitons (see Fig. 3). The ratio of the *D* (prompt/delay . . elow line center for the two samples was 2 and 3.5.

In discussion of these unexpected results, we note that in general the polarization dependence of the FWM signal depends on the details of the symmetry of the electronic excitation. Quantum confinement lifts the valence band degeneracy at k=0 resulting in hh-lh splitting. However, if the energy level diagram represented in Fig. 1 is a good approximation, it is easy to determine what is expected. The conduction band is m=±1/2 character and the valence band is m=±3/2. The axis of quantization and the incident k-vectors are perpendicular to the plane of the layers. The dipole selection rules are Δm=±1 with equal transition moments. For $\mathbf{E_1}\|\mathbf{E_2}$, a population grating (for each frequency group) is induced (E_3 scatters off this grating giving rise to the signal). In the absence of optical alignment and orientation effects [18] the two transitions (-3/2 → -1/2 and +3/2 → +1/2) are independent and at a given frequency each has its own spatial grating. This is also true for $\mathbf{E_1}\perp\mathbf{E_2}$, however the gratings for the two transitions are spatially out of phase. Hence, although the polarization of the incident fields determines the polarization of the signal, the temporal dependence is not expected to be affected. Note that if the scattering from each grating does not depend on the polarization of $\mathbf{E_3}$, then the signal vanishes for $\mathbf{E_1}\perp\mathbf{E_2}$.

Current measurements provide an indication of the mechanism leading to the suppression of the echo for $\mathbf{E_1}\perp\mathbf{E_2}$. Complete randomization of the gratings (corresponding to Δm=+1 or -1 transitions) on the time scale of the excitation pulse would explain the absence of the echo as would the possibility that the scattering of $\mathbf{E_3}$ from the gratings is polarization independent. Randomization occurs due to spin relaxation but we have shown that this occurs on the time scale of 40 ps, in agreement with earlier measurements [19, 20], much longer than the pulse width. However, our measurements show the unexpected result that co-rotating circularly polarized $\mathbf{E_1}$ and $\mathbf{E_2}$ with a linearly polarized $\mathbf{E_3}$ gives a *linearly* polarized echo, i.e., the grating induced by the circularly polarized $\mathbf{E_1}$ and $\mathbf{E_2}$ scatters left and right circularly polarized light with equal efficiency. The absence of the echo in the cross-polarized experiments above is thus due to the destructive interference between the two third order induced polarizations. The linearly polarized echo

observed using circularly polarized E_1 and E_2 shows that both left and right circularly polarized fields couple with the induced grating. The existence of coupling between oppositely-rotating fields has been detected in transient absorption experiments using circularly polarized fields reported in earlier work [20] and also observed in our laboratory. The observed coupling is much stronger than expected and is the subject of current studies [21]. However, the coupling may be the result of localization enhanced exciton-exciton interactions.

A detailed understanding of the origin of the prompt signal is incomplete. However, the data shows the response is resonant with the hh1 exciton though the physical properties of this response are distinct from those of the echo. One explanation is that the signal arises from extended excitons. We note that the prompt signal shows no evidence of saturation whereas the echo saturates due to the finite number of localization sites. For an ideal QW, the saturation intensity is over an order of magnitude higher than the range of our measurements [22]. The large wavelength independent dephasing rate is also expected for an extended state exciton where dephasing is due to single phonon scattering. Indeed, both the magnitude and temperature dependence are in agreement with earlier work on a single QW where it is believed that the excitons are extended [7]. And finally as would be expected, the diffusion coefficient associated with this excitation is greater than the diffusion coefficient for the localized exciton, although, the sample dependent nature of this number shows that this state still experiences scattering from the potential fluctuations due to interface roughness. The simultaneous presence of localized and extended states is not expected in the theory of localization [23] though more recent work challenges this thinking [24] Alternatively, the states associated with the prompt signal may not be truly extended but confined to large regions of the QW characterized by reduced interface fluctuations whereas the echo originates in areas characterized by increased fluctuations leading to strong localization, a picture consistent with the concept of a bimodal distribution of interface roughness [4, 5].

Samples were provided by P.K. Bhattacharya and the work was supported by the A.R.O.

1. M. Lindberg and S.W. Koch, Phys. Rev. B **38**, 3342 (1988).
2. C. Weisbuch, R. Dingle, A.C. Gossard, and W. Wiegmann, Solid State Comm. **38**, 709 (1981).
3. A. Ourmazd, D.W. Taylor, J. Cunningham, and C.W. Tu, Phys. Rev. Lett. **62**, 933 (1989).
4. C.A. Warwick, W.Y. Jan, A. Ourmazd, and T.D. Harris, App. Phys. Lett. **56**, 2666 (1990).
5. D. Gammon, B.V. Shanabrook, and D.S. Katzer, Phys. Rev. Lett. **67**, 1547 (1991).
6. L. Schultheis, M.D. Sturge, and J. Hegarty, Appl. Phys. Lett. **47**, 995 (1985).
7. L. Schultheis, A. Honold, J. Kuhl, K. Köhler, and C.W. Tu., Phys. Rev. B **34**, 9027 (1986).
8. J. Hegarty and M.D. Sturge, J. Opt. Soc. Am. B. **2**, 1143 (1985).
9. T. Takagahara, Phys. Rev. B **31**, 6552 (1985); T. Takagahara, Phys. Rev. B **32**, 7013 (1985).
10. H. Wang, M. Jiang, and D.G. Steel, Phys. Rev. Lett. **65**, 1255 (1990).
11. M.D. Webb, S.T. Cundiff, and D.G. Steel, Phys. Rev. B **43**, 12658 (1991).
12. A.M. Weiner, S. De Silvestri, and E.P. Ippen, J. Opt. Soc. Am. B. **2**, 654 (1985).
13. M. Lindberg, R. Binder, and S.W. Koch, Phys. Rev. A **45**, 1865 (1992); W. Schaefer, F. Jahnke, and S. Schmitt-Rink, preprint.
14. H.H. Yaffe, Y. Prior, J.P. Harbison, and L.T. Florez, in Quantum Electronics Laser Science, 1991 Technical Digest Series (OSA, 1991.); K. Leo, J. Shah, S. Schmitt-Rink, and K. Köhler, in VIIth Int. Symp. on Ultrafast Proc. in Spectr., 1991, proceeding to be published.
15. The energy range over which data is obtained is limited by decreasing signal. However, work by Weiner [12] shows that use of the simple form $\exp(-2\Gamma\tau)$ for determining Γ also limits the detuning range.
16. T. Takagahara, Phys. Rev. B **32**, 7013 (1985).
17. The relationship between the linear absorption line shape and the spectral response of FWM for a homogeneously broadened resonance is in general quite complex and must be determined numerical integration of the equations of motion.

18. The more complex effects of optical orientation and alignment of magnetic substates can give rise to similar polarization effects [P.R. Berman, et al. Phys. Rev. A **38**, 252 (1988)] but such effects are not expected in semiconductors..
19. T.C. Damen, K. Leo, J. Shah, and J.E. Cunningham, App. Phys. Lett. **58**, 1902 (1991).
20. S. Bar-Ad and I. Bar-Joseph, Phys. Rev. Lett. **68**, 349 (1992).
21. S. Koch, personal communication 1992.
22. D.S. Chemla, S. Schmitt-Rink, and D.A.B. Miller, Nonlinear Optical Properties of Semiconductor Quantum Wells, in Optical Nonlinearities and Instabilities in Semiconductors, H. Haug, Editor. (1988, Academic Press, San Diego) p. 83.
23. L. Fleishman and P.W. Anderson, Phys. Rev. B **21**, 2366 (1980).
24. J.C. Phillips, Solid State Commun. **47**, 191 (1983).

Figure Captions

Figure 1: Time resolved signal for all fields co-polarized (a) and for $\mathbf{E_1} \perp \mathbf{E_2} \| \mathbf{E_3}$, $\mathbf{E_s} \| \mathbf{E_1}$ (b). Delay between $\mathbf{E_1}$ and $\mathbf{E_2}$ is 0 ps for (1), 2 ps for (2), 4 ps for (3) in (a) and (b), all are taken 0.4 meV below absorption line center. Left inset in (a) is experimental geometry. Subscript on fields also correspond to time ordering. Right inset in (a) shows magnetic substate structure. Inset in (b) shows dependence of signal strength on incident flux (photons/cm^2), closed circles are for $\mathbf{E_1} \| \mathbf{E_2}$, open are for $\mathbf{E_1} \perp \mathbf{E_2}$, straight lines indicate cubic behavior.

Figure 2: a) Energy dependence of dephasing rates for co-polarized fields (closed circles, dotted line to guide the eye) and for $\mathbf{E_1} \perp \mathbf{E_2}$ (open circles). The signal strength is clearly decreasing away from line center. Solid line is linear absorption. b) Temperature dependence of both signals 1.0 meV below absorption line center, note difference in scales associated with each. Solid line is fit to single phonon scattering, dashed lines are fit to phonon assisted migration ($T < 10K$) and thermal activation ($T > 10K$).

Figure 3: Grating relaxation rate at absorption line center for SPE and FPD as a function of inverse grating spacing.

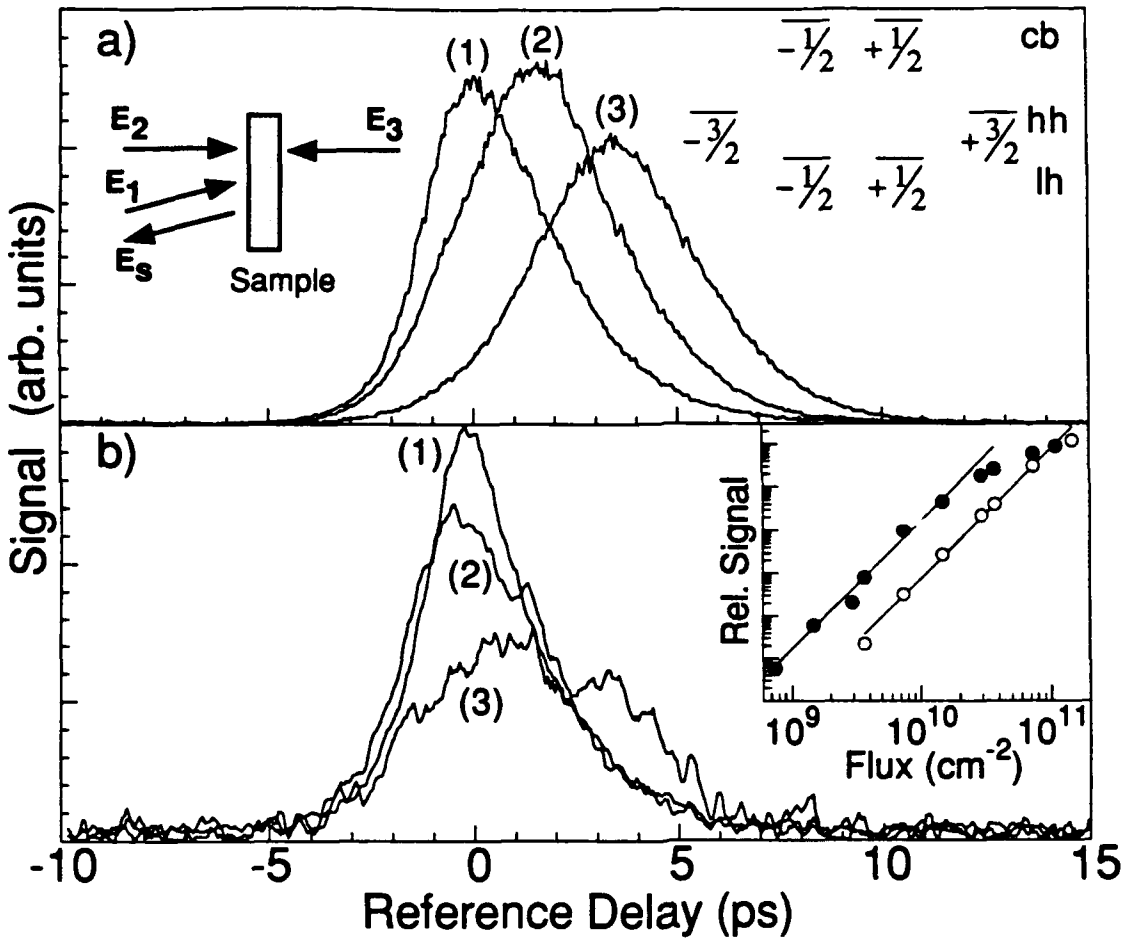
a)
(1)
(2)
(3)
cb
hh
lh
E2
E3
E1
Es
Sample
b)
Signal (arb. units)
Rel. Signal
Flux (cm-2)
Reference Delay (ps)

Fig 1.

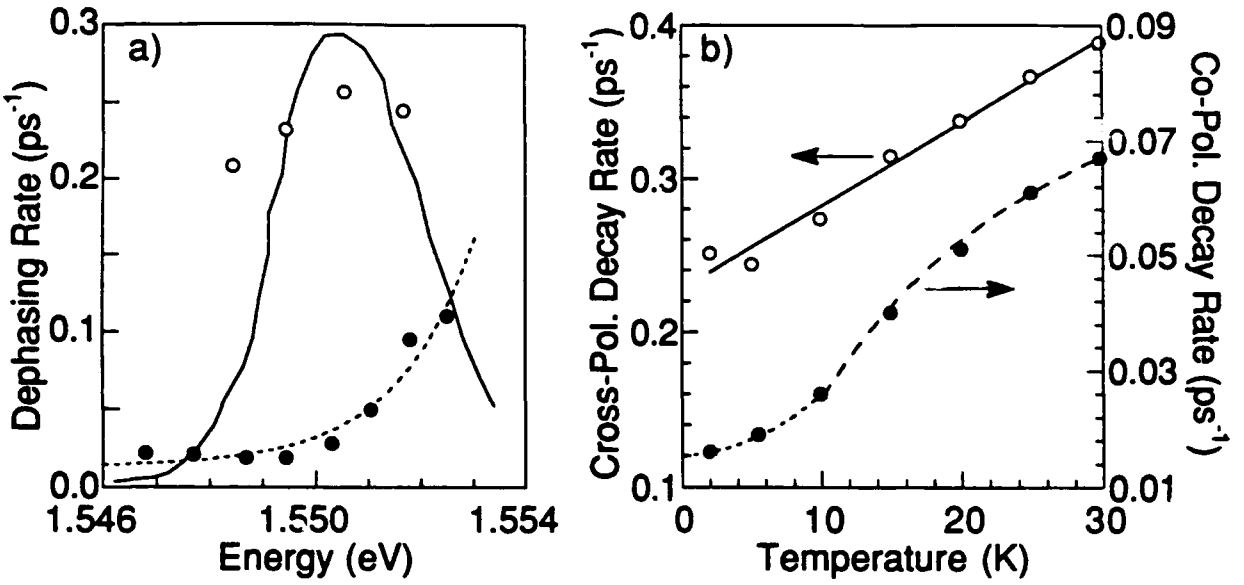
a)
Dephasing Rate (ps^{-1})
0.0
0.1
0.2
0.3
1.546
1.550
1.554
Energy (eV)
b)
Cross-Pol. Decay Rate (ps^{-1})
Co-Pol. Decay Rate (ps^{-1})
0.1
0.2
0.3
0.4
0.01
0.03
0.05
0.07
0.09
0
10
20
30
Temperature (K)

Fig 2.

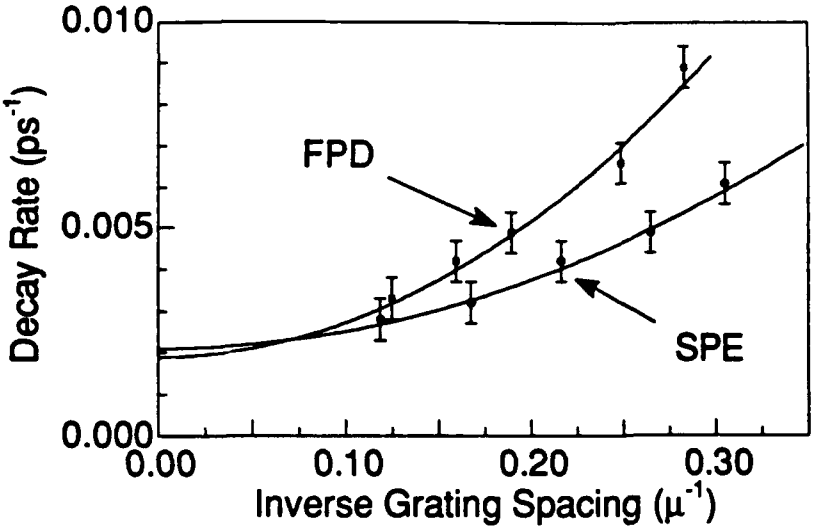
0.010
0.005
0.000
Decay Rate (ps^{-1})
FPD
SPE
0.00
0.10
0.20
0.30
Inverse Grating Spacing (μ^{-1})

Figure 3

Picosecond Excitonic Nonlinearities in the Presence of Disorder

Steven T. Cundiff and Duncan G. Steel

Harrison M. Randall Laboratory of Physics, University of Michigan
Ann Arbor, Mi. 48109, USA

Abstract. The polarization dependence of the low temperature excitonic nonlinear optical susceptibility in $GaAs/Al_{0.3}Ga_{0.7}As$ multiple quantum wells (MQW) exhibits unexpected properties. In a three pulse transient four wave mixing experiment (TFWM), the emitted signal becomes prompt when the first field is cross-linearly-polarized (with respect to the second and third fields), in contrast to the delayed signal observed for co-polarized fields. This demonstrates the presence of both a homogeneously broadened and an inhomogeneously broadened resonance. The characteristics of the nonlinear response indicate that the inhomogeneous resonance is due disorder localized excitons and is suppressed by cross-polarizing the first field, and that the homogeneously broadened resonance is due to extended excitons. Circularly polarized TFWM and transient absorption measurements indicate that this suppression occurs due to coupling between opposite spin excitonic transitions.

The optical and electronic properties of semiconductor heterostructures depend on the energy level structure and dynamics of the electronic excitations. These in turn are sensitive to the presence of disorder, which arises in heterostructures from non-ideal growth conditions. The inhomogeneous broadening of the excitonic resonance reflects the modification of the energy level structure due to the presence of disorder induced localization of the states [1]. Migration between the localization sites, an entirely new dynamical process resulting from disorder, is responsible for relaxation of the excitation at a given energy [2]. To probe the effects of disorder in GaAs MQW we use resonant TFWM and non-degenerate circularly polarized transient absorption at low excitation density. Examination of the polarization dependences yields results which are unexpected for an ideal semiconductor (i.e. no disorder), but which can be explained by the presence of disorder.

Recent results have shown that in a two-pulse TFWM experiment the decay of the signal for increasing interval between pulses changes dramatically in time scale and strength when the pulses are cross-polarized [3]. However a more dramatic effect is observed if the time resolved signal is examined in a three pulse experiment for all fields co-polarized (Fig. 1a) and for $\mathbf{E}_1 \perp \mathbf{E}_2 \| \mathbf{E}_3$, $\mathbf{E}_s \| \mathbf{E}_1$ (Fig. 1b). The shifting of the signal with increasing delay between $\mathbf{E}_1$ and $\mathbf{E}_2$ for co-polarized fields makes it apparent that it is a stimulated photon echo (SPE), arising from an inhomogeneously broadened resonance. However for $\mathbf{E}_1 \perp \mathbf{E}_2$, the emission time of the primary signal is independent of delay between $\mathbf{E}_1$ and $\mathbf{E}_2$, and hence is a free polarization decay (FPD) and arises from a homogeneously broadened resonance (there is a weak SPE present in Fig 1b, however it arises from a resonance which is 2.5 meV Stokes shifted from linear absorption peak, we tentatively assign this to an impurity bound exciton). The signal saturation characteristics for $\mathbf{E}_1 \| \mathbf{E}_2$ and $\mathbf{E}_1 \perp \mathbf{E}_2$ (Fig. 1b inset) are also quite different. For $\mathbf{E}_1 \| \mathbf{E}_2$ the signal exhibits strong saturation at fluxes above 3×10^{10}, whereas no saturation occurs for $\mathbf{E}_1 \perp \mathbf{E}_2$ at densities up to 2×10^{11}.

These differences indicate that the signals must be arising from separate resonances. The disparity in strength suggests that if both resonances are contributing for co-polarized fields only the signal from the inhomogeneously broadened one would be observable. This is confirmed by the presence of both a prompt and delayed contribution at high intensity where the inhomogeneously broadened resonance is strongly saturated.

The SPE for co-polarized fields has been attributed to localized excitons, where the dephasing and population relaxation are due to migration of excitons amongst localization sites [4]. The rapid dephasing and homogeneous nature of the resonance for cross-polarized fields is characteristic of the response from extended excitons. The observed dephasing rate of 5 ps is comparable to that observed for homogeneously broadened excitons in a high quality single quantum well [5]. Comparison of the temperature dependence of the dephasing

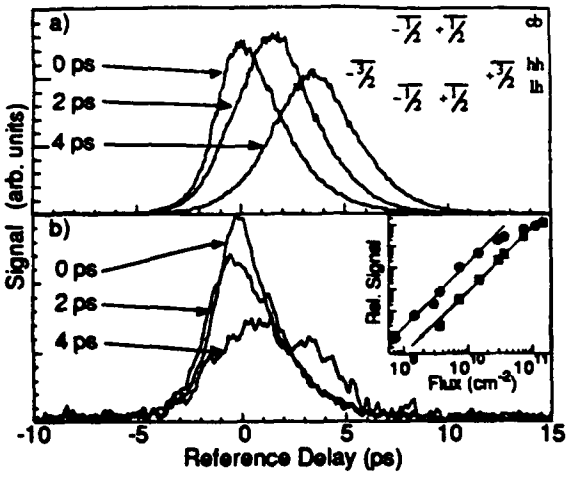

Figure 1. Cross correlation between the TFWM signal and a reference pulse. Upper panel is for co-polarized fields, the lower for $E_1 \perp E_2 \| E_3$, $E_S \| E_1$. In each panel the curves are for increasing E_1-E_2 delay. Upper inset is energy level structure for a GaAs quantum well, lower inset is saturation behavior of the two signals (circles for $E_1 \| E_2$, squares for $E_1 \perp E_2$, straight lines shows cubic behavior).

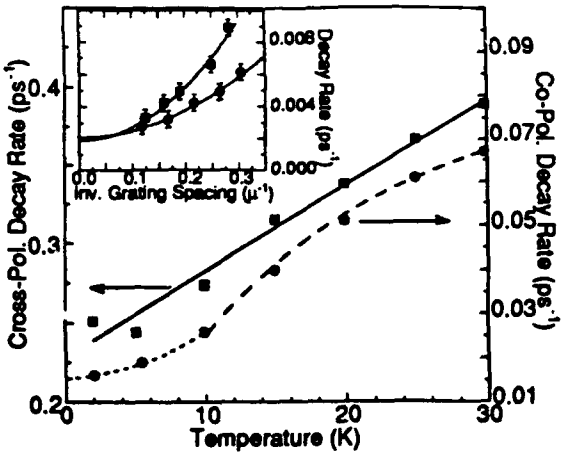

Figure 2. Temperature dependence of dephasing rates for co-polarized (circles, right axis) and cross-polarized (squares, left axis) signals. Lines are fit to theory. Note difference in axis scales. Inset shows grating spacing dependence of grating decay (same legend). The quadratic dependence shows that the diffusion coefficient, D, is larger for the prompt signal (D=10) than the echo (D=5).

rates (Fig. 2) and the relative mobilities (Fig. 2 inset) are consistent with this distinction. The temperature dependence of the co-polarized signal dephasing rate has the same functional form, as observed earlier, and matches theoretical predictions for phonon-assisted-migration of excitons at low temperature and thermal activation at slightly higher ones [4]. The dephasing rate for the cross-polarized signal exhibits a linear dependence on temperature, as expected for single phonon scattering of excitons and as observed in a single quantum well [5]. The increase in relaxation rate with decreasing grating spacing is due to spatial diffusion and shows that the excitation responsible for the prompt signal has a greater mobility than that responsible for the SPE, as would be expected for extended and localized states respectively (here the differing saturation characteristics are used to separate the two signals).

To understand the suppression of the signal for co-polarized fields we need to consider the origin of the TFWM signal and structure of the magnetic substates in a GaAs quantum well. Because the only allowed "transitions" are $\Delta m = \pm 1$ (since the heavy-hole-light-hole degeneracy is lifted by confinement) the incident fields should be considered in terms of circularly polarized components. A separate grating will be formed for each transition (although there is no net grating for an inhomogeneously broadened resonance, there is one for each frequency group). Cross-polarizing the fields which form the grating results in the grating for each transition being spatially 180° out of phase with each other. In an ideal semiconductor this will result in a cross-polarized signal. However, it is apparent that if there is a coupling between the excitation of the two transitions it will result in a reduction of the grating contrast for both, and a suppression of the signal.

To probe for such a coupling of the transitions we examine the polarization of the signal in a TFWM experiment with the first two fields co-circularly-polarized and the third field linearly polarized. These results are given in Fig. 3 as function of incident flux. At low density the signal is linearly polarized, demonstrating that both circular components of the third field are strongly scattered. Hence, there exists a coupling of the two transitions. At increasing density the inhomogeneous resonance saturates, and the signal is more circularly polarized (in the same sense as the first two fields) as would be expected in an ideal semiconductor.

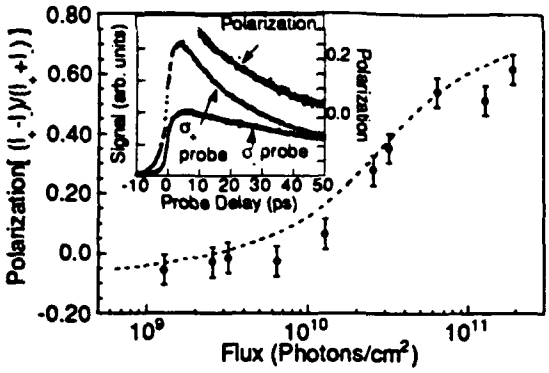

Figure 3. Polarization of signal field for co-circularly-polarized E_1 and E_2, and linearly polarized E_3 (dashed lined is a guide to the eye). Inset shows transient absorption response for probe fields co- and cross-circularly-polarized with respect to a circularly (σ_+) polarized pump, upper curve shows decay of polarization (offset for clarity)

Further evidence of a coupling is observed in transient absorption experiments using circularly polarized fields. Using a circularly polarized pump and a linearly polarized probe, which is resolved into circular components after passing through the sample, we are able to simultaneously probe the response of both transitions. The inset in Fig. 3 shows that both transitions respond essentially simultaneously. This has been confirmed with 200 fsec pulses.

The observed coupling is unexpected for an ideal semiconductor, however the presence of disorder modifies the response. Although spin relaxation results in a coupling of the transitions, it occurs on slower time scales [6, 7]. The relaxation of the polarization in Fig. 3 inset shows that it occurs on a 40 ps time scale in our sample. Based on circularly polarized transient absorption measurements in a narrow stepped quantum well it has been suggested that biexcitonic effects are important [7]. The coupling arises because the presence of an exciton in a localization site modifies the eigenstates for the creation of a second exciton in the vicinity, i.e. a biexciton is created. This has the effect of shifting the effective oscillator frequency by the biexciton binding energy and results in an induced transmission resonant with the pump, and an induced absorption Stokes shifted by the biexciton binding energy. This effect has been observed in our non-degenerate circularly polarized transient absorption measurements.

In summary, we have shown that there are two resonances present in GaAs MQW, and that their response can be separated by their polarization properties. The properties of these resonances are consistent with the simultaneous presence of both localized and extended excitons. The apparent simultaneous presence of both localized and extended states is not predicted by localization theory, especially in two dimensions where all states are thought to be localized by any disorder [8]. However, the interface disorder is complicated and recent work has suggested that the roughness spectrum may be bimodal where some regions may permit extended states [9]. Our results also clearly show that there is a strong coupling between opposite spin exciton transitions.

This work was supported by ARO and AFOSR, samples provide by P.K. Bhattacharya.

References

1. C. Weisbuch, R. Dingle, A.C. Gossard, and W. Wiegmann, Solid State Comm. **38**, 709 (1981).
2. J. Hegarty and M.D. Sturge, J. Opt. Soc. Am. B. **2**, 1143 (1985).
3. H.H. Yaffe, Y. Prior, J.P. Harbison, and L.T. Florez, Quant. Electr. Laser Sci., 1991; K. Leo, J. Shah, S. Schmitt-Rink, and K. Köhler, VIIth Int. Sym. Ultrafast Pro. Spec., 1991.
4. T. Takagahara, J. Lumin. **44**, 347 (1989); M.D. Webb, S.T. Cundiff, and D.G. Steel, Phys. Rev. B **43**, 12658 (1991).
5. L. Schultheis, A. Honold, J. Kuhl, K. Köhler, and C.W. Tu., Phys. Rev. B **34**, 9027 (1986).
6. T.C. Damen, K. Leo, J. Shah, and J.E. Cunningham, App. Phys. Lett. **58**, 1902 (1991).
7. S. Bar-Ad and I. Bar-Joseph, Phys. Rev. Lett. **68**, 349 (1992).
8. E. Abrahams, P.W. Anderson, D.C. Licciardello, and T.V. Ramakrishnan, Phys. Rev. Lett. **42**, 673 (1979).
9. D. Gammon, B.V. Shanabrook, and D.S. Katzer, Phys. Rev. Lett. **67**, 1547 (1991).

Polarization Dependent Coherent Nonlinear Spectroscopy: A Probe of Exciton Localization in Quantum Wells

S.T. Cundiff, H. Wang and D.G. Steel

Harrison M. Randall Laboratory of Physics, University of Michigan, Ann Arbor, Mi. 48109

(313)764-4469

Abstract

The polarization properties for linearly polarized light of the time resolved emission of the hh1 exciton picosecond four-wave-mixing response, yielding a photon echo and a free polarization decay, indicates that both localized and delocalized excitons are present. Measurements using circularly polarized light exhibit a strong and unexpected coupling between magnetic substates.

Polarization Dependent Coherent Nonlinear Spectroscopy: A Probe of Exciton Localization in Quantum Wells

S.T. Cundiff, H. Wang and D.G. Steel

Harrison M. Randall Laboratory of Physics, University of Michigan, Ann Arbor, Mi. 48109

(313)764-4469

Semiconductor heterostructures display optical and electronic properties which are influenced by the dynamics of electronic excitations. The nature of the dynamical processes is sensitive to disorder due to nonideal growth conditions. Carrier localization is a new process which arises in the presence of disorder, and measurements have shown that at low temperature excitons in multiple quantum wells (MQW) are localized and that localization effects are responsible for their relaxation [1]. We use resonant picosecond four-wave-mixing (FWM) to probe the disorder induced effects near the bandedge of GaAs/AlGaAs MQW. The observed optical response suggests that two distinct classes of excitons are present, and that their contribution to the optical response can be separated based upon their polarization properties. The unique energy and temperature dependences of the two classes indicate that the two classes correspond to localized and delocalized excitons. Picosecond transient absorption experiments using circularly polarized light are employed to further examine the polarization properties of the excitonic optical response.

A three pulse transient FWM experiment generates a signal which is emitted promptly on arrival of the third pulse if the system is homogeneously broadened and is called a free polarization decay (FPD). In the presence of inhomogeneous broadening the signal becomes delayed and is termed a stimulated photon echo (SPE). The signal from the hh1 exciton in a MQW is delayed when all three incident fields are linearly co-polarized. However, when the first field is cross-polarized the signal is transformed from a SPE to an FPD (Fig. 1). Clearly the signal for $\mathbf{E}_1 \| \mathbf{E}_2$ arises from an inhomogeneously broadened population, whereas the signal for $\mathbf{E}_1 \perp \mathbf{E}_2$ arises from a *homogeneously broadened transition*. Both the SPE and FPD are resonant with the hh1 exciton.

Measurement of the dephasing rate as a function of temperature and energy show a distinct difference between $\mathbf{E_1}\|\mathbf{E_2}$ and $\mathbf{E_1}\perp\mathbf{E_2}$ (Fig. 2). The complex functional form of the temperature dependence of the dephasing rate associated with the inhomogeneously broadened exciton corresponds to that expected for localized excitons [2], while the temperature dependence for the homogeneously broadened exciton is linear and corresponds to that expected for delocalized excitons [3]. Based on these data we believe that localized excitons give rise to the SPE and delocalized excitons are responsible for the FPD, and that their response can be separated based on their polarization properties.

The separation of the responses of localized and delocalized excitons occurs because the SPE from the localized excitons is suppressed for $\mathbf{E_1}\perp\mathbf{E_2}$. Such a suppression occurs when the excitations due to σ_+ and σ_- polarized light are coupled together (σ_+ and σ_- is the natural polarization description description in a quantum well because the axis of quantization is parallel to the direction of propagation for normal incidence). This coupling is directly demonstrated by frequency degenerate circularly polarized transient absorption measurements using a 3 ps pulse (1 meV spectral width) at low excitation density ($\approx 5\times10^7$ excitons/cm^2/layer). We observe that the response on both σ_+ and σ_- transitions is essentially *simultaneous* when only one is pumped. This coupling does indeed explain the suppression of the SPE, but the origin of such strong rapid coupling is itself of considerable interest. There are several mechanisms which can produce the observed effects. The results of non-degenerate transient absorption and circularly polarized SPE and FPD measurements for various time orderings provide a means to more clearly distinguish the different mechanisms contributing to the nonlinear response and will be presented.

This work is supported by ARO and AFOSR.

1. C. Weisbuch, R. Dingle, A.C. Gossard, and W. Wiegmann, Solid State Comm. **38**, 709 (1981); J. Hegarty and M.D. Sturge, J. Opt. Soc. Am. B. **2**, 1143-1154 (1985).

2. H. Wang, M. Jiang, and D.G. Steel, Phys. Rev. Lett. **65**, 1255-1258 (1990).

3. L. Schultheis, A. Honold, J. Kuhl, K. Köhler, and C.W. Tu., Phys. Rev. B **34**, 9027 (1986).

Figure Captions:

Fig 1: The cross correlation signal obtained by mixing the transient FWM signal with a reference pulse in a second harmonic crystal allows determination of the temporal characteristic of the signal. In a) the fields are co-polarized, and the signal emission clearly depends on the delay between $\mathbf{E_1}$ and $\mathbf{E_2}$, demonstrating its SPE nature. In b) $\mathbf{E_1} \perp \mathbf{E_2} \| \mathbf{E_3}$, $\mathbf{E_s} \| \mathbf{E_1}$, and the signal emission time is independent of the $\mathbf{E_1}$ - $\mathbf{E_2}$ delay. A weak SPE is evident in b), however this arises from a resonance which is 2.5 meV Stokes shifted.

Fig 2: Comparison of the dephasing rate as a function of temperature for $\mathbf{E_1} \| \mathbf{E_2}$ and $\mathbf{E_1} \perp \mathbf{E_2}$. For $\mathbf{E_1} \| \mathbf{E_2}$ the data are fit to phonon-assisted migration for T<10 K (short dash) and thermal activation for T > 10 K (long dash). A linear temperature dependence is observed for $\mathbf{E_1} \perp \mathbf{E_2}$ indicative of single phonon scattering. Note the difference in scales for left and right axes. The inset shows the dephasing rates as a function of energy at 5.5 K. All measurements are performed at low excitation density ($< 5 \times 10^7$).

Fig 3: Transient absorption for various energies within the exciton line for a circularly polarized pump. For each energy the response for a probe co-rotating with the pump (designated by dots) and counter-rotating is given. The upper panel shows the spectral position of the measurements with respect to the heavy and light hole exciton, where the width of the bar roughly denotes the laser bandwidth (FWHM). The autocorrelation of the incident pulses is given at the bottom for reference.

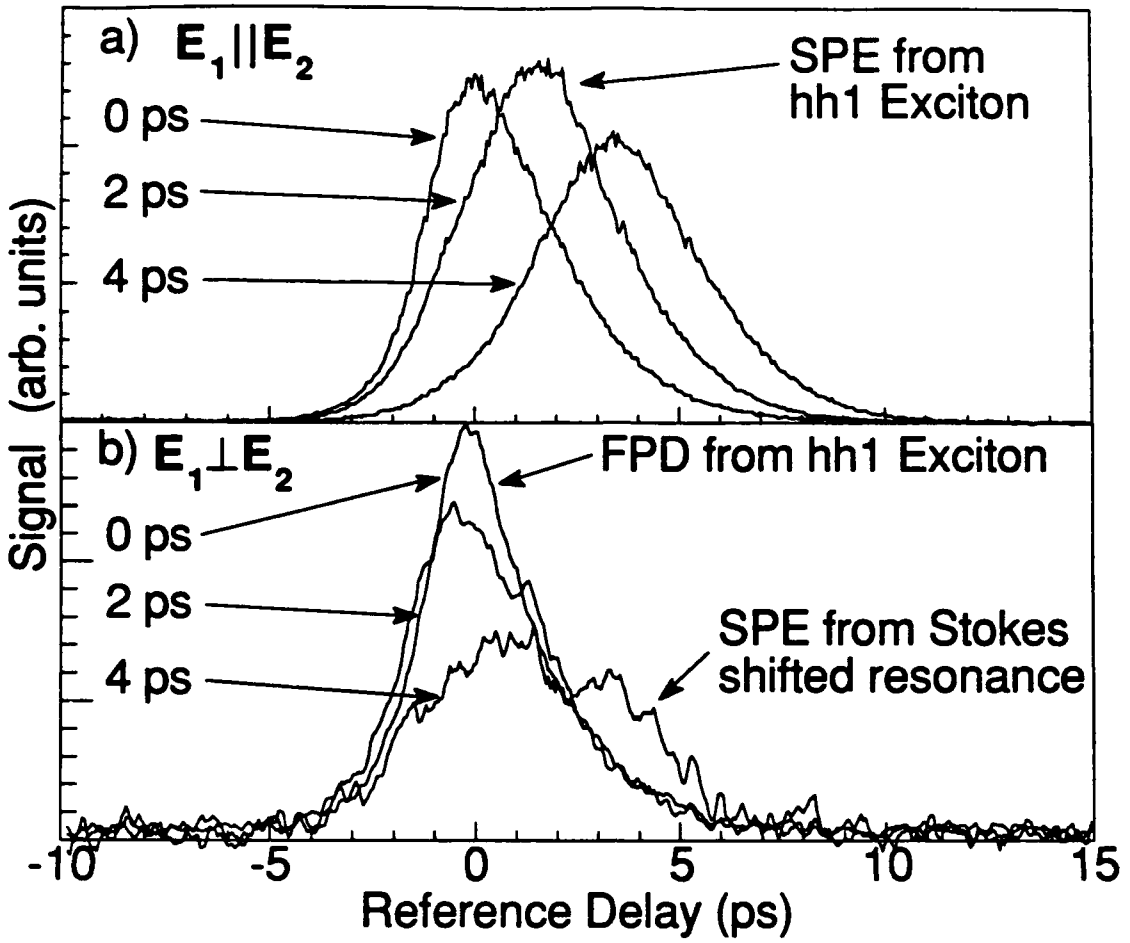
a) $E_1 || E_2$
0 ps
2 ps
4 ps
SPE from
hh1 Exciton
b) $E_1 \perp E_2$
0 ps
2 ps
4 ps
FPD from hh1 Exciton
SPE from Stokes
shifted resonance
Signal (arb. units)
-10
-5
0
5
10
15
Reference Delay (ps)

Figure 1.

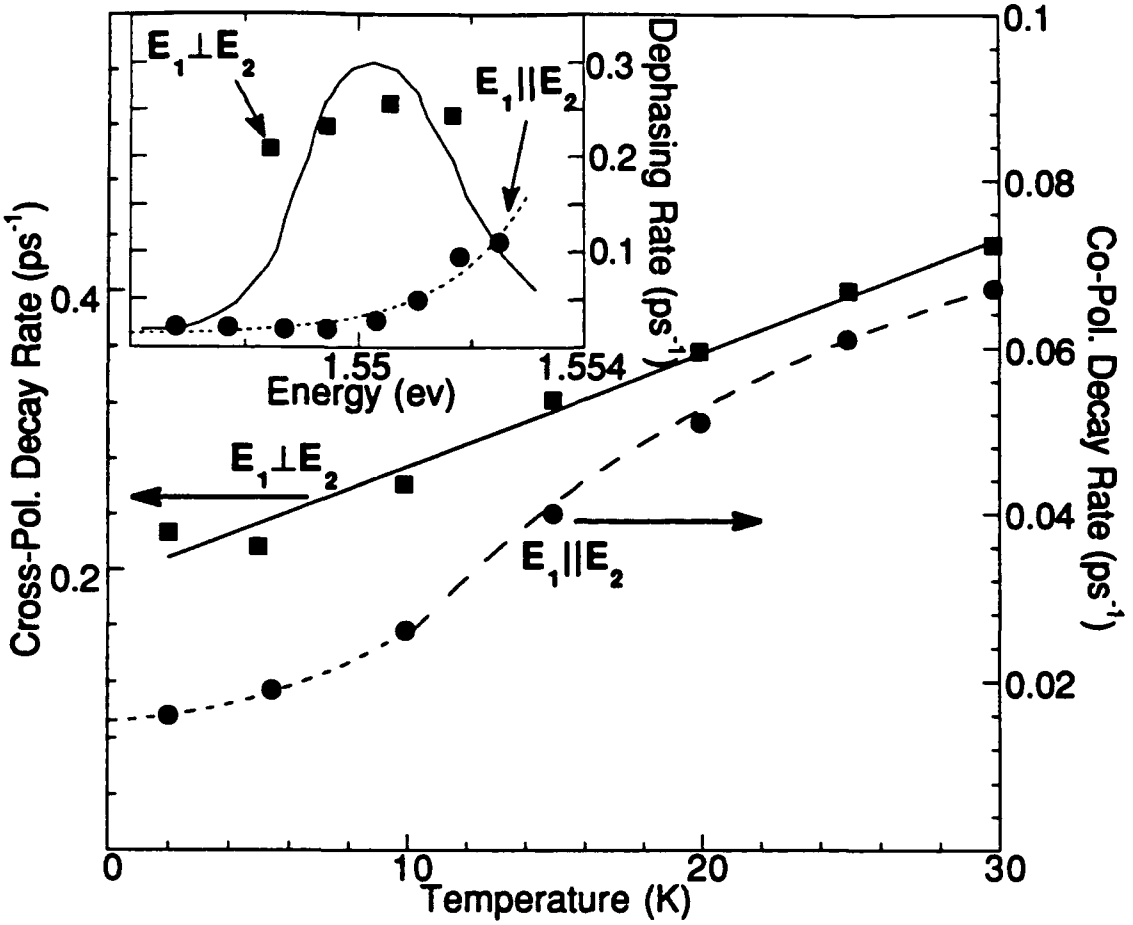
E1⊥E2
E1||E2
Dephasing Rate (ps-1)
0.3
0.2
0.1
1.55
1.554
Energy (ev)
Cross-Pol. Decay Rate (ps-1)
Co-Pol. Decay Rate (ps-1)
0.4
0.2
0.1
0.08
0.06
0.04
0.02
E1⊥E2
E1||E2
0
10
20
30
Temperature (K)

Figure 2.

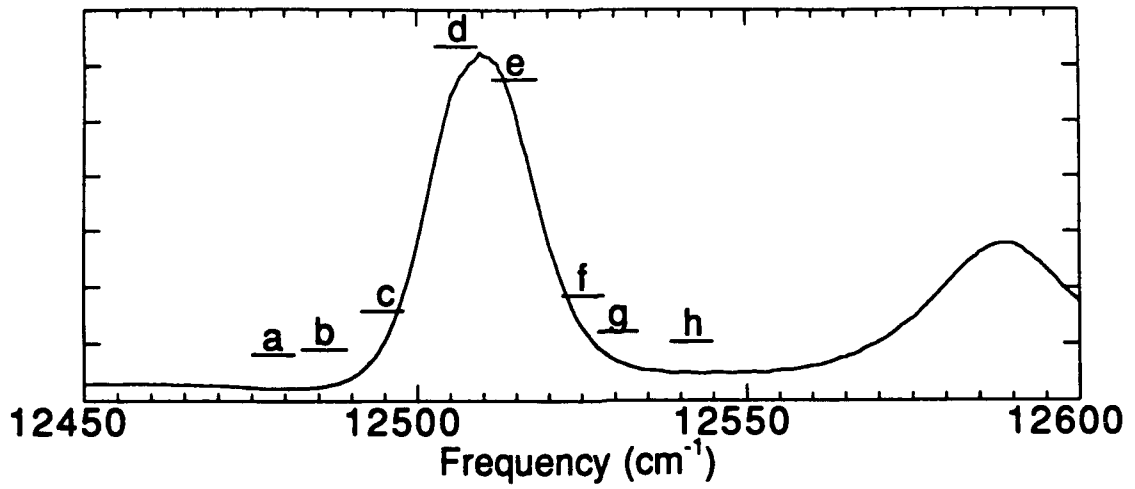
d
e
f
c
g
h
a
b
12450
12500
12550
12600
Frequency (cm-1)

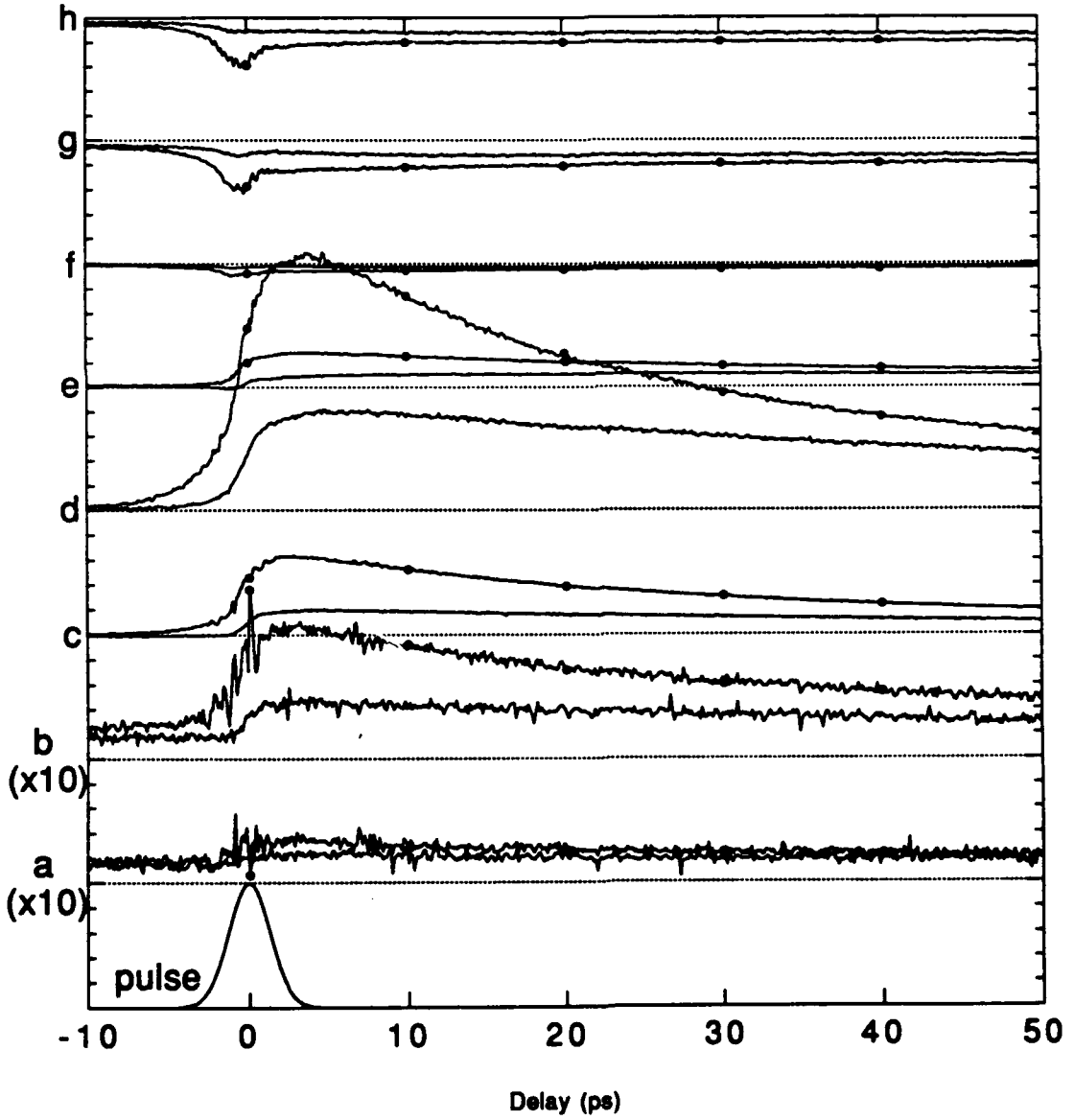
h
g
f
e
d
c
b
(x10)
a
(x10)
pulse
-10
0
10
20
30
40
50
Delay (ps)

Picosecond Photon Echoes and Free Polarization Decay from Localized and Delocalized States in GaAs Quantum Wells

S.T. Cundiff, H. Wang and D.G. Steel

Harrison M. Randall Laboratory of Physics, University of Michigan, Ann Arbor, Mi. 48109

(313)764-4469

Abstract

The time resolved emission of the hh1 exciton picosecond backward four-wave-mixing response in multiple quantum wells is either delayed (photon echo) or prompt (free polarization decay), depending on the relative polarization of the excitation beams, indicating the presence of both localized and delocalized excitons.

Picosecond Photon Echoes and Free Polarization Decay from Localized and Delocalized States in GaAs Quantum Wells

S.T. Cundiff, H. Wang and D.G. Steel

Harrison M. Randall Laboratory of Physics, University of Michigan, Ann Arbor, Mi. 48109

(313)764-4469

Many of the optical and electronic properties of semiconductor heterostructures depends on the dynamics of electronic excitations. Disorder due to nonideal growth conditions can modify these properties and allow new dynamical processes not present in an ideal crystal. One such process is carrier localization on an atomic scale. Indeed measurements have shown the presence of exciton localization [1], the presence of a mobility edge [2], and that low temperature excitonic relaxation proceeds via phonon assisted migration between localization sites [3]. Using resonant picosecond four-wave-mixing (FWM) laser spectroscopy we probe the complex nature of disorder induced effects near the bandedge of GaAs/AlGaAs multiple quantum well (MQW) structures at low temperature. The results suggest that two distinct classes of excitons contribute to the optical response, and that their response is separable based upon their polarization properties. The unique energy and temperature dependences of the dephasing rate indicate the two classes correspond the localized and delocalized excitons.

In the presence of inhomogeneous broadening the signal emitted by a three pulse transient FWM experiment is delayed with respect to the third pulse and termed a stimulated photon echo (SPE). The emission from a homogeneously broadened system is prompt and is called a free polarization decay (FPD). When all three incident pulses are linearly co-polarized the signal from the hh1 excitonic resonance in a MQW is indeed delayed. However, when the first field is cross-polarized the signal is transformed from a SPE to a FPD (Fig. 1). Clearly the signal for $\mathbf{E}_1 \| \mathbf{E}_2$ is arising from an inhomogeneously broadened population, whereas the signal for $\mathbf{E}_1 \perp \mathbf{E}_2$ must be arising from a *homogeneously broadened transition*. The amplitude for $\mathbf{E}_1 \perp \mathbf{E}_2$ is reduced by one

to two orders of magnitude, depending on the excitation wavelength, however both the SPE and FPD are resonant with the hh1 exciton.

Measurement of the dephasing rate as a function of exciton energy shows a distinct difference between that for $\mathbf{E_1}\|\mathbf{E_2}$ and $\mathbf{E_1}\perp\mathbf{E_2}$ (Fig. 2). For $\mathbf{E_1}\|\mathbf{E_2}$ the rate is 0.016 ± 0.001 ps^{-1} on the low energy side, and increases through line center to a rate of 0.1 ± 0.02 ps^{-1} on the high energy side. In contrast for $\mathbf{E_1}\perp\mathbf{E_2}$ the rate is much faster (0.20-0.25 ps^{-1}) and nearly constant across line center. The temperature dependence of the dephasing rates also show the very different behavior for the two cases (Fig. 3). For $\mathbf{E_1}\|\mathbf{E_2}$ the rates follow the functional form expected for dephasing due to migration between localization sites [3]. However for $\mathbf{E_1}\perp\mathbf{E_2}$ the rate is linearly dependent on temperature, as would be expected for single phonon scattering. Both the magnitude of the low temperature dephasing rate, and the temperature dependence are in reasonable agreement with results observed for delocalized excitons in a high quality single quantum well [4]. Based on these data we believe that localized excitons give rise to the SPE, while delocalized excitons give rise to the FPD. The two classes of excitons may be isolated by their polarization properties. These results show that both localized and delocalized excitons contribute to the optical response and is mostly likely the result of microscopic spatial inhomogeneity in the interface roughness spectrum [5]. This work was supported by ARO and AFOSR.

1. C. Weisbuch, R. Dingle, A.C. Gossard, and W. Wiegmann, Solid State Comm. **38**, 709 (1981).

2. J. Hegarty and M.D. Sturge, J. Opt. Soc. Am. B. **2**, 1143-1154 (1985).

3. H. Wang, M. Jiang, and D.G. Steel, Phys. Rev. Lett. **65**, 1255-1258 (1990).

4. L. Schultheis, A. Honold, J. Kuhl, K. Köhler, and C.W. Tu., Phys. Rev. B **34**, 9027 (1986).

5. D. Gammon, B.V. Shanabrook, and D.S. Katzer, Phys. Rev. Lett. **67**, 1547 (1991); C.A. Warwick, W.Y. Jan, A. Ourmazd, and T.D. Harris, App. Phys. Lett. **56**, 2666 (1990).

Figure Captions

Fig. 1: The cross correlation signal obtained by mixing transient FWM signal with a reference pulse in a second harmonic crystal allows determination of the temporal characteristics of the signal. In a) all fields are co-polarized, and the signal is emission clearly depends upon the delay between $\mathbf{E_1}$ and $\mathbf{E_2}$, demonstrating its SPE nature. In b) $\mathbf{E_1} \perp \mathbf{E_2} \| \mathbf{E_3}$, $\mathbf{E_s} \| \mathbf{E_1}$, and the signal emission time is independent of the $\mathbf{E_1}$-$\mathbf{E_2}$. A weak echo is evident in b), however this arises from a resonance which is 2.5 meV Stokes shifted.

Fig. 2: Comparison of the dephasing rate for $\mathbf{E_1} \| \mathbf{E_2}$ and $\mathbf{E_1} \perp \mathbf{E_2}$ as a function of energy at 5.5 K. The linear absorption spectrum (solid line) is displayed for comparison. All measurements are performed at low excitation density ($< 5 \times 10^7$).

Fig. 3: Comparison of the dephasing rate as function of temperature for $\mathbf{E_1} \| \mathbf{E_2}$ and $\mathbf{E_1} \perp \mathbf{E_2}$. For $\mathbf{E_1} \| \mathbf{E_2}$ the data are fit to phonon-assisted migration for T<10 (short dash) K and thermal activation for T>10K (long dash). A linear temperature dependence if observed for $\mathbf{E_1} \perp \mathbf{E_2}$ indicative of single phonon scattering. Note the difference in scale for left and right axes.

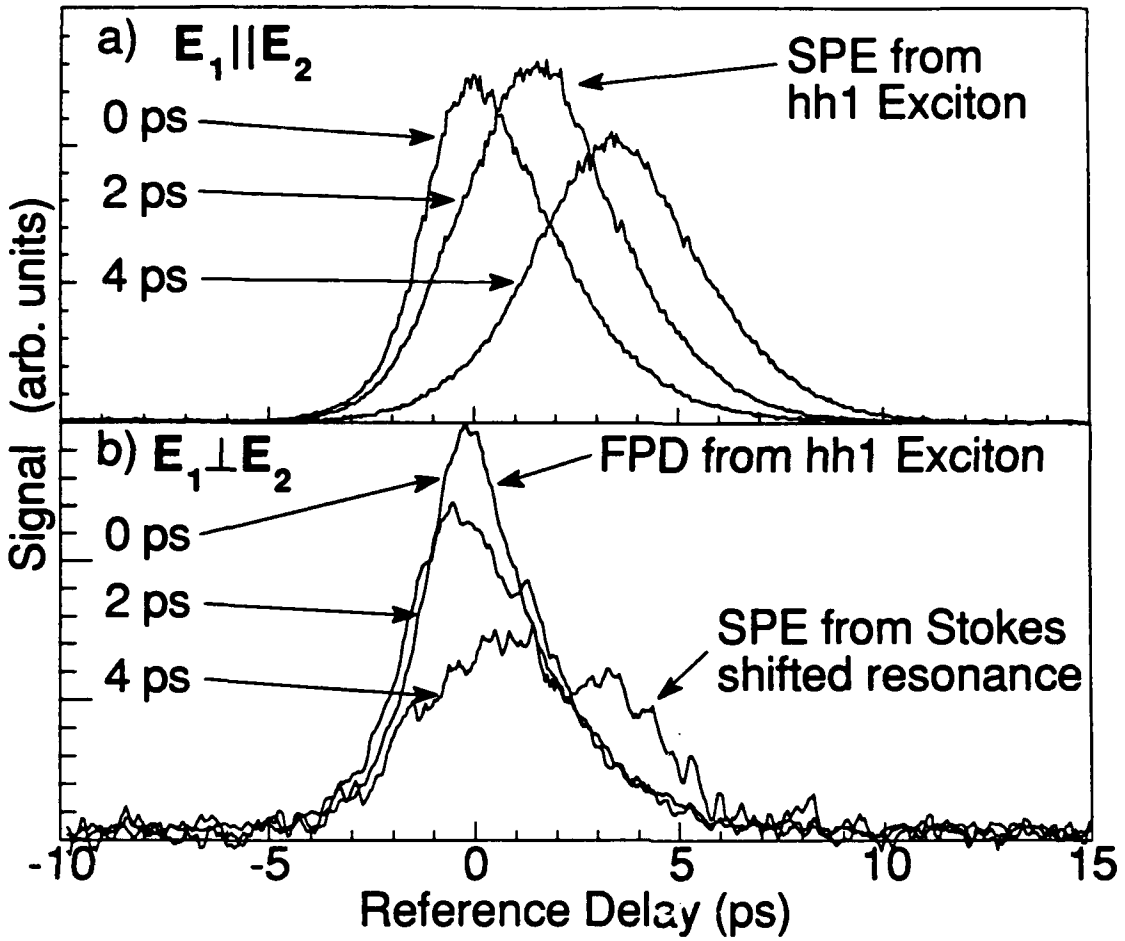
a) $E_1 || E_2$
0 ps
2 ps
4 ps
SPE from
hh1 Exciton
b) $E_1 \perp E_2$
0 ps
2 ps
4 ps
FPD from hh1 Exciton
SPE from Stokes
shifted resonance
Signal (arb. units)
-10
-5
0
5
10
15
Reference Delay (ps)

Figure 1.

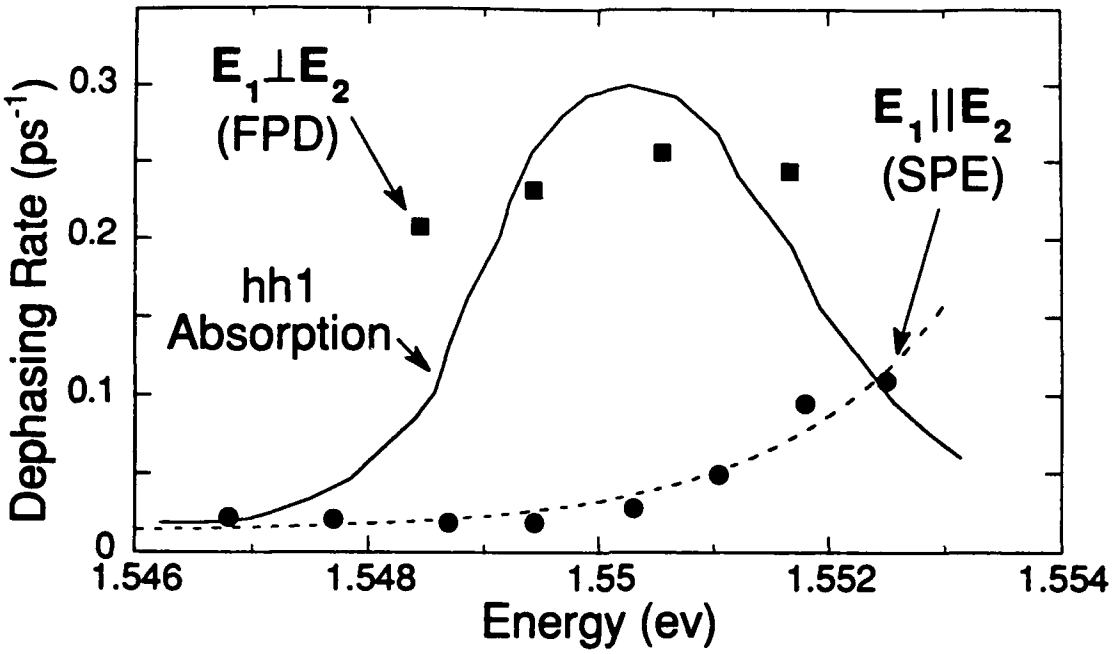
$E_1 \perp E_2$
(FPD)
$E_1 \| E_2$
(SPE)
hh1
Absorption
Dephasing Rate (ps^{-1})
0.3
0.2
0.1
0
1.546
1.548
1.55
1.552
1.554
Energy (ev)

Figure 2.

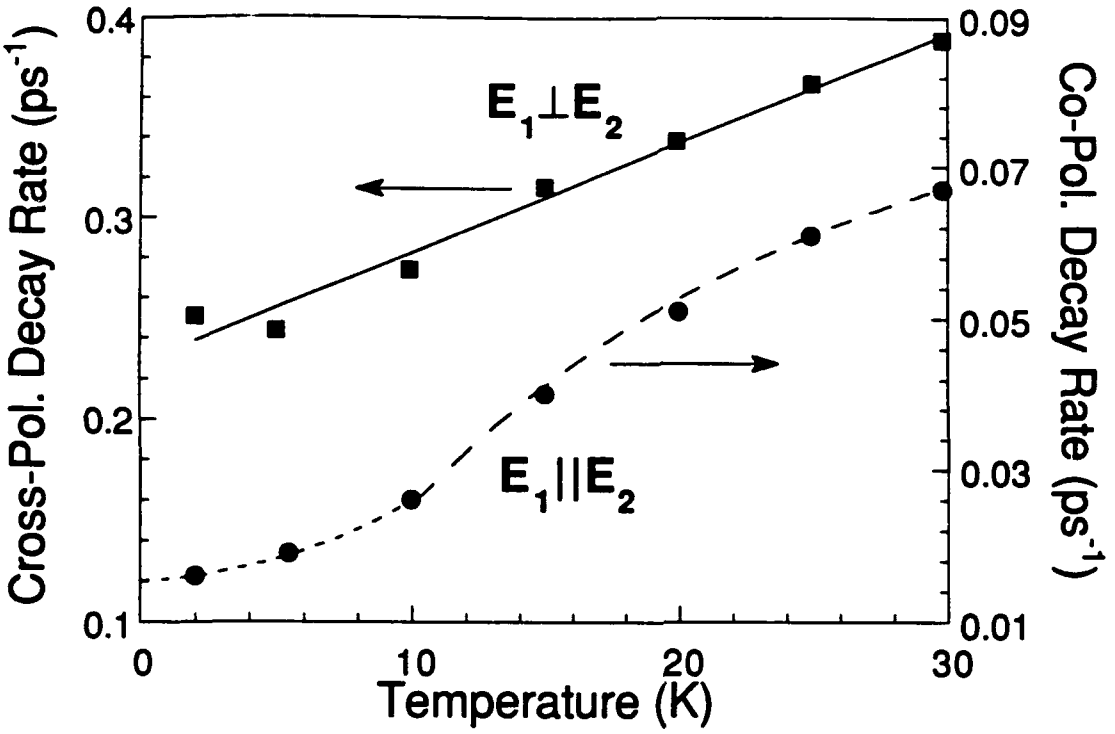
Cross-Pol. Decay Rate (ps^{-1})
Co-Pol. Decay Rate (ps^{-1})
Temperature (K)
$E_1 \perp E_2$
$E_1 \| E_2$
0.4
0.3
0.2
0.1
0.09
0.07
0.05
0.03
0.01
0
10
20
30

Figure 3.

Coupling Between Excitonic Magnetic Substates in GaAs Multiple Quantum Wells

S.T. Cundiff, V. Subramaniam, H. Wang and D.G. Steel

Harrison M. Randall Laboratory of Physics

University of Michigan, Ann Arbor, Mi. 48109

(313)764-4469

Abstract

Low temperature picosecond and femtosecond transient absorption measurements on GaAs/AlGaAs multiple quantum wells using circularly polarized light demonstrate strong and unexpected coupling between excitonic magnetic substates. The data suggests the coupling may be due in part to a combination of band hybridization and biexciton effects in the presence of disorder.

Coupling Between Excitonic Magnetic Substates in GaAs Multiple Quantum Wells

S.T. Cundiff, V. Subramaniam, H. Wang and D.G. Steel

Harrison M. Randall Laboratory of Physics

University of Michigan, Ann Arbor, Mi. 48109

(313)764-4469

Recent three pulse transient four-wave-mixing (FWM) measurements on hh1 excitons in GaAs/AlGaAs multiple quantum wells (MQW) using linearly polarized incident fields have shown that the nature of the emitted signal is transformed from a stimulated photon echo (SPE) to a free polarization decay (FPD) by rotating the polarization of the first field [1]. Dephasing rate data indicates that the SPE and FPD arise from separate populations of excitons present in the MQW, corresponding to excitons localized by disorder and delocalized excitons. The SPE is unexpectedly suppressed for cross polarized fields due to coupling between the excitations induced by σ_+ and σ_- polarized light (σ_+ and σ_- is the natural polarization description in a quantum well because the axis of quantization is parallel to the direction of propagation for normal incidence).

To demonstrate the coupling and investigate the mechanisms responsible we perform transient absorption measurements with a circularly polarized light, where the pump and probe are degenerate in frequency. Using a 3 ps pulse (1 meV spectral width) to allow spectrally selective probing of the excitons we observe that the response of both transitions is essentially *simultaneous*. These data are taken at 5.5 K and at low excitation density ($\approx 5\text{x}10^7$ excitons/cm^2/layer) where the results are density independent.

The observation of such rapid coupling indeed explains the suppression of the SPE signal, however the origin of the strong coupling is itself of considerable interest. The instantaneous nature of the coupling is confirmed by observations using 200 fsec pulses. However the induced

transmission observed with 3 psec pulses on the low energy side of the exciton distribution in Fig.1 becomes an induced absorption when 200 fsec pulses are used (Fig. 2).

Time resolved circularly polarized luminescence measurements have demonstrated that spin relaxation does occur in quantum wells, however the time scale is of order of tens of picoseconds [2]. Indeed spin relaxation is an important mechanism for the long time behavior of our observations, however, it is unlikely that spin relaxation plays a role on sub-picosecond time scales. Band hybridization between the light and heavy hole in a quantum well results in a $m = \pm 1/2$ component in the hh1 exciton wavefunction [3] and qualitatively explains the low energy results in Fig. 1, although it does not seem to explain the induced absorption observed in both Fig. 1 and 2. There are a number of possible explanations for the latter effect, including two photon absorption and coherent effects. Two photon absorption can proceed coherently, resulting in a biexciton, or stepwise resulting in a biexciton, a process which in enhanced by the presence of disorder. The results of SPE and FPD measurements using circularly polarized excitation for various time orderings provide a means to more clearly distinguish the different nonlinear processes contributing to these interactions and will be presented. This work is supported by ARO and AFOSR.

1. S.T. Cundiff, H. Wang, and D.G. Steel, submitted to Phys. Rev. Lett. (1991).
2. T.C. Damen, K. Leo, J. Shah, and J.E. Cunningham, App. Phys. Lett. **58**, 1902 (1991).
3. G.D. Sanders and Y.-C. Chang, Phys. Rev. B **32**, 5517-5520 (1985).

Figure Captions

Figure 1: Transient absorption for various energies within the exciton line for a circularly polarized pump. For each energy the response for a probe co-rotating with the pump (designated by dots) and counter-rotating is given. The upper panel shows the spectral position of the measurements with respect to the heavy and light hole exciton, where the width of the bar roughly denotes the laser bandwidth (FWHM). The autocorrelation (3 ps) of the incident pulses is given at the bottom for reference.

Figure 2: Transient absorption using a 200 fsec pulse. Note that the response has become purely an induced absorption and is still essentially instantaneous. Weak quantum beats between the hh1 and lh1 excitons are evident.

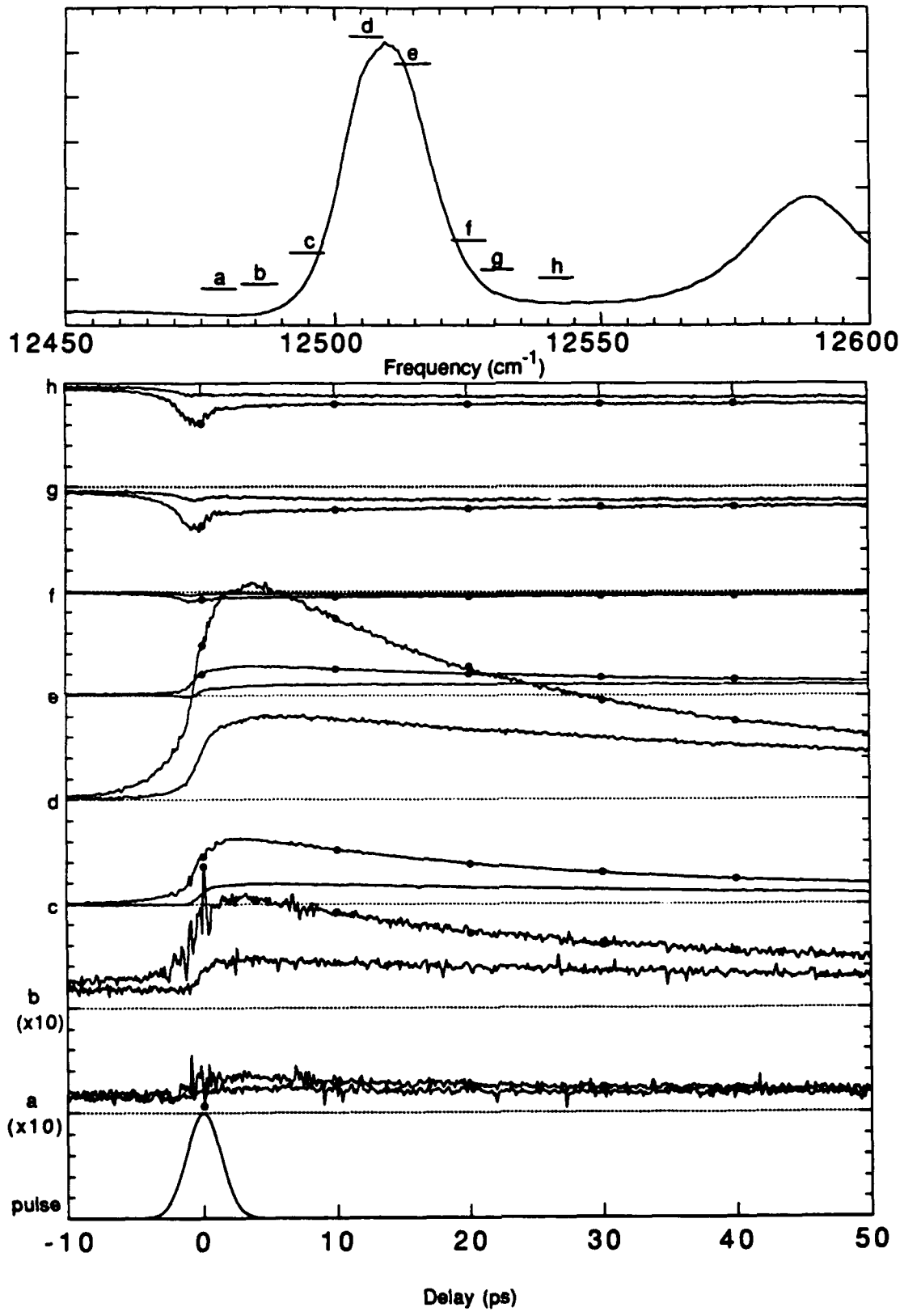
d
e
f
c
g
a
b
h
12450
12500
12550
12600
Frequency (cm-1)
h
g
f
e
d
c
b
(x10)
a
(x10)
pulse
-10
0
10
20
30
40
50
Delay (ps)

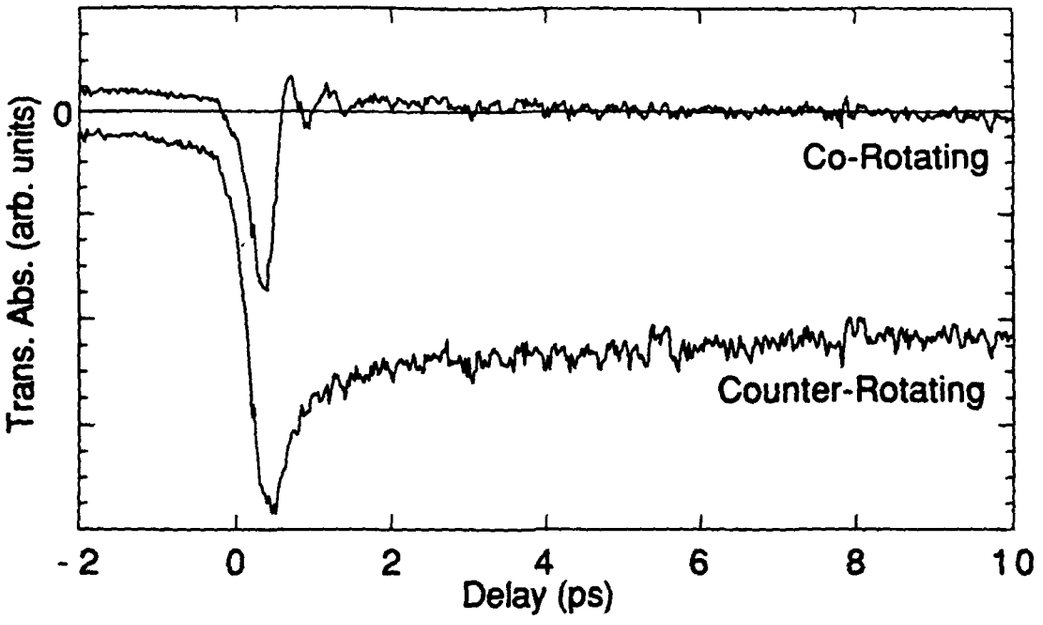
Trans. Abs. (arb. units)
0
Co-Rotating
Counter-Rotating
-2
0
2
4
6
8
10
Delay (ps)

Figure 2

Spin-Flip Induced Spectral Hole Burning of Magnetoexcitons in GaAs/AlGaAs Quantum Wells

Hailin Wang, Min Jiang, R. Merlin, Duncan G. Steel

The Randall Laboratory of Physics
The University of Michigan, Ann Arbor, MI 48109-1120

313-764-4469

Abstract

High resolution frequency domain four wave mixing measurements show spectral hole burning due to the "spin"-flip of localized magnetoexcitons in GaAs quantum wells. The results show the Zeeman doublet and provide a direct measure of the magnetoexciton Zeeman splitting.

Spin-Flip Induced Spectral Hole Burning of Magnetoexcitons in GaAs/AlGaAs Quantum Wells

Hailin Wang, Min Jiang, R. Merlin, Duncan G. Steel

The Randall Laboratory of Physics
The University of Michigan, Ann Arbor, MI 48109-1120

The density of states in a quantum well structure is fully quantized under a magnetic field parallel to the growth axis. As a result, relaxation of carriers or excitons between spin-split levels can only take place via inelastic processes, leading to a substantial increase of the spin relaxation time[1]. Using frequency domain four wave mixing (FWM) and selective optical excitation, we are able to probe for the first time the "spin"-flip transitions of localized magnetoexcitons and measure directly their Zeeman splitting.

The experimental configuration is based on backward FWM [2]. Two nearly degenerate beams designated the forward pump and probe interact in the sample exciting a narrow spectral hole within the inhomogeneous profile. A third beam, designated the backward pump, probes the steady-state distribution of the excitation. The width of the hole burning FWM response as a function of the backward pump frequency can be shown to be twice the homogeneous line width. Note that in contrast to the conventional hole burning, complications due to the exciton spectral diffusion can be substantially reduced in FWM measurements by appropriately detuning the forward pump and probe [2].

Samples used in our measurement consist of 10 periods of 98 Å GaAs and 96 Å $Al_{0.3}Ga_{0.7}As$. The structures show a 1 meV absorption line width for the lowest heavy hole (HH1) exciton. The nonlinear measurements are carried out at 2.5 K and at 4 T in the range of HH1 excitons (see Fig. 1 for the energy level diagram in a magnetic field). In the first set of measurements, three circularly polarized optical beams rotating in the same direction in the lab frame were used. The nonlinear optical response, shown in Fig. 2a, involves only excitons associated with the -3/2 to -1/2 transition. The width of the response corresponds to a

magnetoexciton homogeneous width of 0.03 meV, confirming the localized nature of the exciton [3]. If an exciton created with the forward pump and probe flips its "spin" at the same localization site, it appears as an exciton created in 3/2 to 1/2 transition. Experimentally, spin-flipped magnetoexcitons can be probed by reversing the polarization direction of the backward pump. The resulting nonlinear response shown in Fig. 2b clearly shows narrow hole burning at a new energy with the energy difference being the exciton Zeeman splitting. The small residual signal at the previous hole burning position is most likely due to the small residual ellipticity of the circularly polarized beams. The relatively constant background signal in Fig. 2b is due to excitons that have spectrally diffused [3]. Furthermore, using linearly polarized light for the backward pump and keeping the forward pump and probe exciting only the -3/2 to -1/2 transition, we probed simultaneously the hole burning associated with the -3/2 to -1/2 transition and the spin-flip induced hole burning associated with the 3/2 to 1/2 transition. The nonlinear response obtained (see Fig. 3) shows two well resolved peaks. The separation gives a Zeeman splitting of 0.19 meV at 4 T, which is smaller than that reported previously in a quantum beat experiment [4]. The small response for the 3/2 to 1/2 transition indicates that the exciton "spin"-flip time is longer than the spectral diffusion time. A rate equation estimate gives a spin flip time of order 100 ps. In addition, and as expected, we found that the spin-flip rate decreases rapidly with increasing magnetic fields.

This work is supported by AFOSR and ARO.

References:

(1) M. Potemski, J.C. Maan, A. Fasolino, K. Ploog, and G. Weimann, Phys. Rev. Lett. **20**, 2409 (1989).

(2) H. Wang and D. G. Steel, Phys. Rev. **A43**, 3823 (1991).

(3) H. Wang, M. Jiang, and D.G. Steel, Phys. Rev. Lett. **65**, 1255 (1990).

(4) S. Bar-Ad and I. Bar-Joseph, Phys. Rev. Lett. **66**, 2491 (1991).

Figure Captions.

Figure 1. Electron and heavy hole energy levels in GaAs quantum well in a magnetic field parallel to the growth axis.

Figure 2. FWM nonlinear optical responses as a function of the backward pump energy. A forward pump and probe detuning of 140 MHz is used in all measurements to avoid complication due to spectral diffusion. (a) All three beams interact with the -3/2 to -1/2 transition. (b) The backward pump beam interacts with the 3/2 to 1/2 transition. Dashed lines are Lorentzian fits to the response.

Figure 3. FWM nonlinear optical response with the backward pump beam linearly polarized. The forward pump and probe interact only with the -3/2 to -1/2 transition. The line shape shows well resolved Zeeman doublet. The Solid line is the exciton absorption spectrum. Dashed lines are a guide to the eye.

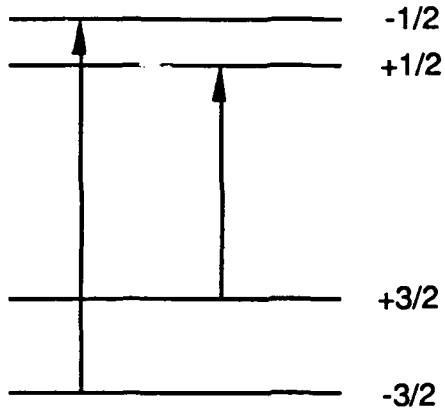

Fig. 1

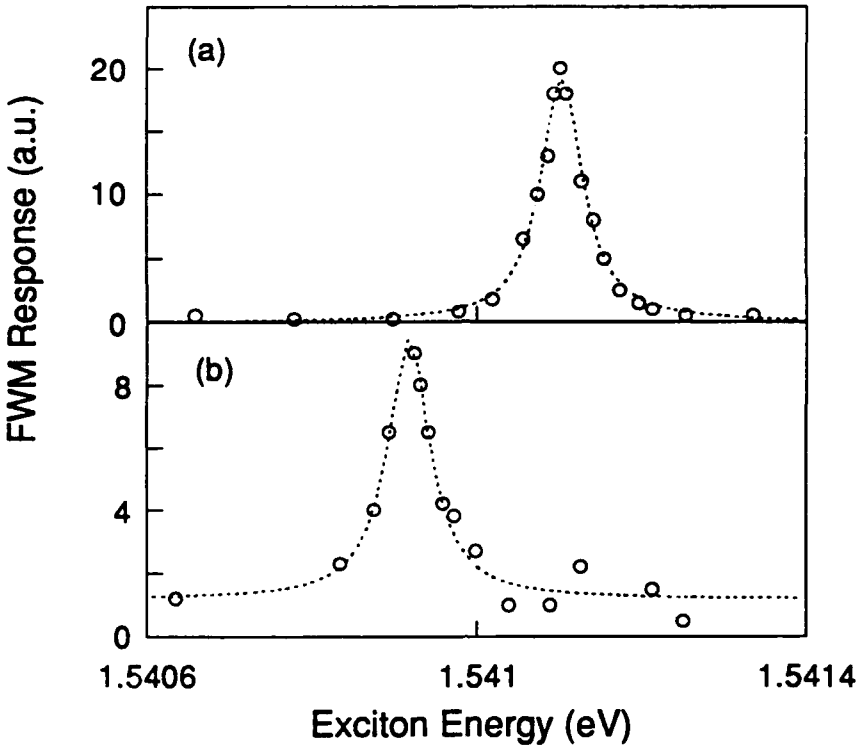
(a)
(b)
20
10
0
8
4
0
FWM Response (a.u.)
1.5406
1.541
1.5414
Exciton Energy (eV)

Fig. 2

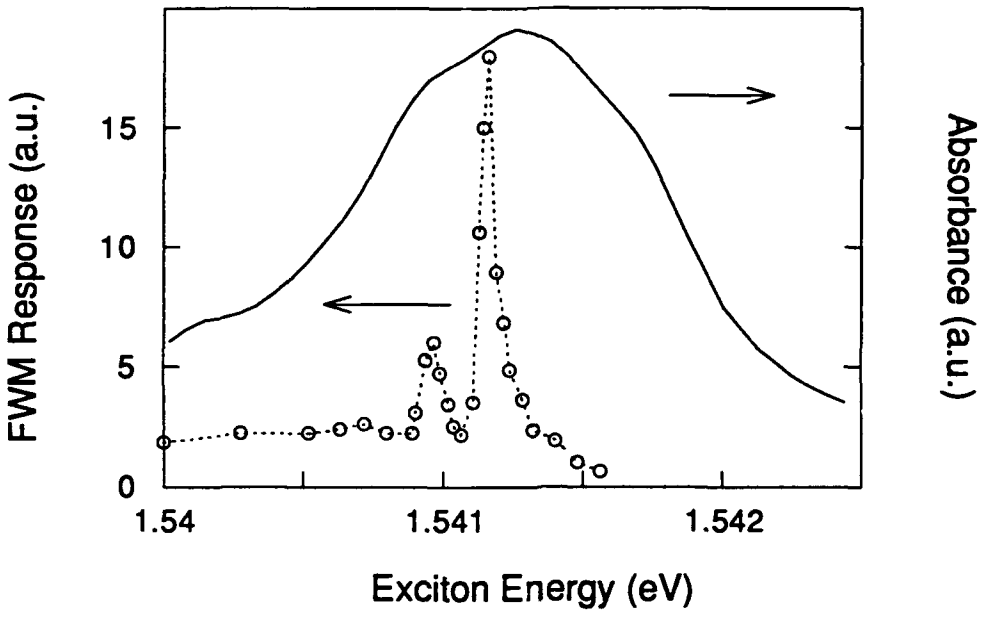
FWM Response (a.u.)
15
10
5
0
1.54
1.541
1.542
Exciton Energy (eV)
Absorbance (a.u.)

Fig. 3

High Resolution Nonlinear Magneto-Optical Spectroscopy in MBE Grown GaAs

Min Jiang, Hailin Wang, R. Merlin, D.G. Steel

The Harrison M. Randall Laboratory of Physics

The University of Michigan, Ann Arbor, MI 48109-1120

313-764-4469

Abstract

We present results of high resolution nonlinear magneto-optical studies in GaAs thin film. Measurements show an enhancement of the nonlinear optical response and a reduction of the magnetoexciton mobility. High Landau-level excitonic nonlinear optical processes is also discussed.

High Resolution Nonlinear Magneto-Optical Spectroscopy in MBE Grown GaAs

Min Jiang, Hailin Wang, R. Merlin, D.G. Steel
The Harrison M. Randall Laboratory of Physics
The University of Michigan, Ann Arbor, MI 48109-1120
313-764-4469

The presence of strong magnetic fields significantly modifies electronic states of a semiconductor, such as quantization of energy levels (Landau levels) and shrinkage of exciton wave functions [1]. Consequently, significant changes in optical as well as transport properties of the material are expected. In this paper, we report observations of an enhanced nonlinear optical response and a dramatic reduction of mobilities for magnetoexcitons in GaAs. We also discuss nonlinear optical measurements of excitons associated with higher Landau levels.

Our measurements are based on frequency domain four wave mixing (FWM) [2], and are carried out at 2.5 K on MBE grown GaAs film of 0.2 μm thickness. At zero field, the sample is homogeneously broadened, and has a 1s exciton absorption line width of 0.2 meV as shown in Fig.1a. The light-heavy hole degeneracy is lifted by strain introduced during the etching process. The linear absorption displays a rich structure at 6 T (see Fig. 1b). The features are likely the combined result of strain and impurity bound excitons. However, the nonlinear optical response (Fig. 1c) obtained through cw degenerate FWM exhibits a quite different structure. The energy separation and the magnetic field dependence of the dominant peaks in the nonlinear spectrum suggest that these peaks are due to magnetoexcitons associated with Landau levels, indicating a significant enhancement of the excitonic nonlinear magneto-optical response above the heavy hole exciton compared to the nonlinear response at 0 T.

The exciton diffusion coefficient is obtained using standard nearly degenerate FWM methods in which grating decay rates are measured as a function of the grating spacing [3]. Figure 2a and 2b display nearly degenerate FWM line shapes obtained at two different field strengths.

The width of the response is given by $\Gamma=\gamma+4\pi^2D/\Lambda^2$, where γ is the excitation decay rate and Λ is the grating spacing. Dramatic field-induced changes in the grating decay rate are evident in Fig. 2b. Figure 2c plots the magnetic dependence of the exciton diffusion coefficient which at 1 T is reduced by a factor of 5 compared to the value at zero field. The reduction of the exciton mobility is likely the result of the smaller Bohr radius in the presence of a magnetic field. In this case exciton scattering by weak or small scale disorder may become important. Note that the smaller grating decay rates also lead to enhanced nonlinear optical responses for magnetoexcitons.

Nearly degenerate FWM measurements on excitons associated with the second and third Landau levels also reveal interesting phenomena. First, decay of the CW nonlinear response is of the order of the exciton recombination time. Second, measurements using selective optical excitation show that the nonlinear signal arises from excitons associated with the σ^- transition. If the nonlinear optical response is primarily due to phase space filling and exchange effects, the first observation would imply that the inter-Landau level transfer rate is slower than or comparable with the exciton recombination rate. If the inter-Landau level interaction is responsible for the nonlinear optical response of excitons associated with high Landau levels, the second observation would suggest a spin dependent inter-exciton interaction. Further studies including magnetoexciton photoluminescence and CW pump-probe measurements, which are helpful in understanding current nonlinear measurements, will also be presented.

This work is supported by ARO and AFOSR.

References

1. R. J. Elliot and R. Loudon: J. Phys. Chem. Solids, **15**, 196(1991)

2. H. Wang, M. Jiang, D. G. Steel, Phys. Rev. Lett. **65**,1255 (1990)

3. J.T. Remillard et al., Optics Letters **14**, 1131(1989)

Figure Captions:

Fig.1 (a) Low temperature linear absorption at zero field. Peaks above 1.538 eV are due to a QW structure contained in the sample. (b) Low temperature linear absorption and degenerate FWM response at 6 T.

Fig.2 Nearly degenerate FWM responses for measurement of grating decay rate. (a) At zero field (b) At 2 T, same grating spacing as in (a). (c) The magnetic field dependence of the diffusion coefficient of magnetoexcitons.

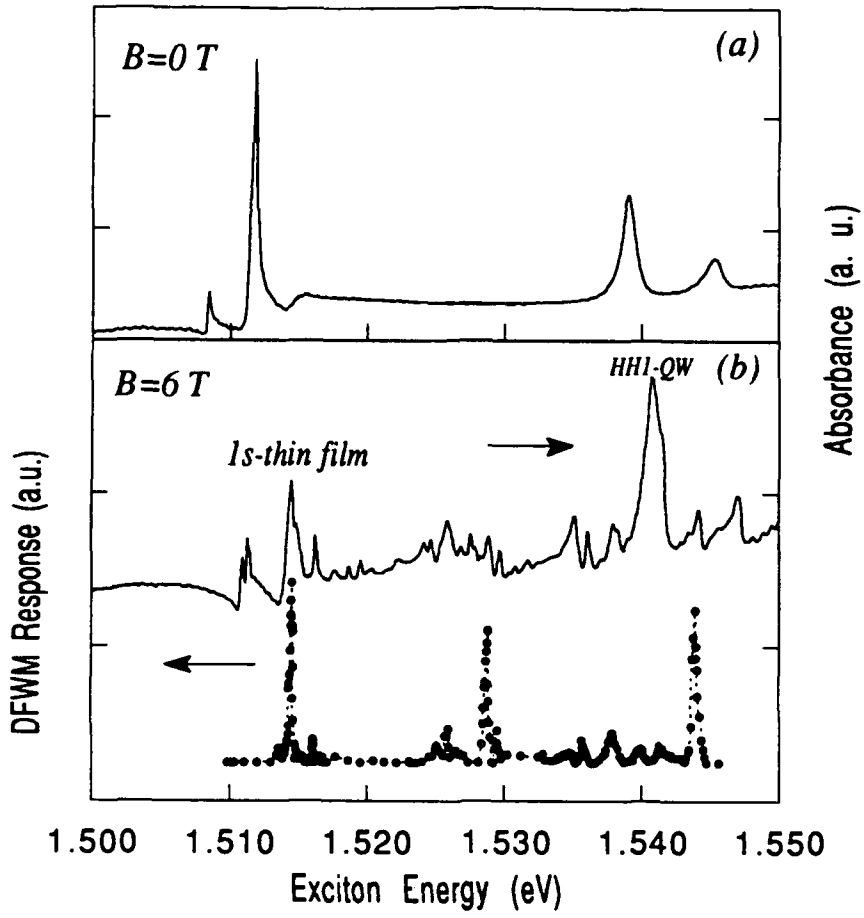
B=0 T
(a)
B=6 T
HH1-QW
(b)
1s-thin film
DFWM Response (a.u.)
Absorbance (a. u.)
1.500
1.510
1.520
1.530
1.540
1.550
Exciton Energy (eV)

Figure.1

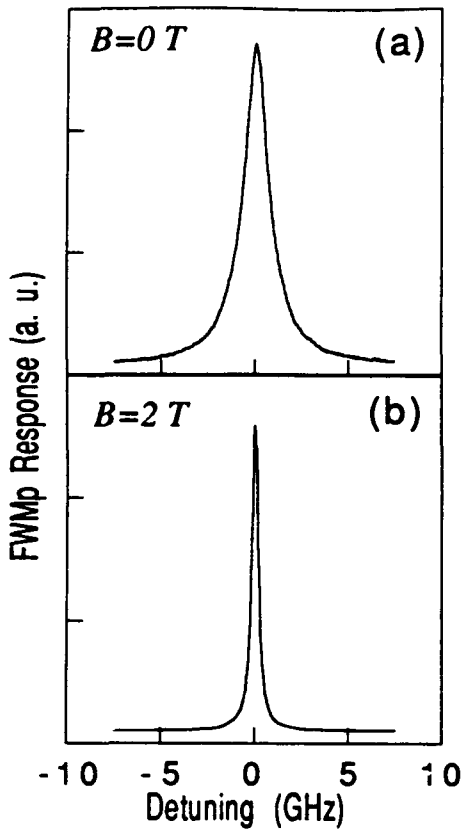
B=0 T
(a)
B=2 T
(b)
FWMp Response (a. u.)
-10
-5
0
5
10
Detuning (GHz)

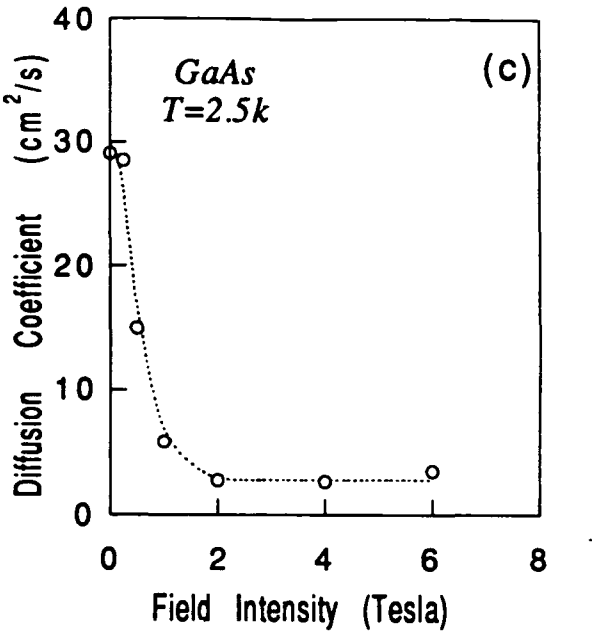
GaAs
T=2.5k
(c)
Diffusion Coefficient (cm²/s)
40
30
20
10
0
0
2
4
6
8
Field Intensity (Tesla)

Figure.2

Accepted for Publ.
IEEE J. Quant. Elect.
Spec. Issue on Ultrafast Opt.
and Elect., Nov. '92
INVITED

Coherent Transient Spectroscopy of Excitons in GaAs/AlGaAs Quantum Wells

S.T. Cundiff and D.G. Steel

Harrison M. Randall Laboratory of Physics

University of Michigan, Ann Arbor, Mi. 48109

(313)764-4469

Coherent transient optical spectroscopy techniques provide a means of studying the relaxation of electronic excitations in solids. Using these techniques we examine the relaxation of excitons in GaAs/AlGaAs multiple quantum wells at low temperature. Localization of excitons due to interface disorder results in inhomogeneous broadening of the absorption spectrum and relaxation due to migration between localization sites. The temperature and energy dependence of the relaxation indicate the presence of complex scattering mechanisms. The dependence of the optical response on the polarization of the incident excitation fields is shown to result in a dramatic change of the dephasing and broadening characteristics of the optical response. This result is interpreted in terms of the presence of both localized and delocalized excitons. Mechanisms for the polarization dependence are discussed.

The early development of tunable pulsed lasers was followed by the demonstration of numerous coherent transient optical spectroscopic techniques. Primarily, early measurements focused on gas phase systems where the corresponding loss of optical coherence (dephasing) occurs on a time scale long compared to the available pulse widths. The work provided considerable new insight into the interaction of light and matter. Although some of the first time domain measurements were performed in ion-doped solids characterized by relatively slow relaxations (~100 ns) [1, 2], it is only recently that it has been possible to use these techniques on fundamental excitations of extended electronics states present in crystals, where the dephasing rate is orders of magnitude faster. This ability is due to the rapid development of ultrafast laser technology producing tunable pulses in the femtosecond to picosecond range. Indeed many coherent effects have now been observed from electronic excitations in semiconductors, both bulk material (often thin layers) and heterostructures. The observed phenomena, briefly reviewed below, include free polarization decays (FPD), various kinds of photon echoes, and quantum beats.

Coherent transient effects arising from atomic transitions are now fairly well understood and have provided extensive information on decay processes of isolated atoms [3] as well as atoms undergoing collisions with neutral ground state perturbers [4-10]. However interpretation of the results of coherent spectroscopy measurements in semiconductors have been more difficult and have revealed the complex nature of the optical response of extended states. These complexities arise both from the underlying fundamental physics of the many body processes [11-14] that determine the nonlinear response as well as the further complication of the presence of impurities and disorder due for example to alloy scattering, or in the case of heterostructures due to nonideal conditions during growth of the samples. While the latter effects may seem to be artificial and the result of technological limitations they are important for two reasons: they limit the performance of devices and they present an avenue for studying the physics of disorder [15]. The presence of disorder effects the nature of electronic excitation as well as transport and relaxation of the excitation [16-18] and relaxation of the optically induced polarization [19]. In this paper we

present measurements that suggest that the nonlinear optical properties and the details of relaxation of excitons in GaAs/AlGaAs multiple quantum wells (MQW) are significantly modified by the presence of disorder.

Initial linear spectroscopic measurements, mainly photoluminescence and photoluminescence excitation spectroscopy, were able to show that the luminescence from GaAs quantum wells was primarily intrinsic in nature [20] and that the inhomogeneous broadening arose from intrawell width fluctuations [21]. These measurements were important in that they showed that, in contrast to most bulk samples, intrinsic excitons dominated the optical response and that disorder within the individual wells was the dominant broadening mechanism. For a review of the linear and nonlinear optical properties of quantum wells see Refs. [22, 23].

Early nonlinear experiments demonstrated resonant degenerate four wave mixing due to intrinsic Wannier excitons in MQWs could be observed at low relatively low excitation density [24]. This demonstrated their large nonlinear response and allowed use of nonlinear spectroscopy techniques based on the third order susceptibility. This led to the use of transient four wave mixing (TFWM) experiments at low temperature in high quality GaAs epilayers and single quantum wells to demonstrate the rapid dephasing of the exciton. In a series of measurements Schultheis and coworkers demonstrated the rapid dephasing due to scattering by longitudinal acoustic phonons of excitons in GaAs on time scales of 7 ps [25], and found time scales of 2-3 ps for homogeneously broadened excitons in a high quality GaAs/AlGaAs single quantum well [26]. In separate measurements they demonstrated and characterized dephasing due to exciton-exciton and exciton-carrier collisions [27-29].

In the presence of inhomogeneous broadening TFWM can generate a photon echo signal [1, 2, 30]. An inhomogeneously broadened medium excited by a short pulse ($\tau << \gamma_{ph}^{-1}$, where τ is the pulsewidth and γ_{ph} is the dephasing rate) exhibits a rapid decay of the FPD signal due to destructive interference between the radiated fields from different frequency groups. However, application of a second pulse can induce a rephasing, resulting in the emission of delayed signal pulse do to constructive interference when the original phases are restored [31]. Although the first

observation by Hu et al. of a photon echo signal in semiconductors was a Raman echo from donor bound excitons in *n*-CdS [32] where the dephasing time is of order 100 ns, the first demonstrated photon echoes from intrinsic excitons in GaAs/AlGaAs multiple quantum wells was reported more recently by Schultheis, Hegarty and Sturge [33]. Disorder at the interface between the GaAs in the quantum well and the AlGaAs barrier, resulting in well width fluctuations and hence fluctuations in the exciton energy, provided the inhomogeneous broadening necessary for the production of an echo. Echoes from interband transitions in GaAs were reported by Becker et al. where the large carrier-carrier scattering rates for free carriers resulted in femtosecond dephasing [34]. Noll et al. observed dephasing times of 200-500 ps using stimulated photon echoes (SPE, a three pulse echo) from disorder localized excitons in CdS_xSe_{1-x} mixed crystals [35]. The long dephasing times were attributed to the fact that the excitons were localized by disorder. As shown in detail below, SPE allow the simultaneous measurement of dephasing and population and were employed by Webb et al [36] to demonstrate the presence of extra dephasing processes in GaAs quantum wells. It was also shown that both inhomogeneously and homogeneously resonances are present [37].

Quantum beats arise from interference effects between distinct resonances which are simultaneously excited by the incident pulses. The first observation of beats in the optical response of GaAs/AlGaAs MQWs was by Göbel et al. [38], where the observed beats were between resonances not sharing a common state and hence are really polarization beats. The beats occurred between the radiated field from excitons in regions of the wells that differed by one monolayer. Shortly thereafter quantum beats between the heavy-hole and light-hole excitons in quantum wells [39, 40] were reported as were beats between free and bound excitons [41]. In a related experiment Leo et al. used TFWM to observe coherent oscillations of a wavepacket in a double quantum well [42]. In this experiment two wells of differing width are separated by a thin barrier; carriers are excited in one well and shown to spatially oscillate between the wells.

Transient coherent spectroscopy of excitons has been important for the study of disorder in quantum well systems. The sensitivity of four-wave-mixing to diffusion due to the resultant washout of the spatial hole burning (also called a light induced grating), was exploited by Hegarty,

Sturge and coworkers to demonstrate the abrupt increase in exciton mobility near the linear absorption line center [43]. This along with earlier resonant Rayleigh scattering measurements which demonstrated a similar increase in the exciton dephasing rate [44] were taken as evidence for a mobility edge. The mobility edge is thought to separate localized states below line center from extended, quasi-delocalized ones above line center. Theoretical predictions were made that dephasing of localized excitons at low temperature results from phonon-assisted-migration [16, 17], producing a characteristic temperature dependence of the dephasing rate. This was observed in InGaAs/InP quantum wells where alloy fluctuation result in localization of all excitonic states [45]. An attempt was made to observe this behavior in GaAs QWs using resonant Raman scattering, however it was not possible to distinguish between phonon-assisted-migration and variable range hopping [46]. Frequency domain techniques demonstrated this characteristic dependence for low energy excitons (below the mobility edge) in GaAs/AlGaAs MQW, confirming the presence of phonon-assisted-migration [47]. Coherent transient spectroscopy measurements discussed below have also observed the presence of phonon-assisted-migration and shown the change over to thermally activated behavior [36]. Takagahara has assembled a comprehensive review of the theory and experiments relevant to excitonic relaxation in quantum wells [18].

The large optical density of these systems leads to coherent coupling of excitons through exciton-exciton interactions which are related to local field effects. This can complicate the interpretation of results. Many of these effects can be predicted by extending the simple two level model [48] and have been observed [49, 50]. In particular the signal observed for "negative" delay can be calculated using the standard third order perturbation theory if the fields radiated by the polarization induced at first order is included at higher order. Indeed these effects had been observed earlier in accumulated photon echo experiments [51]. Of more fundamental interest is the presence of strong Coulomb coupling in semiconductors. This can lead to dramatic modification of the nonlinear optical response for sufficiently strong excitation, as demonstrated by recent numerical calculations [12, 14, 52, 53]. Additional temporal structure predicted by these calculations has been observed [54].

We have used coherent transient techniques, primarily TFWM, to closely examine the nonlinear response of GaAs/AlGaAs MQWs. The important results, discussed in detail below, are: (i) verification that the TFWM signal is indeed an echo by time resolving the emission and that its temporal width is in agreement with the observed inhomogeneous line width, confirming the presence of inhomogeneous broadening corresponding to the entire absorption width; (ii) observation of the signature characteristic of spectral diffusion for three pulse techniques, as expected for relaxation due to exciton migration between localization sites; (iii) examination of dephasing and population relaxation rates which shows the presence of additional complex scattering mechanisms at high energy or high temperature; and (iv) determination of the dependence of the TFWM response on the polarization of the incident fields which shows that both the dephasing rate and homogeneity are surprisingly polarization dependent, indicating the presence of two distinct classes of excitons; the temperature and energy dependencies and transport properties suggest that they are localized and delocalized excitons.

The measurements presented in this paper were obtained from various molecular beam epitaxially grown GaAs/$Al_{0.3}Ga_{0.7}As$ multiple quantum wells, typically with 100 Å wells and barriers and between 10 and 65 periods. The samples are mounted on a sapphire disk (*c*-axis normal) and the substrate removed by selective etching. A typical sample from which many of the results are obtained consists of 65 periods of 96 Å wells and 98 Å barriers. The HH1 absorption linewidth for this sample was approximately 2.2 meV, and there is a Stokes shift of 1 meV between absorption and luminescence. Although the basic physical effects were observed in all samples, the bulk of the measurements reported in this paper were performed on the larger linewidth samples (~2 meV) to permit spectral resolution that was not limited by the laser bandwidth (except for pulses below ~2 ps).

The coherent transient spectroscopy measurements in this work are based on degenerate three pulse TFWM in a backwards geometry (the so called phase conjugate geometry). The backward geometry is used since phase matching is assured and there is considerable improvement in the signal to noise. In this geometry the first pulse is incident at a small angle with respect to the

second pulse, which in turn is counter-propagating with respect to the third pulse. The signal pulse counter-propagates with respect to the first pulse. See inset in Figure 1 for experimental configuration and timing. The signal pulse can be either time integrated in a photo-multiplier, or time-resolved by mixing with a reference pulse in a $LiIO_3$ second harmonic crystal. The second pulse is mechanically chopped at 1 KHz to allow phase sensitive detection (for the most demanding measurements both the first and second pulses are mechanically chopped and the signal detected at the difference frequency, which allows rejection of scattered light from the sample and further enhances signal to noise). For the time integrated measurements the signal pulse is passed through a polarizer followed by a spatial filter to reject scattered laser light before detection. The input pulses are produced by a synchronously pumped hybrid mode locked dye laser, using Styryl 9 as the gain jet and IR 140 or NCI as the saturable absorber. The pulse width can be adjusted between 1 ps and 8 ps autocorrelation width by selection of the birefringent filter (1, 2 or 3 plate) and saturable absorber density (including no jet). Use of longer pulses is required for the spectrally sensitive measurements and the bandwidth of the short (1 ps) pulses is similar to the absorption linewidth of the sample. The dye laser is pumped at 76 MHz by second harmonic from an actively mode locked Nd:YAG laser. For transient differential absorption measurements to examine polarization coupling a 100 fsec self modelocked Ti:Al_2O_3 laser was used.

Three pulse TFWM allows the simultaneous measurement of both relaxation of the optically induced coherence (dephasing) and population (or excitation) [30]. For time intervals greater than the pulsewidth the time integrated signal strength as a function of the time interval between the first two pulses is determined by the dephasing rate (near zero delay the pulse shape determines the signal). The signal strength is proportional to $\exp\left(-4\gamma'_{ph}\tau\right)$ for an inhomogeneously broadened resonance, where γ'_{ph} is the total dephasing rate, and τ is the interval between the first and second pulses. For a homogeneously broadened resonance the signal strength is proportional to $\exp\left(-2\gamma'_{ph}\tau\right)$. The population decay rate determines the strength of the time integrated signal with respect to the interval between the second and third pulses and is proportional to $\exp\left(-2\gamma'_{pop}T\right)$ for

either a homogeneously or an inhomogeneously broadened resonance. γ'_{pop} is the total population decay rate and T is the delay between the second and third pulses.

As mentioned above TFWM in an inhomogeneously broadened media results in the photon echo, where the output signal emission is delayed with respect to the incident pulses. In an ordinary two pulse (or spontaneous) photon echo the output pulse is emitted at a time after the arrival of the second pulse which is equal to the interval between the two incident pulses. In the three pulse (or stimulated) photon echo the output pulse is emitted at a time after the arrival of the third pulse equal to the interval between the first two pulses. In contrast the FPD signal arising from a homogeneous system is emitted promptly upon the arrival of the third pulse and is independent of the interval between the first two pulses. Hence observation of the time resolved signal for various delays between the first two pulses allows unambiguous discrimination between homogeneously and inhomogeneously broadened systems. In a simple resonant system it is possible to distinguish between a homogeneous and inhomogeneously broadened system based upon the symmetry of the time integrated signal strength as a function of delay between the first two pulses. When there is non-zero delay between the second and third pulses, the signal from a homogeneously broadened system is symmetric about zero delay, whereas for an inhomogeneously broadened system a signal is only emitted for the "correct" time ordering resulting in an asymmetric response. However, as we will show, the complex nature of the optical response in a semiconductor heterostructure can make interpretation difficult, and time resolving the signal unambiguously demonstrates the nature of the broadening. The width of the echo pulse is determined by the inhomogeneous broadening. In the limit of delta function pulses and strong Gaussian inhomogeneous broadening, the width of echo is given by $\Delta t = 2\sqrt{2}\ln 2 / \pi\Delta\nu$ where Δt is the echo pulsewidth and $\Delta\nu$ is the full width half maximum of the Gaussian inhomogeneous distribution in hertz.

In early photon echo experiments the time scales were sufficiently slow that it was possible to time resolve the echo by simply observing the output of a photomultiplier on a fast oscilloscope. Unfortunately time scales characteristic of semiconductor systems do not permit this, hence, as

mentioned abcve, we must employ cross correlation techniques (on the slightly longer time scales observed in Ref. [35] it is possible to use a streak camera). Figure 1a is a typical cross-correlation between an echo signal from a GaAs/AlGaAs MQW and a reference pulse. To confirm that this is indeed an echo Figure 1b shows the output pulse position as a function of delay between the first to pulses. The expected linear relationship is obtained. The slight deviation near zero is due to finite pulse effects, as shown in numerical solutions to the Optical Bloch Equations (OBEs) [36, 55]. A fit to the echo pulse based upon numerical solution to the OBEs provides an estimate of 2.25±0.25 meV for the inhomogeneous width, in good agreement with that observed in linear absorption for this sample.

Having confirmed that the signal is an echo we can now make time integrated measurements as a function of pulse delay knowing that the signal strength as function of delay, τ, between the first two pulses is proportional to $\exp\left(-4\gamma'_{ph}\tau\right)$ allowing us to determine the dephasing rate. Figure 2 shows the results: in a) the signal strength as a function of delay between the first two pulses (second and third pulse arrive simultaneously) yields a dephasing time of 68 ps and in b) the signal strength as a function of delay between the second and third pulse (first and second simultaneous) yields a population decay time of 34 ps (the data are offset for clarity). These results indicate that $\gamma'_{ph} = \frac{1}{2}\gamma'_{pop}$ as expected. These results are for low energy excitons (see inset) at low density (8×10^7) and are intensity independent. The longest pulses (8 ps) were used, providing the greatest spectral resolution (~0.1 meV). This dephasing rate corresponds to a homogeneous linewidth of 19 μeV, much less than the inhomogeneous width and much less than that reported in earlier work, although typical in all our samples. It is interesting to note that the rapid population relaxation is much too fast to be due to recombination, which occurs on time scales of 0.5-1.0 ns at low temperature in these materials [56].

To understand this rapid population decay we must consider the possibility of exciton migration between localization sites. If an exciton created at a given site migrates to site of differing energy where the change in energy exceeds the pulse bandwidth, then the exciton will no longer interact with the incident fields. As this process transfers energy from one spectral region to

another it is known as "spectral diffusion" and is analogous to velocity changing collisions in Doppler broadened gas phase systems [57]. It has been shown that spectral diffusion produces a characteristic signature for three pulse TFWM [30]. For large delay between second and third pulses, the dependence of the time integrated signal on first-second pulse delay is transformed from a simple exponential decay to a strong contribution at zero delay followed by a sharp fall and an exponential decay determined by the dephasing rate. Insight into this can be obtained by considering how the echo is formed. During the interval between the first two pulses each frequency group acquires a phase and the third pulse causes the groups to rephase. However if an oscillator undergoes spectral diffusion between the arrival of the second and third pulses, it does not rephase and the coherent emission is suppressed. When there is no delay between the first two pulses, the phase factor is the same for all frequency groups, i.e. identically zero, hence spectral diffusion has no effect and a strong coherent emission is still present producing the spike at zero delay. This spike is due to excitons which spectrally diffuse, but remain within the laser bandwidth, there is also a loss of signal due to excitons which spectrally diffuse out of the laser bandwidth. This behavior is displayed in Figure 3. In 3a) the signal as a function of first-second pulse delay for zero two-three pulse delay is shown and it is accurately described by a simple exponential decay. In 3b) a large (50 ps) delay is introduced between the second and third pulse, a strong spike for zero first-second pulse delay now dominates the signal, as expected in the presence of strong spectral diffusion.

The rapid population decay, coupled with the presence of spectral diffusion suggests that exciton relaxation is indeed primarily due to excitons migrating between localization sites of different energy. To obtain insight into the mechanism for migration among localization sites, we examine the temperature dependence of the dephasing rate (Fig. 4). At low temperature (T< 10 K) the dependence closely matches that predicted for phonon assisted migration [16, 17]. Phonon assisted migration is due to tunneling between localization sites and is predicted to have a temperature dependence with a functional form of $\gamma = \Gamma_0 \exp(\beta T^{1.6})$. Both β and Γ_0 depend on the exciton energy, here $\beta = 0.016$ and $\Gamma_0 = 0.02$ meV. This functional form is distinct from that

predicted for variable range hopping ($\gamma = \Gamma_0 \exp\left(B / T^{n+1}\right)$ in n dimensions) [58], which is usually applied to electronic conduction in the localized regime. Variable range hopping only considers site-to-site transfer due to wavefunction overlap. The presence of long range dipole-dipole interactions for excitons is responsible for the distinct temperature dependence. At slightly higher temperatures, thermal activation becomes the dominant mechanism as is manifest by the clear Arrhenius behavior. In this regime acoustic phonons activate excitons from the localized states below line center to delocalized ones above line center. They subsequently relax into other available sites.

In Figure 5 we compare of the dephasing rate and population relaxation rate as function of temperature (Fig. 5a) and exciton energy (Fig. 5b). While both increase with increasing temperature or exciton energy, as expected based upon phonon-assisted-migration and the transition from localized to delocalized states at higher energy [44], the dephasing rate increases more rapidly. At low temperature and energy the dephasing time is exactly twice the population relaxation time, or terms of rates, $\gamma'_{ph} = \frac{1}{2}\gamma'_{pop}$. This is exactly the behavior expected for a simple two level system in the absence of ground state relaxation. This is easily seen heuristically by considering a two level system consisting of a ground state $|0\rangle$ and an excited state $|1\rangle$, the excited state population is $\langle 1|1\rangle$ hence if it decays as $\exp(-\gamma t)$ then the coherent superposition $\langle 1|0\rangle$ must decay as $\exp\left(-\frac{1}{2}\gamma t\right)$. The dashed lines in Fig. 5 shows $\gamma'_{ph} - \frac{1}{2}\gamma'_{pop}$. The extra dephasing is either the result of $\gamma'_{ph} = \frac{1}{2}\gamma'_{pop} + \gamma_{ph}(T,E)$, where $\gamma_{ph}(T,E)$ represents pure dephasing processes or the possible presence of ground state scattering processes at higher temperature and energy. The observation that in some samples the dephasing rate can exceed the population decay rate indicates that pure dephasing processes do contribute to the relaxation. The presence of such terms indicate that pure elastic scattering is present, where elastic means that there is no change in the energy of the exciton after scattering. The dependence on temperature suggests a phonon scattering process, although such a process would require at least two phonons in a second order process in order to be elastic.

For the measurements presented above the incident fields were co-polarized, perpendicular to the plane of the incident beams. Several studies have reported that the dephasing rate increases dramatically when the first field is cross polarized [59, 60]. However an even more fundamental change in the response is noted upon comparison of the time resolved signal from a MQW for all fields co-polarized (Fig. 6a) to that for $\mathbf{E}_1 \perp \mathbf{E}_2 \parallel \mathbf{E}_3$, $\mathbf{E}_s \parallel \mathbf{E}_1$ (Fig. 6b). The data clearly show that in the former case the emission time depends on the interval between $\mathbf{E}_1$ and $\mathbf{E}_2$ while in the second case it does not. This demonstrates that the signal for $\mathbf{E}_1 \perp \mathbf{E}_2$ is an FPD, while that for $\mathbf{E}_1 \parallel \mathbf{E}_2$ is an SPE (as we had discussed above) corresponding to a homogeneously broadened resonance and an inhomogeneously broadened resonance, respectively. A weak echo signal is evident in Fig. 6b, however this arises from a resonance which is 2.5 meV Stokes shifted from the absorption peak. On resonance the strength of this Stokes shifted resonance is comparable to that which produces the FPD. The observed SPE from this resonance in Fig. 6b is weak due to the large detuning, but observable because of the long dephasing time (~70 ps). Both the FPD (Fig. 6b) and co-polarized SPE (Fig. 6a) are resonant and show very similar spectral dependence. The TFWM signal strength for the FPD and SPE are spectrally coincident, and line up within experimental error with the linear absorption spectrum after correction for the effects of the strong linear absorption on the TFWM signal. The FPD is approximately 2 orders of magnitude weaker than the co-polarized SPE at low intensity at the peak of the response.

This behavior is somewhat surprising. Based on the energy level structure (see Fig. 6 insert) no difference in the nature of the signal is expect other than the polarization. More specifically, for GaAs the conduction band is $m=\pm 1/2$ character and the heavy-hole valence band is $m=\pm 3/2$; in a quantum well the spherical symmetry is lifted by the two dimensional nature of the structure and the axis of quantization is perpendicular to the plane of the layers. Quantum confinement lifts the valence band degeneracy at $k=0$ resulting in heavy-hole-light-hole splitting. Dipole allowed transitions require $\Delta m=\pm 1$, where in this material transition moments are equal. Hence linearly polarized fields propagating perpendicular to the layers must be taken as a superposition of two circularly polarized fields. We will designate the exciton created by a σ_+ polarized field as $|+1\rangle$

(consisting of a +3/2 hole and a -1/2 electron) and the exciton created by a σ_- polarized field as $|-1\rangle$ (consisting of a -3/2 hole and a 1/2 electron) [61]. The signal is produced by the scattering of E_3 off the grating produced by $E_1^* E_2$. (This picture is for a homogeneously broadened system but still provides insight for an inhomogeneously broadened system. Although there is no net grating, there is a grating for each frequency group within the inhomogeneous distribution. Each group results in a component of the scattered signal and it is the phase relationship between these components which results in the signal delay.) We see then that for linear co-polarized $\mathbf{E}_1$ and $\mathbf{E}_2$, two spatial gratings consisting of $|+1\rangle$ and $|-1\rangle$ excitons respectively, are created and are spatially coincident. For $\mathbf{E}_1 \perp \mathbf{E}_2$, the two gratings are exactly spatially out of phase. However, E_3 must also be decomposed into circularly polarized components, each of which independently scatters from one of the gratings, resulting in a linearly polarized signal field. Hence the change in the nonlinear response in Fig. 6 is clearly unexpected.

A further distinction between the two signals is seen by examining the dephasing rates in Figure 7 for $\mathbf{E}_1 \perp \mathbf{E}_2$ and $\mathbf{E}_1 \| \mathbf{E}_2$. The rate for $\mathbf{E}_1 \perp \mathbf{E}_2$ is much greater, 0.20-0.25 ps^{-1} and essentially energy independent, whereas for $\mathbf{E}_1 \| \mathbf{E}_2$ the rate varies from 0.016 ± 0.001 ps^{-1} on the low energy side to 0.1 ± 0.02 ps^{-1} on the high energy side. The tuning range over which a meaningful dephasing measurement can be made in a homogeneously broadened resonance is limit since the observed decay of the signal will be more rapid with increased laser detuning from resonance. The exact nature of this effect is sensitive to the details of the line shape and the pulse envelope [30].

These differences between the TFWM signal for $\mathbf{E}_1 \perp \mathbf{E}_2$ and $\mathbf{E}_1 \| \mathbf{E}_2$ strongly suggest that there are two distinct classes of excitons present. The signal for $\mathbf{E}_1 \| \mathbf{E}_2$ matches that expected for localized excitons, in agreement with previous observations. However, the homogeneous broadening and dephasing rate for $\mathbf{E}_1 \perp \mathbf{E}_2$ is comparable to that observed for excitons believed to be delocalized in high quality single quantum wells [26].

We note that the combined response of the FPD and the Stokes shifted SPE observed for $\mathbf{E}_1 \perp \mathbf{E}_2$ resulted in biexponential decays below line center where the dephasing rate associated

with this SPE is 0.014±0.002 ps^{-1}, slower than for the co-polarized SPE. Due to the 2.5 meV Stokes shift and slow dephasing we tentatively assign the SPE in Fig. 6b to impurity bound excitons [62, 63].

The temperature dependence of the dephasing rate for the co-polarized SPE and the FPD also show distinctly different behavior (Fig. 8). While the temperature dependence of the dephasing rate measured for the SPE corresponds to relaxation of localized excitons as described above, the dephasing rate for the prompt signal shows a linear temperature dependence of the form $\gamma = \gamma_0 + \gamma^* T$, where $\gamma^* = 4\mu eV / K$. The scattering mechanism is attributed to single phonon scattering of delocalized excitons along the two-dimensional exciton dispersion curve and the scattering coefficient is similar to that observed by Schultheis in the single quantum well [26].

Additionally, we note that measurement of the TFWM signal strength as a function of incident intensity for fixed pulse delay and energy again reveals a difference between the two signals. Figure 9 shows that at low excitation density, less than 10^8 excitons/cm^2/layer, both depend cubically on the total incident intensity as expected for a third order nonlinear optical process. The SPE is two orders of magnitude larger than the FPD, an enhancement expected for localized excitons compared to excitons in an ideal quantum well due to the increased oscillator strength for localized states resulting from an increase in the electron-hole overlap [64]. However the SPE shows a strong deviation from cubic behavior and saturation at an excitation density above 2×10^8. This behavior is expected for the SPE since the number of sites to localize an exciton is finite and clearly well below the density necessary to saturate the response in an ideal quantum well. Simple estimates of the latter saturation density based for free two-dimensional excitons give a value on the order of 10^{10} excitons/cm^2 [22].

The above measurements are consistent with the hypothesis that the FPD arises from delocalized excitons. Indeed, recent theoretical work on the nonlinear response for excitons in an ideal semiconductor shows that the TFWM signal is indeed a prompt FPD for low intensity excitation resonant with the exciton [14, 53]. While it is not possible at this time to directly prove

such an interpretation, we note that transport measurements provide a further indication of the differences between the two states.

To examine this aspect of the behavior, we studied the angle dependence of the excitation relaxation rate to probe the spatial "washout" time due to motion of the excitation. This is the typical approach in transient grating experiments to measure spatial diffusion [65]. At an angle θ between $\mathbf{E}_1$ and $\mathbf{E}_2$ in the material, wavelength λ and index of refraction n, the total signal decay is given by $\gamma = 2\gamma_{pop} + 8\pi^2 D\Lambda^{-2}$, where γ_{pop} is the excitation decay rate, D is the spatial diffusion coefficient and $\Lambda = n\lambda / 2\sin\theta$ is the grating spacing. It would be expected that delocalized states should have a larger D than localized states.

While such measurements are complicated by spectral diffusion (the spectral diffusion rate is much greater than the spatial diffusion rate), measurement of D can still be estimated by measuring the spatial diffusion rate of the quasi-equilibrium excitons that are long lived (~recombination time). For these measurements we work at a slightly higher temperature in order to increase the number of spectrally diffused excitons resonant with the laser and thereby increase the signal component of the long lived excitons. In addition, to observe the long lived component of the FPD signal, it is necessary to use co-polarized fields since in the cross-polarized geometry spin relaxation destroys the $|+1\rangle$ and $|-1\rangle$ exciton spatial gratings on a time scale of 30-50 ps [66, 67]. To discriminate between the FPD and SPE in this case, we note that at densities below 5×10^8 only the SPE is observable whereas at densities above 10^{10} the SPE is saturated and only the FPD is observable (at intermediate densities both signals can be observed [37]).

Figure 10 shows γ as a function of inverse grating spacing for the FPD and SPE, fitting to a quadratic dependence yields D=5.2 for the SPE and D=10.1 for the FPD. This data is taken at an exciton energy 0.5 meV below line center and at a temperature of 15 K. This difference is clear evidence of the greater mobility of the excitons which are responsible for the FPD signal. The diffusion coefficient for localized excitons is dependent on the exciton energy [43] and this measurement is taken at a point where it is beginning to undergo a transition from its low energy (small D) to high energy (large D) values.

It is important to consider, however, why the polarization of the fields distinguishes between the two kinds of excitons. The relative strength of the two signals indicates that while both localized and delocalized excitons are contributing to the co-polarized response, the response due the localized excitons completely dominates the signal at low density, although at higher density both signals can be observed. Hence, the real question is how does cross-polarizing the incident fields suppress the response of the localized excitons? While resolution of this remains incomplete, some insight into this problem is had by extending our earlier discussion of the origin of the TFWM signal and the structure of the electronic transitions.

In particular, coupling between the $|+1\rangle$ and $|-1\rangle$ excitons for $\mathbf{E}_1 \perp \mathbf{E}_2$ will result in suppression of a scattered signal. This is a consequence of the fact that the spatial modulations for the two excitons are spatially out of phase and hence coupling of $|+1\rangle$ ($|-1\rangle$) exciton to a $|-1\rangle$ ($|+1\rangle$) exciton in a region of $|+1\rangle$ ($|-1\rangle$) excited excitons will reduce the fringe contrast ratio for each spatial modulation. We note that TFWM using circularly polarized excitation beams supports the idea that the apparent change in dephasing rate is due to the suppression of the response giving rise to the slow dephasing (SPE) since we have experimentally shown that under no combination of circular polarizations is the rapid dephasing for crossed linearly polarized excitation observed. In addition, our measurements show the unexpected result that co-rotating circularly polarized $\mathbf{E}_1$ and $\mathbf{E}_2$ with a linearly polarized $\mathbf{E}_3$ gives a *linearly polarized* echo. This shows that the grating induced by co-rotating circularly polarized fields scatters both left and right circularly polarized fields with equal efficiency. Hence the absence of the echo in the linearly polarized experiments is due to destructive interference between the two third order induced polarizations.

To probe for a coupling between the $|+1\rangle$ and $|-1\rangle$ excitons, we used circularly polarized light in a simple (incoherent) transient absorption measurement, where the pump and probe have opposite circular polarization. Using a circularly polarized pump beam and a linearly polarized probe, which is resolved into circularly polarized components after passing through the sample, we discover that there is indeed a strong *instantaneous* coupling. This is evident in Figure 11, where the induced transmission for both circular components as a function of delay is shown. These

measurements were made with 2.8 ps pulses, however the coupling still appears instantaneous even when 300 fs pulses are used.

Although coupling will reduce the magnitude of the SPE, we must still consider the origin of the coupling. The instantaneous nature of the coupling rules out spin relaxation, which occurs on a time scale of 30-50 ps [66, 67] (the convergence of the two curves in Fig. 11 is due to spin relaxation, and the decay of the polarization indicates a spin relaxation time of 40 ps). In addition, although band mixing between the HH1 and LH1 valence bands will result in an instantaneous coupling, current estimates suggest the effect is not sufficiently large to explain our results [68-70] We currently believe it is at least in part due to localization enhanced biexcitonic effects, where the presence of one exciton at a localization site means that creating a second one of opposite spin results in formation of a biexciton, and hence a shift of the resonance by the biexciton binding energy. Evidence for biexcitonic effects has been observed as beats in transient absorption measurements [67], as well as in two-pulse TFWM [71].

Non-degenerate transient absorption measurements allow more direct observation of biexcitonic effects (Figure 12). A Stokes shifted induced absorption appears when the probe is oppositely circularly polarized with respect to the pump, as expected if biexcitons are being formed. For pump energy below line center, the Stokes shift is *constant with respect to the pump frequency*. A more complete presentation of these results will be made elsewhere [72]. Any biexcitonic effect will indeed only effect the localized excitons giving rise to the SPE as the formation of biexcitons is considerably smaller for delocalized excitons at the low densities employed.

Although it is clear that a strong coupling exists between $|+1\rangle$ and $|-1\rangle$ excitons and that it is likely due to localization enhanced biexcitonic effects, the apparent complete suppression of the SPE from localized excitons is not yet fully understood. To determine if the coupling observed in transient absorption is sufficient for complete suppression of the SPE a careful calculation of the pertinent coherent processes must be undertaken.

Our measurements clearly show that two distinct resonances are present in the quantum wells, and that they exist at the same energy. Similar results have been obtained in all our samples including very high quality samples. The measurements are also consistent with the possibility that the two resonances are due to the simultaneous presence of both localized and delocalized excitons. This apparent coexistence of both localized and delocalized states is unexpected from weak localization theory. Disorder results in localization due to the constructive interference of the back scattered wave function [73]. In two dimensions any disorder is thought to localize all states according to arguments based upon scaling theory [74]. For $T > 0$ inelastic scattering by phonons can lead to delocalized states. Coupling between localized and delocalized states at the same energy is thought to lead to decay of the localized ones into the delocalized ones [75] preventing them from coexisting at the same energy. Arguments have been presented that coexistence and separability may indeed be possible [76]. Unfortunately, the complex nature of the interface disorder in quantum wells makes a simple application of these theoretical considerations difficult, since the recent evidence for a bimodal distribution of roughness length scales [77, 78] may provide regions where excitons are strongly localized and others regions where the wave functions are more extended. Indeed, an alternate explanation is that excitons are localized according to these two different scale lengths. If one of the scale lengths is sufficiently large, phonon-assisted-tunneling will be reduced while the large spatial extent of the wave function will reduce the oscillator strength and increase the dephasing rate. However, in this picture it is somewhat surprising that the SPE and FPD have the same spectral dependence.

In summary, we have used coherent transient spectroscopic techniques to probe the very complex nonlinear optical response of excitons in quantum well structures. Our results demonstrate that much of this complexity is due to the presence of disorder and the new relaxation mechanisms which it introduces.

The authors would like to thank H. Wang for many helpful and insightful discussions, M. Webb who collaborated on portions of this work and V. Subramaniam and K. Ferrio for technical

assistance. The MBE grown samples were provided by P.K. Bhattacharaya. This work was supported by ARO, AFOSR and NSF.

1. N. A. Kurnit, I. D. Abella, and S. R. Hartmann, "Observation of a Photon Echo", *Phys. Rev. Lett.*, vol. 13, pp. 567-568, 1964.

2. I. D. Abella, N. A. Kurnit, and S. R. Hartmann, "Photon Echoes", *Phys. Rev.*, vol. 141, pp. 391-406, 1966.

3. S. Stenholm, *Foundations of Laser Spectroscopy* , New York: Wiley, 1984.

4. P. F. Liao, N. P. Economou, and R. R. Freeman, "Two-Photon Coherent Transient Measurements of Doppler-Free Linewidths with Broadband Excitation", *Phys. Rev. Lett.*, vol. 39, pp. 1473-1476, 1977.

5. T. Mossberg, *et al.*, "Tri-Level Echoes", *Phys. Rev. Lett.*, vol. 39, pp. 1523-1526, 1977.

6. A. Flusberg, *et al.*, "Observation and Relaxation of the Two-Photon Echo in Na Vapor", *Phys. Rev. Lett.*, vol. 41, pp. 305-308, 1978.

7. A. Flusberg, *et al.*, "Foreign-gas-induced relaxation of Rydberg S and D states in atomic sodium", *Phys. Rev. A*, vol. 19, pp. 1607-1621, 1979.

8. R. Kachru, T. W. Mossberg, and S. R. Hartmann, "Stimulated Photon Echo Study of Na(3 $^2S_{1/2}$)-CO Velocity-changing Collisions", *Opt. Comm.*, vol. 30, pp. 57-62, 1979.

9. T. W. Mossberg, *et al.*, "Total Scattering Cross Section for Na on He Measured by Stimulated Photon Echoes", *Phys. Rev. Lett.*, vol. 42, pp. 1665-1669, 1979.

10. R. Kachru, T. W. Mossberg, and S. R. Hartmann, "Noble-gas-induced broadening of transitions to Rydberg S and D states in atomic sodium", *Phys. Rev. A*, vol. 21, pp. 1124-1133, 1980.

11. S. Schmitt-Rink, D. S. Chemla, and D. A. B. Miller, "Theory of transient excitonic optical nonlinearities in semiconductor quantum-well stuctures", *Phys. Rev. B*, vol. 32, pp. 6601-6609, 1985.

12. M. Lindberg and S. W. Koch, "Effective Bloch Equations for semiconductors", *Phys. Rev. B*, vol. 38, pp. 3342-3350, 1988.

13. J. R. Kuklinski and S. Mukamel, "Generalized semiconductor Bloch equations: Local fields and transient gratings", *Phys. Rev. B*, vol. 44, pp. 11253-11259, 1991.

14. M. Lindberg, R. Binder, and S. W. Koch, "Theory of the semiconductor photon echo", *Phys. Rev. A*, vol. 45, pp. 1865-1875, 1992.

15. P. A. Lee and T. V. Ramakrishnan, "Disordered electronic systems", *Rev. Mod. Phys.*, vol. 57, pp. 287-337, 1985.

16. T. Takagahara, "Localization and homogeneous dephasing relaxation of quasi-two-dimensional excitons in quantum-well heterostructures", *Phys. Rev. B*, vol. 32, pp. 7013-7015, 1985.

17. T. Takagahara, "Localization and energy transfer of quasi-two-dimensional excitons in GaAs-AlAs quantum-well heterstructures", *Phys. Rev. B*, vol. 31, pp. 6552-6573, 1985.

18. T. Takagahara, "Excitonic relaxation processes in quantum well structures", *J. Lumin.*, vol. 44, pp. 347-366, 1989.

19. C. Lonsky, P. Thomas, and A. Weller, "Optical Dephasing in Disordered Semiconductors", *Phys. Rev. Lett.*, vol. 63, pp. 652-655, 1989.

20. C. Weisbuch, *et al.*, "Intrinsic Radiative Recombination from Quantum States in GaAs-AlGaAs Multi-Quantum Well Structures", *Solid State Commun.*, vol. 37, pp. 219-222, 1981.

21. C. Weisbuch, *et al.*, "Optical characterization of interface disorders in GaAs-AlGaAs multiple quantum well structures", *Solid State Comm.*, vol. 38, pp. 709-712, 1981.

22. D. S. Chemla, S. Schmitt-Rink, and D. A. B. Miller, "Nonlinear Optical Properties of Semiconductor Quantum Wells", in *Optical Nonlinearities and Instabilities in Semiconductors*, H. Haug, ed. San Diego: Academic Press, 1988, pp. 83-120.

23. S. Schmitt-Rink, D. S. Chemla, and D. A. B. Miller, "Linear and nonlinear optical properties of semiconductor quantum wells", *Advances in Physics*, vol. 38, pp. 89-188, 1989.

24. J. Hegarty, *et al.*, "Resonant degenerate four-wave mixing in GaAs multiquantum well structures", *Appl. Phys. Lett.*, vol. 40, pp. 132-134, 1982.

25. L. Schultheis, *et al.*, "Picosecond Phase Coherence and Orientational Relaxation of Excitons in GaAs", *Phys. Rev. Lett.*, vol. 57, pp. 1797-1800, 1986.

26. L. Schultheis, *et al.*, "Optical dephasing of homogeneously broadened two-dimensional exciton transitions in GaAs quantum wells", *Phys. Rev. B*, vol. 34, pp. 9027-9030, 1986.

27. L. Schultheis, *et al.*, "Ultrafast Phase Relaxation of Excitons via Exciton-Exciton and Exciton-Electron Collisions", *Phys. Rev. Lett.*, vol. 57, pp. 1635-1638, 1986.

28. A. Honold, *et al.*, "Relation between homogeneous linewidth and radiative lifetime of excitons in quantum wells". in *XVI Int. Conf. on Qu. Elect.*, 1988.

29. A. Honold, *et al.*, "Collision broadening of two-dimensional excitons in a GaAs single quantum well", *Phys. Rev. B*, vol. 40, pp. 6442-6445, 1989.

30. A. M. Weiner, S. De Silvestri, and E. P. Ippen, "Three-pulse scattering for femtosecond dephasing studies: theory and experiment", *J. Opt. Soc. Am. B.*, vol. 2, pp. 654-661, 1985.

31. T. Yajima and Y. Taira, "Spatial Optical Parametric Coupling of Picosecond Light Pulses and Transverse Relaxation Effect in Resonant Media", *J. Phys. Soc. of Japan*, vol. 47, pp. 1620-1626, 1979.

32. P. Hu, S. Geschwind, and T. M. Jedju, "Spin-Flip Raman Echo in n-Type CdS", *Phys. Rev. Lett.*, vol. 37, pp. 1357-1360, 1976.

33. L. Schultheis, M. D. Sturge, and J. Hegarty, "Photon echoes from two-dimensional excitons in GaAs-AlGaAs quantum wells", *Appl. Phys. Lett.*, vol. 47, pp. 995-997, 1985.

34. P. C. Becker, *et al.*, "Femtosecond Photon Echoes from Band-to-Band Transitions in GaAs", *Phys. Rev. Lett.*, vol. 61, pp. 1647-1649, 1988.

35. G. Noll Siegner, U., Shevel, S.G. and Göbel, E.O., "Picosecond Stimulated Photon Echo Due to Intrinsic Excitations in Semiconductor Mixed Crystals", *Phys. Rev. Lett.*, vol. 64, pp. 792-795, 1990.

36. M. D. Webb, S. T. Cundiff, and D. G. Steel, "Stimulated Picosecond Photon Echo Studies of Localized Exciton Relaxation and Dephasing in GaAs/AlGaAs Multiple Quantum Wells", *Phys. Rev. B*, vol. 43, pp. 12658-12661, 1991.

37. M. D. Webb, S. T. Cundiff, and D. G. Steel, "Observation of Time-Resolved Picosecond Stimulated Photon Echoes and Free Polarization Decay in GaAs/AlGaAs Multiple Quantum Wells", *Phys. Rev. Lett.*, vol. 66, pp. 934-937, 1991.

38. E. O. Göbel, *et al.*, "Quantum Beats of Excitons in Quantum Wells", *Phys. Rev. Lett.*, vol. 64, pp. 1801-1804, 1990.

39. K. Leo, *et al.*, "Quantum beats of light hole and heavy hole in quantum wells", *App. Phys. Lett.*, vol. 57, pp. 19-21, 1990.

40. B. F. Feuerbacher, *et al.*, "Quantum beats between the light and heavy hole excitons in a quantum well", *Solid State Commun.*, vol. 74, pp. 1279-1283, 1990.

41. K. Leo, *et al.*, "Quantum beats of free and bound excitons in GaAs/$Al_xGa_{1-x}As$ quantum wells", *Phys. Rev. B*, vol. 42, pp. 11359-11361, 1990.

42. K. Leo, *et al.*, "Coherent Oscillations of a Wave Packet in a Semiconductor Double-Quantum-Well Structure", *Phys. Rev. Lett.*, vol. 66, pp. 201-204, 1991.

43. M. D. Sturge, J. Hegary, and L. Goldner, "Localization of two-dimensional excitons in GaAs-AlGaAs quantum-well layers". in *17th Int. Conf. on the Physics of Semicon.*, pp. 367-370, San Francisco: Springer-Verlag, 1984.

44. J. Hegarty, *et al.*, "Resonant Rayleigh Scattering from an Inhomogeneously Broadened Transition: A New Probe of the Homogeneous Linewidth", *Phys. Rev. Lett.*, vol. 49, pp. 930-932, 1982.

45. J. Hegarty, K. Tai, and W. T. Tsang, "Enhanced inelastic scattering and localization of excitons in InGaAs/InP alloy quantum wells", *Phys. Rev. B*, vol. 38, pp. 7843-7845, 1988.

46. J. E. Zucker, *et al.*, "Resonant Raman study of low-temperature exciton localization in GaAs quantum wells", *Phys. Rev. B*, vol. 35, pp. 2892-2895, 1987.

47. H. Wang, M. Jiang, and D. G. Steel, "Measurement of Phonon-Assisted Migration of Localized Excitons in GaAs/AlGaAs Multiple-Quantum-Well Structures", *Phys. Rev. Lett.*, vol. 65, pp. 1255-1258, 1990.

48. M. Wegener, *et al.*, "Line shape of time-resolved four-wave mixing", *Phys. Rev. A*, vol. 42, pp. 5675-5683, 1990.

49. K. Leo, *et al.*, "Effects of Coherent Polarization Interactions on Time-Resolved Degenerate Four-Wave Mixing", *Phys. Rev. Lett.*, vol. 65, pp. 1340-1343, 1990.

50. K. Leo, *et al.*, "Subpicosecond four-wave mixing in GaAs/$Al_xGa_{1-x}As$ quantum wells", *Phys. Rev. B*, vol. 44, pp. 5726-5737, 1991.

51. S. Saikan, *et al.*, "Optical-density effect in heterodyne-detected accumulated photon echo", *Phys. Rev. B*, vol. 36, pp. 5074-5077, 1987.

52. S. W. Koch, R. Binder, and M. Lindberg, "Many-body theory of Rabi flopping and photon echo in semiconductors". in *Quant. Elect. Laser Sci.*, OSA Technical Digest Series vol. 11, 1991.

53. W. Schaefer, F. Jahnke, and S. Schmitt-Rink, "Many-particle effects on transient four-wave-mixing signals in semiconductors", *manuscript*..

54. J. Shah, personal communication.

55. M. D. Webb, *Picosecond Nonlinear Optical Studies of Exciton Relaxation in Multiple Quantum Well Structures*, Ph.D. dissertation, University of Michigan, 1990.

56. J. Feldman, *et al.*, "Linewidth Dependence of Radiative Exciton Lifetimes in Quantum Wells", *Phys. Rev. Lett.*, vol. 59, pp. 2337-2340, 1987.

57. P. R. Berman, "Effects of Collisions on linear and non-linear spectroscopic line shapes", *Phys. Rep.*, vol. 43, pp. 101-149, 1978.

58. N. F. Mott and E. A. Davis, *Electronic Processes in Non-Crystalline Materials* 2nd ed., Oxford: Clarendon Press, 1979.

59. H. H. Yaffe, *et al.*, "Polarization and wavelegth dependence of relaxation processes as measured by time delayed four wave mixing in quantum wells". in *Quantum Electronics Laser Science*, OSA Technical Digest Series vol. 11, 1991.

60. K. Leo, *et al.*, "Subpicosecond Spectroscopy of Excitons in GaAs/AlGaAs Heterostructures". in *VIIth International Symposium on Ultrafast Processes in Spectroscopy*, proceeding to be published, 1991.

61. R. Planel and C. Benoit a la Guillaume, "Optical Orientation of Excitons", in *Optical Orientation*, F. Meier and B.P. Zakharchenya, Eds. Amsterdam: Elsevier, 1984, pp. 353-380.

62. D. A. Kleinman, "Binding energy of biexcitons and bound excitons in quantum wells", *Phys. Rev. B*, vol. 28, pp. 871-879, 1983.

63. S. Charbonneau, T. Steiner, and M. Thewalt, "Photoluminescence decay times of the defect-induced bound exciton lines in GaAs grown by molecular beam epitaxy", *Phys. Rev. B*, vol. 41, pp. 2861-2864, 1990.

64. T. Takagahara and E. Hanamura, "Giant-Oscillator-Strength Effect on Excitonic Optical Nonlinearities Due to Localization", *Phys. Rev. Lett.*, vol. 56, pp. 2533-2536, 1986.

65. H. J. Eichler, P. Günter, and D. W. Pohl, *Laser-Induced Dynamic Gratings* , Berlin: Springer-Verlag, 1986.

66. T. C. Damen, *et al.*, "Spin relaxation and thermalization of excitons in GaAs quantum wells", *App. Phys. Lett.*, vol. 58, pp. 1902-1904, 1991.

67. S. Bar-Ad and I. Bar-Joseph, "Exciton Spin Dynamics in GaAs Heterostructures", *Phys. Rev. Lett.*, vol. 68, pp. 349-352, 1992.

68. R. Ferreira and G. Bastard, ""Spin"-flip scattering of holes in semiconductor quantum wells", *Phys. Rev. B*, vol. 43, pp. 9687-9691, 1991.

69. W. T. Masselink, *et al.*, "Absorption coefficients and exciton oscillator strengths in AlGaAs-GaAs superlattices", *Phys. Rev. B*, vol. 32, pp. 8027-8034, 1985.

70. G. D. Sanders and Y.-C. Chang, "Effect of band hybridization on exciton states in GaAs-Al_xGa_{1-x} quantum wells", *Phys. Rev. B*, vol. 32, pp. 5517-5520, 1985.

71. B. F. Feuerbacher, J. Kuhl, and K. Ploog, "Biexcitonic contributionto the degenerate-four-wave-mixing signal from a GaAs/AlGaAs quantum well", *Phys. Rev. B*, vol. 43, pp. 2439-2441, 1991.

72. S. T. Cundiff and D. G. Steel, to be published.

73. P. W. Anderson, "Absence of Diffusion in Certain Random Lattices", *Phys. Rev.*, vol. 109, pp. 1492-1505, 1958.

74. E. Abrahams, *et al.*, "Scaling Theory of Localization: Absence of Quantum Diffusion in Two Dimensions", *Phys. Rev. Lett.*, vol. 42, pp. 673-676, 1979.

75. L. Fleishman and P. W. Anderson, "Interactions and the Anderson transition", *Phys. Rev. B*, vol. 21, pp. 2366-2377, 1980.

76. J. C. Phillips, "Why localized and extended impurity band states can coexist and be separated", *Solid State Commun.*, vol. 47, pp. 191-193, 1983.

77. D. Gammon, B. V. Shanabrook, and D. S. Katzer, "Excitons, Phonons and Interfaces in GaAs/AlAs Quantum-Well Structures", *Phys. Rev. Lett.*, vol. 67, pp. 1547-1550, 1991.

78. C. A. Warwick, *et al.*, "Does luminescence show semiconductor interfaces to be atomically smooth?", *App. Phys. Lett.*, vol. 56, pp. 2666-2668, 1990.

Figure Captions

Figure 1: (a) Cross correlation signal showing time resolved echo, (b) echo position as a function of delay between first and second pulses, dashed line it fit based upon numerical solutions of the Optical Bloch Equations, deviation from linearity near zero is due to finite pulse effects. Inset in (a) shows experimental configuration. Arrows designate incident pulses, labeled by time ordering, S is emitted signal pulse.

Figure 2: TFWM signal as function of delay between first and second pulses (a), and second and third pulse (b), data offset for clarity. Lines are exponential fits, demonstrating a dephasing time of 68 ps in (a) and a population relaxation time of 34 ps in (b). Inset shows spectral position (arrow) at which these measurements were made relative to linear absorption curve.

Figure 3: TFWM signal as function of delay between first two pulses for zero delay between second and third pulses (a) and 50 ps delay (b). The sharp spike at zero evident in (b) demonstrates the presence of spectral diffusion.

Figure 4: Dephasing as a function of temperature (diamonds). Lines are fits: solid line is fit to activation behavior for high temperature, dashed line is fit to phonon-assisted-migration for low temperature. Note difference in scales.

Figure 5: Comparison of dephasing and population relaxation rates as a function of temperature (a) and energy (b). In both the circles are population relaxation rate and squares are dephasing rate, lines are to guide the eye. Dashed line is "extra-dephasing". Short dash line in (b) is linear absorption for reference.

Figure 6: Cross correlation signal (a) for $\mathbf{E}_1 \parallel \mathbf{E}_2$ and (b) for $\mathbf{E}_1 \perp \mathbf{E}_2$ for 0,2 and 4 ps delay between $\mathbf{E}_1$ and $\mathbf{E}_2$. Inset shows energy level diagram for GaAs in a quantum well.

Figure 7: Dephasing rate as a function of photon energy for $\mathbf{E}_1 \parallel \mathbf{E}_2$ (circles) and $\mathbf{E}_1 \perp \mathbf{E}_2$ (squares). Solid line is linear absorption for reference.

Figure 8: Dephasing rate as function of temperature for $\mathbf{E}_1 \parallel \mathbf{E}_2$ (circles, right axis) and $\mathbf{E}_1 \perp \mathbf{E}_2$ (squares, left axis). Solid line is fit showing linear temperature dependence for $\mathbf{E}_1 \perp \mathbf{E}_2$ and dashed lines are fit to phonon-assisted-migration (short dash) and thermal activation (long dash) for $\mathbf{E}_1 \parallel \mathbf{E}_2$. Note the difference in scales for left and right axes.

Figure 9: Density dependence of signal strength for $\mathbf{E}_1 \parallel \mathbf{E}_2$ (open circles) and $\mathbf{E}_1 \perp \mathbf{E}_2$ (solid circle). Lines are fit to cubic dependence for low density.

Figure 10: Decay rate of signal as a function of delay between second and third pulses for various grating spacings for the FPD (density of 2×10^{10} excitons/cm^2/layer) and SPE (2×10^8). The solid lines are a fit to the expected quadratic dependence, yielding a diffusion coefficient of 10.1 for the FPD and 5.2 for the SPE.

Figure 11: Transient absorption signal strength as a function of delay for opposite circular probe polarizations, pump is σ_+ polarized. Upper trace shows polarization (right axis, offset for clarity), fit to exponential behavior demonstrates spin relaxation time of 40 ps (solid line).

Figure 12: Non-degenerate transient absorption for σ_+ (solid square) and σ_- (open circle) probes, pump is σ_+ polarized and the arrow designates its energy (1 meV bandwidth). Dashed line is linear absorption for reference.

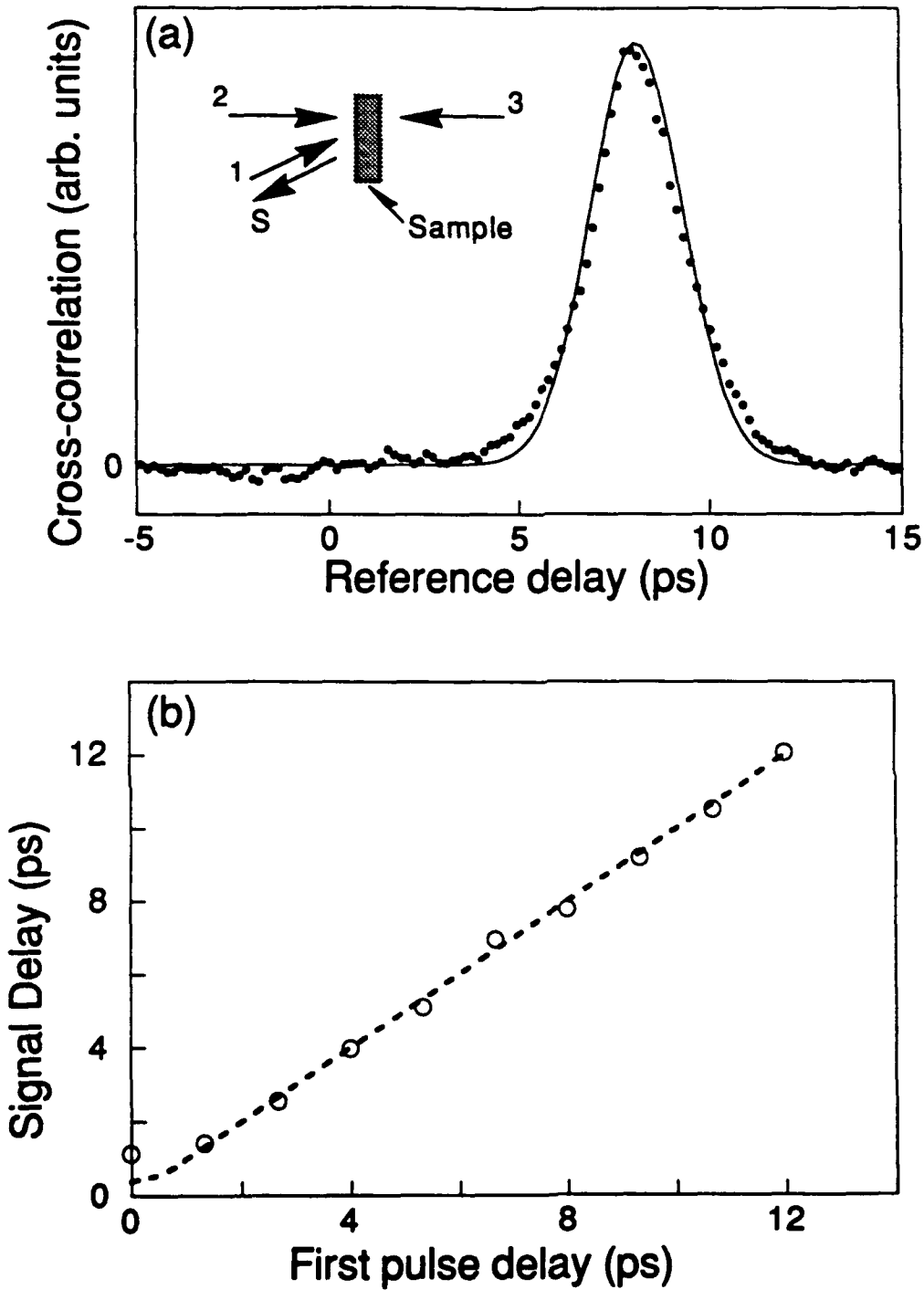
(a)
2
3
1
S
Sample
Cross-correlation (arb. units)
0
-5
0
5
10
15
Reference delay (ps)
(b)
12
8
4
0
Signal Delay (ps)
0
4
8
12
First pulse delay (ps)

Fig 1

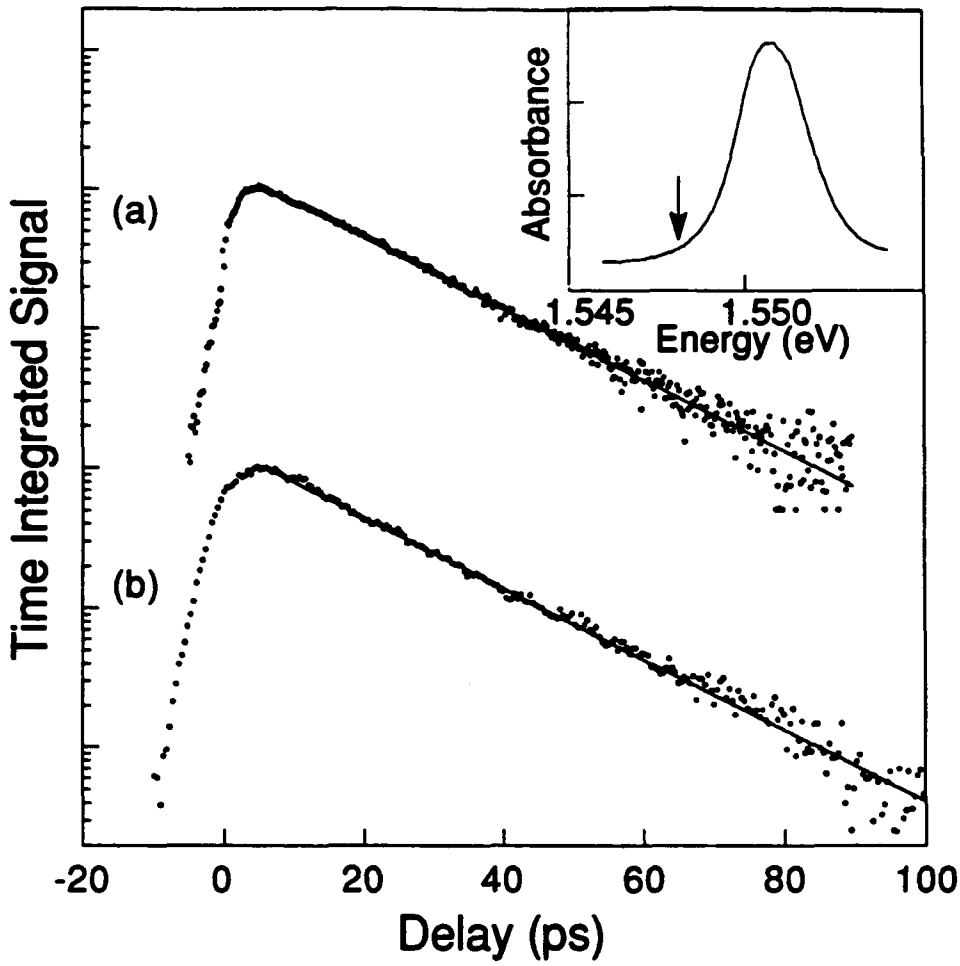
Time Integrated Signal
(a)
(b)
Absorbance
1.545
1.550
Energy (eV)
-20
0
20
40
60
80
100
Delay (ps)

Fig 2.

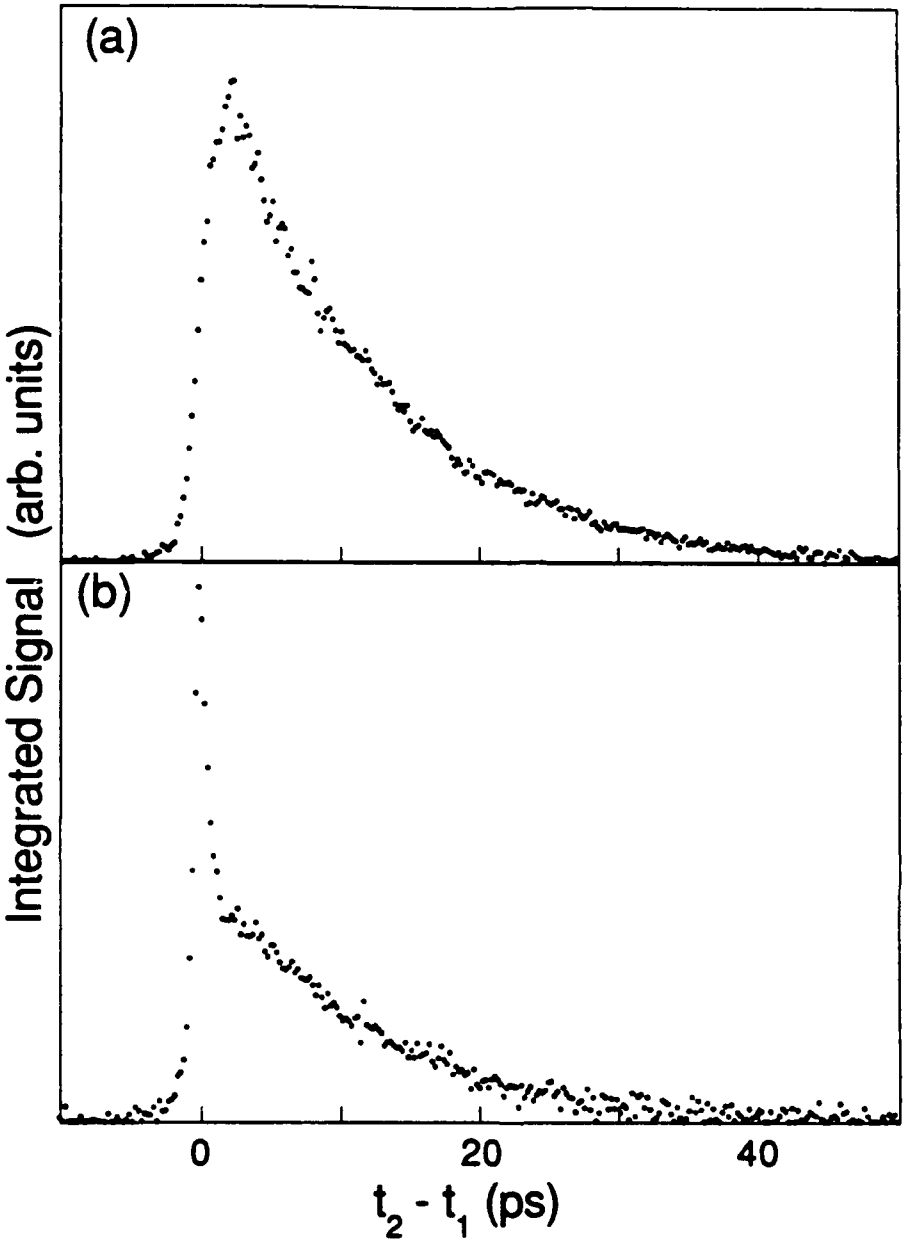

Fig 3

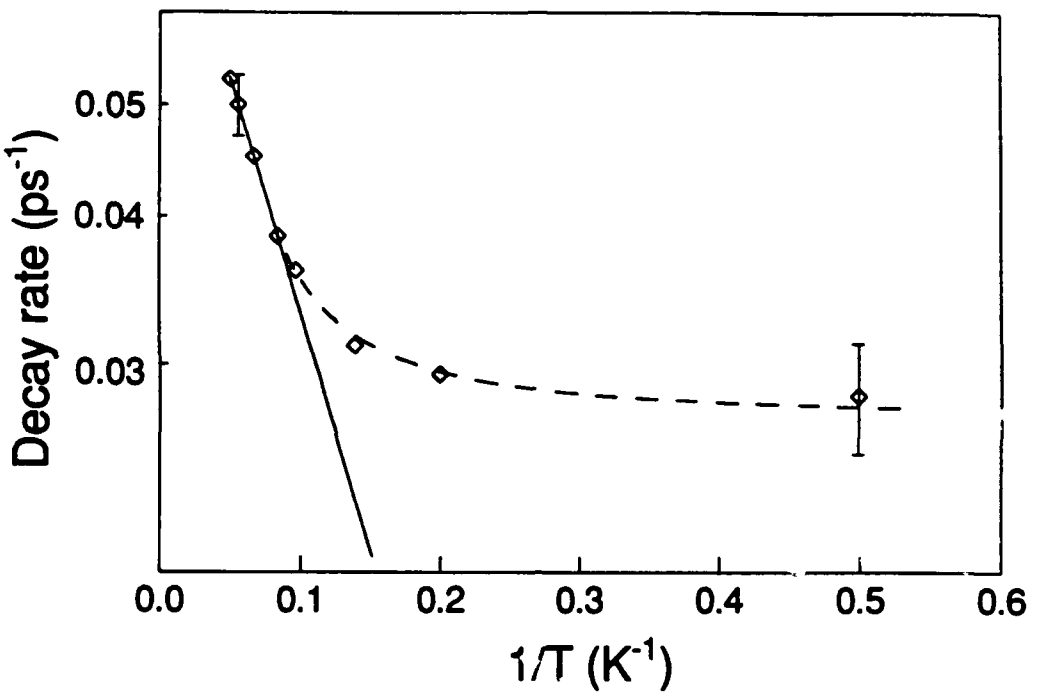

Fig 4.

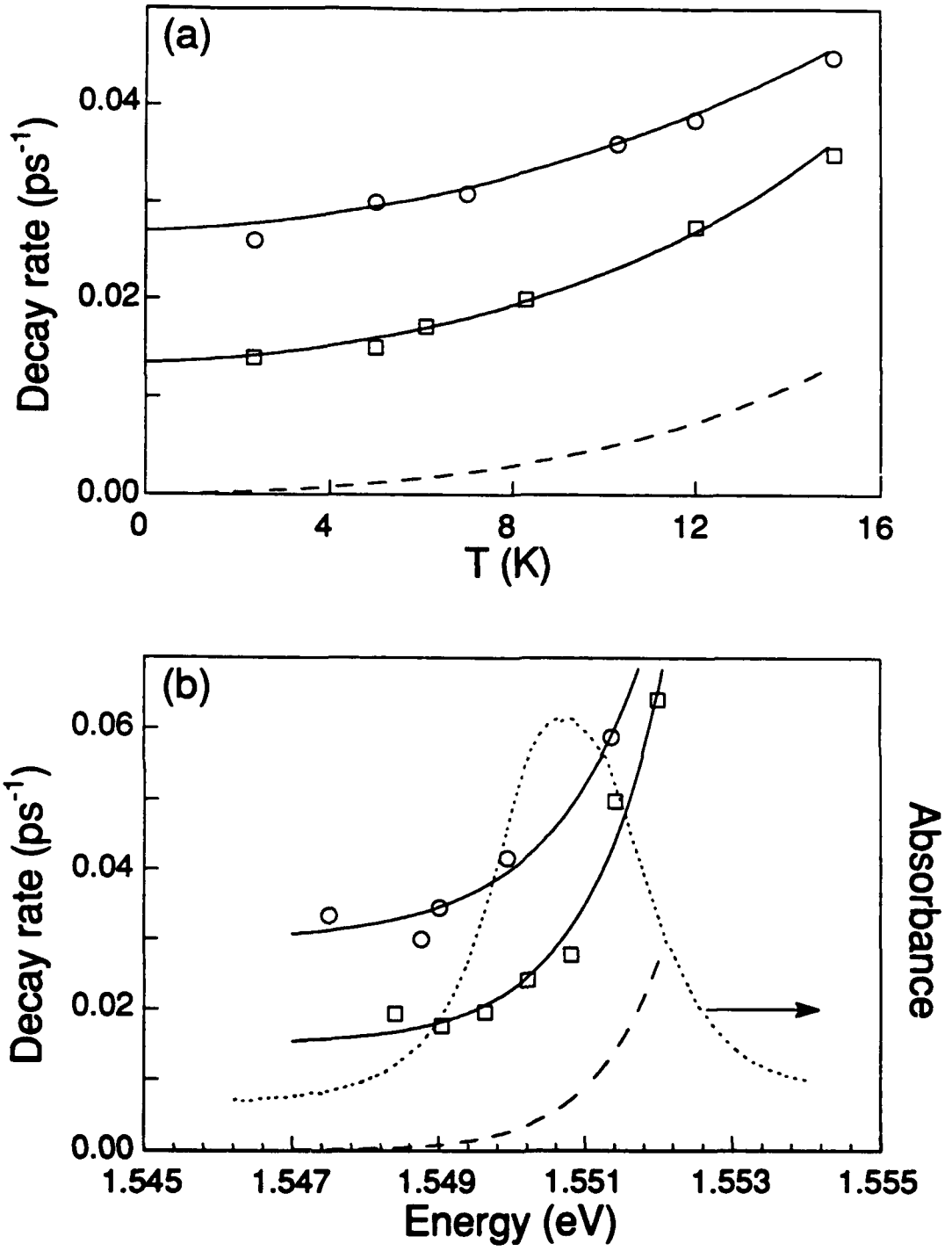
(a)
Decay rate (ps^{-1})
0.04
0.02
0.00
0
4
8
12
16
T (K)
(b)
Decay rate (ps^{-1})
0.06
0.04
0.02
0.00
1.545
1.547
1.549
1.551
1.553
1.555
Energy (eV)
Absorbance

Fig. 5

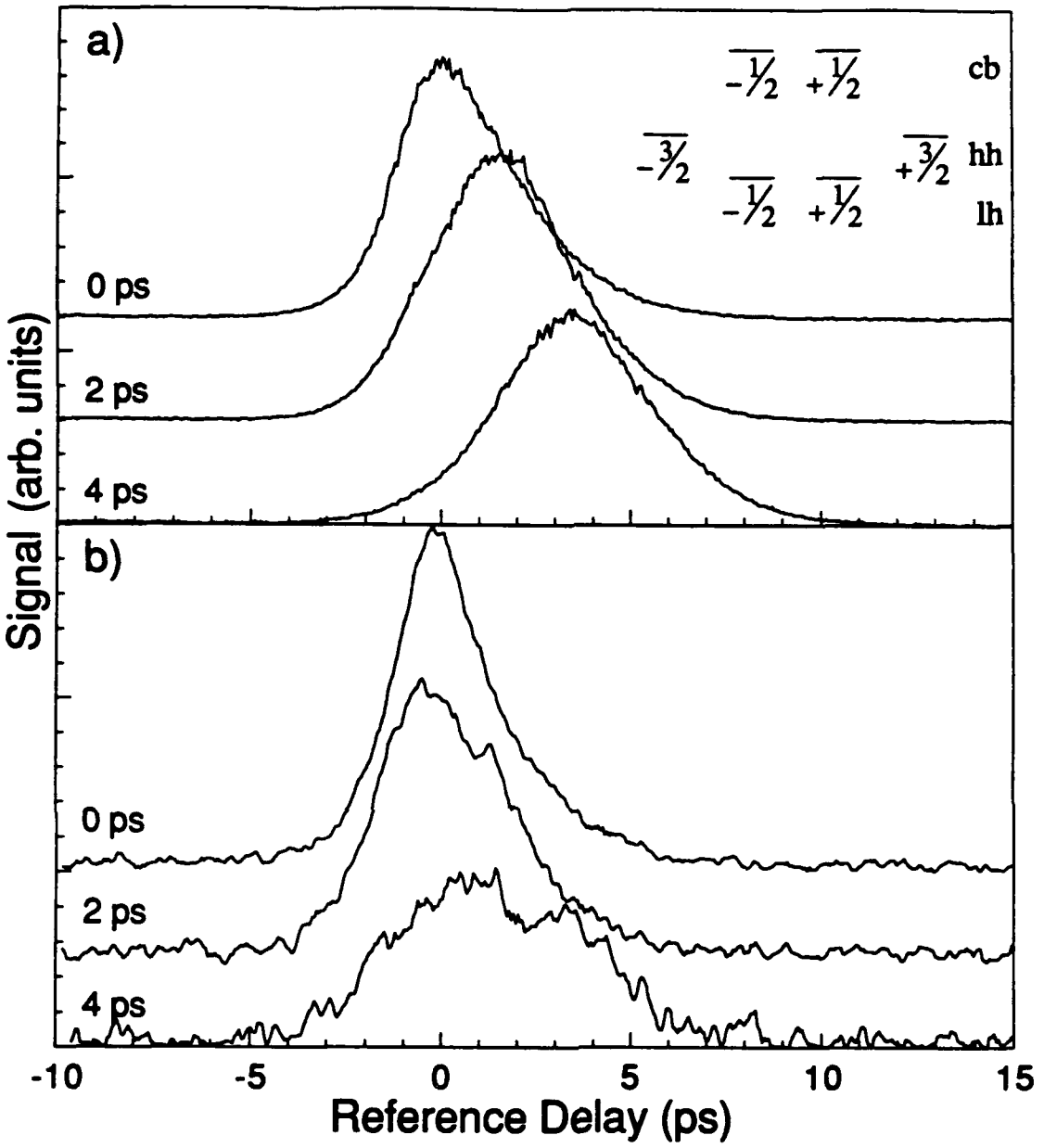
a)
-1/2 +1/2 cb
-3/2 +3/2 hh
-1/2 +1/2 lh
0 ps
2 ps
4 ps
b)
0 ps
2 ps
4 ps
Signal (arb. units)
-10
-5
0
5
10
15
Reference Delay (ps)

Figure 6.

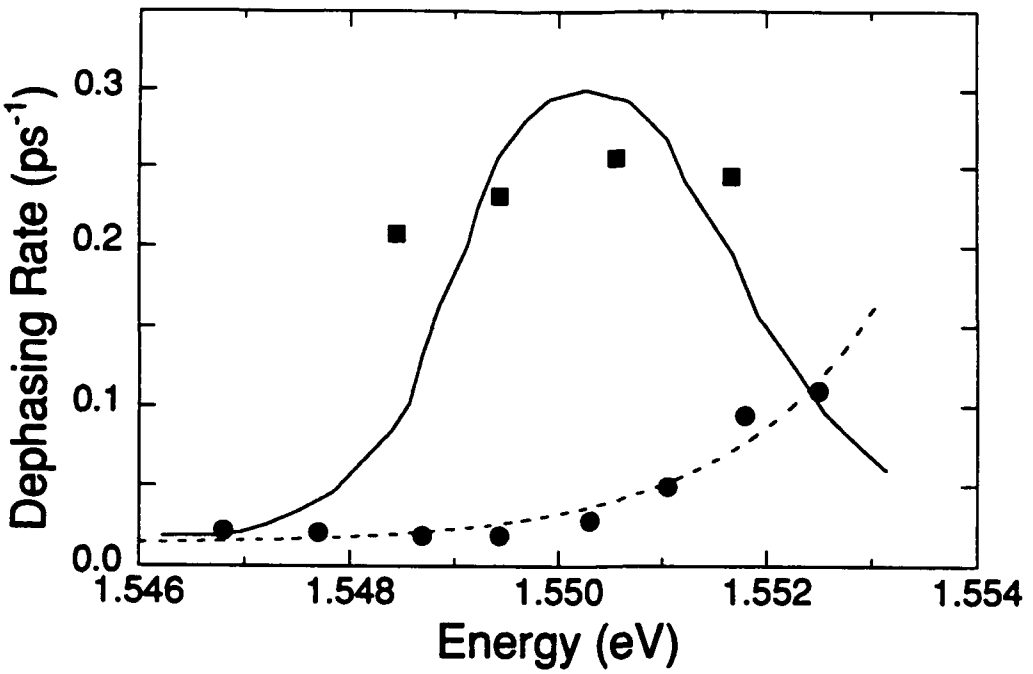
Dephasing Rate (ps^{-1})
0.3
0.2
0.1
0.0
1.546
1.548
1.550
1.552
1.554
Energy (eV)

Figure 7.

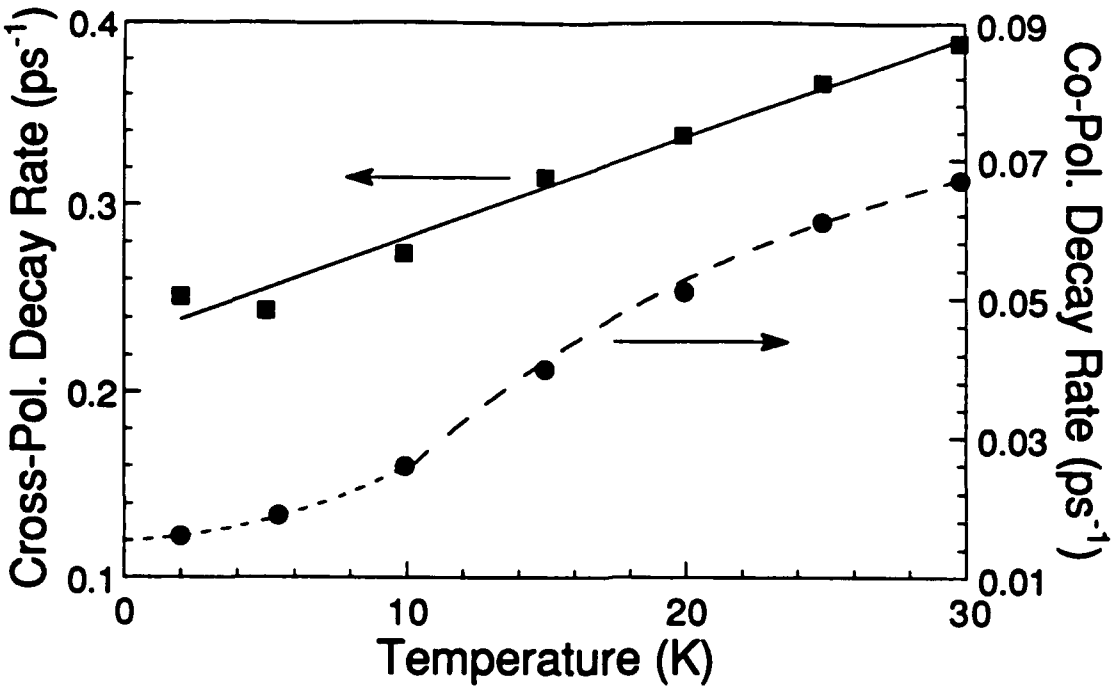
Cross-Pol. Decay Rate (ps^{-1})
Co-Pol. Decay Rate (ps^{-1})
Temperature (K)
0.4
0.3
0.2
0.1
0.09
0.07
0.05
0.03
0.01
0
10
20
30

Figure 8.

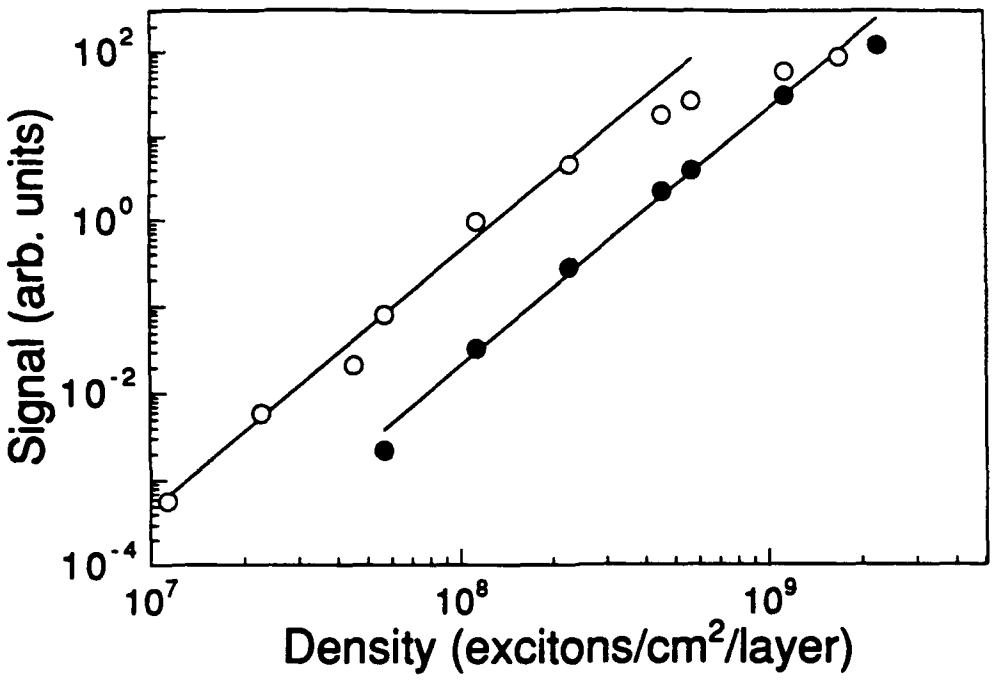
Signal (arb. units)
10^{2}
10^{0}
10^{-2}
10^{-4}
10^{7}
10^{8}
10^{9}
Density (excitons/cm^2/layer)

Fig. 9

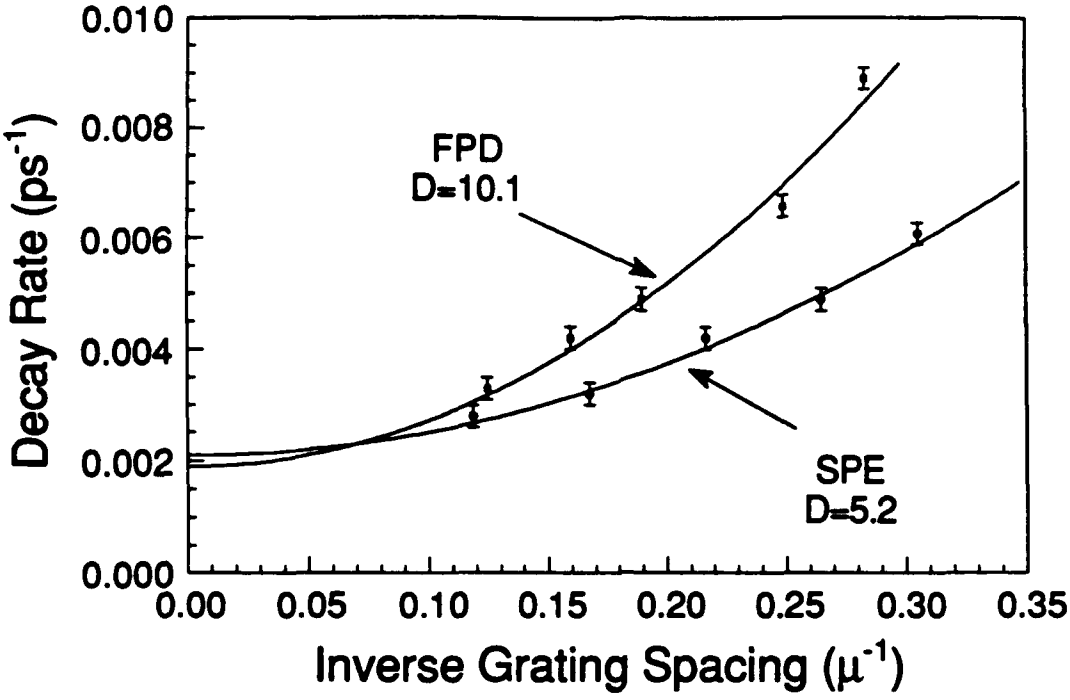
0.010
0.008
0.006
0.004
0.002
0.000
Decay Rate (ps^{-1})
FPD
D=10.1
SPE
D=5.2
0.00
0.05
0.10
0.15
0.20
0.25
0.30
0.35
Inverse Grating Spacing (μ^{-1})

Fig. 10

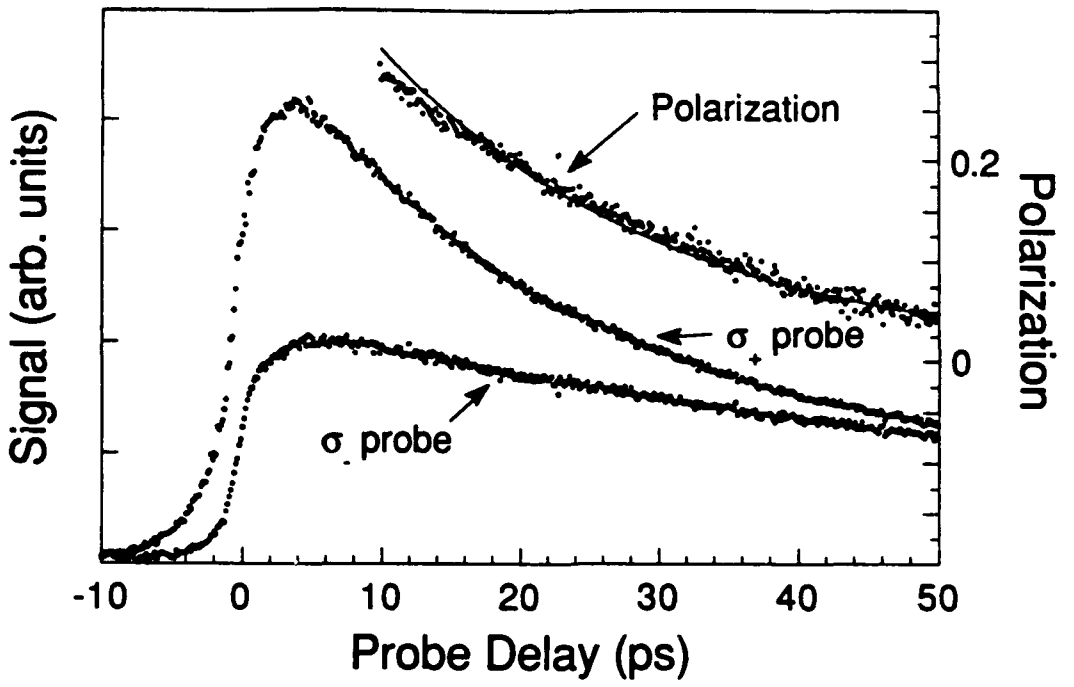
Polarization
σ+ probe
σ- probe
Signal (arb. units)
Polarization
0.2
0
-10
0
10
20
30
40
50
Probe Delay (ps)

Fig 11

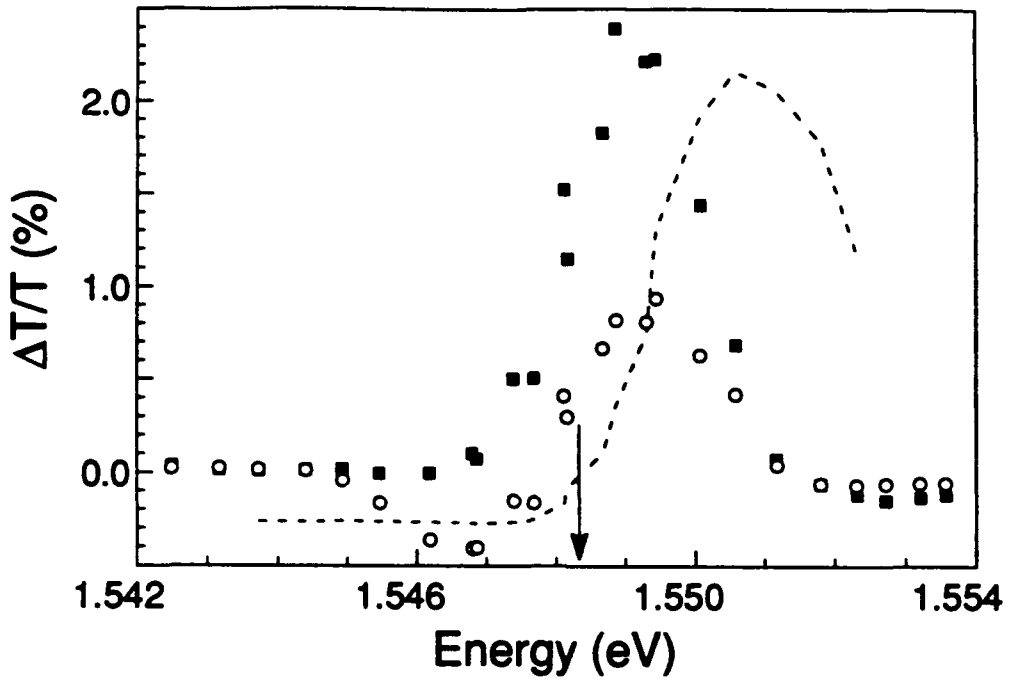

Fig. 12

Invited chapter in *Optics of Semiconductor Nanostructures*, Fritz Henneberger and Stefan Schmitt-Rink, eds (VCH-Germany, 1992)

Coherent Nonlinear Spectroscopy of Excitons in Quantum Wells

Duncan G. Steel, Hailin Wang, Steven T. Cundiff
Harrison M. Randall Laboratory
University of Michigan, Ann Arbor, MI 48109

Introduction

The development of tunable narrow band cw lasers and ultrafast pulsed lasers has resulted in the discovery and development of numerous nonlinear optical effects in materials. These nonlinear phenomena have been studied extensively and have provided considerable understanding of the interaction of light with matter. However, in recent years, these effects have been explored as powerful laser based optical spectroscopy methods for the study of materials. While these methods were first applied extensively in the area of basic atomic physics, they are now extensively used in the study of solids such as semiconductors, impurity doped crystals and the complex problem of molecules in solution. The increased interest in nonlinear laser spectroscopy is very evident in the study of direct bandgap semiconductors and corresponding heterostructures such as quantum wells, superlattices and quantum wires and dots. These materials are of considerable interest for application to electronic, optical and optoelectronic devices. Both linear and nonlinear laser spectroscopic methods have played a major role in the study of the material properties in these systems. These methods have also been important in the characterization of corresponding electronic and optical device performance.

Studies of the nonlinear optical properties of semiconductor heterostructures have also been important in the area of basic physics. For example, as discussed elsewhere in this book, there is now considerable understanding regarding the fundamental origin of the nonlinear optical response in ideal semiconductors (for a review see [.1, .2]). The response is considerably more complicated than that of simple atomic systems as a result of the carrier-carrier Coulomb interactions and their Fermionic nature. Disorder is an additional complication in these systems. In a heterostructure disorder can be caused by fluctuations in the confinement potential or alloy concentration. Disorder is of fundamental interest as discussed below since it leads to fundamental phenomena such as localization [.3]. Disorder can also profoundly effect the performance of devices.

In this chapter we review recent results obtained in the study of excitons in GaAs/AlGaAs quantum well (QW) structures based on frequency domain and time domain coherent nonlinear spectroscopy. The discussion emphasizes the study of the dynamical behavior of excitons at low

temperature, where the excitons are stable against ionization by LO phonons. At sufficiently low excitation densities the coherent emission arises only from the third order optical susceptibility. In this regime the excitonic susceptibility is dominated by the effects of disorder induced localization of the excitons. This approach is in contrast to other work discussed in this book which has emphasized studies at higher excitation density to examine the many body nature of the interaction. At these high densities the effects of disorder are reduced due to saturation of that part of the response. By working at low excitation density, it has been the objective of our group and others to learn more about the nature of the material.

As is well known, the exciton dominates the linear and nonlinear optical properties just below the bandedge in GaAs QW structures. In these structures, quasi two dimensional excitons are confined in the thin GaAs layer by the larger band gap of the $Al_xGa_{1-x}As$ layers. Enhancement of the electron-hole correlation due to confinement leads to an increase in the exciton oscillator strength, exciton transition energy and the exciton binding energy with no corresponding increase in phonon interactions. This results in well resolved excitonic resonances even at room temperature. In an ideal quantum well, the origin of the nonlinear response is dominated by the effects of the Pauli exclusion principle including phase space filling, exchange and exciton-exciton interactions. The effects of Coulomb screening are significantly reduced due to the reduced dimensionality [.1]. However, as indicated above, the nature of the response can be strongly affected by the presence of disorder that results from alloy fluctuations or defects that are the intrinsic result of material growth [.4]. In this case, the assumption that the fundamental states of the system are described by extended states must be corrected to account for the localization induced effects. This behavior is especially important in nanostructures since it has been shown that in the presence of disorder, all states are localized in a system confined to two or less dimensions [.3, .5]. The theory for the nonlinear response in the presence of disorder is not nearly as well developed as is the theory in an ideal system. However, the experimental results discussed in this chapter provide physical insight and are compared to theory where possible.

The nonlinear optical properties of the exciton also strongly depend on the dynamical interaction of the exciton with the surrounding crystal lattice and vacuum radiation. Relaxation of the exciton and the associated polarization (i.e., the induced coherence) due to these interactions determine both the frequency dependence and dynamics of the nondegenerate nonlinear response. Here again, disorder can significantly alter these details. Therefore measurements of these properties are not only important for any application of these materials but also provide a quantitative description of the exciton relaxation process. This description can in turn be related to both the fundamental manybody physics and the physics associated with disordered systems. As

we discuss below in the latter case, exciton relaxation in a QW in part reflects properties of the $GaAs/Al_xGa_{1-x}As$ interface, an issue of importance in crystal growth.

Early insight into the effects of disorder was obtained in studies of exciton luminescence which showed the emission was inhomogeneously broadened due to the corresponding potential fluctuations [.6]. These studies were followed by results that indicated that this interface roughness is characterized by a scale length large compared to the Bohr radius of the exciton (see, for example, [.7, .8]); however, more recent studies by chemical lattice imaging have shown the presence of monolayer flat islands with a smaller spatial extent of 50-100 Å [.9]. These observations lead to the proposal that at least two scale lengths for interface roughness are required in order to account for the observations [.10]. While these results are presently somewhat controversial [.11, .12], further evidence that the island size distribution is bimodal has been recently presented in luminescence and Raman scattering measurements [.13]. Details of the interface roughness also depend on specific growth processes, such as interrupted or non-interrupted growth [.8], or whether GaAs is grown on $Al_xGa_{1-x}As$ or $Al_xGa_{1-x}As$ is grown on GaAs [.14]. The effects of interface roughness are significant. For example, an exciton confined to a thin GaAs layer (typically 100 Å) experiences an energy shift of order several meV for a monolayer well-width change. As the exciton moves inside the well, it will be scattered by the random potential due to the interface roughness. As a result, low energy excitons are expected to become *localized*, *i.e. the wave function* envelope decays exponentially in space. This dependence of the exciton energy on the local environment leads to inhomogeneous broadening of the linear absorption spectrum.

The resultant dynamics for localized and delocalized excitons have qualitatively different relaxation properties [.15]. Even at low temperature (<10K), localized excitons do not remain truly localized, instead they can migrate among localization sites by emitting or absorbing acoustic phonons (phonon assisted migration). Phonon assisted migration was first proposed to explain the slow and non-exponential energy relaxation observed in time resolved luminescence measurements in a GaAs QW structure [.16] and directly observed in InGaAs/InP QW where all excitons are localized by alloy disorder [.17] and in GaAs QW where excitons are localized due to interface disorder [.18, .19]. At higher temperatures, excitons can absorb phonons with sufficient energy to become activated to delocalized states at higher energies. The activation process has been observed in a number of measurements such as spectral hole burning [.20], resonant Raleigh scattering [.21], and resonant Raman scattering [.22]. Estimation of the activation energy have suggested that the onset for the delocalized exciton in GaAs QW structures is near the absorption line center [.20]. In contrast, decay of the delocalized exciton is determined by the exciton-

phonon scattering along the energy-momentum dispersion curve and the exciton recombination. Furthermore, delocalized excitons also experience elastic scattering from potential fluctuations, which introduces additional dephasing due to the decay of the polarization .

In the balance of this chapter, we present the results of the study of exciton dynamics in QWs based on two coherent nonlinear spectroscopy methods: high resolution frequency domain cw four wave mixing (FWM) and picosecond FWM. In principle, these two methods provide comparable information, but as we show, they are most sensitive to different aspects of the nonlinear response. As a result, we are able to develop a more complete picture of the system based on a combination of the data. The experimental results show: (1) the importance of disorder in determining the nonlinear response, (2) the presence of spectral diffusion due to phonon assisted migrations, (3) measurement of the exciton Zeeman splitting, (4) the presence of extra dephasing, (5) the polarization dependence of the picosecond response due to two distinct resonances, (6) coupling between opposite spin excitons.

Frequency Domain FWM Spectroscopy

High resolution frequency domain spectroscopy based on cw FWM is a powerful coherent spectroscopy method that can provide information on various relaxation phenomena and energy level structure. For example in a single measurement we are able to observe time scales ranging over twelve orders of magnitude [.23]. In addition, this method can eliminate the inhomogeneous broadening due to interface roughness or random crystal fields . This latter feature enables measurement of the homogeneous line shape. Since these measurements are performed in energy space, they are particularly sensitive to relaxation processes involving energy shifts of the excitation (i.e., spectral diffusion) such as the migration of excitons between different energy sites discussed above. The narrow excitation bandwidth also permits improved spectral resolution over the usual time domain measurements which is important since as we show below, many of the relaxation parameters vary spectrally across the exciton absorption feature. As pointed out below, however, the frequency domain measurements lose relative sensitivity with increasing polarization excitation decay rates. In this case, time domain measurements are especially helpful.

Since the theoretical basis for these spectroscopic measurements and a detailed discussion of the experimental approach is discussed in detail elsewhere [.24, .25], we will only summarize the key results in this chapter. The experimental configuration is based on the backward FWM geometry shown in Fig. .1. Since we are measuring the third order susceptibility tensor

$\chi^{(3)}(\omega_s=\omega_1-\omega_2+\omega_3)$, it is essential that the input frequencies of the three input beams shown in Fig. .1 be independent. In this geometry, two beams $E_1(\omega_1, k_1)$ and $E_2(\omega_2, k_2)$ interact in the sample with a third beam $E_3(\omega_3, k_3)$ ($E_1 \| E_2 \perp E_3$) through the resonant third order susceptibility to generate a signal beam $E_s(\omega_s, k_s)$ proportional to $\chi^{(3)}(\omega_s=\omega_1-\omega_2+\omega_3):E_1E_2^*E_3$. In a simple physical picture for this system (though not necessarily in general as we see in the time domain measurements below), $E_1 \cdot E_2^*$ results in a spatial and temporal modulation of the exciton population, which modifies the optical response of the sample leading to a traveling wave grating or modulation of the absorption and dispersion. The coherent nonlinear signal arises from scattering of the backward beam from the grating. Spectroscopic information can be obtained by studying the dependence of the nonlinear optical response on the relative frequency detuning, absolute frequency detuning, the electric field polarization, the input beam intensities and the relative angle of the different input beams, especially the angle between k_1 and k_2. The observed line shapes and corresponding physical information that is obtained depends on which frequency is tuned. In general, tuning ω_1 or ω_2 probes population and grating relaxation, while tuning ω_3 provides a measure of the homogeneous line shape [.26] and of the spectral redistribution of the excitation [.24]. Solution of the modified optical Bloch equations, including spectral diffusion [.24], provides complete understanding of this spectroscopy method. However, considering a few simple examples yields a more physical understanding of the line shapes.

We first consider excitation transfer between neighboring sites through an inter-site interaction (such as the dipole-dipole interaction). The excitation transfer is assumed to be characterized by a redistribution kernel $W(\omega, \omega')$ representing the rate for populations in the excited state to be transferred from sites with resonant frequency ω to sites with resonant frequency ω'. The overall spectral diffusion rate out of sites with frequency ω is then $\Gamma(\omega) = \int W(\omega,\omega')d\omega'$. $W(\omega,\omega')$ is analogous to collision kernels that are used to describe velocity changing collisions in atomic vapor [.27]. In addition, since the excitation transfer is likely to be associated with emission or absorption of thermal phonons, we assume there is no quantum coherence transfer in the spectral diffusion process; i.e., that at the new site the excitation transfer does not induce a superposition state of the ground and excited state that is coherent with the input fields. The validity of this assumption remains to be determined and is the subject of ongoing research.

It is important to note here that since this model is based on simple two-level atom type physics, it clearly does not completely represent the nonlinear response of the exciton nor the physical process of exciton migration during nonlinear optical interactions. However, the basic physical concepts that come from this picture are valid as long as there is no significant effect of an exciton at energy E on an exciton at energy E' in an inhomogeneously broadened system due for

example to screening or local field effects. This latter case clearly plays a role in time domain measurements [.28] although the effect on cw FWM is less clear. It is interesting to note that recent theoretical work has shown that in the limit that phase space filling dominates the exciton nonlinear optical response, the equation of motion governing the nonlinear optical processes in semiconductors is nearly identical to the optical Bloch equation of an atomic system [.29].

We now consider the line shape obtained by tuning ω_3. In this measurement, two nearly degenerate beams $\mathbf{E}_1$ and $\mathbf{E}_2$ interfere in the sample to excite a population modulation of a narrow spectral hole with a full-width $2\gamma_{ph}$ within the much larger inhomogeneous absorption line profile, where γ_{ph} is the polarization decay rate or dephasing rate. The line shape is obtained by measuring the nonlinear signal as a function of the frequency of the backward pump beam. This measurement is analogous to cw hole burning measurements and is also closely related to the standard two pulse or three pulse photon echo measurement discussed below. In hole burning measurements, the response is due to the modulation of the absorption whereas in FWM, a population grating is created and the signal is due to scattering of $\mathbf{E}_3$ by the resultant modulation of both the absorption and dispersion. The resonant response occurs when the signal frequency ω_s is resonant with states excited by $\mathbf{E}_1$ and $\mathbf{E}_2$ [.24]. In the absence of spectral diffusion, the line shape obtained by tuning ω_3 (which tunes ω_s where $\omega_s = \omega_1 - \omega_2 + \omega_3$) simply reflects the spectral details of the hole excited by $\mathbf{E}_1 \cdot \mathbf{E}_2^*$. The line shape reduces to a simple Lorentzian with a width *twice the homogeneous width* (i.e., $4\gamma_{ph}$).

In the presence of spectral diffusion, the problem becomes more complex. The hole excited by $\mathbf{E}_1 \cdot \mathbf{E}_2^*$ diffuses in energy space resulting in a spectral redistribution of the excitation. As before, a signal field is produced by the scattering of $\mathbf{E}_3$ when ω_s is resonant with the spectral hole. However, scattering of $\mathbf{E}_3$ also occurs when ω_s is resonant with states that are excited due to spectral diffusion, i.e., states which have been excited due to the transfer of energy away from the states of initial excitation. Hence, this redistribution can be directly mapped out in the line shape obtained by tuning ω_3.

While there are some apparent similarities between FWM and hole burning spectroscopy (FWM measures the square of the modulus of the third order susceptibility and spectral hole burning measures the imaginary part of the susceptibility), the FWM approach discussed here is considerably more powerful [.25]. The reason is that in frequency domain FWM, it is possible to control the contribution from the spectrally diffused excitation by using a fixed probe-forward pump frequency offset. In particular, the quasi-equilibrium distribution of excitation created by spectral diffusion decays on the time scale of the loss of total excitation (due e.g. to radiative

recombination). However, the primary component of the spectral hole decays at the spectral diffusion rate which is usually much faster than the former rate. The contribution from the spectrally diffused excitation can be effectively eliminated from the response by setting the frequency difference between ω_1 and ω_2 large compared to the life time of the quasi-equilibrium distribution. Furthermore, while the current discussion has focused on a simple resonant system, it is easy to imagine that there are different systems characterized by different excitation and dephasing relaxation rates but having nearly the same resonant frequency. By examining the homogeneous line width measured in this response as a function of different values of ω_1-ω_2, it is possible to differentiate between the different resonant systems.

In another class of measurements in this system, we hold $\omega_2=\omega_3$ and tune ω_1, producing a traveling wave modulation of excitation with amplitude proportional to $[\delta+i\Gamma_{pop}]^{-1}$ where $\delta=\omega_1-\omega_2$. The nonlinear response as a function of δ then measures the decay rate of the modulation formed by excitations that are resonant with the signal beam. The decay rate of the modulation, Γ_{pop}, due to population decay includes contributions from radiative and nonradiative recombination (γ_{rec}) as well as transfer of excitations from energy E to E', where $|E-E'| > \gamma_{ph}$, at the spectral diffusion rate Γ. Spectral diffusion due to intersite energy transfer is also accompanied by a corresponding change in spatial location of the excitation which contributes to the rate of washout of the spatial modulation and hence to Γ_{pop}. However, if the effective mean free path for excitation transfer is small, the effect would be described by a spatial diffusion process. Since we have assumed that the optical coherence is destroyed by the transfer process, the general contribution of spatial diffusion, whether or not it is associated with spectral diffusion, can be phenomenologically included as a spatial diffusion decay term in Γ_{pop}. The decay rate is given by $\Gamma_d= 4\pi^2D/\Lambda^2$ where D is the diffusion coefficient and Λ is the spatial period of the modulation ($\Lambda = \lambda / n2\sin\theta$, where θ is the angle between $\mathbf{E}_1$ and $\mathbf{E}_2$ in the material, λ is the wavelength and n is the index of refraction). The width of the FWM line shape is then given by $\Gamma_{pop}=\Gamma+\gamma_{rec}+\Gamma_d$. Note that in the limiting case where $\gamma_{ph}\sim\Gamma_{pop}/2$ ($\Gamma_d=0$), the FWM line shape obtained by tuning ω_1 is complicated by the fact that tuning ω_1 also changes the frequency of the signal beam and the frequency of the first order polarization. The line shape in this case then experiences an additional resonant effect from the hole burning denominator appearing as $[\delta+2i\gamma_{ph}]^{-1}$, resulting in a deviation from a simple Lorentzian and requiring a small correction (of order 1) in relating Γ_{pop} to the HWHM for absolute decay rate measurements [.18]. The FWM response obtained by tuning ω_2 provides a measurement similar to the line shape obtained by tuning ω_1. However, since $\omega_1=\omega_3$, the hole burning denominator appears as $(\delta+i\gamma_{ph})^{-1}$ resulting in a slightly larger correction. In the case of $\gamma_{ph}>>\Gamma_{pop}/2$, the line shapes obtained by tuning either ω_1 or ω_2 are the same and independent of γ_{ph}.

Spectral diffusion of the excitation between different energy sites also leads to the establishment of a quasi-equilibrium redistribution of the excited state population as we have discussed earlier. This is expected regardless of the functional form of the redistribution kernel. This quasi-equilibrium population contributes to the nonlinear response, and decay of this population is determined by the spontaneous emission of the excited states. If the spontaneous emission rate is slow compared to the spectral diffusion rate, then a narrow resonance with a half-width given by γ_{sp} can be observed on top of the broad resonance. In the limit of a very large spectral diffusion rate, the narrow resonance may even become dominant. In a typical time resolved luminescence measurement of this transition, the measured decay rate would be given by γ_{sp}. However, because of the hole burning achieved in frequency domain FWM, it is possible to separately measure both decay rates.

Measurements have been performed on various GaAs QW samples, differing primarily in the number of layers, the absorption width and Stokes shift in the luminescence. However, a typical GaAs QW sample used in our measurements consisted of 65 periods of 96 Å GaAs wells and 98 Å $Al_{0.3}Ga_{0.7}As$ barriers, characterized by an absorption line width of 2.2 meV for the HH1 exciton, and a Stokes shift of 1 meV between the HH1 exciton absorption and emission. A second sample has only 10 periods with a 0.8 meV line width and a 0.3 meV Stokes shift in the luminescence. The samples are mounted on a sapphire disk (c axis normal) with the substrate removed for the nonlinear measurement. The exciton density for these measurements was kept low, near 10^7 excitons /cm^2. All the nonlinear measurements are carried out on the HH1 exciton.

The overall cw degenerate (i.e., $\omega_s=\omega_1=\omega_2=\omega_3$) nonlinear response is shown in Fig. .2, obtained at 2.5 K. The rapid decrease of the nonlinear response around the absorption line center is partly due to strong exciton absorption. However, the nonlinear response on the high energy side of the absorption line center is extremely small compared to that on the low energy side, signaling a change of the exciton relaxation properties across the absorption line center. The small cw nonlinear optical response indicates a much increased exciton relaxation rate above the absorption line center, as we will show more directly below.

To characterize the relaxation of the exciton population, we examine the FWM line shape obtained by tuning ω_1 [.18]. Figure .3a shows a line shape obtained 1.5 meV below the line center of the HH1 resonance. If only a simple radiative recombination decay process was present, the line shape would be a single Lorentzian with a width given by recombination time of order 0.5 -1 nsec [.30]. The curve shows the relaxation process is considerably more complex, as

anticipated above. The complexity is manifest in the appearance of a small structure at the top of the resonance and the fact that the primary line width corresponds to a relaxation time of 60 ps. This time scale is slow compared to acoustic-phonon scattering of the delocalized exciton (typically on a time scale of 10 ps [.31]) and is an order of magnitude faster than the exciton recombination time. The line shape shown in Fig. .3a is independent of the modulation spacing. Recalling from the above discussion that the spatial diffusion rate varies as the inverse square of the grating spacing, we can infer an upper limit of order 1 cm^2/s for the exciton diffusion coefficient. This result indicates that excitons are strongly localized in this spectral region, as suggested by earlier resonant Raleigh scattering and transient FWM measurement of Hegarty and Sturge [.4]. The data in Fig. .3a suggest that the decay of the exciton population, Γ_{pop}, is characterized by exciton spectral diffusion as a result of scattering of localized excitons from energy E to E' ($|E-E'|>\gamma_{ph}$). The obtained decay rate is in agreement with the calculation based on phonon assisted migration of the localized exciton [.31].

The presence of spectral diffusion suggests that we should be able to detect the quasi-equilibrium distribution of excitons which are the result of this process and which decay at the recombination rate. In fact the FWM response shown in Fig. .3a shows a small and narrow feature at the top of the resonance. The narrow feature becomes more pronounced at higher temperature due to the faster exciton migration rate which also leads to an increase of the quasi-equilibrium population, as shown in Fig. .3b. The width associated with the feature corresponds to a decay time of 1.2 ns consistent with the exciton recombination rate, which also further supports the conclusion that the fast decay time is due to spectral diffusion.

The quasi-equilibrium exciton distribution due to spectral diffusion is readily observable in the FWM line shape obtained by scanning the back beam at ω_3. This enables a direct detection of excitons scattered from energy E to E' [.18, .32]. Figure .4a shows a FWM line shape where excitons are optically excited by $E_1 \cdot E_2^*$ 1.5 meV below the absorption line center. The nonlinear response is corrected for sample absorption. The narrow resonance in the response corresponds to exciton spectral hole burning, and the width of the hole gives an exciton homogeneous line width $2\gamma_{ph} \sim 0.03$ meV, assuming no contribution due to spectral diffusion. (Recall from above that in the absence of spectral diffusion, the observed width is $4\gamma_{ph}$.) The broad Stokes shifted feature is due to the quasi-equilibrium distribution of the exciton population, and the response is a function of the steady state exciton population assuming all excitons in the spectral region concerned give rise to the same cw nonlinear response. The FWM line shape in Fig. .4a can be fit to a simple model which neglects migration to states above the excitation energy. The calculation is based on the nonlinear optical response of a simple two level system and assumes a Gaussian distribution

for the quasi-equilibrium population of excitons that have migrated to states below the excitation energy. The spectral profile of the hole-burning resonance is assumed to be Lorentzian. The result is plotted as the solid line in Fig. .4a. A small but finite detuning of order 100kHz is set between fields 1 and 2 to reduce contributions to the data in Fig. .4a from slower components (discussed elsewhere [.33]).

Further insight into the mechanism of exciton migration is had by returning to the data in Fig. .3a and measuring the spectral diffusion rate as a function of temperature since the migration process is likely to involve absorption or emission of acoustic phonons. The theoretical model for phonon assisted exciton migration was developed recently by Takagahara [.31]. In the model, excitons resonantly excited are in a non-equilibrium state and can migrate to other sites by emitting or absorbing acoustic phonons. Migration is possible due to the overlap of the exciton wave function in different sites when the inter-site distance is small. When the inter-site distance is much greater than the localization length the process occurs by inter-site dipole-dipole coupling. The typical magnitude of participating phonon wave vectors is within a few times of the inverse of the localization length corresponding to phonon energies of order 0.01 to 0.1 meV. The theory predicts a distinctive temperature dependence for the migration rate. At low temperatures, the dependence is described by $\exp(\beta T^{\alpha})$. In this expression, β is positive and independent of temperature but is expected to increase with the exciton energy and depends on details of interface roughness; α is estimated to be between 1.6 and 1.7. The predicted temperature dependence is quite different from that of variable range hopping used by Mott to interpret electronic conduction in the localized regime [.34]. The difference has been attributed to the long-range nature of the inter-site interaction and the phonon emission process involved in the migration of the localized exciton [.15]. The temperature dependence has been observed in transient hole burning experiments in an InGaAs/InP QW where all excitons are localized by alloy disorder [.17].

Figure .5 shows the temperature dependence of the exciton migration rate measured at 0.6 meV and 1.5 meV below the absorption line center. The data is in good agreement with the phonon assisted migration theory discussed above with α=1.6. The measurement indicates that the dominant contribution to relaxation of the localized exciton is phonon assisted migration up to a temperature of 15 K. Earlier measurements have reported observations of an activation type of temperature dependence for the localized exciton at temperatures between 7 and 20 K, indicating that in this temperature region, relaxation for the localized exciton is dominated by thermal activation to delocalized states [.4, .22]. It is quite likely that sample dependent variations in the thermal activation energy are the result of differences in the nature of interface roughness [.35].

In this sample, spectral diffusion due to a thermal activation process is observed at temperatures above 15 K using the stimulated photon echo as we discuss below.

Earlier measurements using transient four wave mixing and resonant Raleigh scattering [.4] have suggested that in a multiple quantum well excitons above the exciton absorption line center may be weakly delocalized. Indeed as seen in Fig. .2, our measurements of the FWM response above the exciton absorption line center are qualitatively different from that below the absorption line center. Physically, excitons can become delocalized when the localization length is comparable with or larger than the scale of inelastic cutoff given by $\sqrt{D\tau}$ [.36], where D is the exciton diffusion coefficient and τ is the time between exciton-phonon scattering. Above line center, the nonlinear response is completely dominated by the recombination component even at our lowest temperature (1.8 K) as seen in Fig. .6a, in contrast to the results seen in Fig. .3. This behavior is expected if excitons experience an extremely rapid inelastic scattering such as in the case of a delocalized exciton. The line width observed by tuning ω_1 is fit by a Lorentzian and corresponds to a recombination time of 1.2 nsec. Measurement of this line shape as a function of the modulation spacing shows a quadratic dependence of the modulation decay rate on the inverse of the modulation spacing, yielding an exciton diffusion coefficient of order 16 cm^2/s, in contrast to the above results which indicated an upper limit of 1 cm^2/sec for the diffusion coefficient for excitons created well below line center.

The general features associated with higher energy excitons is seen in Fig. .4b where we created an exciton grating 2 meV *above* the absorption line center and probe the FWM response by tuning ω_3. A narrow hole burning resonance is not observed in this line shape. The nonlinear signal above the absorption line center is considerably smaller compared to that below the line center, which is due to rapid dephasing of the polarization as well as the much increased exciton population decay rate. A magnified version of the FWM spectrum above the absorption line center is also shown in the figure. A large dephasing rate for the delocalized exciton is expected [.31] since these excitons are expected to experience rapid elastic scattering from interface potential fluctuations in addition to the exciton-acoustic phonon scattering. The large dephasing rate compared to that reported for very high quality single QW [.37] indicates strong elastic scattering from interface disorder. The strong nonlinear optical signal below the absorption line center indicates that most of the excitons created above the absorption line center become localized before they eventually recombine.

Based on the cw frequency domain FWM described thus far, it is clear that the presence of disorder in these systems greatly modifies both the dynamical response of the resonant excitation

as well as the nonlinear optical properties. The discussion has focused on the clearly excitonic contributions to the nonlinear optical response, but as we discuss elsewhere [.33], there are other contributions to the nonlinear response which are nearly resonant with the exciton but appear to arise from correlated electron-hole pairs with relaxation times on the scale of microseconds. These contributions are caused by two-photon transitions, but are not biexcitonic in nature.

While the discussion up to this point has emphasized the use of cw FWM for measurements of relaxation, the great precision afforded in such measurements and the ability to eliminate inhomogeneous broadening can also be used to obtain new information on energy level structure. This is especially powerful in cases where linear spectroscopic methods fail due to the large inhomogeneous broadening compared to the relevant energy scale. The capability has been critical in our studies of spin flip induced hole burning and measurements of the exciton Zeeman splitting in modest magnetic fields.

To understand these experiments, we note that the electronic energy spectrum of quantum well structures is fully quantized under a magnetic field parallel to the growth axis. Optical absorption reveals a ladder of magnetoexcitons corresponding to transitions between electron and hole Landau levels [.38]. The accompanying Zeeman splitting lifts the Kramers degeneracy and is characterized by an effective g-factor which depends sensitively on the details of the band structure. In addition, the energy separation between the different spin leads to an increase in the spin relaxation time since now spin relaxation can only take place via inelastic processes [.39].

There have been numerous studies of the electron g-factor, however, determination of the Zeeman splitting has been more difficult because of the large inhomogeneous broadening due to disorder [.40] and the fact that the exciton Zeeman splitting in a quantum well is much smaller than in the for small magnetic fields. Earlier magneto-reflectance measurements were able to resolve Zeeman splittings for the light-hole but not the heavy-hole exciton [.41]. More recent measurements have inferred the exciton *g*-factor from nonlinear quantum beat spectroscopy [.42]. However, using the methods described above, we have been able to obtain the first direct measurements of the exciton Zeeman splitting in a GaAs quantum wells. The measurements reveal a heavy-hole splitting much smaller than that reported for bulk GaAs at low magnetic field, and show a nonlinear dependence of the splitting on magnetic field strength. The results reflect the effects of the complex band structure of a quantum well.

In these experiments, a nearly monochromatic optical beam with σ_- circular polarization is used to excite a narrow spectral-hole at the lowest heavy-hole (HH1) exciton associated with the 3/2 to

1/2 transition (see Fig. .7 for the 2-D exciton energy level diagram in a magnetic field). The width of the spectral-hole is determined by the homogeneous line width. Spin relaxation of these excitons generate a spectral-hole of excitons associated with the -3/2 to -1/2 transition. The induced spectral hole burning is probed using an optical beam with σ_+ circular polarization. Zeeman splitting can then be obtained by measuring the energy spacing between the spin-flip-induced spectral hole and the original spectral hole resonance.

In practice, the measurements proposed above are complicated by strong spectral diffusion of the localized excitons, as seen in Fig. .4a. In the limit where the spin-flip time is long compared with the spectral diffusion time, nearly all spin-flipped excitons have diffused in energy. Hence, the spin-flip-induced spectral hole burning resonance will be completely smeared out by the spectral diffusion process. To avoid the above complications, we exploit the power of FWM spectroscopy which enables us to eliminate the spectral diffusion contribution to the response. As before, nearly degenerate beams $\mathbf{E}_1$ and $\mathbf{E}_2$ interfere in the sample to excite a traveling wave grating which oscillates at a frequency equal to the detuning between the two beams $\delta=|\omega_1-\omega_2|$. The amplitude of the grating is proportional to $(\delta+i\Gamma_{pop})^{-1}$. Measuring the FWM signal as a function of ω_3 probes the spectral profile of the grating. In the presence of spectral diffusion, the spectral-hole excited by $\mathbf{E}_1\cdot\mathbf{E}_2^*$ diffuses in energy and the FWM response arises from both the spectral-hole and the quasi-equilibrium distribution of the exciton population as discussed above. The decay of the spectral hole is determined by the sum of the exciton spectral diffusion and recombination rates. However, the life time of the quasi-equilibrium distribution is determined solely by the recombination time of the exciton as we discussed earlier . In the limit where the spectral diffusion rate is much larger than the exciton recombination rate, detuning $\mathbf{E}_1$ and $\mathbf{E}_2$ by an amount large compared with the recombination rate (but still smaller than or comparable with the spectral diffusion rate) significantly decreases the amplitude of the grating associated with the quasi-equilibrium distribution. As a result, the FWM nonlinear optical response will be dominated by the spectral hole burning resonance [.25].

For these measurements, experiments were carried out at 2.5 K using a split-coil superconducting magnet. The effects of spectral diffusion were reduced on the spectral hole burning resonance by using two acousto-optic modulators to set the detuning between $\mathbf{E}_1$ and $\mathbf{E}_2$ to 140 MHz. In the first set of measurements, we used three circularly polarized optical beams rotating in the same direction in the lab frame. The nonlinear optical response, shown as squares in Fig. .8, involves only the σ_- excitons associated with the 3/2 to 1/2 transition. As expected, the contribution from spectral diffusion is nearly nonexistent.

When the electron or hole associated with a σ_- exciton created with $E_1 \cdot E_2^*$ flip their spin, the nonlinear response probed by reversing the polarization direction of the third beam will exhibit a resonance associated with a spectral hole located at the energy of the σ_+ exciton. The nonlinear response at the σ_+ exciton arises due to phase space filling caused by the presence of electrons (holes) with -1/2 (+3/2) angular momentum. The resulting resonance, shown as circles in Fig. .8, clearly shows narrow spectral hole burning at a lower energy. The energy difference is the exciton Zeeman splitting, which is 0.19 meV at 4T. The nearly constant background signal in Fig. .8 is due to excitons that have spectrally diffused. Note that spin-flips of σ_+ excitons require absorption of acoustic phonons, and are slower compared with spin-flips of σ_- excitons. The observed spin-flip-induced spectral hole burning resonance is considerably weaker at 4T when $E_1 \cdot E_2^*$ excites σ_+ excitons.

Using linearly polarized light for the third beam, we can simultaneously probe the spectral hole burning and the spin-flip-induced resonance. With $E_1 \cdot E_2^*$ exciting only the σ_- excitons, the FWM response obtained (see Fig. .9) shows the well resolved Zeeman doublet. Because of possible interference between the two resonances, the Zeeman splitting determined from Fig. .9 is less accurate than that from Fig. .8.

Recent measurements have shown that at low and intermediate magnetic field, the electron g-factor at the lowest Landau level in GaAs quantum wells is close to the value for bulk GaAs [.43]. In contrast, the Zeeman splitting of the HH1 exciton obtained above is very small in comparison with that reported for bulk GaAs [.44]. Our results seem to be in agreement with the earlier magneto-reflectance measurements where the heavy hole Zeeman doublet was not resolved. Small Zeeman splittings attributed to the strong valence band mixing in quantum well structures have been recently predicted by numerical calculations of magnetoexcitons using the Luttinger Hamiltonian [.45, .46]. In particular, the mixing of σ_- excitons with excitons at higher energy pushes the σ_- exciton to lower energy. The theory also predicts an eventual sign change of the Zeeman splitting at higher magnetic fields where the band mixing effects overcome those of the Zeeman interaction. However, theoretical determination of the magnetic field at which the zero crossing occurs is difficult since the cancellation of the two competing contributions depends strongly on parameters of the model [.46]. The sign change of the splitting has not been observed in our measurements up to 6 T.

Figure .10 displays the magnetic field dependence of the Zeeman splitting for the HH1 exciton. The validity of the quadratic dependence indicated in the figure (dashed line) is clearly

questionable since our data covers only a relatively small field range. Nevertheless, the observed field dependence is somewhat surprising since the calculations predict a field dependence slower than linear. The observed dependence may be due in part to the nonparabolicity of the conduction band [.47], which was not included in the calculations. Note that our results differ considerably from those obtained from nonlinear quantum beats in a 30 Å stepped GaAs quantum well [.42]. Zeeman splittings reported in the quantum beat measurements are proportional to magnetic fields with a field strength ranging from 1 to 5 T, and are very close to those measured for impurity bound excitons in bulk GaAs [.48].

In summary of this section, we note that frequency domain FWM spectroscopy shows the complex and rich nature of the nonlinear optical response of excitons in quantum wells as well as showing the extra complexity that results due to the presence of disorder. However, while these experiments have provided considerable understanding, we see in the next section that this picture is incomplete.

Picosecond Transient FWM Spectroscopy

In this section, we summarize our experimental results based on using coherent transient techniques, specifically stimulated photon echoes and free polarization decay. Compared to cw FWM spectroscopy, these methods are more sensitive to phenomena characterized by a range of dephasing times since the amplitude of the signal is independent of the dephasing time when the pulse widths are short compared to the different dephasing times. As in the case of cw FWM, coherent nonlinear transient effects can also eliminate the effects of inhomogeneous broadening, although these methods are not as sensitive to energy dependent decay phenomena such as spectral diffusion. In the presence of inhomogeneous broadening, the emission in a transient FWM experiment is delayed with respect to the last pulse and called a photon echo, whereas in a homogeneously broadened system, the signal is prompt and called a free polarization decay.

Coherent optical transient effects arising from atomic transitions are now well understood and have provided extensive information on decay processes of isolated atoms [.49] as well as atoms undergoing collisions with neutral ground state perturbers [.50, .51, .52, .53, .54, .55, .56]. However, there has been recent progress in developing the theoretical formalism for understanding coherent interactions in semiconductors as discussed elsewhere [.57, .58] and in this book. As discussed above, because the carriers are Fermions, this problem is considerably more complex than simple atomic systems.

The first experiments to demonstrate coherent transient effects in semiconductor heterostructures were the transient FWM measurements of Hegarty et al. [.59] performed at low temperature where they observed the large nonlinear response. These experiments demonstrated the use of coherent nonlinear transient spectroscopy techniques for measurement of fundamental parameters in these systems. This led to the use of transient four wave mixing (TFWM) experiments at low temperature in high quality GaAs epilayers and single quantum wells to demonstrate the rapid excitonic dephasing. In a series of measurements Schultheis and coworkers demonstrated the rapid dephasing due to scattering by longitudinal acoustic phonons of excitons in GaAs on time scales of 7 ps [.60], and found time scales of 2-3 ps for homogeneously broadened excitons in a high quality GaAs/AlGaAs single quantum well [.37]. In separate measurements they demonstrated and characterized dephasing due to exciton-exciton and exciton-carrier collisions [.61, .62, .63].

It is clear that based on earlier work [.4, .6] and the work discussed in the previous section that the exciton resonance in most of these systems is inhomogeneously broadened, and hence, the transient FWM response is expected to be an echo. It is useful to understand the physical origin of the echo: An inhomogeneously broadened medium excited by a short pulse ($\tau << \gamma_{ph}^{-1}$, where τ is the pulse width and γ_{ph} is the dephasing rate) exhibits a rapid decay of the free polarization decay (FPD) signal due to destructive interference between the radiated fields from different frequency groups. This decay time, often designated as T_2^*, is given by the inverse of the inhomogeneous width. T_2^* should be distinguished from the more fundamental decay time of the induced coherence in a specific resonance, given by $T_2=\gamma_{ph}^{-1}$, which of course is the inverse free polarization decay rate. However, application of a second pulse induces a rephasing, resulting in the emission of a delayed signal pulse (photon echo) due to constructive interference when the original phases are restored. Photon echoes were first reported by Kurnit et al. [.64, .65] and discussed in detail by Yajima [.66]. Although the first observation by Hu et al. of a photon echo signal in semiconductors was a Raman echo from donor bound excitons in *n*-CdS [.67] where the dephasing time is of order 100 ns, the first demonstrated photon echoes from intrinsic excitons in GaAs/AlGaAs multiple quantum wells was reported only recently by Schultheis, Hegarty and Sturge [.68]. Disorder at the interface between the GaAs in the quantum well and the AlGaAs barrier, resulting in well width fluctuations and hence fluctuations in the exciton energy as well as well-to-well thickness variations, provided the inhomogeneous broadening necessary for the production of an echo. Echoes from interband transitions in GaAs were reported by Becker et al. [.69] where the large carrier-carrier scattering rates for free carriers resulted in femtosecond dephasing. Noll et al. [.70] observed dephasing times of 200-500 ps using stimulated photon

echoes (a three pulse echo) from disorder localized excitons in CdS_xSe_{1-x} mixed crystals. The long dephasing times were attributed to the fact that the excitons were localized by disorder, resulting in a reduced scattering rate.

Another form of coherent optical effects are quantum beats which arise from interference effects between distinct resonances that are simultaneously excited by the incident pulses. The first observation of beats in the optical response of GaAs/AlGaAs MQWs was by Göbel et al. [.71], where the observed beats were between resonances not sharing a common state and hence are really polarization beats. The beats occur between the radiated field from excitons in regions of the wells that differed by one monolayer. Shortly thereafter quantum beats between the heavy-hole and light-hole excitons in quantum wells [.72, .73] were reported as were beats between free and bound excitons [.74]. In a related experiment Leo et al. used TFWM to observe coherent oscillations of a wave packet in a double quantum well [.75]. In this experiment two wells of differing width are separated by a thin barrier; carriers are excited in one well and shown to spatially oscillate between the wells.

The large optical density of these systems leads to coherent coupling of excitons through exciton-exciton interactions which are related to local field effects and can complicate the interpretation of results. The qualitative change in behavior can be seen by extending the simple two level model [.76] leading to so-called "negative" delay signals. This effect was first noted in atomic systems in accumulated photon echo experiments [.77] and recently reported in semiconductor systems [.28, .78]. Of more fundamental interest is the presence of strong Coulomb coupling in semiconductors. This can lead to dramatic modification of the nonlinear optical response for sufficiently strong excitation, as demonstrated by recent numerical calculations [.29, .57, .58]. Additional temporal structure predicted by these calculations has been observed [.79, .80].

Our own measurements have focused on the use of photon echoes and free polarization decay in three pulse FWM. As we discuss below, much of the information we have obtained using the methods of the previous section can be obtained from these experiments, though for many problems, the coherent transient studies are superior. However, as in the case of the cw FWM measurements in the first section, new results are obtained in measurements based on time resolving the emission of the nonlinear response and examining the dependence of the spectroscopic features on the polarization of the input beams. These results are not totally explained by the existing theoretical picture. Supplemental experiments based on non-degenerate pump and probe experiments provide some additional insight into these new effects.

The coherent transient spectroscopy measurements are based on degenerate three pulse TFWM in a backwards geometry (the so called phase conjugate geometry as in Fig. .1). The backward geometry is used since phase matching is assured and there is considerable improvement in the signal to noise. In this geometry the first pulse is incident at a small angle with respect to the second pulse, which in turn is counter-propagating with respect to the third pulse. The signal pulse counter-propagates with respect to the first pulse. The general experimental configuration and timing sequence is shown in Fig. .11. The signal pulse can be either time integrated in a photo-multiplier, or time-resolved by mixing with a reference pulse in a $LiIO_3$ second harmonic crystal. The input pulses are produced by a mode locked dye laser, where the pulse width can be adjusted between 1 ps and 8 ps autocorrelation width. Use of longer pulses is required for the spectrally sensitive measurements. For transient differential absorption measurements to examine polarization coupling, a 200 fsec self modelocked $Ti:Al_2O_3$ laser was used.

Three pulse TFWM allows the simultaneous measurement of both relaxation of the optically induced coherence (dephasing) and population (or excitation) [.81]. The time integrated signal strength as a function of the time interval between the first two pulses is proportional to $\exp(-4\gamma_{ph}\tau)$ for an inhomogeneously broadened resonance, where γ_{ph} is the dephasing rate, and τ is the interval between the first and second pulses. For a homogeneously broadened resonance the signal strength is proportional to $\exp(-2\gamma_{ph}\tau)$. The population decay rate determines the strength of the time integrated signal with respect to the interval between the second and third pulses and is proportional to $\exp(-2\Gamma_{pop}T)$ for either a homogeneously or an inhomogeneously broadened resonance. Γ_{pop} is the total population decay rate and T is the delay between the second and third pulses. As discussed above, Γ_{pop} has contributions from spectral and spatial diffusion as well as recombination.

As indicated above, in an ordinary two pulse (or spontaneous) photon echo the output pulse is emitted at a time after the arrival of the second pulse which is equal to the interval between the two incident pulses. In the three pulse (or stimulated) photon echo the output pulse is emitted at a time after the arrival of the third pulse equal to the interval between the first two pulses. In contrast the free polarization decay signal arising from a homogeneous system is emitted promptly upon the arrival of the third pulse and is independent of the interval between the first two pulses. The corresponding timing sequence is shown in Fig. .11. Hence observation of the time resolved signal for various delays between the first two pulses allows for the unambiguous discrimination between homogeneously and inhomogeneously broadened systems. In a simple resonant system it

is possible to distinguish between a homogeneously and inhomogeneously broadened system based upon the symmetry of the time integrated signal strength as a function of delay between the first two pulses [.81] . When there is non-zero delay between the second and third pulses, the signal from a homogeneously broadened system is symmetric about zero delay, whereas for an inhomogeneously broadened system a signal is only emitted for the "correct" time ordering resulting in an asymmetric response. However, as we will show, the complex nature of the optical response in a semiconductor heterostructure can make interpretation difficult, and time resolving the signal is essential to demonstrate the nature of the broadening.

An important feature of time resolving the emission in a photon echo experiment is that the *amount* of inhomogeneous broadening can be determined *explicitly* if the functional form of the inhomogeneous broadening is known. In the limit of delta function optical excitation pulses and strong Gaussian inhomogeneous broadening, the width of the echo is given by $\Delta t = 2\sqrt{2}\ln 2 / \pi\Delta\nu$ where Δt is the echo pulse width and $\Delta\nu$ is the full width half maximum of the Gaussian inhomogeneous distribution in Hertz. In the following experiments, it is important to consider the details of the pulse shape, and so we determine the inhomogeneous broadening by numerically integrating the optical Bloch equations assuming a Gaussian profile for the inhomogeneous broadening.

Using cross-correlation between the photon echo signal from a GaAs/AlGaAs MQW and a reference pulse, we obtain the time resolved delayed signal seen in Fig. .12a. To confirm that this is indeed a classical echo, we show in Fig. .12b that the output pulse position as a function of delay between the first two pulses varies linearly. The solid line is theory based on numerical integration of the optical Bloch equations and the slight deviation near zero is due to finite pulse effects [.19, .82]. The solid line in Fig. .12a is a fit to the echo pulse based on the numerical integration and provides an estimate of 2.25±0.25 meV for the inhomogeneous width, in good agreement with that observed in linear absorption for this sample.

Typical time integrated decay curves of both the dephasing rate and the excitation decay rate are shown in Fig. .13. These are taken at small angle between the first two fields so that spatial diffusion can be neglected. We see that the dephasing time is 68 ps while the excitation decay time is 34 ps. These results indicate that $\gamma_{ph} = \frac{1}{2}\Gamma_{pop}$. In the case of a simple resonant system this implies no lower level decay and no extra dephasing. These results are for low energy excitons (see inset) at low density (8×10^7) and are *intensity independent*. To obtain such a long dephasing time, it is also important to use long pulses (8 ps) to provide adequate spectral resolution (~0.1 meV). This dephasing rate corresponds to a homogeneous line width of 19 μeV, much less than

the inhomogeneous width. As expected from the above discussion the population relaxation is too fast to be due to recombination, which occurs on time scales of 0.5-1.0 ns at low temperature in these materials [.83], but rather is due to spectral diffusion.

Because of the bandwidth of a short optical pulse, it is difficult to obtain the kind of energy redistribution data that we obtained in cw FWM shown in Fig. .4a clearly demonstrating the presence of spectral diffusion. However, stimulated photon echoes can provide a key signature of this behavior [.81] which can be used to substantiate the above conclusion regarding spectral diffusion. In particular for large delay between second and third pulses (large compared to the spectral diffusion time), the dependence of the time integrated signal on first-second pulse delay is transformed from a simple exponential decay to a strong contribution at zero delay followed by a sharp drop in signal and an exponential decay. The decay rate for the exponential component is independent of the delay between the second and third pulses. To understand this, we recall that in the formation of an echo, each frequency group acquires a different phase during the time evolution between the first and second pulses while the third pulse causes the groups to rephase. However if an oscillator undergoes spectral diffusion between the arrival of the second and third pulses, that oscillator does not rephase at the correct frequency and hence does not contribute constructively to the coherent emission. When there is no delay between the first two pulses, the phase factor is the same for all frequency groups, i.e. identically zero, hence spectral diffusion has no effect and a strong coherent emission is still present, producing the spike at zero delay. This behavior is shown in Figure .14. In (a) the signal as a function of first-second pulse delay for zero two-three pulse delay is shown, and it is accurately described by a simple exponential decay. In (b) a large (50 ps) delay is introduced between the second and third pulse, a strong spike for zero first-second pulse delay now dominates the signal, as expected in the presence of strong spectral diffusion.

Using the stimulated photon echo, we have been able to reproduce the temperature dependence associated with phonon assisted tunneling discussed earlier in Fig. .5. In fact using this echo, we have extended the temperature range of the data shown above to confirm that the behavior of the excitation decay rate transforms from phonon assisted tunneling (varying as $\gamma = \Gamma_0 \exp(\beta T^{1.6})$) to thermal activation with the classical Arrhenius temperature dependence. The activation energy corresponds to the laser detuning from resonance, as expected if an exciton mobility edge exists near absorption line center. The details of these results are discussed elsewhere [.19]. However, the stimulated photon echo enables a more powerful examination of the relaxation processes by allowing us to compare the excitation relaxation rate and the dephasing rate as a function of temperature and energy. In Figure .15 we compare the dephasing rate and population relaxation rate as function of temperature (Fig. .15a) and exciton energy (Fig. .15b). While both increase

with increasing temperature or exciton energy, as expected based upon phonon assisted migration and the transition from localized to delocalized states at higher energy [.21], the dephasing rate increases more rapidly. At low temperature and energy the dephasing time is exactly twice the population relaxation time as seen in Fig. .13, or in terms of rates, $\gamma_{ph} = \frac{1}{2}\Gamma_{pop}$. The dashed lines in Fig. .15 shows $\gamma_{ph} - \frac{1}{2}\Gamma_{pop}$. The extra dephasing is either the result of $\gamma_{ph} = \frac{1}{2}\Gamma_{pop} + \gamma_{ph}^{ex}(T,E)$, where $\gamma_{ph}^{ex}(T,E)$ represents pure dephasing processes, or the fact that ground state scattering processes are present at higher temperature and energy. The observation that in some samples the dephasing rate can exceed the population decay rate indicates that pure dephasing processes do contribute to the relaxation. The presence of such terms indicate that pure elastic scattering is present, where elastic means that there is no change in the energy of the exciton after scattering. The dependence on temperature suggests a phonon scattering process, but such a process would require at least two phonons in a second order process in order to be elastic. The issue of dephasing in these systems is the subject of recent theoretical work [.84].

In the above measurements, the discussion has stressed the basic aspects of relaxation and exciton dynamics. It is clear that disorder plays a major role in these systems since all the dynamical process which we have been investigating, including spectral diffusion and phonon-assisted-migration, are controlled by the nature of disorder. However more recently, several studies have reported that the dephasing rate changes dramatically in two pulse echo experiments in a MQW when the first field is cross polarized [.85, .86] with respect to the other incident field. However an even more fundamental change in the response is noted upon comparison of the time resolved signals. In the above transient FWM experiments, all beams were linearly co-polarized. Figure .16 compares the time resolved emission in a co-polarized experiment (Fig. .16a) to that for $\mathbf{E}_1 \perp \mathbf{E}_2 \parallel \mathbf{E}_3$, $\mathbf{E}_s \parallel \mathbf{E}_1$ (Fig. .16b). The data show that in the former case the emission time depends on the interval between $\mathbf{E}_1$ and $\mathbf{E}_2$ while in the second case it does not. [The weak echo signal evident in Fig. .16b arises from a resonance which is 2.5 meV Stokes shifted from the absorption peak. On resonance the strength of the signal is comparable to the free polarization decay, however, the contribution is observable in Fig. .16b despite the large detuning because the dephasing time, at 70 ps, is even longer than that for the primary stimulated photon echo. Further discussion is given below.] Both the free polarization decay (.16b) and co-polarized stimulated photon echo (.16a) are resonant and show very similar spectral dependence, and after correction for absorption are nearly coincident with the absorption maximum. The free polarization decay is approximately 2 orders of magnitude weaker than the co-polarized stimulated photon echo at low intensity at the peak of the response. Based on the above discussion, it is clear that the signal for $\mathbf{E}_1 \parallel \mathbf{E}_2$ is due to an inhomogeneously broadened resonance while the signal for $\mathbf{E}_1 \perp \mathbf{E}_2$ is due to a homogeneously broadened resonance.

This behavior is completely unexpected. Based on the energy level structure (see Fig. .16a inset) no difference in the nature of the signal is expect other than the polarization. More specifically in GaAs, quantum confinement lifts the valence band degeneracy at k=0 resulting in heavy-hole-light-hole splitting. When the axis of quantization is taken to be perpendicular to the barriers, the heavy-hole valence band has only two degenerate magnetic substates given by m=±3/2 levels while the conduction band substates are given by m=±1/2. The selection rules for optical excitation are Δm=±1. Since linearly polarized fields propagating parallel to the axis of quantization can be taken as a superposition of two circularly polarized fields, we can designate the exciton created by a σ_+ polarized field as $|+1\rangle$ (consisting of a +3/2 hole and a -1/2 electron) and the exciton created by a σ_- polarized field as $|-1\rangle$ (consisting of a -3/2 hole and a 1/2 electron) [.87]. The signal is produced by the scattering of E_3 off the grating produced by $E_1^* E_2$. We see then that for linear co-polarized E_1 and E_2, two spatial gratings consisting of $|+1\rangle$ and $|-1\rangle$ excitons respectively, are created and are spatially coincident. For $E_1 \perp E_2$, the two gratings are exactly spatially out of phase. However, E_3 must also be decomposed into circularly polarized components, each of which independently scatters from one of the gratings, resulting in a linearly polarized signal field. Hence the change in the nonlinear response in Fig. .16 is clearly unexpected. (This picture is for a homogeneously broadened system but still provides insight for an inhomogeneously broadened system. Although there is no net grating, there is a grating for each frequency group within the inhomogeneous distribution. Each group results in a component of the scattered signal, and it is the phase relationship between these components which results in the signal delay.)

In Fig. .17, we compare the dephasing rates for these two components of the response as a function of excitation wavelength. The dephasing rate for the prompt signal ($E_1 \perp E_2$) is much greater than the delayed signal, 0.20-0.25 ps^{-1} and essentially energy independent. The dephasing rate for the delayed signal ($E_1 \| E_2$) varies from 0.016±0.001 ps^{-1} on the low energy side to 0.1±0.02 ps^{-1} on the high energy side. The increase in the dephasing rate with increasing photon energy has been reported earlier [.4, .18] and is expected due to the increase in scattering rate for localized excitons near the mobility edge [.4]. The temperature dependence of these dephasing rates also differs considerably. In Fig. .18 we see that the temperature dependence of the dephasing rate of the delayed component follows the behavior for phonon assisted migration and thermal activation of localized excitons as described above. However, the dephasing rate for the prompt signal shows a linear temperature dependence of the form $\gamma_{ph} = \gamma_0 + \gamma^* T$, where $\gamma^* = 4\mu eV / K$. We note that the magnitude of γ_0, the linear dependence on temperature and the magnitude of γ^* are similar to that observed by Schultheis in a single quantum well which was

believed to be of very high quality [.37]. The sample in that work was believed to be homogeneously broadened with no Stokes shift in the luminescence. Based on the quality of the sample, the homogeneous broadening of the HH1 resonance even at low temperature and the linear temperature dependence of the dephasing rate, Schultheis et al. proposed that the scattering mechanism was single phonon scattering [.88] along the 2-D dispersion curve of an exciton described by an extended (delocalized) wave function.

It is, of course, difficult to determine experimentally if a wave function is truly extended. However, there are several other experimental results consistent with such a potentially interesting explanation for the above data. In Fig. .19 we show that for fixed pulse delay and energy, the magnitude of both signals varies cubically with the incident beam energies (the solid line corresponds to a slope of n=3). However, at densities above 2×10^8, the stimulated photon echo emission deviates from cubic behavior and begins to saturate while there is no evidence of saturation in the prompt signal. Such saturation of the delayed signal which arises due to localized excitons would be expected since there are a finite number of localization sites. The saturation intensity of the nonlinear response in an ideal quantum well where all states are extended is expected to be considerably higher [.89] than that seen for localized states in Fig. .19. At sufficiently high excitation intensity, the co-polarized signal is comprised of both a prompt signal and an echo [.90], but as the intensity increases, the delayed signal completely saturates, leaving only the free polarization decay, as seen in Fig. .20.

Transport measurements also provide an indication of the origin of the differences in these two signals. To examine this aspect of the behavior, we studied the angle dependence of the excitation relaxation rate to probe the spatial "washout" time due to motion of the excitation. This is the typical approach in transient grating experiments to measure spatial diffusion [.91]. the total signal decay is given by Γ_m, as discussed earlier for frequency domain FWM. It would be expected that delocalized states should have a larger D than localized states.

Figure .21 shows $2\Gamma_m$ as a function of inverse grating spacing for the free polarization decay and the stimulated photon echo, fitting to a quadratic dependence yields D=5.2 for the stimulated photon echo and D=10.1 for the free polarization decay. This data is taken at an exciton energy 0.5 meV below line center and at a temperature of 15 K. The measured difference is larger in other samples. This difference is clear evidence of the greater mobility of the excitons which are responsible for the free polarization decay signal. The diffusion coefficient for localized excitons is dependent on the exciton energy [.4] and this measurement is taken at a point where it is beginning to undergo a transition from its low energy (small D) to high energy (large D) values.

The ratio of the two diffusion coefficients is sample dependent as expected where in a 10 period sample, the ratio is as large as 3.5.

There are several theoretical considerations which impact the proposed explanation. First we note that recent theoretical work on the nonlinear response for excitons in an ideal semiconductor shows that the TFWM signal is a prompt free polarization decay for low intensity excitation resonant with the exciton [.57, .58]. We note that this same theory predicts that at higher excitation densities, contributions from the continuum states leads to double pulse structure similar to that shown in the middle curve in Fig. .20. However, this delayed signal is predicted to increases in strength with increasing excitation density, in contrast to our measurements where the delayed signal is clearly due to localized states. In fact the delayed signal predicted by theory is not expected at our excitation level for a 100Å well. Hence, while these measurements constitute no proof, the data is certainly suggestive that both localized and extended state excitons are simultaneously present in the system, and the results provide a strong motivation for further research while clearly showing the complexity of the physics involved in the nonlinear optical response in semiconductor heterostructures. Similar results have been obtained in all our samples including very high quality samples. It is important to note that the coexistence of both localized and delocalized states is unexpected from weak localization theory. Disorder results in localization due to the constructive interference of the back scattered wave function [.3, .92]. In two dimensions any disorder is thought to localize all states according to arguments based upon scaling theory [.5]. For $T > 0$ inelastic scattering by phonons can lead to delocalized states. Coupling between localized and delocalized states at the same energy is thought to lead to decay of the localized ones into the delocalized ones [.93] preventing their coexistence at the same energy, although recently these ideas have been challenged [.94]. However, the complex nature of the interface disorder in quantum wells makes a simple application of these theoretical considerations difficult. The recent evidence for a bimodal distribution of roughness length scales [.10, .13] may provide regions where excitons are strongly localized and others regions where the wave functions are more extended. Indeed, an alternate explanation is that excitons are localized according to these two different scale lengths. If one of the scale lengths is sufficiently large, phonon-assisted-tunneling will be reduced while the large spatial extent of the wave function will reduce the oscillator strength and increase the dephasing rate. However, in this latter picture it is somewhat surprising that the stimulated photon echo and free polarization decay have the same spectral dependence.

The observation of the free polarization decay is a result of the suppression of the stimulated photon echo using orthogonally polarized excitation beams. However, as seen in the discussion of

FWM in the context of the energy level diagram in Fig. .16, it is clear that the absence of the stimulated photon echo with orthogonally polarized light is disturbing. The relative strength of the two signals indicates that while both localized and extended state excitons are contributing to the co-polarized response, the response due to localized excitons completely dominates the signal at low density, although at higher density both signals can be observed. Indeed, the resolution of this issue remains incomplete, however, some insight into this problem is had by extending our earlier discussion of the origin of the TFWM signal and considering additional experimental results.

In particular, coupling between the $|+1\rangle$ and $|-1\rangle$ excitons for $\mathbf{E}_1 \perp \mathbf{E}_2$ will result in suppression of a scattered signal. This is a consequence of the fact that the spatial modulations for the two excitons are spatially out of phase and hence coupling of $|+1\rangle$ ($|-1\rangle$) exciton to a $|-1\rangle$ ($|+1\rangle$) exciton in a region of $|+1\rangle$ ($|-1\rangle$) excited excitons will reduce the fringe contrast ratio for each spatial modulation. We note that TFWM using circularly polarized excitation beams supports the idea that the apparent change in dephasing rate is due to the suppression of the response giving rise to the slow dephasing and the echo since we have experimentally shown that under no combination of circular polarizations is the rapid dephasing for crossed linearly polarized excitation observed. Additionally we have shown that when $\mathbf{E}_1$ and $\mathbf{E}_2$ are co-circularly-polarized and $\mathbf{E}_3$ is linearly polarized, the resultant signal is also linearly polarized. This is demonstrated in Fig. .22, where the polarization of the signal field, for $\mathbf{E}_1$ and $\mathbf{E}_2$ are co-circularly-polarized, is shown as a function of incident flux. At low excitation density the polarization is zero, within experimental accuracy, i.e. the signal field is linearly polarized. At higher excitation the signal field becomes polarized in the same sense as $\mathbf{E}_1$ and $\mathbf{E}_2$ as is expected for an ideal semiconductor. This low excitation density result is surprising as the grating should only exist for one of the two transitions, and hence only scatter one of the two circular components which make up $\mathbf{E}_3$, resulting in a circularly polarized signal. This result is consistent with a coupling between the $|+1\rangle$ and $|-1\rangle$ excitons for localized states resulting in the destructive interference and hence suppression of the emitted signal for crossed-linearly-polarized fields. The transition from a linearly polarized to a circularly polarized signal occurs at incident fluxes comparable to those at which the photon echo component saturates (Fig. .19), this is consistent with the echo signal scattering from both transitions.

To probe for a coupling between the $|+1\rangle$ and $|-1\rangle$ excitons, we used circularly polarized light in a simple (incoherent) transient absorption measurement, where the pump and probe have opposite circular polarization. Using a circularly polarized pump beam and a linearly polarized probe, which is resolved into circularly polarized components after passing through the sample, we

discover that there is indeed a strong *instantaneous* coupling. This is evident in Figure .23, where the induced transmission for both circular components as a function of delay is shown. These measurements were made with 2.8 ps pulses (0.5 meV below absorption line center), however the coupling still appears instantaneous even when 300 fs pulses are used.

Although coupling will reduce the magnitude of the simulated photon echo, we must still consider the origin of the coupling. The instantaneous nature of the coupling rules out spin relaxation, which occurs on a time scale of 30-50 ps [.95, .96] (the convergence of the two curves in Fig. .23 is due to spin relaxation, and indicates a spin relaxation time of 40 ps). In addition, although band mixing between the HH1 and LH1 valence bands will result in an instantaneous coupling, current estimates suggest the effect is not sufficiently large to explain our results [.97, .98]. We currently believe it is at least in part due to localization enhanced biexcitonic effects, where the presence of one exciton at a localization site means that creating a second one of opposite spin results in formation of a biexciton, and hence a shift of the resonance by the biexciton binding energy. Evidence for biexcitonic effects has been observed as beats in transient absorption measurements [.96], as well as in two-pulse TFWM [.99].

Non-degenerate transient absorption measurements allow more direct observation of biexcitonic effects (Figure .24). A Stokes shifted induced absorption appears when the probe is oppositely circularly polarized with respect to the pump, as expected if biexcitons are being formed. For pump energy below line center, the Stokes shift is *constant with respect to the pump frequency*. A more complete presentation of these results will be made elsewhere [.100]. Any biexcitonic effect will indeed only effect the localized excitons giving rise to the stimulated photon echo as the probability for formation of biexcitons is considerably smaller for delocalized excitons at the low densities employed.

Although it is clear that a strong coupling exists between $|+1\rangle$ and $|-1\rangle$ excitons and that it is likely due to localization enhanced biexcitonic effects, the apparent complete suppression of the stimulate photon echo from localized excitons is not yet fully understood. To determine if the coupling observed in transient absorption is sufficient for complete suppression of the simulated photon echo a careful calculation of the pertinent coherent processes must be undertaken.

Summary

In this chapter, we have shown that coherent nonlinear optical interactions in quantum well structures exhibit a rich spectrum of behavior which reflects not only on the differences between these systems and simple atomic systems but also on the complexity due to the manybody nature of the interaction and the effects of disorder. The experimental methods required to extract meaningful information in these experiments is also more complex than in simpler systems, but the results provide a basis for the understanding of the interaction of light with semiconductors as well as providing a powerful means for the study of complex materials.

There are of course numerous other kinds of coherent nonlinear optical effects which have yet to be observed in these systems. For example, the presence of higher lying levels due sub-bands suggests that two-photon echoes [.52] or tri-level echoes [.51] could be observed. Coherent excitation from HH1 to E1 to E2, involving two photons could be used to probes higher lying energy level structure as well as the new relaxation processes. A very significant question would be to understand the nature of the correlations between the inhomogeneous broadening mechanisms involves with these different resonances. Coherent spectroscopy methods could also be used to better understand the role of the biexciton. Alternatively, based on the understanding had in quantum wells, it would be useful to explore the nature of the coherent nonlinear optical interactions in structures with increased quantum confinement such as quantum wires and dots. These importance of these methods will increase in systems where "dark states", i.e., states which participate in the optical interactions but do not radiate, may dominate in relaxation processes.

References

[.1] Schmitt-Rink, S., Chemla, D. S. and Miller, D. A. B., Phys. Rev. B **32**, (1985) 6601.

[.2] Haug, H. and Koch, S. W., Quantum Theory of the Optical and Electronic Properties of Semiconductors, World Scientific, Singapore 1990.

[.3] Lee, P. A. and Ramakrishnan, T. V., Rev. Mod. Phys. **57**, (1985) 287.

[.4] Hegarty, J. and Sturge, M. D., J. Opt. Soc. Am. B. **2**, (1985) 1143.

[.5] Abrahams, E., Anderson, P. W., Licciardello, D. C. and Ramakrishnan, T. V., Phys. Rev. Lett. **42**, (1979) 673.

[.6] Weisbuch, C., Dingle, R., Gossard, A. C. and Wiegmann, W., Solid State Comm. **38**, (1981) 709.

[.7] Miller, R. C., Tu, C. W., Sputz, S. K. and Kopf, R. F., Appl. Phys. Lett. **49**, (1986) 1245.

[.8] Tu, C. W., Miller, R. C., Wilson, B. A., Petroff, P. M., et al., J. Cryst. Growth **81**, (1987) 159.

[.9] Ourmazd, A., Taylor, D. W., Cunningham, J. and Tu, C. W., Phys. Rev. Lett. **62**, (1989) 933.

[.10] Warwick, C. A., Jan, W. Y., Ourmazd, A. and Harris, T. D., App. Phys. Lett. **56**, (1990) 2666.

[.11] Ourmazd, A. and Cunningham, J., Phys. Rev. Lett. **65**, (1990) 2318.

[.12] Deveaud, B., Guenais, B., Poudoulec, A., Regreny, A., et al., Phys. Rev. Lett. **65**, (1990) 2317.

[.13] Gammon, D., Shanabrook, B. V. and Katzer, D. S., Phys. Rev. Lett. **67**, (1991) 1547.

[.14] Tanaka, T. and Sakaki, H., J. Cryst. Growth **81**, (1987) 153.

[.15] Takagahara, T., J. Lumin. **44**, (1989) 347.

[.16] Masumoto, Y., Shionoya, S. and Kawaguchi, H., Phys. Rev. B **29**, (1984) 2324.

[.17] Hegarty, J., Tai, K. and Tsang, W. T., Phys. Rev. B **38**, (1988) 7843.

[.18] Wang, H., Jiang, M. and Steel, D. G., Phys. Rev. Lett. **65**, (1990) 1255.

[.19] Webb, M. D., Cundiff, S. T. and Steel, D. G., Phys. Rev. B **43**, (1991) 12658.

[.20] Hegarty, J., Goldner, L. and Sturge, M. D., Phys. Rev. B **30**, (1984) 7346.

[.21] Hegarty, J., Sturge, M. D., Weisbuch, C., Gossard, A. C., et al., Phys. Rev. Lett. **49**, (1982) 930.

[.22] Zucker, J. E., Pinczuk, A., Chemla, D. S. and Gossard, A. C., Phys. Rev. B **35**, (1987) 2892.

[.23] Remillard, J. T., Wang, H., Steel, D. G., Oh, J., et al., Phys. Rev. Lett. **62**, (1989) 2861.
[.24] Wang, H. and Steel, D. G., Phys. Rev. A **43**, (1991) 3823.
[.25] Wang, H. and Steel, D. G., App. Phys. **A33**, (1991) 514.
[.26] Steel, D. G. and Remillard, J. T., Phys. Rev. A **36**, (1987) 4330.
[.27] Berman, P. R., Phys. Rep. **43**, (1978) 101.
[.28] Leo, K., Wegener, M., Shah, J., Chemla, D. S., et al., Phys. Rev. Lett. **65**, (1990) 1340.
[.29] Lindberg, M. and Koch, S. W., Phys. Rev. B **38**, (1988) 3342.
[.30] Göbel, E. O., Jung, H., Kuhl, J. and Ploog, K., Phys. Rev. Lett. **51**, (1983) 1588.
[.31] Takagahara, T., Phys. Rev. B **32**, (1985) 7013.
[.32] Wang, H., Remillard, J. T., Webb, M. D., Steel, D. G., et al., Surf. Sci. **228**, (1990) 69.
[.33] Jiang, M., Wang, H. and Steel, D. G., to be published (1992)
[.34] Mott, N. F. and Davis, E. A., Electronic Processes in Non-Crystalline Materials, 2nd, Clarendon Press, Oxford 1979.
[.35] Takagahara, T., private communication.
[.36] Thouless, D. J., Phys. Rev. Lett. **39**, (1977) 1167.
[.37] Schultheis, L., Honold, A., Kuhl, J., Köhler, K., et al., Phys. Rev. B **34**, (1986) 9027.
[.38] Shinada, M. and Tanaka, K., J. Phys. Soc. Jpn **29**, (1970) 1258.
[.39] Potemski, M., Maan, J. C., Fasolino, A., Ploog, K., et al., Phys. Rev. Lett. **63**, (1989) 2409.
[.40] Snelling, M. J., Blackwood, E., McDonagh, C. J. and Harley, R. T., Phys. Rev. B **45**, (1992) 3922.
[.41] Lefebvre, P., Gil, B., Lascaray, J. P., Mathieu, H., et al., Phys. Rev. B **37**, (1988) 4171.
[.42] Bar-Ad, S. and Bar-Joseph, I., Phys. Rev. Lett. **66**, (1991) 2491.
[.43] Dobers, M., Klitzing, K. and Weimann, G., Phys. Rev. B **38**, (1988) 5453.
[.44] Bimberg, B., Advan. in Solid State Phys. **XVIII**, (1977) 195.
[.45] Bauer, G. E. W. and Ando, T., Phys. Rev. B **37**, (1988) 3130.
[.46] Bauer, G. E. W., in High Magnetic Fields in Semiconductor Physics II, G. Landwehr ed. Spring-Verlag, Berlin 1989.
[.47] Lommer, G., Malcher, F. and Rossler, U., Phys. Rev. B **32**, (1985) 6965.
[.48] White, A. M., Hinchliffe, I. and Dean, P. J., Solid State Commun. **10**, (1972) 497.
[.49] Stenholm, S., Foundations of Laser Spectroscopy, Wiley, New York 1984.

[.50] Liao, P. F., Economou, N. P. and Freeman, R. R., Phys. Rev. Lett. **39**, (1977) 1473.

[.51] Mossberg, T., Flusberg, A., Kachru, R. and Hartmann, S. R., Phys. Rev. Lett. **39**, (1977) 1523.

[.52] Flusberg, A., Mossberg, T., Kachru, R. and Hartmann, S. R., Phys. Rev. Lett. **41**, (1978) 305.

[.53] Flusberg, A., Kachru, R., Mossberg, T. and Hartmann, S. R., Phys. Rev. A **19**, (1979) 1607.

[.54] Kachru, R., Mossberg, T. W. and Hartmann, S. R., Opt. Comm. **30**, (1979) 57.

[.55] Mossberg, T. W., Flusberg, A., Kachru, R. and Hartmann, S. R., Phys. Rev. Lett. **42**, (1979) 1665.

[.56] Kachru, R., Mossberg, T. W. and Hartmann, S. R., Phys. Rev. A **21**, (1980) 1124.

[.57] Lindberg, M., Binder, R. and Koch, S. W., Phys. Rev. A **45**, (1992) 1865.

[.58] Schaefer, W., Jahnke, F. and Schmitt-Rink, S., manuscript (1992)

[.59] Hegarty, J., Sturge, M. D., Gossard, A. C. and Wiegman, W., Appl. Phys. Lett. **40**, (1982) 132.

[.60] Schultheis, L., Kuhl, J., Honold, A. and Tu, C. W., Phys. Rev. Lett. **57**, (1986) 1797.

[.61] Schultheis, L., Kuhl, J., Honold, A. and Tu, C. W., Phys. Rev. Lett. **57**, (1986) 1635.

[.62] Honold, A., Schultheis, L., Kuhl, J. and Tu, C. W., XVI Int. Conf. on Qu. Elect., 1988.

[.63] Honold, A., Schultheis, L., Kuhl, J. and Tu, C. W., Phys. Rev. B **40**, (1989) 6442.

[.64] Kurnit, N. A., Abella, I. D. and Hartmann, S. R., Phys. Rev. Lett. **13**, (1964) 567.

[.65] Abella, I. D., Kurnit, N. A. and Hartmann, S. R., Phys. Rev. **141**, (1966) 391.

[.66] Yajima, T. and Taira, Y., J. Phys. Soc. of Japan **47**, (1979) 1620.

[.67] Hu, P., Geschwind, S. and Jedju, T. M., Phys. Rev. Lett. **37**, (1976) 1357.

[.68] Schultheis, L., Sturge, M. D. and Hegarty, J., Appl. Phys. Lett. **47**, (1985) 995.

[.69] Becker, P. C., Fragnito, H. L., Brito Cruz, C. H., Fork, R. L., et al., Phys. Rev. Lett. **61**, (1988) 1647.

[.70] Noll, G., Siegner, U., Shevel, S. G. and Göbel, E. O., Phys. Rev. Lett. **64**, (1990) 792.

[.71] Göbel, E. O., Leo, K., Damen, T. C., Shah, J., et al., Phys. Rev. Lett. **64**, (1990) 1801.

[.72] Leo, K., Damen, T. C., Shah, J., Göbel, E. O., et al., App. Phys. Lett. **57**, (1990) 19.

[.73] Feuerbacher, B. F., Kuhl, J., Eccleston, R. and Ploog, K., Solid State Commun. **74**, (1990) 1279.

[.74] Leo, K., Damen, T. C., Shah, J. and Köhler, K., Phys. Rev. B **42**, (1990) 11359.

[.75] Leo, K., Shah, J., Göbel, E. O., Damen, T. C., et al., Phys. Rev. Lett. **66**, (1991) 201.

[.76] Wegener, M., Chemla, D. S., Schmitt-Rink, S. and Schäfer, W., Phys. Rev. A **42**, (1990) 5675.

[.77] Saikan, S., Miyamoto, H., Tosaki, Y. and Fujiwara, A., Phys. Rev. B **36**, (1987) 5074.

[.78] Leo, K., Göbel, E. O., Damen, T. C., Shah, J., et al., Phys. Rev. B **44**, (1991) 5726.

[.79] Kim, D.-S., Shah, J., Cunningham, J. E. and Damen, T. C., Phys. Rev. Lett. **68**, (1992) 2838.

[.80] Kim, D.-S., Shah, J., Damen, T. C., Cunningham, J. E., et al., Quantum Electronics and Laser Science, Anaheim, 1992.

[.81] Weiner, A. M., De Silvestri, S. and Ippen, E. P., J. Opt. Soc. Am. B. **2**, (1985) 654.

[.82] Webb, M. D., Thesis, University of Michigan, 1990.

[.83] Feldman, J., Peter, G., Gobel, E. O., Dawson, P., et al., Phys. Rev. Lett. **59**, (1987) 2337.

[.84] Lonsky, C., Thomas, P. and Weller, A., Phys. Rev. Lett. **63**, (1989) 652.

[.85] Yaffe, H. H., Prior, Y., Harbison, J. P. and Florez, L. T., Quantum Electronics Laser Science, Baltimore, 1991.

[.86] Leo, K., Shah, J., Schmitt-Rink, S. and Köhler, K., VIIth International Symposium on Ultrafast Processes in Spectroscopy, Bayreuth (Germany), 1991.

[.87] Planel, R. and Benoit a la Guillaume, C., Optical Orientation of Excitons in Optical Orientation, F. Meier and B. P. Zakharchenya ed. Elsevier, Amsterdam 1984.

[.88] Miyata, T., J. Phys. Soc. Jap. **31**, (1971) 529.

[.89] Chemla, D. S., Schmitt-Rink, S. and Miller, D. A. B., Nonlinear Optical Properties of Semiconductor Quantum Wells in Optical Nonlinearities and Instabilities in Semiconductors, H. Haug ed. Academic Press, San Diego 1988.

[.90] Webb, M. D., Cundiff, S. T. and Steel, D. G., Phys. Rev. Lett. **66**, (1991) 934.

[.91] Eichler, H. J., Günter, P. and Pohl, D. W., Laser-Induced Dynamic Gratings, Springer-Verlag, Berlin 1986.

[.92] Anderson, P. W., Phys. Rev. **109**, (1958) 1492.

[.93] Fleishman, L. and Anderson, P. W., Phys. Rev. B **21**, (1980) 2366.

[.94] Phillips, J. C., Solid State Commun. **47**, (1983) 191.

[.95] Damen, T. C., Leo, K., Shah, J. and Cunningham, J. E., App. Phys. Lett. **58**, (1991) 1902.

[.96] Bar-Ad, S. and Bar-Joseph, I., Phys. Rev. Lett. **68**, (1992) 349.

[.97] Masselink, W. T., Pearah, P. J., Klem, J., Peng, C. K., et al., Phys. Rev. B 32, (1985) 8027.

[.98] Sanders, G. D. and Chang, Y.-C., Phys. Rev. B 32, (1985) 5517.

[.99] Feuerbacher, B. F., Kuhl, J. and Ploog, K., Phys. Rev. B 43, (1991) 2439.

[.100] Cundiff, S. T. and Steel, D. G., to be published (1992)

Figure .1 Geometry for backward four-wave mixing spectroscopy. The cross-hatched regions schematically represent the excitation grating created by fields 1 and 2.

Figure .2 The degenerate four-wave mixing nonlinear response of the HH1 exciton at 2.5K. While the reduction in the nonlinear response near line center is due in part to absorption of the applied fields and emitted signal, the weak response on the high energy compared to the low energy side indicates a dramatic change in the fundamental nature of the nonlinear across line center.

Figure .3 The nondegenerate FWM response observed below the absorption line center obtained by tuning ω_1. The line width measures the energy relaxation rate. (a). The width corresponds to a relaxation time of 60 ps, the time scale for spectral diffusion. (b). The measurement seen in (a) is repeated at higher temperature. The spectral diffusion rate increases as well as the dominance of the narrow structure seen at the top of the response in (a). The width of the narrow resonance is determined by the exciton recombination time.

Figure .4 The nondegenerate four-wave mixing response obtained by tuning ω_3. The line shape is determined by homogeneous broadening as well as contributions from spectral diffusion in the limit that $|\omega_2-\omega_1|<<\Gamma$, the spectral diffusion rate. (a) The grating is written below line center. The narrow feature is the spectral hole produced by $\mathbf{E}_1\cdot\mathbf{E}_2^*$ 1.5 meV below absorption line center. The broad feature represents the quasi-equilibrium distribution of excitons produced by spectral diffusion. (b). The FWM spectrum observed when $\mathbf{E}_1\cdot\mathbf{E}_2^*$ is tuned 2 meV above line center. Note the absence of hole burning.

Figure .5 Temperature dependence of the spectral diffusion rate determined by measuring the line width of the broad feature in Fig. .3. The dashed lines are a fit of the theory based on phonon assisted migration.

Figure .6 (a) The nondegenerate FWM response observed above the absorption line center obtained by tuning ω_1 (compare with Fig. .3). The narrow feature corresponds to exciton recombination. (b) The line width in Fig. .3 as a function of the inverse grating spacing. The rate varies quadratically with the inverse grating spacing due to spatial diffusion. Far below line center, the rate depends very weakly on the grating spacing showing the greatly reduced spatial diffusion.

Figure .7 Energy level diagram and experimental configuration for FWM studies of magnetoexcitons in a quantum well.

Figure .8 The FWM response of magnetoexcitons in a quantum well obtained by tuning ω_3. The grating is written using σ_- polarized E_1 and E_2 The high frequency resonance is the original spectral hole observed when E_3 is σ_- polarized while the lower frequency resonance is the result of spin flip induced hole burning, observed when E_3 is σ_+ polarized.

Figure .9 The FWM response obtained as in Fig. .8 except that E_3 is linearly polarized.

Figure .10 Magnetic field dependence of the magnetoexciton Zeeman splitting.

Figure .11 Experimental geometry and timing sequence for three pulse TFWM. In (b), the system is homogeneously broadened and the signal field is a free polarization decay emitted coincidently with the third field. In (c), the system is inhomogeneously broadened, and the signal is a stimulated photon echo emitted at a time after the third pulse equal to the time difference between the first and second pulses.

Figure .12 (a) The time resolved emission in a three pulse stimulated photon echo experiment obtained by cross-correlating the emission with a reference pulse from the laser. The solid line is a fit of the numerically integrated density matrix equations from which we can obtain the inhomogeneous width. (b) A plot of the signal delay as a function of the time delay between the first two pulses. The dashed line is the prediction of the numerically integrated optical Bloch equations which accounts for the finite pulse delay and the deviation from a linear delay around t=0.

Figure .13 Time integrated decay curves. (a). The signal amplitude as a function of the time delay between E_1 and E_2 measures the dephasing rate. (b) The signal amplitude as a function of the time delay between E_2 and E_3 measures the energy relaxation time. The inset shows the energy of excitation.

Figure .14 Measuring the signal decay as a function of the first-second pulse delay for (a) zero and (b) finite delay between the second and third pulses confirms the presence of spectral diffusion. The decay at long times is identical in both (a) and (b).

Figure .15 Measurement of the dephasing rate and energy decay rate as a function of (a) temperature and (b) excitation energy. The dashed line in each figure is given by $\gamma_{ph} - \frac{1}{2}\Gamma_{pop}$ and potentially represents the so-called pure dephasing.

Figure .16 Comparison of the time resolved emission in the TFWM experiment for (a) all incident fields linearly co-polarized and (b) for $\mathbf{E}_1 \perp \mathbf{E}_2 \parallel \mathbf{E}_3$, $\mathbf{E}_s \parallel \mathbf{E}_1$. In (a), the signal shows increasing delay with increasing time between the first two pulses. In (b), the signal is clearly prompt, corresponding to a free polarization decay (see text for discussion of the weak echo in 16b.) The inset shows the energy structure and corresponding magnetic quantum numbers for the heavy and light hole valence bands and conduction band.

Figure .17 Comparison of the dephasing rates for the free polarization decay (squares) and stimulated photon echo (circles) as a function of excitation energy.

Figure .18 Comparison of the dephasing rates for the free polarization decay (squares) and stimulated photon echo (circles) as a function of temperature.

Figure .19 The signal amplitude of the stimulated photon echo (circles) and free polarization decay (squares) as a function of photon flux. The solid lines have a slope corresponding to n=3, as expected for a simple third order nonlinear optical response. The stimulated photon echo signal arises from localized excitons and saturates due to the finite number of excitons.

Figure .20 The time resolved emission for moderate (a) and high (b) excitation intensity. Panel (b) is taken on a 10 layer sample with 1.0 ps pulses.

Figure .21 The measured decay rate as a function of inverse grating spacing for both the stimulated photon echo (circles) and the free polarization decay (squares). The stronger dependence of the free polarization decay on the inverse grating spacing shows the greater mobility (diffusivity) of the excitons giving rise to the free polarization decay compared to those giving rise to the stimulated photon echo. Solid lines are fit to quadratic dependence.

Figure .22 The signal depolarization as a function of incident flux when E_1 and E_2 are co-circularly-polarized and E_3 is linearly polarized. For the vertical axis I_+ is the intensity for the signal component co-polarized with E_1 and E_2 and I_- is the component cross-polarized, hence a polarization of zero indicates linear polarization and a value of 1 indicates circular polarization of the same sense as the first two fields. At low intensity, the scattering of E_3 is nearly independent of the E_3 polarization.

Figure .23 Transient absorption decay for both a σ_+ and a σ_- circularly polarized probe beam and a σ_+ polarized pump. The data show an instantaneous coupling between these two different polarizations which is unexpected given the energy level diagram in Fig. 16. The upper curve (right axis, offset for clarity) represent the polarization where the long time decay is given by spin-flip relaxation.

Figure .24 Different transmission spectra for co-rotating and counter-rotating pump and probe beams.

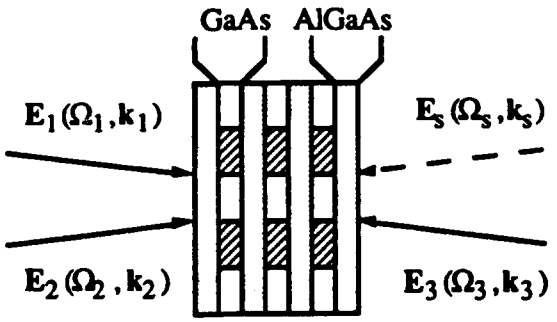
GaAs
AlGaAs
$E_1(\Omega_1, k_1)$
$E_s(\Omega_s, k_s)$
$E_2(\Omega_2, k_2)$
$E_3(\Omega_3, k_3)$

Figure 1

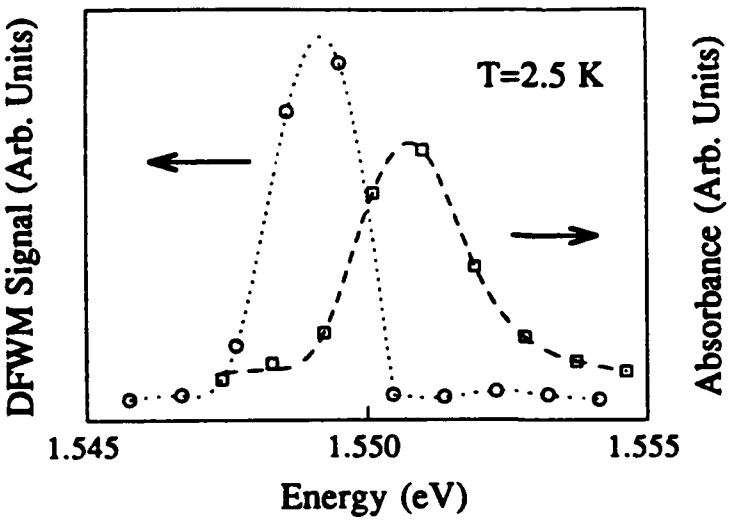
T=2.5 K
DFWM Signal (Arb. Units)
Absorbance (Arb. Units)
1.545
1.550
1.555
Energy (eV)

Fig. 2

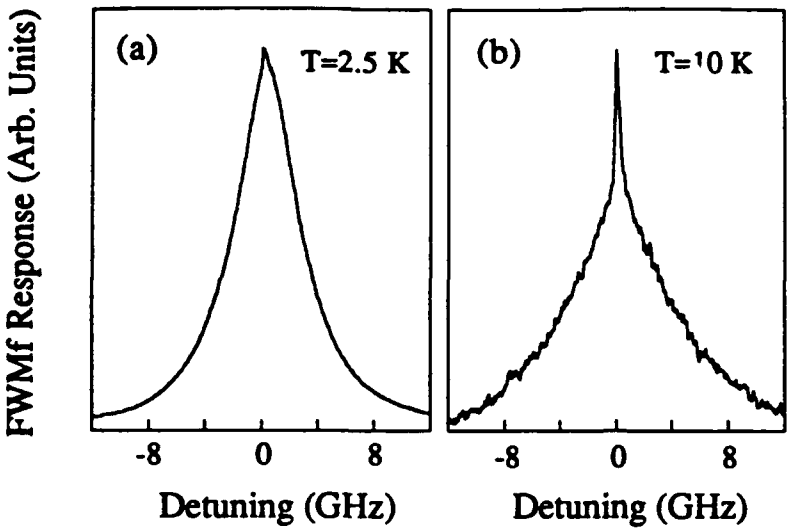
FWMf Response (Arb. Units)
(a)
T=2.5 K
(b)
T=10 K
-8
0
8
-8
0
8
Detuning (GHz)
Detuning (GHz)

Figure 3.

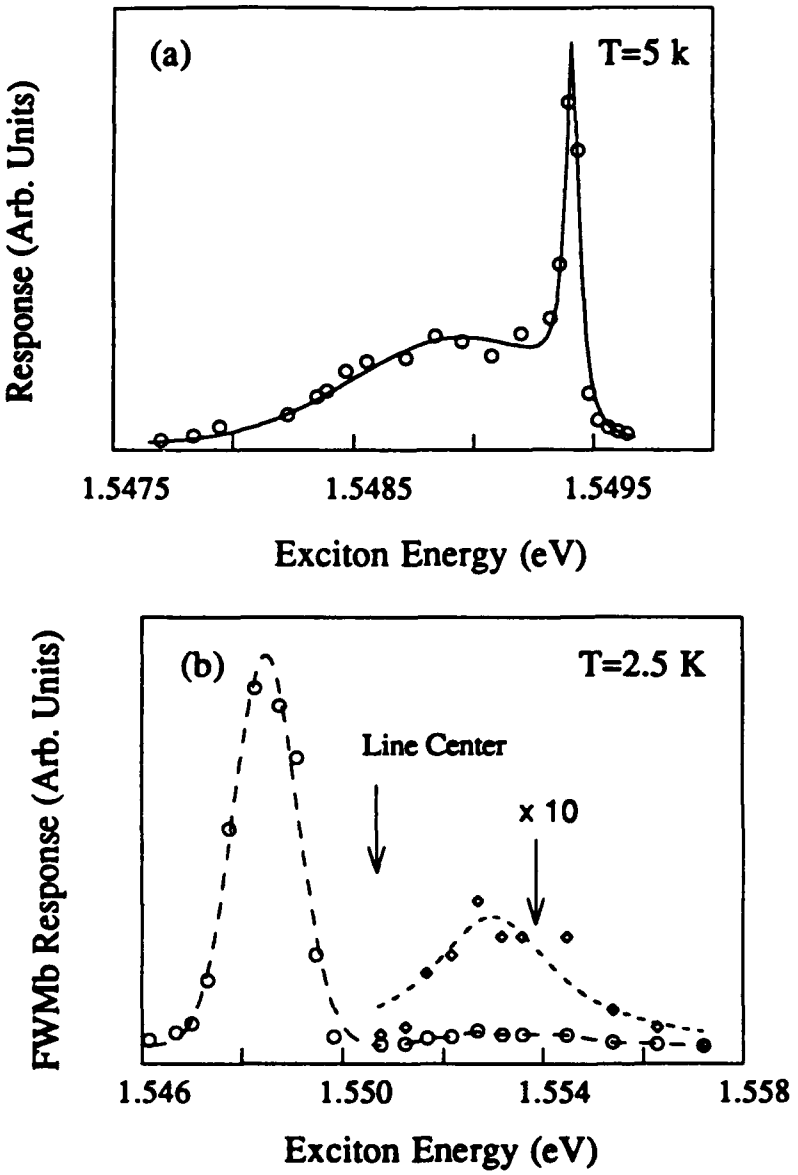
(a)
T=5 k
Response (Arb. Units)
1.5475
1.5485
1.5495
Exciton Energy (eV)
(b)
T=2.5 K
Line Center
x 10
FWMb Response (Arb. Units)
1.546
1.550
1.554
1.558
Exciton Energy (eV)

Figure 4

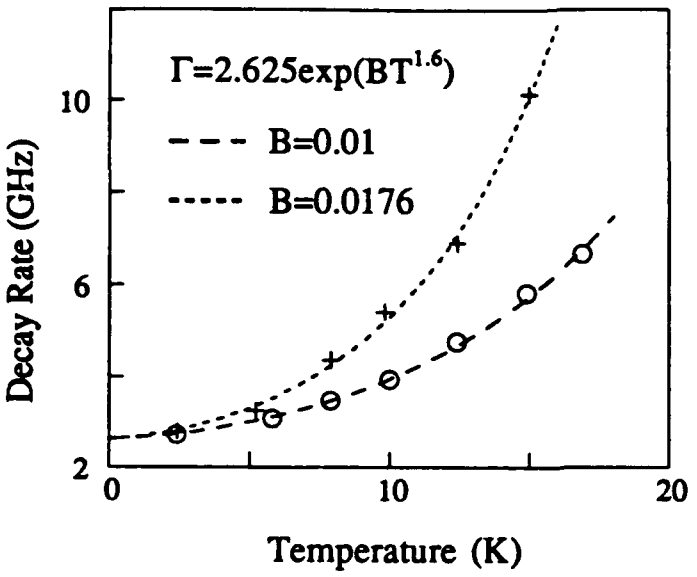
Γ=2.625exp(BT^1.6)
B=0.01
B=0.0176
Decay Rate (GHz)
10
6
2
0
10
20
Temperature (K)

Figure 5

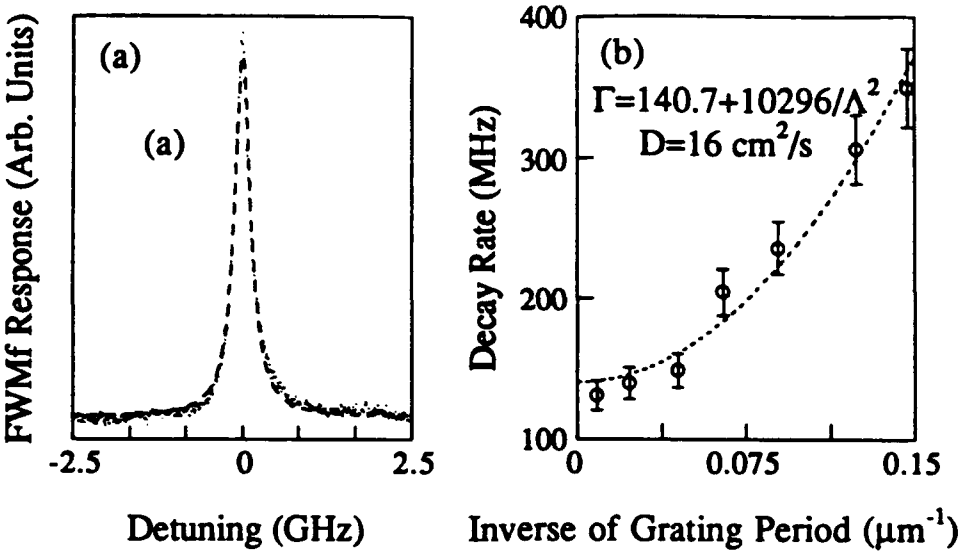
(a)
(a)
FWMf Response (Arb. Units)
-2.5
0
2.5
Detuning (GHz)
(b)
Γ=140.7+10296/Λ²
D=16 cm²/s
Decay Rate (MHz)
400
300
200
100
0
0.075
0.15
Inverse of Grating Period (μm⁻¹)

Figure 6

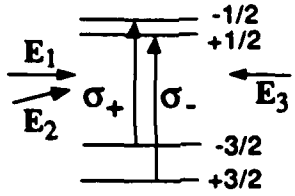

Figure 7

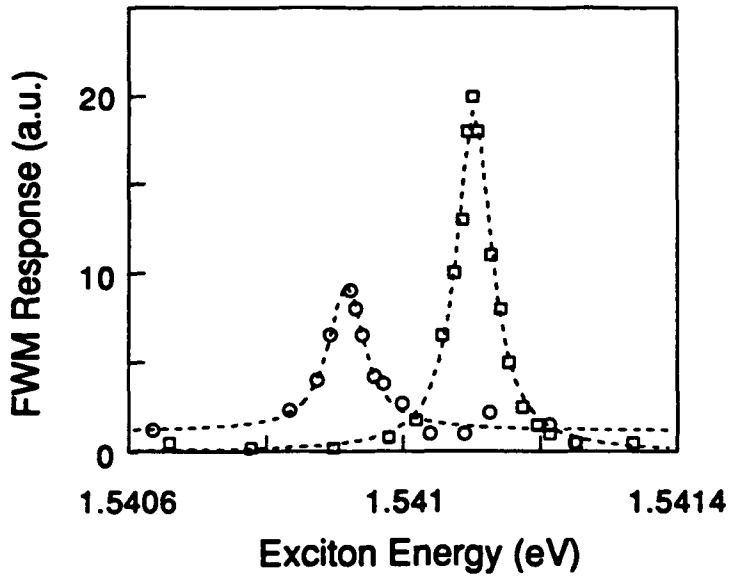

Figure 8.

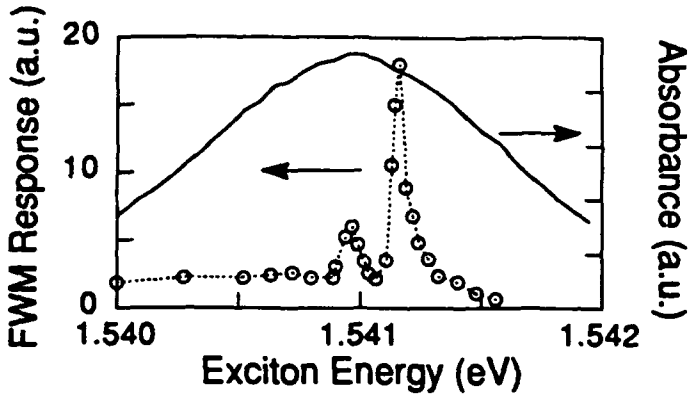
FWM Response (a.u.)
20
10
0
1.540
1.541
1.542
Exciton Energy (eV)
Absorbance (a.u.)

Figure 9

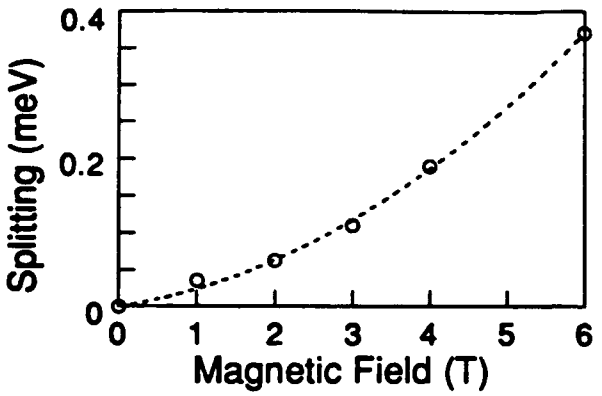

Figure 10

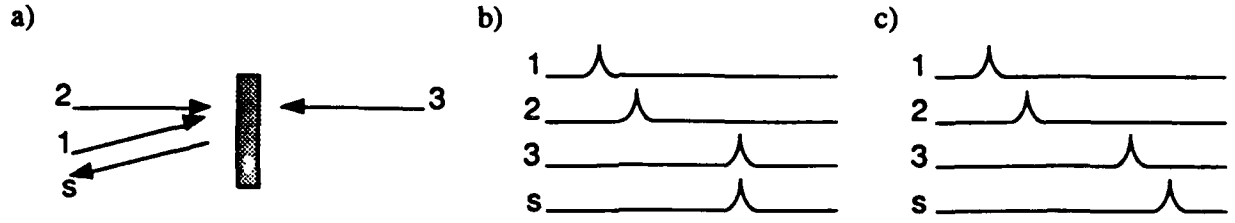

Figure 11

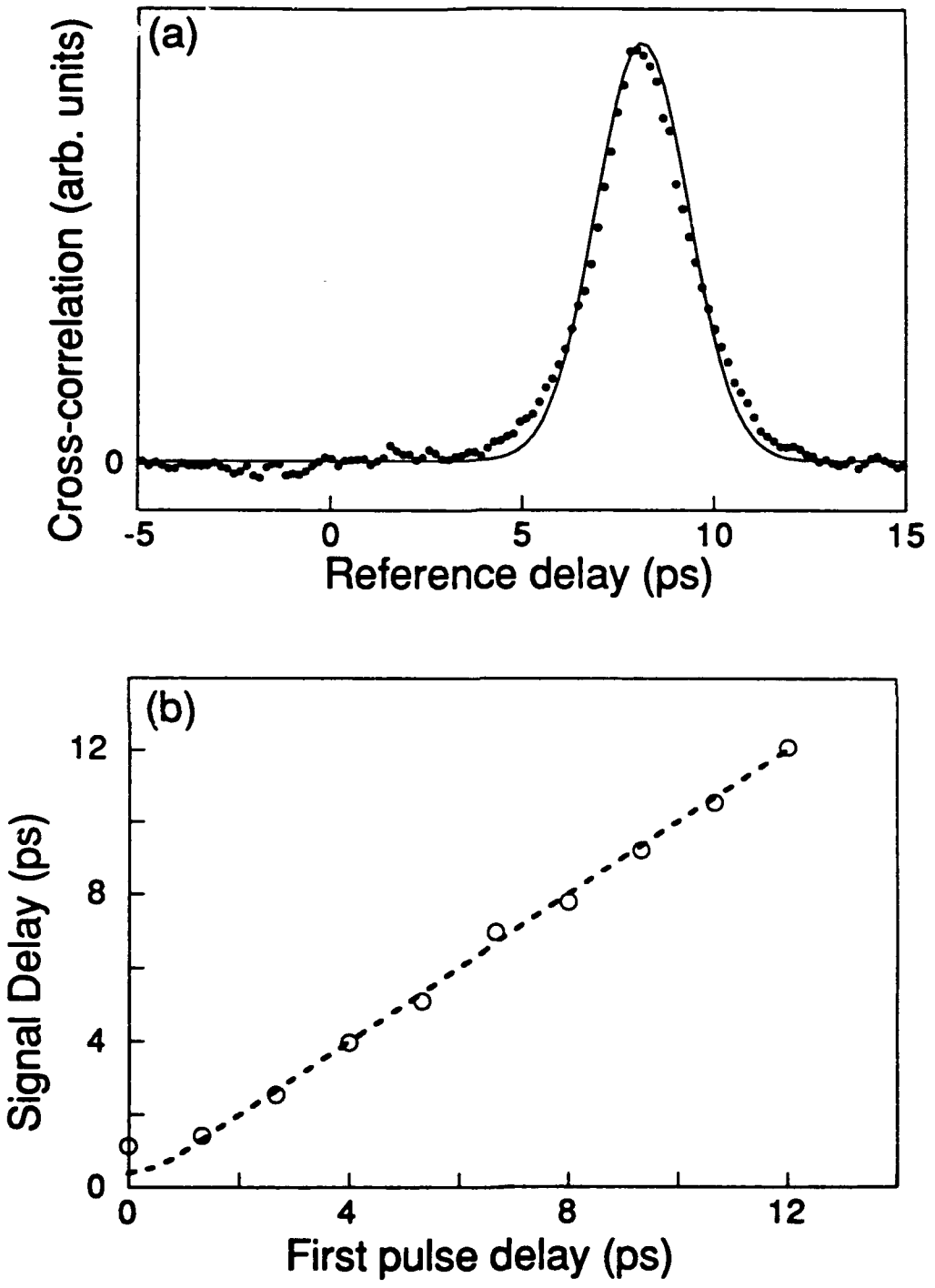
(a)
Cross-correlation (arb. units)
0
-5
0
5
10
15
Reference delay (ps)
(b)
Signal Delay (ps)
0
4
8
12
0
4
8
12
First pulse delay (ps)

Figure 12.

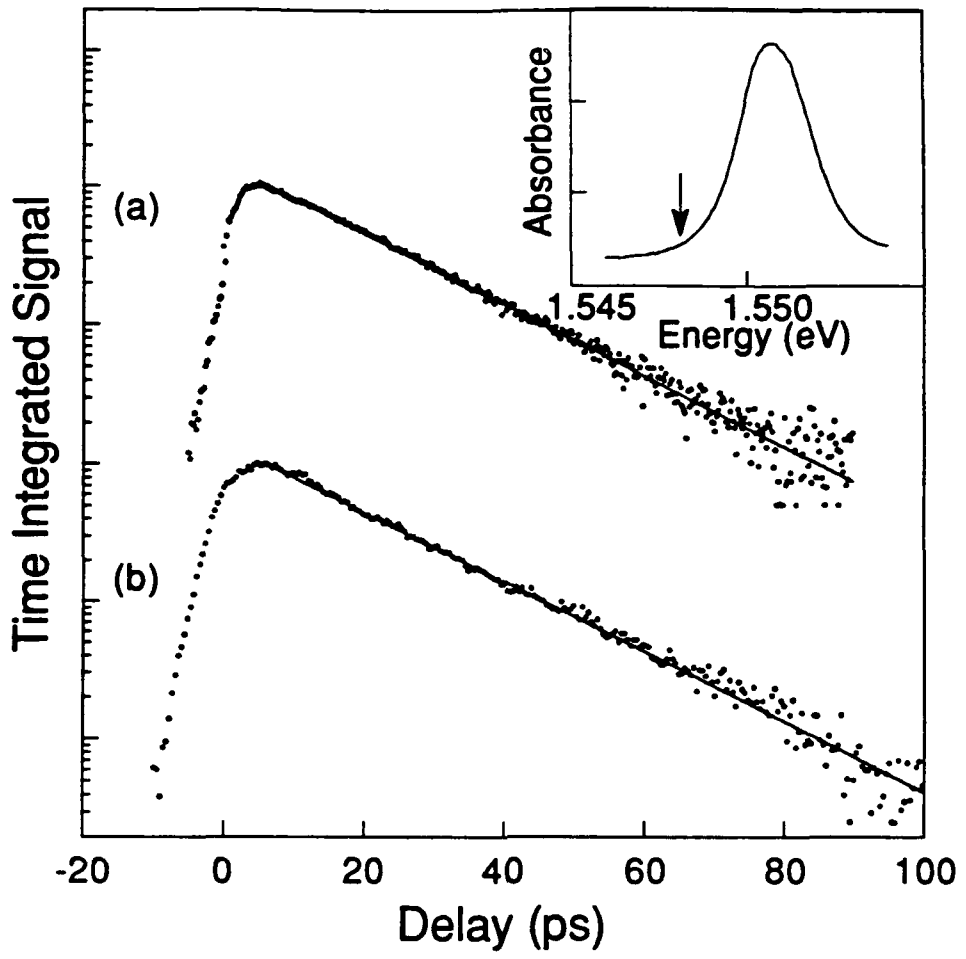
Time Integrated Signal
(a)
(b)
Absorbance
1.545
1.550
Energy (eV)
-20
0
20
40
60
80
100
Delay (ps)

Figure 13

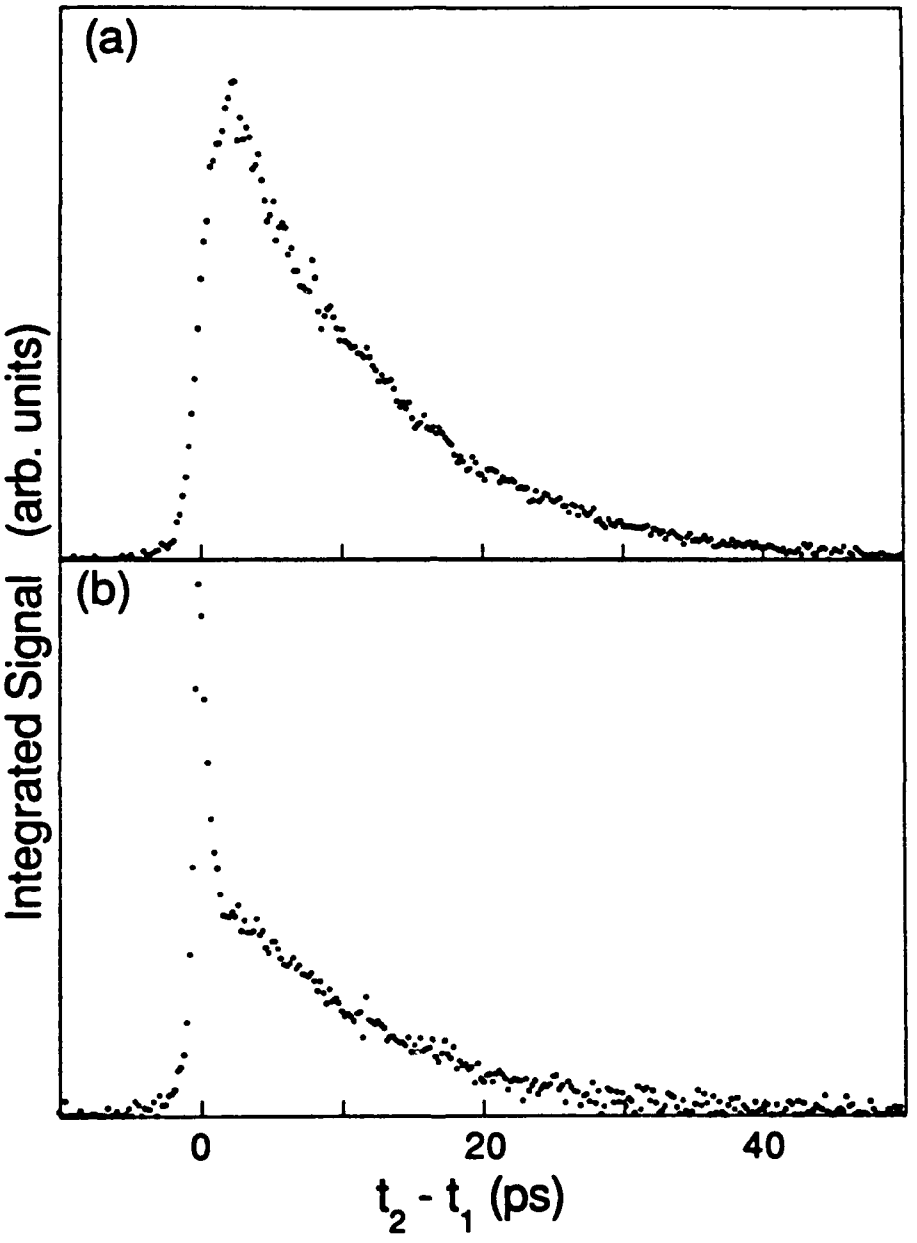

Fig 14

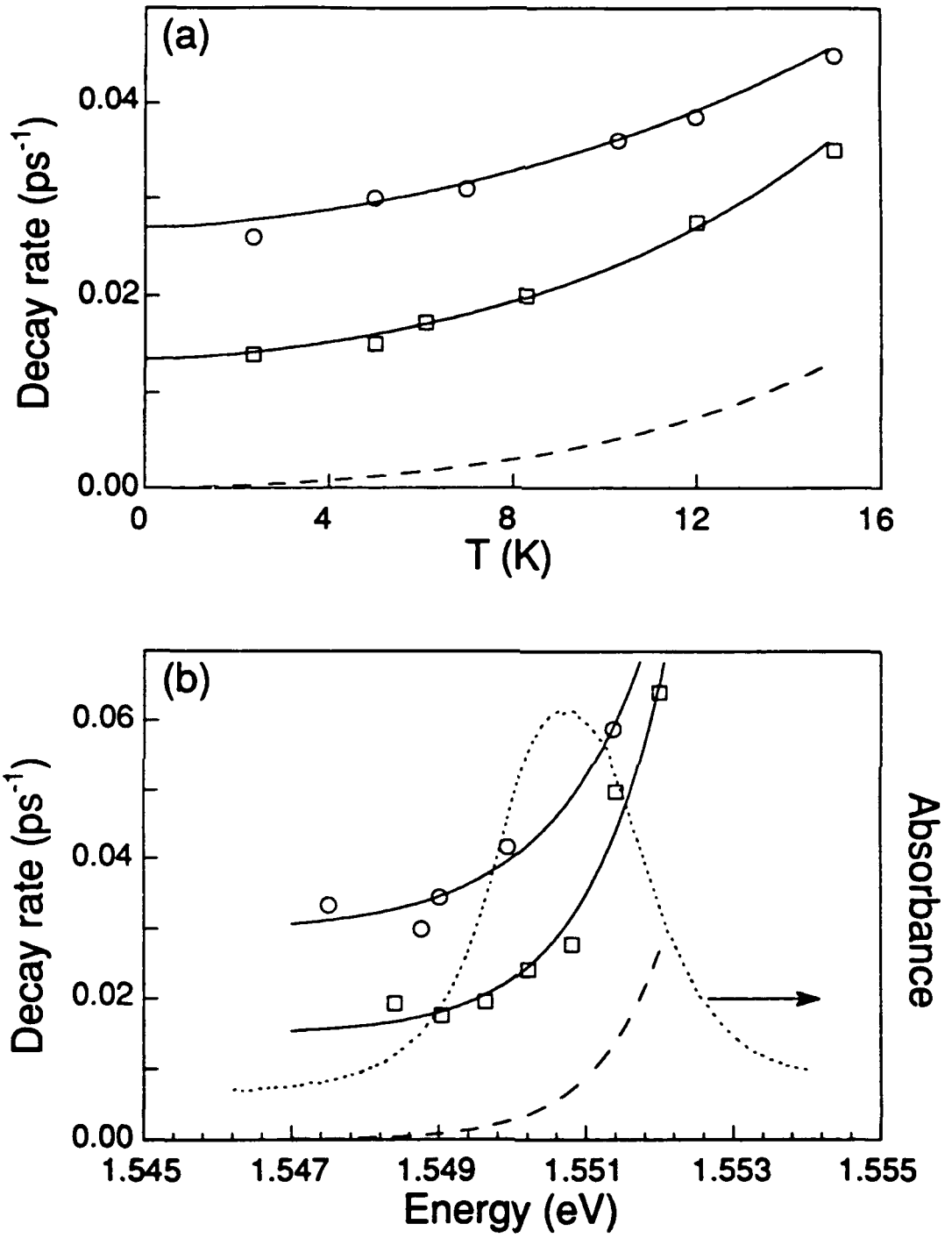
(a)
Decay rate (ps^{-1})
0.04
0.02
0.00
0
4
8
12
16
T (K)
(b)
Decay rate (ps^{-1})
0.06
0.04
0.02
0.00
1.545
1.547
1.549
1.551
1.553
1.555
Energy (eV)
Absorbance

Fig. 15

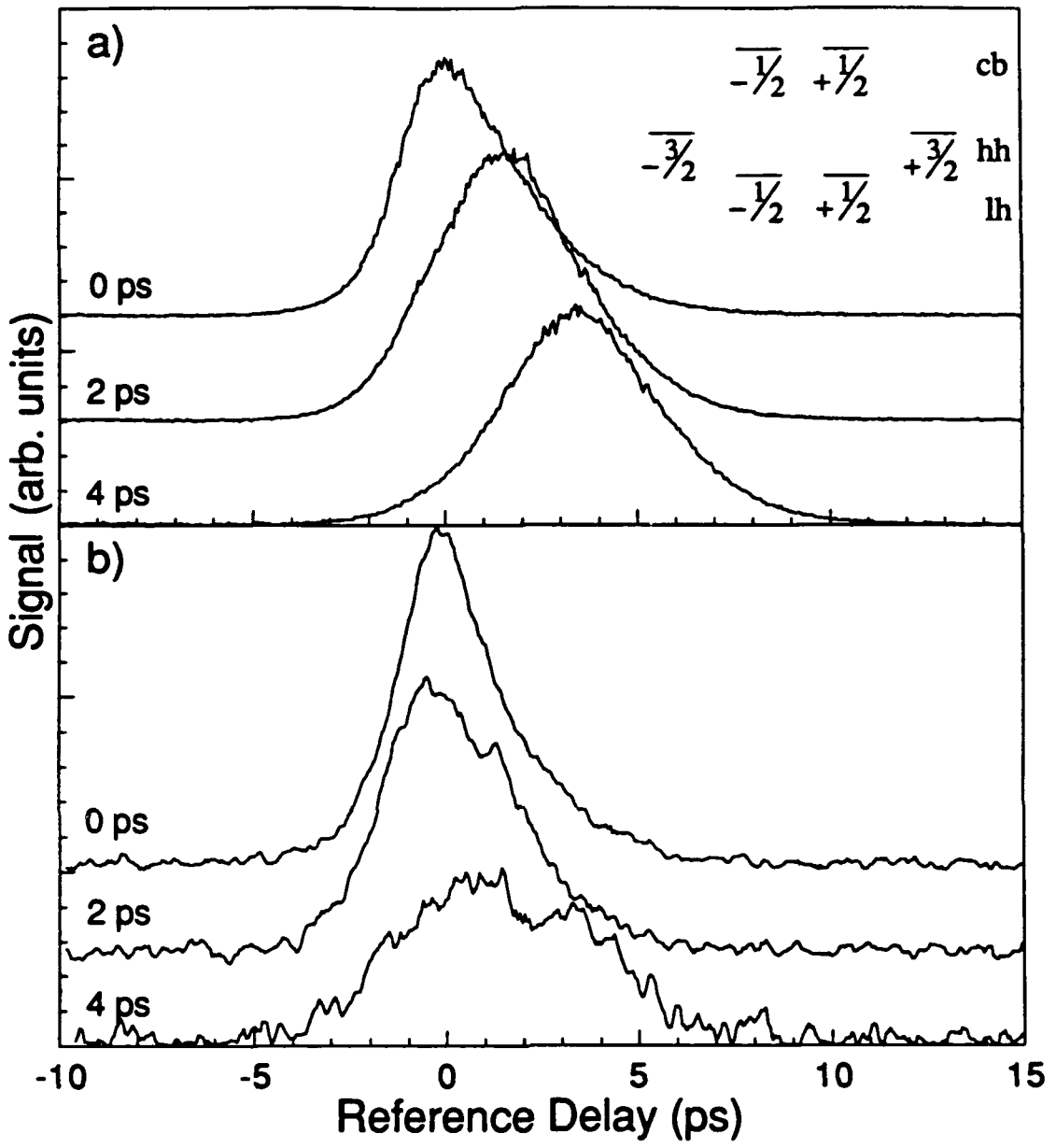
a)
-1/2 +1/2
cb
-3/2
+3/2
hh
-1/2 +1/2
lh
0 ps
2 ps
4 ps
b)
0 ps
2 ps
4 ps
Signal (arb. units)
-10
-5
0
5
10
15
Reference Delay (ps)

Figure 16.

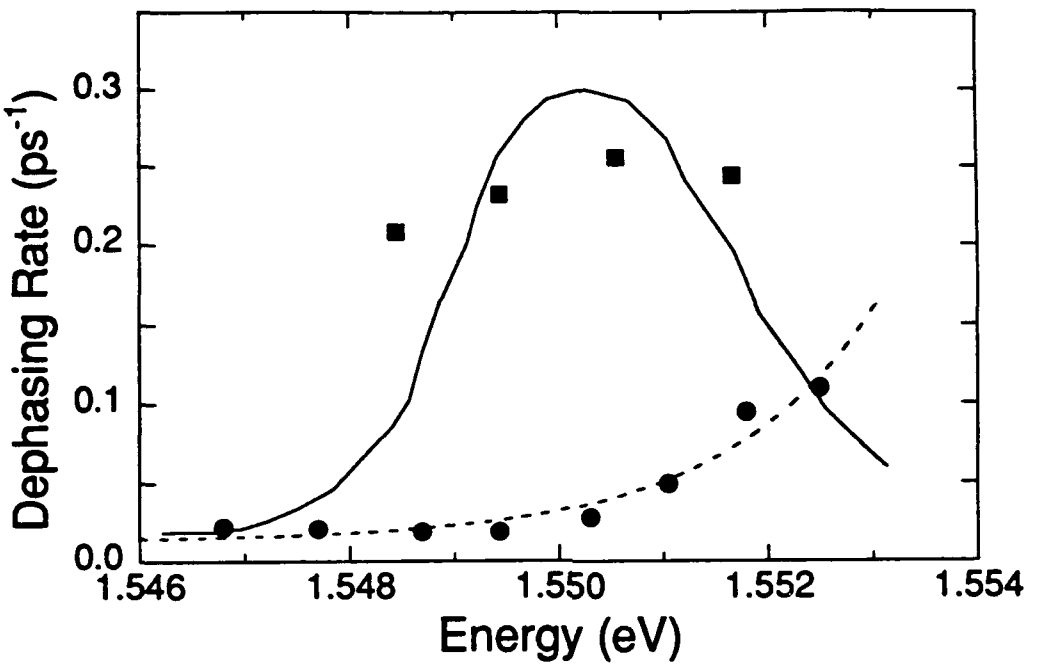
Dephasing Rate (ps^{-1})
0.0
0.1
0.2
0.3
1.546
1.548
1.550
1.552
1.554
Energy (eV)

Figure 17.

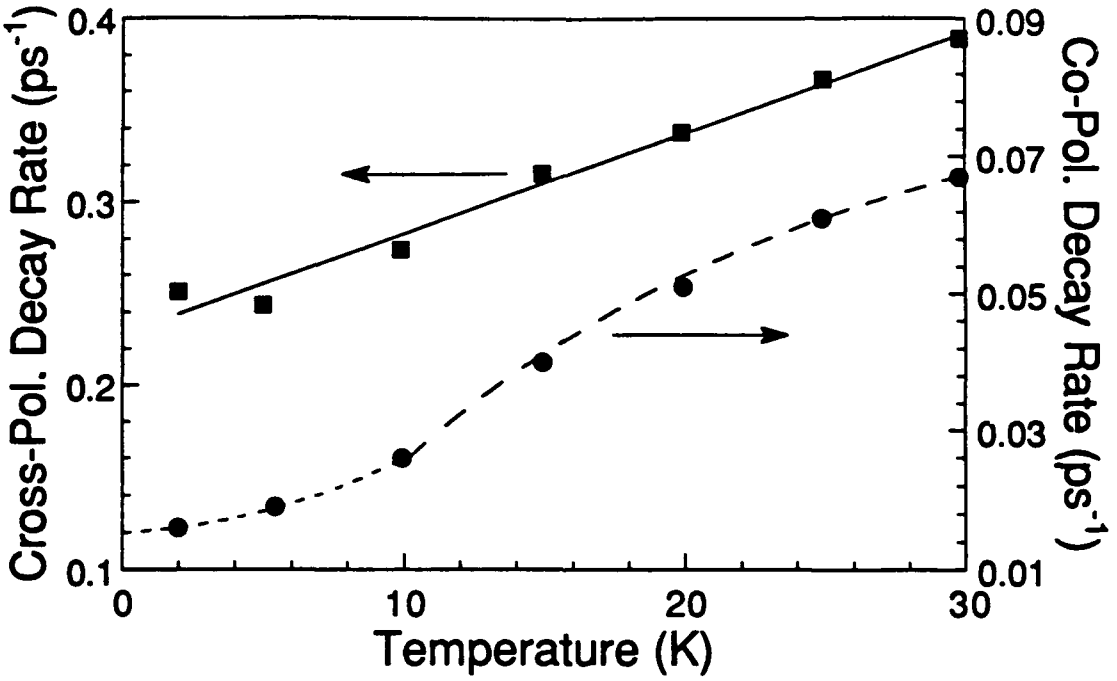
Cross-Pol. Decay Rate (ps^{-1})
Co-Pol. Decay Rate (ps^{-1})
Temperature (K)
0.4
0.3
0.2
0.1
0.09
0.07
0.05
0.03
0.01
0
10
20
30

Figure 18.

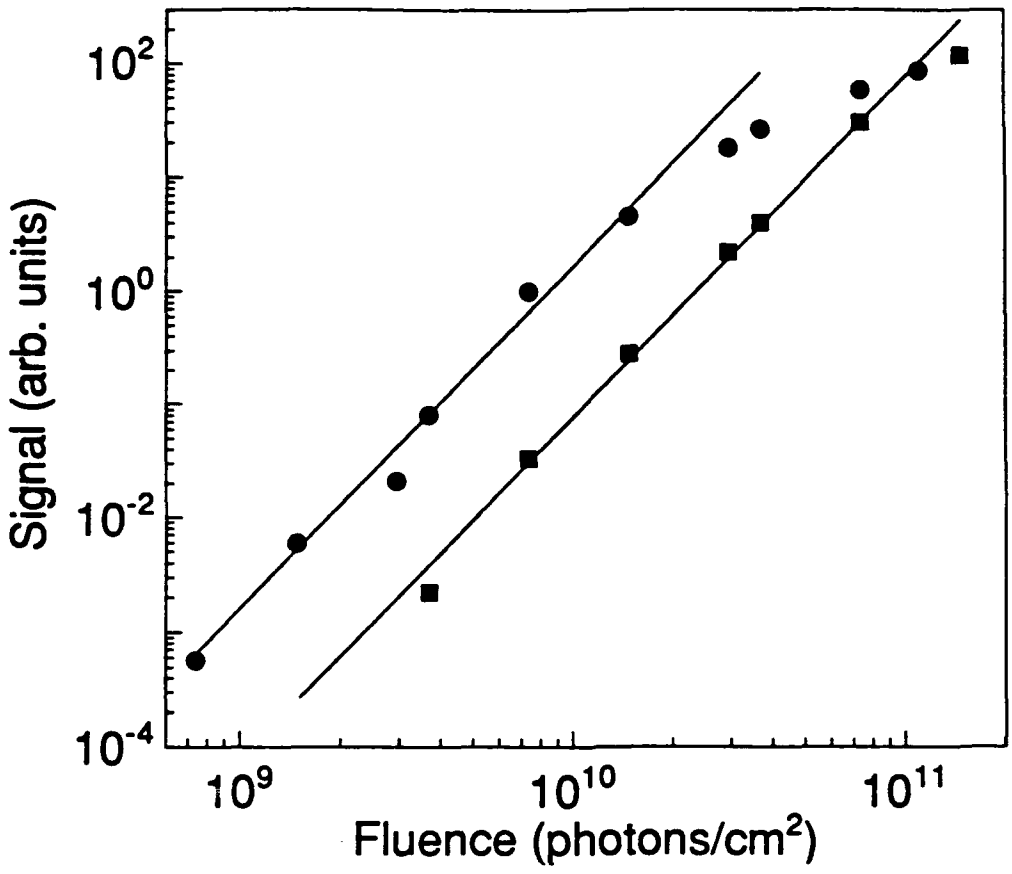
10^2
10^0
10^{-2}
10^{-4}
Signal (arb. units)
10^9
10^{10}
10^{11}
Fluence (photons/cm^2)

Fig. 19

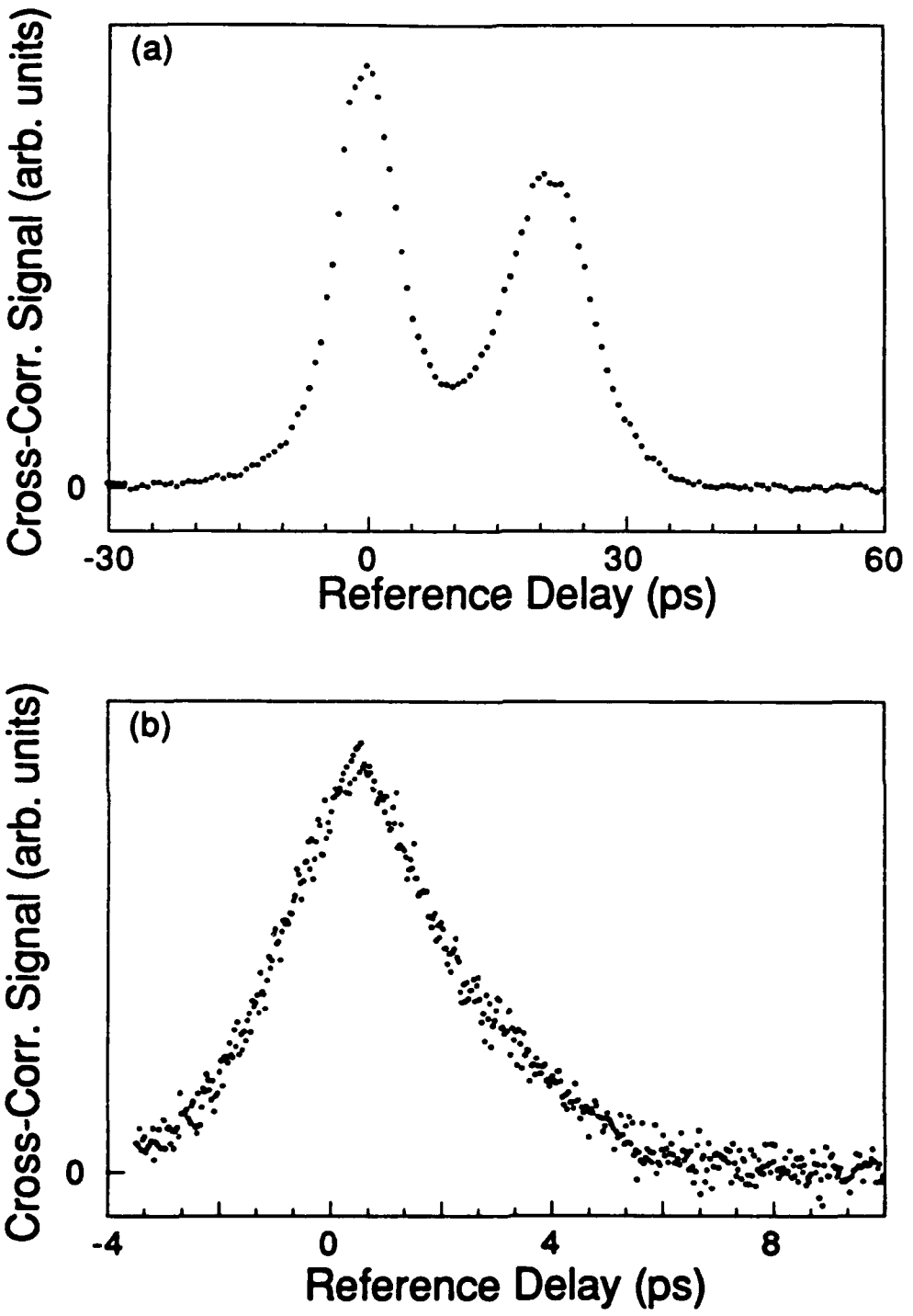
(a)
Cross-Corr. Signal (arb. units)
0
-30
0
30
60
Reference Delay (ps)
(b)
Cross-Corr. Signal (arb. units)
0
-4
0
4
8
Reference Delay (ps)

Fig. 20.

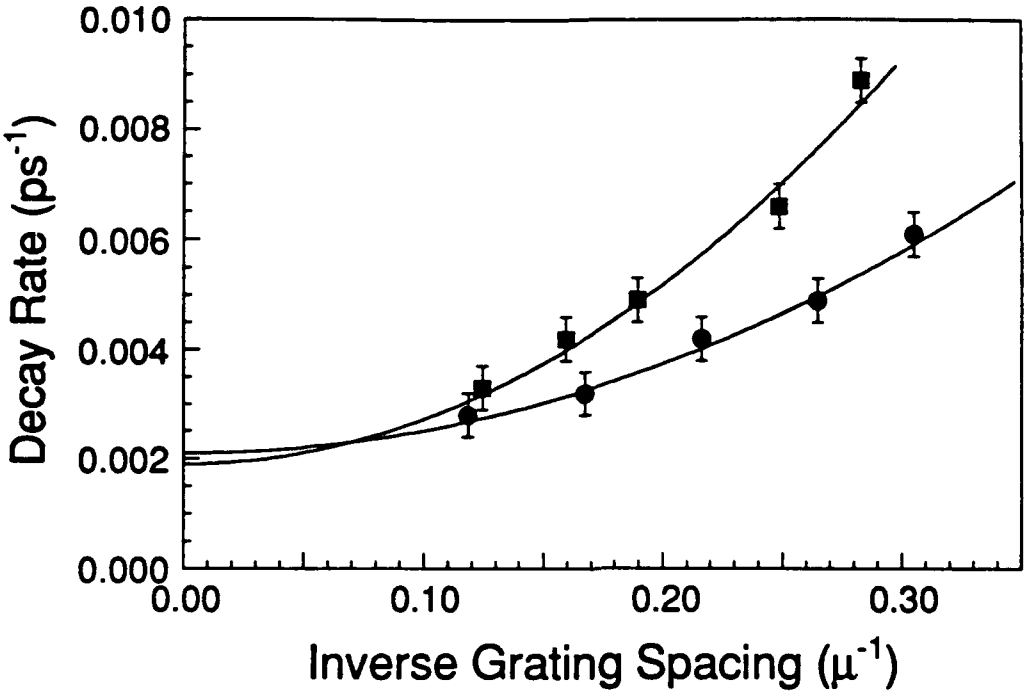
0.010
0.008
0.006
0.004
0.002
0.000
Decay Rate (ps^{-1})
0.00
0.10
0.20
0.30
Inverse Grating Spacing (μ^{-1})

Fig. 21

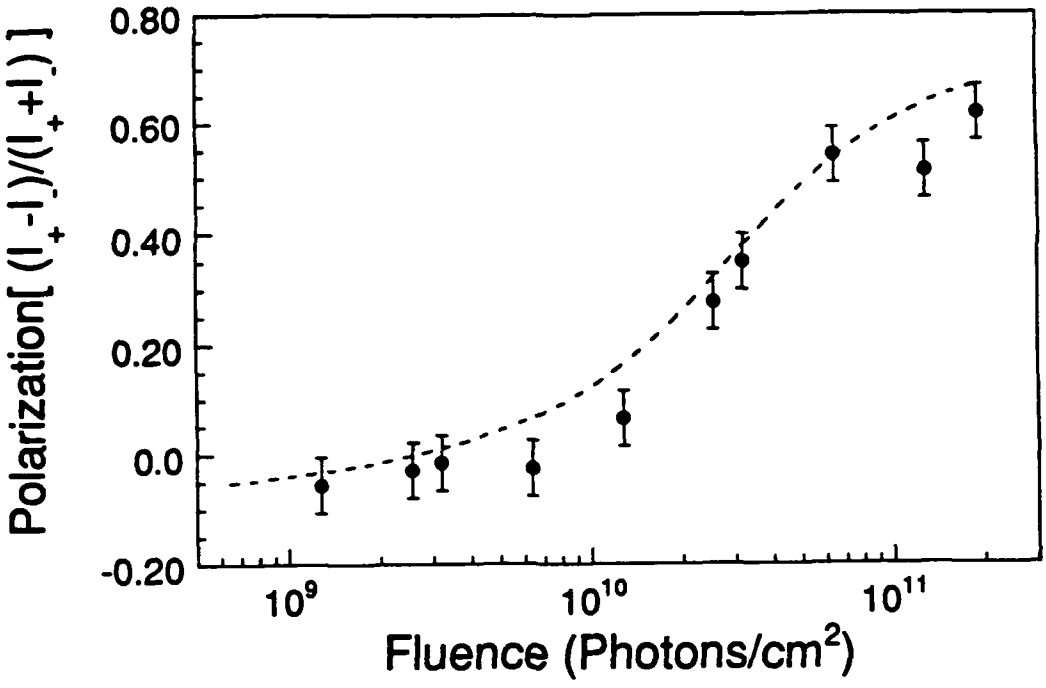
0.80
0.60
0.40
0.20
0.0
-0.20
Polarization[(I+ -I-)/(I+ +I-)]
10^9
10^10
10^11
Fluence (Photons/cm^2)

Fig. 22

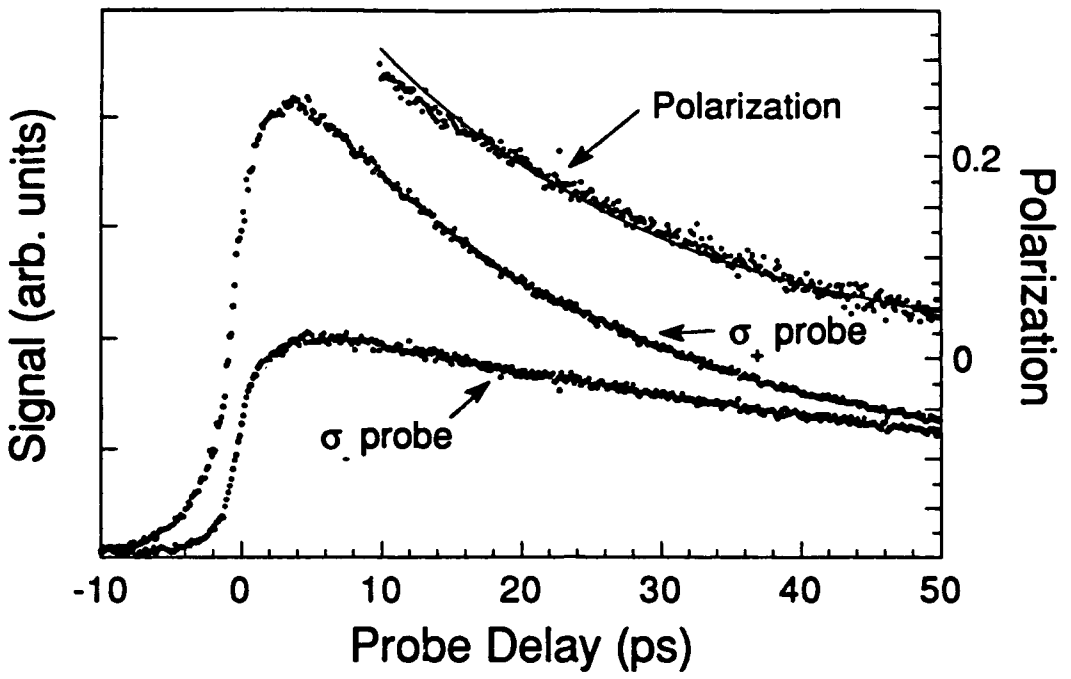
Polarization
σ+ probe
σ- probe
Signal (arb. units)
Polarization
0.2
0
-10
0
10
20
30
40
50
Probe Delay (ps)

Fig 23

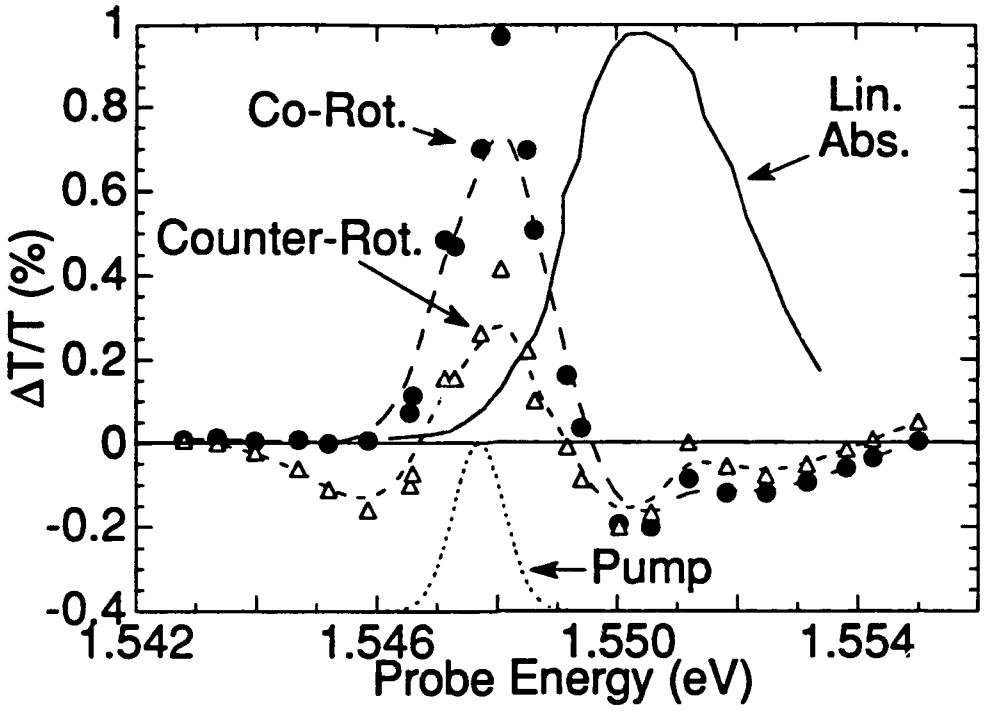
1
0.8
0.6
0.4
0.2
0
-0.2
-0.4
ΔT/T (%)
Co-Rot.
Counter-Rot.
Lin.
Abs.
Pump
1.542
1.546
1.550
1.554
Probe Energy (eV)

Figure 24

To be published, Proceedings NATO ARW in *Frontiers of Optical Phenomena in Semiconductor Structures of Reduced Dimensions*, 1992.

Coherent Nonlinear Laser Spectroscopy of Excitons in Quantum Wells

D. G. Steel, S. T. Cundiff, and H. Wang

The Harrison M. Randall Laboratory of Physics

The University of Michigan, Ann Arbor, MI 48109

313-764-4469

ABSTRACT

Coherent nonlinear laser spectroscopy of excitons in quantum wells based on frequency domain four wave mixing and picosecond photon echoes shows the presence of long dephasing times due to disorder. Measurements demonstrate that these excitons relax primarily by phonon assisted migration between localization sites. However, measurements of the polarization dependence of the nonlinear response shows the simple picture of excitons is inadequate for describing the interaction. Furthermore, the measurements indicate that there are two distinct resonant contributions to the nonlinear response which are characterized by different relaxation, saturation and transport properties.

The strong excitonic resonance observed in optical spectroscopy of semiconductors just below the bandedge is the result of the Coulomb interaction between electrons and holes. Quantum confinement of the carriers in semiconductor heterostructures results in an increase in the transition energy as well as an increase in the electron-hole correlation leading to an increase in the binding energy and electronic oscillator strength. The persistence of a strong resonance even at room temperature has resulted in considerable interest in these materials for potential optoelectronic applications based on the strong nonlinear optical susceptibility associated with a resonant response.

However, complete understanding of the nonlinear optical response has been difficult. In contrast to simple atomic systems, the excitations are described by extended states subject to Fermi statistics and characterized by strong Coulomb interactions. In simple atomic systems, optical interactions have been described by optical Bloch equations and more recently by modified optical Bloch equations [1]. In an effort to parallel this successful formalism for semiconductors, a set of effective optical Bloch equations has been developed which reveals that although many similar coherent nonlinear optical effects are present in semiconductors, their physical origin and interpretation is considerably more complex (for a review see [2, 3]). In an ideal semiconductor, the origin of the nonlinear response is dominated by effects of Coulomb screening and the Pauli exclusion principle including phase space filling and exciton-exciton interactions. Coulomb screening and effects of the Pauli exclusion principle lead to manybody contributions to the nonlinear response causing such effects as optically induced changes in the oscillator strength as well as shifts in the transition energy and the bandedge. In the presence of quantum confinement, Coulomb screening effects are reduced due to the reduced dimensionality [2]. The large optical density of these systems is also not common in simple low density atomic systems and leads to coherent coupling of excitons through exciton-exciton interactions which are related to local field effects. The qualitative change in behavior can be seen by extending the simple two level model [4] which can lead to so-called "negative" delay signals and nonexponential decays. This effect is closely related to the Lorentz-Lorenz law in gases [5] and

was first noted in coherent transient effects in atomic systems in accumulated photon echo experiments [6] and recently reported in semiconductor systems [7-9]. Of more fundamental interest is the presence of strong Coulomb coupling in semiconductors. This can lead to dramatic modification of the nonlinear optical response for sufficiently strong excitation, as demonstrated by recent numerical calculations [10, 11].

In semiconductor heterostructures, the description of nonlinear optical behavior has been greatly complicated by the presence of disorder which is also an issue of fundamental interest [12]. In quantum wells fluctuations in the confinement potential due to interface roughness lead to localization of the exciton where the exciton envelope function decays exponentially in space. The optical response in these systems becomes inhomogeneously broadened, resulting in an increase in the linear absorption linewidth due to small fluctuations in the exciton transition energy . In addition exciton localization also results in reduced phonon scattering leading to a decrease in the homogeneous linewidth (i.e., decreased dephasing rate) compared to an ideal quantum well at low temperature where the linewidth and energy relaxation are determined by phonon scattering along the two-dimensional dispersion curve (~psec, [13]). For localized excitons energy relaxation proceeds by phonon assisted migration between localization sites and thermal activation to delocalized states [14, 15].

In this paper we describe a series of nonlinear optical measurements based on frequency domain cw four-wave mixing and picosecond transient four-wave mixing. The measurements show a rich diversity in the coherent nonlinear optical phenomena which can be observed in these systems but also demonstrate the complexity induced by disorder. The results show that existing theoretical understanding in these systems is inadequate for describing the observations.

Early insight into the effects of disorder was obtained in studies of exciton luminescence which confirmed the emission was inhomogeneously broadened due to the corresponding potential fluctuations [16]. These studies were followed by results that indicated that this interface roughness is characterized by a scale length large compared to the Bohr radius of the exciton (see, for example, [17, 18]); however, more recent studies by chemical lattice imaging

have shown the presence of monolayer flat islands with a smaller spatial extent of 50-100 Å [19]. While these results are presently somewhat controversial [20, 21], they have led to the proposal that at least two scale lengths for interface roughness are required in order to account for the observations [22]. Further evidence that the island size distribution is bimodal has been recently presented in luminescence and Raman scattering measurements [23]. Details of the interface roughness also depend on specific growth processes, such as interrupted or non-interrupted growth [18], or whether GaAs is grown on $Al_xGa_{1-x}As$ or $Al_xGa_{1-x}As$ is grown on GaAs [24].

Localized and extended excitons have qualitatively different relaxation properties [15]. Even at low temperature (<10K), localized excitons do not remain truly localized, instead they can migrate among localization sites by emitting or absorbing acoustic phonons. Such phonon assisted migration was first proposed to explain the slow and non-exponential energy relaxation observed in time resolved luminescence measurements in a GaAs QW structure [25] and directly observed in InGaAs/InP QW where all excitons are localized by alloy disorder [26] and in GaAs QW where excitons are localized due to interface disorder [27, 28]. At higher temperatures, excitons can absorb phonons with sufficient energy to become activated to delocalized states at higher energies. The activation process has been observed in a number of measurements such as spectral hole burning [29], resonant Raleigh scattering [30], and resonant Raman scattering [31]. Estimates of the activation energy have suggested that the onset for the delocalized exciton in GaAs QW structures is near the absorption line center [32]. In contrast, decay of the delocalized exciton is determined by the exciton-phonon scattering along the energy-momentum dispersion curve and the exciton recombination. Furthermore, delocalized excitons also experience elastic scattering from potential fluctuations, which introduces additional dephasing due to the decay of the polarization. Indeed as we show below in typical quantum wells, the dephasing time is >45 psec whereas in near ideal quantum well, the dephasing time is an order of magnitude shorter [13].

To study the nonlinear optical response in these systems, experiments were performed on various GaAs quantum well structures. Typical samples were comprised of 96Å GaAs wells and

98Å $Al_{0.3}Ga_{0.7}As$ barriers. The substrate was removed for transmission and four wave mixing measurements. The number of periods was either 10 or 60. In 60 period wells, the typical linear absorption linewidth was 2 meV with a 1 meV Stokes shift in the luminescence. In the 10 period sample, the absorption linewidth was 0.9 meV and there was a negligible Stokes shift in the luminescence (<0.2 meV.)

In the first set of measurements, we use a new method of saturation spectroscopy based on cw frequency domain four-wave mixing to demonstrate spectral hole burning and phonon assisted migration of excitons in these systems. Since the theoretical basis for these spectroscopic measurements is discussed in detail elsewhere [33], we summarize the basic approach for completeness. The experimental configuration is based on the backward FWM geometry where two beams $\mathbf{E}_1(\omega_1, \mathbf{k}_1)$ and $\mathbf{E}_2(\omega_2, \mathbf{k}_2)$ separated by an angle θ interact in the sample with a third beam $\mathbf{E}_3(\omega_3, \mathbf{k}_3)$ ($\mathbf{E}_1 \| \mathbf{E}_2 \perp \mathbf{E}_3$) through the resonant third order susceptibility to generate a signal beam $\mathbf{E}_S(\omega_S, \mathbf{k}_S)$ proportional to $\chi^{(3)}(\omega_S=\omega_1-\omega_2+\omega_3):\mathbf{E}_1\mathbf{E}_2^*\mathbf{E}_3$. In these experiments, $\mathbf{k}_3$ is counter-propagating with respect to $\mathbf{k}_1$ and the signal counter-propagates with respect to $\mathbf{k}_2$. In a simple physical picture for the response of this system (though not necessarily in general as we see in the time domain measurements below), $\mathbf{E}_1 \cdot \mathbf{E}_2^*$ results in a spatial and temporal modulation of the exciton population, which modifies the optical response of the sample and leads to a traveling wave grating or modulation of the absorption and dispersion. The coherent nonlinear signal arises from scattering of the third beam, $\mathbf{E}_3$, from the grating. Spectroscopic information can be obtained by studying the dependence of the nonlinear optical response on the relative frequency detuning, absolute frequency detuning, the electric field polarization, the input beam intensities and the relative angle of the different input beams, especially the angle between $\mathbf{k}_1$ and $\mathbf{k}_2$. The observed line shapes and corresponding physical information that is obtained depends on which frequency is tuned. In general, tuning ω_1 or ω_2 probes population and grating relaxation, while tuning ω_3 provides a measure of the homogeneous line shape similar to spectral hole burning and of the spectral redistribution of the excitation.

In Fig. 1a, we show the four wave mixing response obtained by scanning the frequency of the third beam (ω_3) [27, 34]. This enables a direct detection of the spectral hole produced by excitons excited by $\mathbf{E}_1 \cdot \mathbf{E}_2^*$ at energy E (1.5 meV below the absorption line center) as well as detecting any excitons scattered from energy E to E' due to spectral diffusion. The nonlinear response is corrected for sample absorption. The narrow resonance in the response corresponds to exciton spectral hole burning. The width of the hole gives an exciton homogeneous line width $2\gamma_{ph} \sim 0.03$ meV, corresponding to a dephasing time of 45 psec, assuming no contribution due to spectral diffusion. (In the absence of spectral diffusion, the observed width is $4\gamma_{ph}$.) The broad Stokes shifted feature is due to the quasi-equilibrium distribution of the exciton population produced by the migration of excitons from energy E to E'. The response is a function of the steady state exciton population assuming all excitons in the spectral region concerned give rise to the same cw nonlinear response. The line shape in Fig. 1a can be fit to a simple model which neglects migration to states above the excitation energy. The calculation is based on the nonlinear optical response of a simple two level system and assumes a Gaussian distribution for the quasi-equilibrium population of excitons that have migrated to states below the excitation energy. The spectral profile of the hole-burning resonance is assumed to be Lorentzian. The result is plotted as the solid line in the figure. A small but finite detuning of order 100kHz is set between fields 1 and 2 to reduce contributions to the data from slower components (discussed elsewhere [35]).

In the simple picture of spectral hole burning in the presence of spectral diffusion, the lifetime of the excitation created by $\mathbf{E}_1 \cdot \mathbf{E}_2^*$ is characterized by two time scales. The initial excitation decays on a short time scale due to spectral diffusion. However, assuming equilibrium is established on a time scale short compared to the recombination time, a second time scale is observed due to decay of the equilibrium population; i.e., the recombination time. The presence of two time scales in clearly seen in Fig. 1b (T=10K) where we show the four-wave mixing lineshape obtained by tuning ω_1. Recall that tuning ω_1 varies the frequency difference ω_1-ω_2 which determines the oscillation time of the grating. The signal decreases when the frequency

difference exceeds the relaxation rate (similar to the Fourier transform picture of a time-resolved pump-probe measurement.) The narrow resonance corresponds to a lifetime of 1 nsec and represents the decay time of the quasi-equilibrium exciton distribution (the broad feature in Fig. 1a.) The wide feature corresponds to a lifetime of 45 psec and is the inverse of the spectral diffusion rate. Indeed, setting the detuning of ω_1-ω_2 large compared to the width of the narrow feature greatly reduces the contribution of the broad feature in Fig. 1a and in fact further narrows the sharp resonance, confirming that the broad feature in Fig. 1a corresponds to spectral diffusion.

The theoretical model for phonon assisted exciton migration was developed recently by Takagahara [14]. In the model, excitons resonantly excited are in a non-equilibrium state and can migrate to other sites by emitting or absorbing acoustic phonons. Migration is possible due to the overlap of the exciton wave function in different sites when the inter-site distance is small. When the inter-site distance is much greater than the localization length the process occurs by inter-site dipole-dipole coupling. The typical magnitude of participating phonon wave vectors is within a few times of the inverse of the localization length corresponding to phonon energies of order 0.01 to 0.1 meV. The theory predicts a distinctive temperature dependence for the migration rate. At low temperatures, the dependence is described by $\exp(\beta T^{\alpha})$. In this expression, β is positive and independent of temperature but is expected to increase with the exciton energy and depends on details of interface roughness; α is estimated to be between 1.6 and 1.7. The predicted temperature dependence is quite different from that of variable range hopping used by Mott to interpret electronic conduction in the localized regime [36]. The difference has been attributed to the long-range nature of the inter-site interaction and the phonon emission process involved in the migration of the localized exciton [15]. This temperature dependence has been observed in transient hole burning experiments in an InGaAs/InP QW where all excitons are localized by alloy disorder [26]. Figure 2 shows the temperature dependence of the exciton migration rate measured at 0.6 meV and 1.5 meV below the absorption line center. The data is in good agreement with the phonon assisted migration theory

discussed above with α=1.6. The measurement indicates that the dominant contribution to relaxation of the localized exciton is phonon assisted migration up to a temperature of 15 K. The slow scattering rates and observed temperature dependence are quite different from the faster rates and linear temperature dependence reported in material with reduced disorder [13].

The strong inhomogeneous broadening of the hh1 linear absorption spectrum compared to the intrinsic homogeneous width suggests that such a system is ideal for observing a classical photon echo. In the classical picture of the three pulse transient resonant four wave mixing response, a homogeneously broadened system gives rise to a free polarization decay signal which is coincident in time with the third excitation pulse. However, in the presence of strong inhomogeneous broadening, the fields from the different resonances initially interfere, destroying the free polarization decay. At a time after the third pulse given by the time between the first two pulses, a rephasing occurs giving rise to a constructive interference and coherent emission designated as an echo. Recent theoretical work has predicted that in an ideal semiconductor, exciton-exciton interactions and coupling to the continuum lead to complex temporal structure in the emitted radiation in a coherent transient four-wave mixing experiment producing time delays in the emission as seen in a photon echo experiment [11]. However, in a classical two pulse (spontaneous) or three pulse (stimulated) photon echo, an inhomogeneously broadened resonant system produces a time delay in the emitted signal with respect to the last pulse that is given by the time between the first two pulses. In addition, the emission is a single peak with a width determined by the inhomogeneous width. Early work on GaAs MQW demonstrated the existence of a spontaneous photon echo [37] while more recently, transient four-wave mixing in the mixed crystal CdSSe demonstrated a stimulated photon echo [38].

Using the identical geometry as in the above cw measurements, we have examined the time resolved emission generated in a three pulse transient four-wave mixing experiment in the limit where the Rabi flopping frequency, $\mu E/\hbar$ is much less than the exciton binding energy [39]. A psec laser system (pulsewidth adjustable between 200 fsec and 8 psec) was used to excite the system. A portion of the laser beam was mixed with the coherent signal to produce an up-

converted signal for time resolution. Figure 3a shows the time resolved emission where the inset confirms that the time delay in the emission is given by the time delay between the first two pulses. In these experiments, the normal time ordering is E_2 followed by E_1 followed by E_3. (Note that the contributions due to polarization scattering which give rise to so-called negative time signals [4, 7, 8, 11] for E_1 followed by E_2 are not observed in these experiments on time scales of T_2 since local field effects decay on the time scale of T_2^*, the inverse of the inhomogeneous width.) The solid line in Fig. 3a represents a numerical integration of the optical Bloch equations including finite pulsewidth effects where the only fitting parameters are the amplitude and the inhomogeneous width (in the limit of delta-function pulses, the temporal width of the echo is given by $\Delta t = 4\hbar\sqrt{2}\ln 2 / \Delta E$ where Δt is the echo pulse width and ΔE is the full width half maximum of the Gaussian inhomogeneous distribution in energy.) The fit gives $\Delta E = 2.25 \pm 0.25\, eV$, in excellent agreement with the 2.2 eV linear absorption width of this particular sample. Fig. 3b shows the excellent single exponential decays associated with the energy relaxation rate and the dephasing rate corresponding to 35 psec and 69 psec, respectively. Based on this approach, we have reported measurements of the energy and temperature dependence of the relaxation rates further confirming the details of phonon assisted migration in disordered systems [28].

Through the above discussion, we have provided a self-consistent picture of the nonlinear optical response and associated dynamics. It is clear that disorder plays a major role in these systems since the dynamical processes which we have been investigating are controlled by the nature of disorder. In the above experiments all fields were linearly co-polarized, however, several studies have recently reported that the dephasing rate changes dramatically in two pulse transient four-wave mixing experiments in a MQW when $\mathbf{E}_2 \perp \mathbf{E}_1$ [40, 41]. In Fig. 4 we demonstrate a fundamental change under these conditions in the time resolved emission by comparing the time resolved emission in a co-polarized experiment (Fig. 4a) to that for $\mathbf{E}_2 \perp \mathbf{E}_1 \parallel \mathbf{E}_3$, $\mathbf{E}_s \parallel \mathbf{E}_2$ (Fig. 4b). The data show that in the former case the emission time depends on the interval between $\mathbf{E}_1$ and $\mathbf{E}_2$ while in the second case it does not. [The weak echo signal

evident in Fig. 4b arises from a resonance which is 2.5 meV Stokes shifted from the absorption peak. On resonance the strength of the signal is comparable to the free polarization decay, however, the contribution is observable in Fig. 4b despite the large detuning because the dephasing time of this signal, 70 ps, is much longer than the dephasing time of the primary peak and hence decays far more slowly with increasing time delay between the first and second pulse.] Both the free polarization decay (4b) and co-polarized stimulated photon echo (4a) are resonant and show very similar spectral dependence; after correction for absorption, they are nearly coincident with the absorption maximum. The free polarization decay is approximately 2 orders of magnitude weaker than the co-polarized stimulated photon echo at low intensity at the peak of the response. Based on the above classical picture, it is clear that the signal for $\mathbf{E}_1 \parallel \mathbf{E}_2$ is due to an inhomogeneously broadened resonance while the signal for $\mathbf{E}_1 \perp \mathbf{E}_2$ is due to a homogeneously broadened resonance.

This behavior is completely unexpected. Based on the energy level structure (see Fig. 4a inset) no difference in the nature of the signal is expected other than the polarization. In GaAs, quantum confinement lifts the valence band degeneracy at k=0 resulting in heavy-hole-light-hole splitting which for these experiments is large compared to the laser bandwidth and the Rabi flopping frequency. When the axis of quantization is taken to be perpendicular to the barriers, the heavy-hole valence band has only two degenerate magnetic substates given by $m=\pm 3/2$ levels while the conduction band substates are given by $m=\pm 1/2$. The selection rules for optical excitation are $\Delta m=\pm 1$. Since linearly polarized fields propagating parallel to the axis of quantization can be taken as a superposition of two circularly polarized fields, we can designate the exciton created by a σ_+ polarized field as $|+1\rangle$ and the exciton created by a σ_- polarized field as $|-1\rangle$. The signal is produced by the scattering of $\mathbf{E}_3$ off the grating produced by $\mathbf{E}_1^* \mathbf{E}_2$. We see then that for linear co-polarized $\mathbf{E}_1$ and $\mathbf{E}_2$, two spatial gratings consisting of $|+1\rangle$ and $|-1\rangle$ excitons are created and are spatially coincident. For $\mathbf{E}_1 \perp \mathbf{E}_2$, the two gratings are exactly spatially out of phase. However, $\mathbf{E}_3$ must also be decomposed into circularly polarized components, each of which independently scatters from one of the gratings, resulting in a linearly

polarized signal field. Hence the change in the nonlinear response in Fig. 4 is clearly unexpected. (This picture is for a homogeneously broadened system but still provides insight for an inhomogeneously broadened system. Although there is no net grating, there is a grating for each frequency group within the inhomogeneous distribution. Each group results in a component of the scattered signal, and it is the phase relationship between these components which results in the signal delay.)

In Fig. 5a we compare the energy dependence of the dephasing rates for these two components of the response. The dephasing rate for the prompt signal ($\mathbf{E}_1 \perp \mathbf{E}_2$) is much greater than the delayed signal, 0.20-0.25 ps^{-1} and essentially energy independent. The dephasing rate for the delayed signal ($\mathbf{E}_1 \| \mathbf{E}_2$) varies from 0.016±0.001 ps^{-1} on the low energy side to 0.1±0.02 ps^{-1} on the high energy side. The increase in the dephasing rate with increasing photon energy has been reported earlier [27, 28, 42] and was suggested to be due to the increase in scattering rate for localized excitons near the mobility edge. The temperature dependence of these dephasing rates also differs considerably. In Fig. 5b we see that the temperature dependence of the dephasing rate of the delayed component follows the behavior for phonon assisted migration and thermal activation of localized excitons as described above. However, the dephasing rate for the prompt signal shows a linear temperature dependence of the form $\gamma_{ph} = \gamma_0 + \gamma^* T$, where $\gamma^* = 4\mu eV / K$. We note that the magnitude of γ_0, the linear dependence on temperature and the magnitude of γ^* are similar to that observed by Schultheis in a single quantum well which was believed to be of very high quality [13] . The sample in that work was believed to be homogeneously broadened with no Stokes shift in the luminescence. Based on the quality of the sample, the homogeneous broadening of the HH1 resonance even at low temperature and the linear temperature dependence of the dephasing rate, Schultheis *et al.* proposed that the scattering mechanism was single phonon scattering [43] along the 2-D dispersion curve of an exciton described by an extended (delocalized) wave function.

It is, of course, difficult to determine experimentally if a wave function is truly extended. However, there are several additional experimental observations in the current experiments

which are consistent with the proposal that the resonance involved in the emission in Fig. 4b arises from excitons with extended wave functions. In Fig. 6a we show that for fixed pulse delay and energy, the magnitude of both signals vary cubically as expected with the incident beam energies (the solid line corresponds to a slope of n=3) for a true four-wave mixing process. However, at densities above 2×10^8 excitons-cm^{-2}-layer^{-1} (corresponding to a fluence of 2×10^{10} photons$-$cm^{-2}, where the density was calculated based on the absorbed energy) the stimulated photon echo emission deviates from cubic behavior and begins to saturate while there is no evidence of saturation in the prompt signal. Such saturation of the delayed signal which arises due to localized excitons would be expected since there are a finite number of localization sites. The saturation intensity of the nonlinear response in an ideal quantum well where all states are extended is considerably higher than that seen for localized states. At sufficiently high excitation intensity, the co-polarized signal is comprised of both a prompt signal and an echo [39] but as the intensity increases, the delayed signal completely saturates, leaving only the free polarization decay.

Transport measurements also provide an indication of the origin of the differences in these two signals. To examine this aspect of the behavior, we studied the angle dependence of the excitation relaxation rate to probe the spatial "washout" time due to motion of the excitation. This is the typical approach in transient grating experiments to measure spatial diffusion [44]. In these experiments measurement of the signal as a function of the delay between the second and third fields measures the decay rate of the excitation induced by the first two fields. The total signal decay is given by $\Gamma_{pop} = \gamma_{rec} + \Gamma_{SD} + \Gamma_D$ where γ_{rec} is the recombination rate, Γ_{SD} is the spectral diffusion rate and Γ_D is the spatial diffusion rate given by $4\pi^2 D / \Lambda^2$. Λ is the grating spacing: $\Lambda = \lambda / n2\sin(\theta/2)$. It is expected that delocalized states should have a larger D than localized states. Figure 6b shows $2\Gamma_{pop}$ as a function of inverse grating spacing for the free polarization decay and the stimulated photon echo, fitting to a quadratic dependence yields D=5.2 for the stimulated photon echo and D=10.1 for the free polarization decay. This data is taken at an exciton energy 0.5 meV below line center and at a temperature of 15 K. The

measured difference is larger in other samples. This difference is clear evidence of the greater mobility of the excitons which are responsible for the free polarization decay signal. The diffusion coefficient for localized excitons is dependent on the exciton energy [42] and this measurement is taken at a point where it is beginning to undergo a transition from its low energy (small D) to high energy (large D) values. The ratio of the two diffusion coefficients is sample dependent as expected where in a 10 period sample, the ratio is as large as 3.5.

The difference in the diffusion coefficients supports the earlier data suggesting that the emission shown in Fig. 4 arises from two different resonant effects and the larger dephasing rate and increased mobility observed for the resonance studied with orthogonal excitation indicates this exciton may not be as strongly localized. Indeed, the conclusion that the prompt signal arises from a homogeneously broadened resonance is not completely accurate in view of recent theoretical work [11]. These results show that for low intensity resonant excitonic excitation in the transient four-wave mixing geometry, the emission time does not depend on the time between the first two pulses. At higher excitation density, additional temporal structure is observed at later times which does depend on the time between the first two pulses. The intensity dependence shown in this model for this delayed structure is opposite that reported in the above discussion. However, the intensities for the observation in these experiments are all well below that predicted in the theoretical work for observing the additional temporal structure. In fact, we believe that the emission in Fig. 4b is indeed the low intensity response predicted in reference [11].

We note that the proposal that these resonances are distinguished by different degrees of localization is certainly unexpected in the usual picture of localized and delocalized states [45]. However, an alternative explanation may be that these resonances coincide in energy but not in space, a possibility consistent with the recent proposals that interface roughness is characterized by a bimodal distribution in scale lengths [22, 23]. However, even in material characterized as high quality, we have shown that these effects can dominate optical studies.

We also note that the disappearance of the echo for orthogonal polarization remains unexplained. Experimentally, the absence of the signal demonstrates the absence of a grating. Recalling that there are two induced gratings associated with $|+1\rangle$ and $|-1\rangle$ excitons, respectively, we note that complete spatial mixing of the two gratings on a time scale of the measurement would indeed destroy the signal. One such mechanism is spin relaxation. However, measurements show the spin relaxation time in this system is on the order of 40 psec, in agreement with other measurements [46, 47], far too slow to account for the observed behavior.

Additional insight into these results is seen in the experimental study of the unexpected intensity dependence and depolarization of the four-wave mixing response. In these experiments, the first two fields $\mathbf{E}_1$ and $\mathbf{E}_2$ are circularly co-polarized σ_+. Hence, in the simple picture where m is a good quantum number, only $|+1\rangle$ excitons are created. Using a *linearly* polarized field for $\mathbf{E}_3$, we would expect that only the σ_+ component of the $\mathbf{E}_3$ polarization would be scattered, giving rise to a completely circularly polarized signal. In Fig. 7a, we plot the polarization given by the intensity difference between left and right circularly polarized light normalized to the sum. At low intensity, we see the surprising result that the polarization of the system is lost; i.e., the scattered signal is linearly polarized. As the excitation intensity increases, the polarization of the system is recovered and the emitted radiation is circularly polarized. While the physical basis for this response is not understood, the disappearance of the echo with orthogonally linearly polarized fields is now clear. Since linearly polarized light couples equally well to the $|+1\rangle$ and $|-1\rangle$ exciton gratings, there is no effective modulation of the optical response and hence no scattering of $\mathbf{E}_3$. Alternatively, the scattering of radiation from the $|+1\rangle$ exciton grating is exactly out of phase with the radiation scattered from the $|-1\rangle$ exciton grating, resulting in complete destructive interference.

The origin of this behavior is not fully understood, but it is unlikely that dynamical effects such as relaxation can explain the above behavior. Incoherent transient spectroscopy pump-probe measurements using circularly polarized radiation show that the coupling appears to be

instantaneous, as seen in Fig. 7b. Similar results are obtained with 200 fsec pulses, though the sign of the response depends on pulsewidth and detuning. It is unlikely that any relaxation effects would occur on such a short time scale. Alternatively, the above discussion has been based on the assumption that m is a good quantum number. Recently, it has been shown in numerical studies in an ideal GaAs quantum well, that band mixing is not strong enough to account for the observed coupling in the nonlinear response although mixing of the magnetic substates may occur due to interface roughness [48]. An alternative explanation is based on disorder enhanced exciton-exciton interactions. Nondegenerate pump-probe measurements using orthogonally circularly polarized light show a pump induced increased absorption due to a Stokes shifted resonance when the pump is tuned just below the hh1 absorption line center. The Stokes shift is of order 1-1.5 meV and is constant with respect to the pump frequency rather than the hh1 resonance. These measurements are consistent with the presence of a resonantly produced biexciton. These measurements show that the net coupling for co-rotating and oppositely rotating circularly polarized fields is comparable and may explain the behavior observed in the photon echo experiments. Recent evidence for biexciton effects in the nonlinear response have been reported in both quantum beat experiments [47] and in transient four-wave mixing [49].

In summary, we have shown that the nonlinear response in these systems is highly complex. Based on the classical interpretation of the nonlinear response, there appear to be two contributions to the hh1 resonance with similar spectral structure but differing in dynamics, transport and symmetry. The above measurements show the importance of including the effects of disorder in the interpretation of any optical measurement and in future theoretical work to enable comparison with experiment.

This work was supported by AFOSR, ARO and NSF.

REFERENCES

1. P.R. Berman and R.G. Brewer, Phys. Rev. A **32**, 2784 (1985).
2. S. Schmitt-Rink, Phys. Rev. B **32**, 6601 (1985).
3. H. Haug and S.W. Koch, *Quantum Theory of the Optical and Electronic Properties of Semiconductors* (World Scientific, Singapore, 1990)
4. M. Wegener, D.S. Chemla, S. Schmitt-Rink, and W. Schäfer, Phys. Rev. A **42**, 5675 (1990).
5. R.P. Srivastava and H.R. Saidi, J. Quant. Spectrosc. Radiat. Transfer. **16**, 301 (1976).
6. S. Saikan, H. Miyamoto, Y. Tosaki, and A. Fujiwara, Phys. Rev. B **36**, 5074 (1987).
7. B. Fluegel, N. Peyghambarian, G. Olbright, M. Lindberg, S.W. Koch, M. Joffre, D. Hulin, A. Migus, and A. Antonetti, Phys. Rev. Lett. **59**, 2588 (1987).
8. K. Leo, M. Wegener, J. Shah, D.S. Chemla, E.O. Göbel, T.C. Damen, S. Schmitt-Rink, and W. Schäfer, Phys. Rev. Lett. **65**, 1340 (1990).
9. K. Leo, E.O. Göbel, T.C. Damen, J. Shah, S. Schmitt-Rink, W. Schaefer, J.W. Müller, K. Köhler, and P. Ganser, Phys. Rev. B **44**, 5726 (1991).
10. M. Lindberg and S.W. Koch, Phys. Rev. B **38**, 3342 (1988).
11. M. Lindberg, R. Binder, and S.W. Koch, Phys. Rev. A **45**, 1865 (1992).
12. P. Lee A., T.V. Ramakrishnan, Rev. Mod. Phys. **57**, 287 (1985).
13. L. Schultheis, A. Honold, J. Kuhl, K. Kohler, and C.W. Tu, Phys. Rev. B **34**, 9027 (1986).
14. T. Takagahara, Phys. Rev. B **32**, 7013 (1985).
15. T. Takagahara, Jr. Lumin. **44**, 347 (1989).
16. C. Weisbuch, R. Dingle, A.C. Gossard, and W. Wiegmann, Solid State Comm. **38**, 709 (1981).
17. R.C. Miller, C.W. Tu, S.K. Sputz, and R.F. Kopf, Appl. Phys. Lett. **49**, 1245 (1986).

18. C.W. Tu, R.C. Miller, B.A. Wilson, P.M. Petroff, T.D. Harris, R.F. Kopf, S.K. Sputz, and M.G. Lamon, J. Cryst. Growth **81**, 159 (1987).

19. A. Ourmazd, D.W. Taylor, J. Cunningham, and C.W. Tu, Phys. Rev. Lett. **62**, 933 (1989).

20. B. Deveaud, B. Guenais, A. Poudoulec, and A. Regreny, Phys. Rev. Lett. **65**, 2317 (1990).

21. A. Ourmazd and J. Cunningham, Phys. Rev. Lett **65**, 2318 (1990).

22. C.A. Warwick, W.Y. Jan, A. Ourmazd, and T.D. Harris, Appl. Phys. Lett. **56**, 2666 (1990).

23. D. Gammon, B.V. Shanabrook, and D.S. Katzer, Phys. Rev. Lett. **67**, 1547 (1991).

24. T. Tanaka and H. Sakaki, J. Cryst. Growth **81**, 153 (1987).

25. Y. Masumoto, S. Shionoya, and H. Kawaguchi, Phys. Rev. B **29**, 2324 (1984).

26. J. Hegarty, K. Tai, and W.T. Tsang, Phys. Rev. B **38**, 7843 (1988).

27. H. Wang, M. Jiang, and D.G. Steel, Phys. Rev. Lett. **65**, 1255 (1990).

28. M.D. Webb, S.T. Cundiff, and D.G. Steel, Phys. Rev. B **43**, 12658 (1991).

29. J. Hegarty and M.D. Sturge, J. Lumin. **31&32**, 494 (1984).

30. J. Hegarty, M.D. Sturge, C. Weisbuch, A.C. Gossard, and W. Wiegmann, Phys. Rev. Lett. **49**, 930 (1982).

31. J.E. Zucker, A. Pinczuk, D.S. Chemla, and A.C. Gossard, Phys. Rev. B **35**, 2892 (1987).

32. J. Hegarty, L. Goldner, and M.D. Sturge, Phys. Rev. B **30**, 7346 (1984).

33. H. Wang and D.G. Steel, Phys. Rev. A **43**, 3823 (1991).

34. H. Wang and D.G. Steel, App. Phys. **A33**, 514 (1991).

35. M. Jiang, H. Wang, and D.G. Steel, Appl. Phys. Lett. (1992).

36. N.F. Mott and E.A. Davis, *Electronic Processes in Non-Crystalline Materials* (Clarendon Press, Oxford, 1979) 2nd ed.

37. L. Schultheis, M.D. Sturge, and J. Hegarty, Appl. Phys. Lett. **47**, 995 (1985).

38. G. Noll, U. Siegner, S.G. Shevel, and E.O. Göbel, Phys. Rev. Lett. **64**, 792 (1990).

39. M.D. Webb, S.T. Cundiff, and D.G. Steel, Phys. Rev. Lett. **66**, 934 (1991).

40. H.H. Yaffe, Y. Prior, J.P. Harbison, and L.T. Florez, in Quantum Electronics Laser Science, 1991 Technical Digest Series (OSA, 1991.)

41. K. Leo, J. Shah, S. Schmitt-Rink, and K. Köhler, in VIIth International Symposium on Ultrafast Processes in Spectroscopy, (IOP, 1992, 1991.)

42. J. Hegarty and M.D. Sturge, J. Opt. Soc. Am. B **2**, 1143 (1985).

43. T. Miyata, Jr. Phys. Soc. Japan **31**, 529 (1971).

44. H.J. Eichler, P. Günter, and D.W. Pohl, *Laser-Induced Dynamic Gratings* (Springer-Verlag, Berlin, 1986) 256.

45. L. Fleishman and P.W. Anderson, Phys. Rev. B **21**, 2366 (1980).

46. T.C. Damen, L. Viña, J.E. Cunningham, J. Shah, and L.J. Sham, Phys. Rev. Lett. **67**, 3432 (1991).

47. S. Bar-Ad and I. Bar-Joseph, Phys. Rev. Lett. **68**, 349 (1992).

48. S. Koch, personal communication. 1992,

49. B.F. Feuerbacher J. Kuhl, K. Ploog, Phys. Rev. B **43**, 2439 (1991).

Figure Captions

Fig. 1. (a) The four-wave mixing response as a function of the third beam frequency at 5 K showing the spectral hole with a width determined by the homogeneous width. The four-wave mixing response also shows a broad pedestal at lower energy due to the quasi-equilibrium distribution of excitons produced by exciton migration. This migration may also contribute to the width of the narrow feature. (b) The four wave mixing response at 10 K as a function of the detuning between the first and second beams. Unlike Fig. 1a, this lineshape reflects the energy relaxation rate. The broad feature measures the rate of decay of the narrow spectral hole in Fig. 1a while the narrow feature measures the rate of decay of the quasi-equilibrium distribution giving rise to the pedestal.

Fig. 2. The temperature dependence of the exciton decay rate. Circles and crosses are data obtained at 1.5 meV and at 0.6 meV below line center respectively. Dashed lines are fit to the theory of phonon assisted migration.

Fig. 3. (a) The time resolved transient four-wave mixing response demonstrating delay of the emission. The inset shows a linear dependence on incident pulse interval characteristic of a classic photon echo. (b) The transient four-wave mixing signal as a function of delay between first two pulses (curve (i)), and second and third pulses (curve (ii)). Straight lines are fit to exponential behavior, yielding a dephasing time of 69 psec for curve (i) and an excitation relaxation time of 35 psec for curve (ii).

Fig. 4 The time resolved transient four-wave mixing signal for co-polarized fields (a) and $\mathbf{E}_1 \perp \mathbf{E}_2 \| \mathbf{E}_3$, $\mathbf{E}_s \| \mathbf{E}_1$ (b). The response for a series of delays between $\mathbf{E}_1$ and $\mathbf{E}_2$ are given in each panel. The inset in the upper panel is the energy level structure for the magnetic substates in a GaAs MQW.

Fig. 5 Dependence of dephasing rates on (a) energy and (b) temperature. Solid squares are for $\mathbf{E}_1 \perp \mathbf{E}_2$ and open circles for $\mathbf{E}_1 \| \mathbf{E}_2$. In (b) dashed line is fit to theoretical predictions for excitons migrating between localization sites, solid line is fit for single phonon scattering.

Fig. 6 (a) Signal strength as a function of incident intensity, straight lines are for cubic behavior. (b) Decay of grating as a function of grating spacing, lines are fits to quadratic dependence expected for spatial diffusion. In both solid squares are for $\mathbf{E}_1 \perp \mathbf{E}_2$ and open circles for $\mathbf{E}_1 \| \mathbf{E}_2$.

Fig. 7 (a) Polarization $(I_+ - I_-)/(I_+ + I_-)$ of signal field as a function of incident intensity, dashed line is to guide the eye. (b) Transient absorption response for a circularly polarized (σ_+) pump. Upper curve is decay of polarization (right axis, offset for clarity).

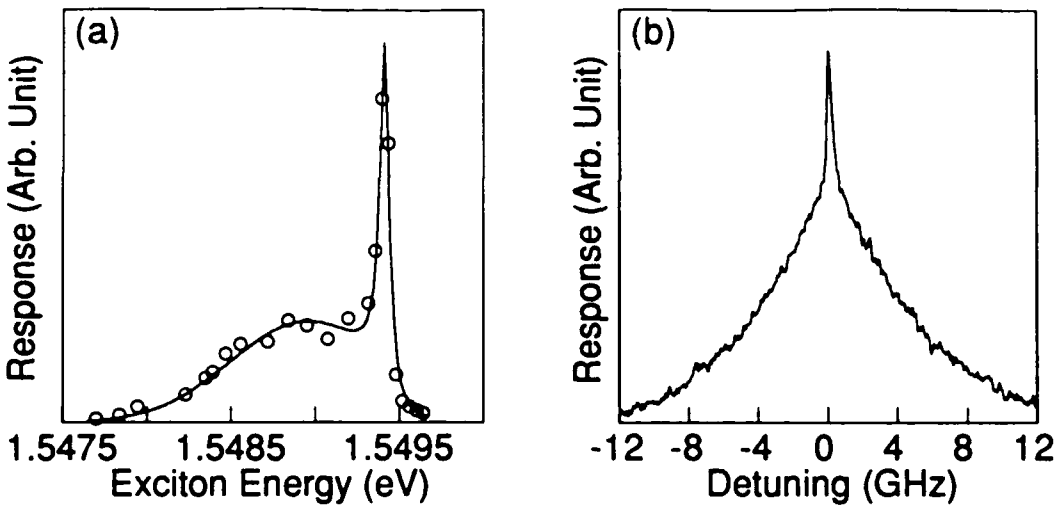
(a)
Response (Arb. Unit)
1.5475
1.5485
1.5495
Exciton Energy (eV)
(b)
Response (Arb. Unit)
-12
-8
-4
0
4
8
12
Detuning (GHz)

Figure 1.

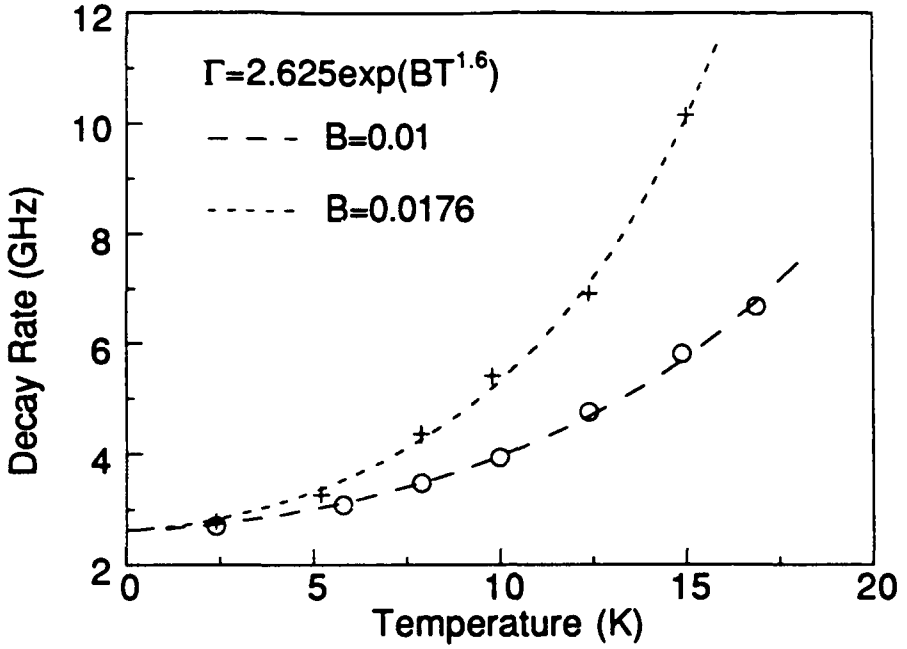
Γ=2.625exp(BT^1.6)
B=0.01
B=0.0176
Decay Rate (GHz)
Temperature (K)
12
10
8
6
4
2
0
5
10
15
20

Figure 2.

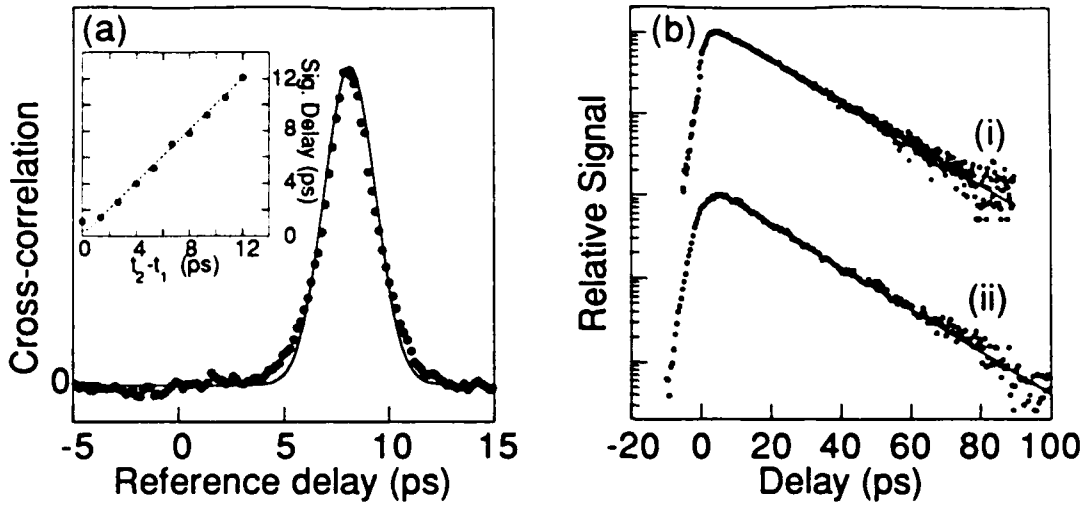
(a)
Cross-correlation
0
-5
0
5
10
15
Reference delay (ps)
Sig Delay (ps)
0
4
8
12
t_2-t_1 (ps)
(b)
Relative Signal
(i)
(ii)
-20
0
20
40
60
80
100
Delay (ps)

Figure 3

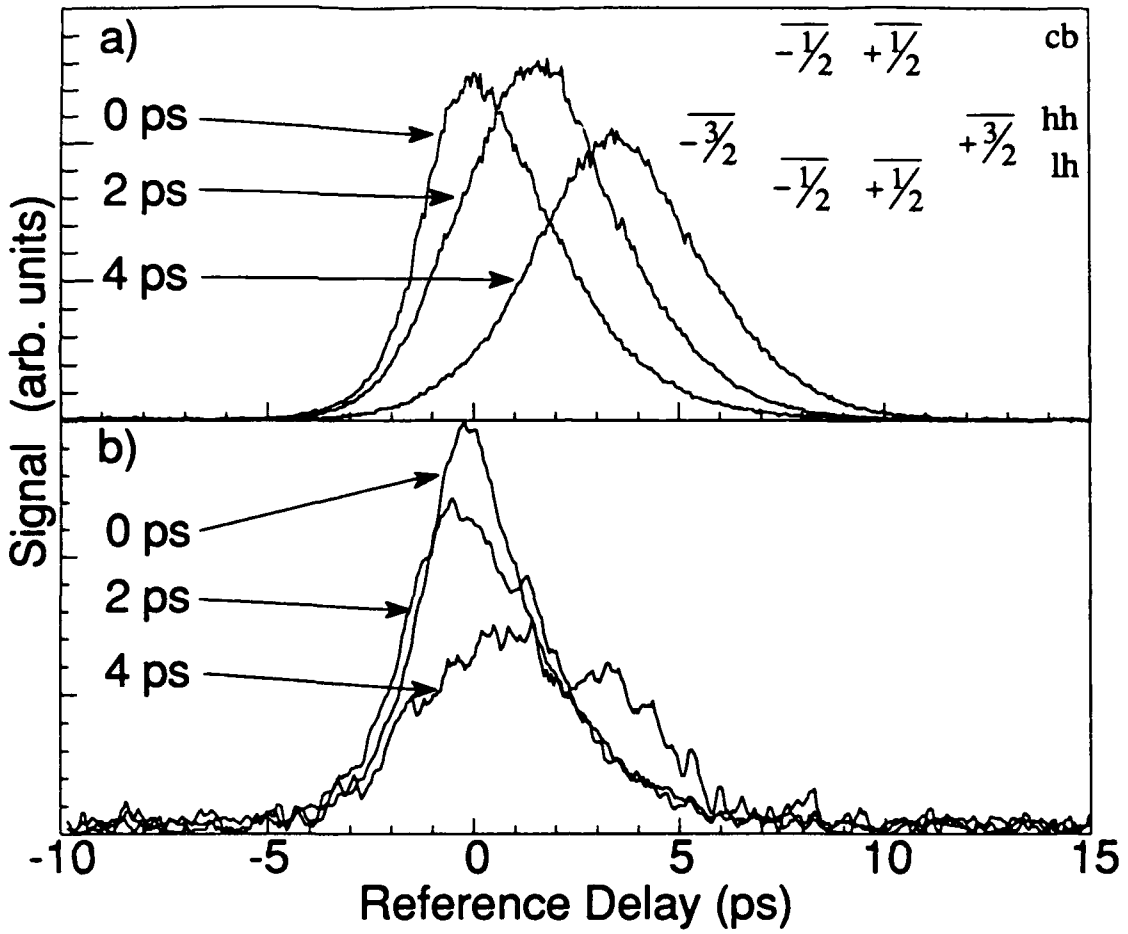
a)
0 ps
2 ps
4 ps
-1/2 +1/2
cb
-3/2
+3/2
hh
-1/2 +1/2
lh
b)
0 ps
2 ps
4 ps
Signal (arb. units)
-10
-5
0
5
10
15
Reference Delay (ps)

Figure 4

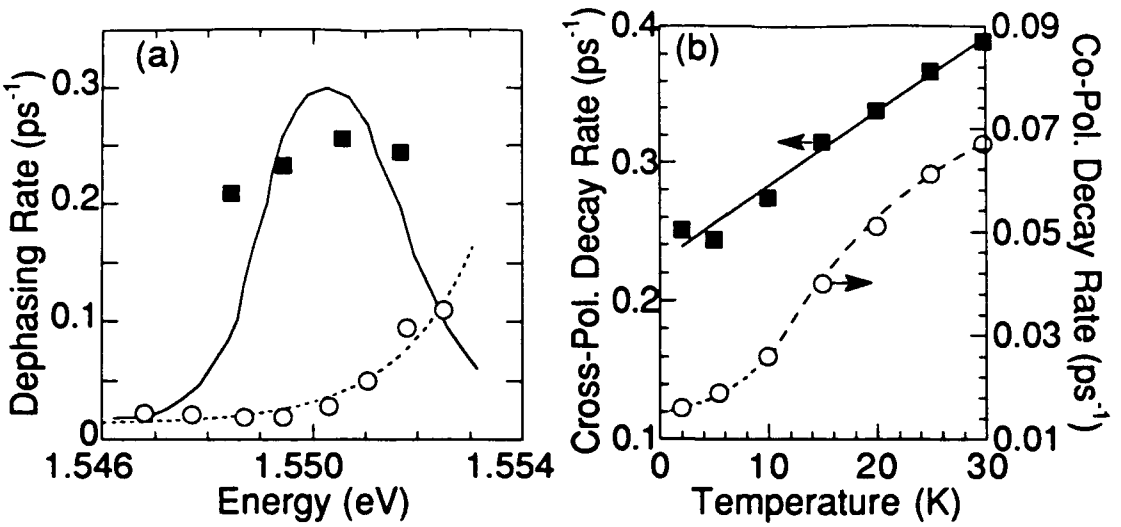
(a)
Dephasing Rate (ps^{-1})
0.3
0.2
0.1
0
1.546
1.550
1.554
Energy (eV)
(b)
Cross-Pol. Decay Rate (ps^{-1})
0.4
0.3
0.2
0.1
0.09
0.07
0.05
0.03
0.01
Co-Pol. Decay Rate (ps^{-1})
0
10
20
30
Temperature (K)

Figure 5

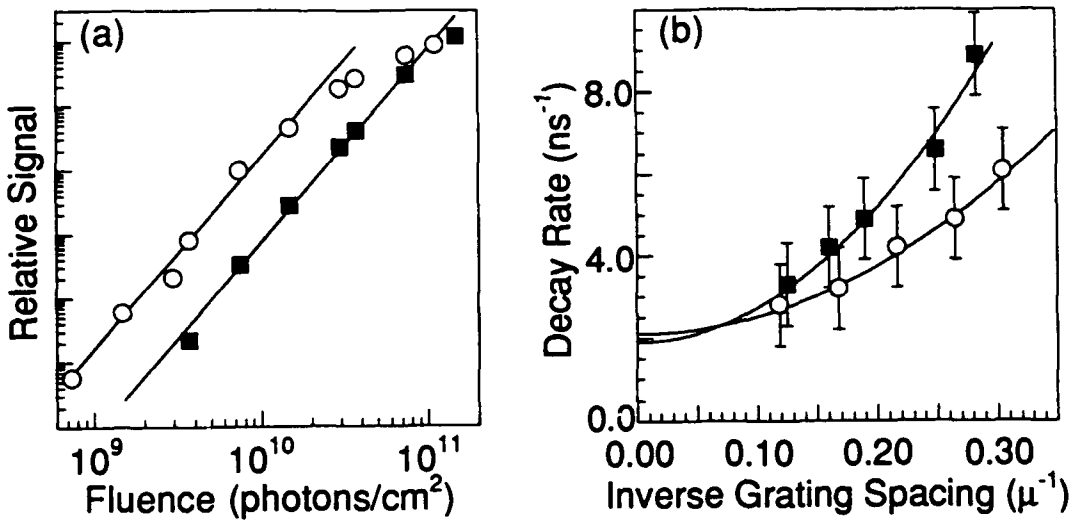
(a)
Relative Signal
10^9
10^{10}
10^{11}
Fluence (photons/cm^2)
(b)
Decay Rate (ns^{-1})
8.0
4.0
0.0
0.00
0.10
0.20
0.30
Inverse Grating Spacing (μ^{-1})

Fig. 6

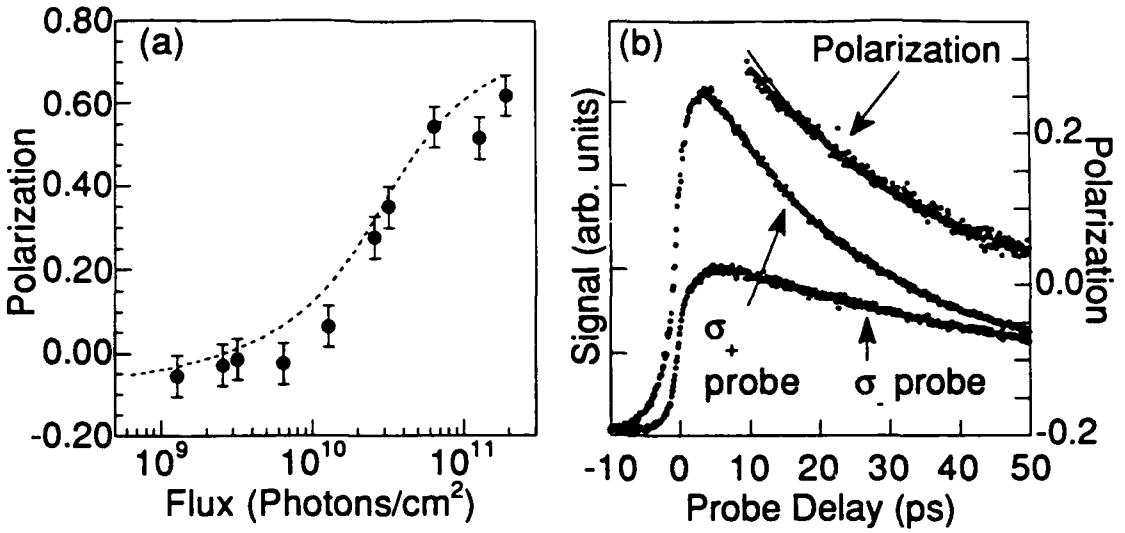
(a)
Polarization
0.80
0.60
0.40
0.20
0.00
-0.20
10^9
10^{10}
10^{11}
Flux (Photons/cm^2)
(b)
Polarization
Signal (arb. units)
σ_+ probe
σ_- probe
0.2
0.0
-0.2
Polarization
-10
0
10
20
30
40
50
Probe Delay (ps)

Fig 7.